

Doctoral Dissertation

**Isolation and Evaluation of Biological Activities of
Compounds from *Cordyceps militaris* (L.) Link Fruiting Body**

TRAN NGOC QUY

Graduate School for International Development and Cooperation
Hiroshima University

March 2020

**Isolation and Evaluation of Biological Activities of
Compounds from *Cordyceps militaris* (L.) Link Fruiting Body**

D172758


TRAN NGOC QUY

A Dissertation Submitted to
the Graduate School for International Development and Cooperation
of Hiroshima University in Partial Fulfillment
of the Requirement for the Degree of
Doctor of Agriculture

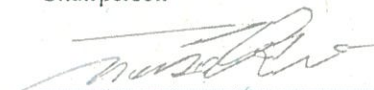
March 2020

We hereby recommend that the dissertation by Mr. TRAN NGOC QUY entitled "Isolation and Evaluation of Biological Activities of Compounds from *Cordyceps militaris* (L.) Link Fruiting Body" be accepted in partial fulfillment of the requirements for the degree of DOCTOR OF AGRICULTURE.

Committee on Final Examination:




TRAN Dang Xuan, Associate Professor
Chairperson



TSUDZUKI Masaaki, Professor



MAEDA Teruo, Professor

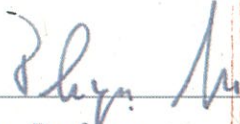


HOSAKA Tetsuro, Associate Professor

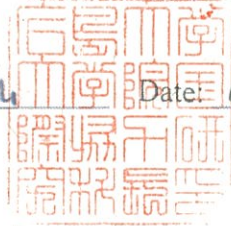


MORIMOTO Masanori, Associate Professor of Graduate
School of Agriculture, Kindai University

Date: January 30, 2020

Approved: 

BABA Takuya, Professor
Dean



Date: February 21, 2020

Graduate School for International Development and Cooperation
Hiroshima University

Table of contents

Table of contents	i
List of figures	iv
List of tables	xiii
List of appendixes	xix
Abstract	xx
Acknowledgments	xxv
1 Introduction	1
1.1 Background	1
1.2 Research objectives	4
1.3 Scientific contributions of the present study	4
1.4 Dissertation structure.....	5
2 Xanthine oxidase (XO) inhibitory and antioxidant activities of Cordyceps militaris (L.) Link fruiting body	6
2.1 Introduction	6
2.2 Materials and methods	8
2.2.1 Chemicals	8
2.2.2 Plant materials	9
2.2.3 Preparation of fungus extract	9
2.2.4 Fractionation of ethyl acetate extract	10
2.2.5 Xanthine oxidase (XO) inhibitory activity	11
2.2.6 DPPH radical scavenging activity	12
2.2.7 ABTS radical scavenging activity	12
2.2.8 Identification of chemical constituents by gas chromatography-mass spectrometry (GC-MS).....	13
2.2.9 Statistical analysis	14
2.3 Results	14
2.3.1 Xanthine oxidase inhibitory activity of crude extracts and fractions of <i>C. militaris</i>	14
2.3.2 Antioxidant activities of 14 fractions from EtOAc extract of <i>C. militaris</i> ...	16
2.3.3 GC-MS of analysis of <i>C. militaris</i> fractions from EtOAc extract.....	17
2.4 Discussion	19
2.5 Conclusion.....	21
3 Antibacterial activity of Cordyceps militaris (L.) Link fruiting body	22

3.1	Introduction	22
3.2	Materials and methods	25
3.2.1	Chemicals	25
3.2.2	Plant materials and fractions preparation	25
3.2.3	Antibacterial activity	25
3.2.4	Identification of chemical constituents of active fractions by gas chromatography-mass spectrometry (GC-MS)	26
3.2.5	Statistical analysis	26
3.3	Results	27
3.3.1	Antibacterial activity of crude extracts of <i>C. militaris</i>	27
3.3.2	Antibacterial activity of fractions from EtOAc extract of <i>C. militaris</i>	27
3.3.3	Compounds identification by GC-MS of active fractions from EtOAc extract of <i>C. militaris</i>	29
3.4	Discussion	30
3.5	Conclusion.....	31
4	Allelopathic activity and identification of allelochemicals from fruiting body of <i>Cordyceps militaris</i> (L.) Link fruiting body.....	32
4.1	Introduction	32
4.2	Materials and methods	34
4.2.1	Reagents	34
4.2.2	Plant materials	34
4.2.3	Preparation of plant extract	34
4.2.4	Fractionation of ethyl acetate extract	35
4.2.5	Germination and growth bioassays	35
4.2.6	Identification of chemical constituents by gas chromatography-mass spectrometry (GC-MS).....	36
4.2.7	Quantification of cordycepin by HPLC	37
4.2.8	Determination identification of cordycepin by LC-ESI-MS.....	37
4.2.9	Cordycepin content in different extractions	38
4.2.10	Statistical analysis	38
4.3	Results	38
4.3.1	Inhibitory effects of crude extracts of <i>C. militaris</i>	38
4.3.2	Effects of fractions from the EtOAc extract of <i>C. militaris</i>	39
4.3.3	Identification chemical compounds in CM4 fraction.....	40
4.3.4	Determination and quantification of cordycepin by high-performance	

liquid chromatography (HPLC)	41
4.3.5 Cordycepin detection by liquid chromatography-electrospray ionization-mass spectrometry (LC-ESI-MS).....	42
4.3.6 Comparison of cordycepin yields in different extractions	42
4.4 Discussion	43
4.5 Conclusion.....	45
5 Cordycepin isolated from <i>Cordyceps militaris</i>: Its newly discovered herbicidal property and potential plant-based novel alternative to glyphosate and paraquat.	46
5.1 Introduction	46
5.2 Materials and methods	47
5.2.1 Chemicals	47
5.2.2 Plant materials and CM4 fraction.....	48
5.2.3 Germination and growth bioassays	48
5.2.4 Physiological responses.....	49
5.2.5 Biochemical responses	50
5.2.6 Statistical analysis	51
5.3 Results	52
5.3.1 Effects of cordycepin, CM4 fraction, BA, glyphosate and paraquat on radish and barnyard grass.....	52
5.3.2 Physiological responses to cordycepin, CM4 fraction and benzoic acid	53
5.3.3 Biochemical responses to the CM4 Fraction, cordycepin and benzoic acid	56
5.4 Discussion	59
5.5 Conclusion.....	63
6 General discussion and conclusion	65
6.1 General discussion.....	65
6.2 Xanthine oxidase inhibition	66
6.3 Antibacterial activity	68
6.4 Allelopathic activity	69
6.5 Conclusion.....	72
References	73

List of figures

Figure 1.	The figure of <i>C. militaris</i> cultivating in artificial solid medium.	2
Figure 2.	The fruiting-bodies of <i>C. militaris</i> (L.) from Truc Anh company.	9
Figure 3.	Process of extraction and fractionation of <i>C. militaris</i> fruiting-bodies	10
Figure 4.	ABTS and DPPH radical scavenging activities of EtOAc fractions from <i>C. militaris</i> and antioxidant butylated hydroxytoluene (BHT) standard.	16
Figure 5.	Process of extraction and fractionation of the fruiting-bodies of <i>C. militaris</i>	35
Figure 6.	Germination and growth bioassays on radish.....	36
Figure 7.	Figure of inhibition on radish of CM4 fraction and control.....	40
Figure 8.	(a) HPLC chromatogram of cordycepin standard, (b) HPLC chromatogram of cordycepin in the fraction CM4 compared with the cordycepin standard (0.5 mg/mL).....	41
Figure 9.	Total ion chromatogram and mass of cordycepin detected in the CM4 fraction by LC-ESI-MS.....	42
Figure 10.	Chlorophylls and carotenoids contents of radish treated by cordycepin, CM4 fraction and BA at 40 ppm.	54
Figure 11.	Electrolyte leakage of radish treated by cordycepin, CM4 fraction and BA at 40 ppm.	55
Figure 12.	Lipid peroxidation accumulation in radish among control and treatments (cordycepin, CM4 fraction and BA) at 40 ppm.	56
Figure 13.	Total phenolic contents in the roots and aerial parts of radish among cordycepin, CM4 fraction and BA at 40 ppm.	57
Figure 14.	Total flavonoid contents in the roots and aerial parts of radish among cordycepin, CM4 fraction, and BA at 40 ppm.	57
Figure 15.	Proline contents in root and aerial parts of radish treated by cordycepin, CM4 fraction, and BA at 40 ppm.	58
Figure 16.	Comparison structure of cordycepin, allopurinol and xanthine.	68

Figure 17.	GC-MS chromatogram of F1 fraction from ethyl acetate extract of <i>C. militaris</i>	110
Figure 18.	Mass-spectra of palmitic acid methyl ester (Rt = 16.72) in F1 fraction from ethyl acetate extract of <i>C. militaris</i> detected by GC-MS	111
Figure 19.	ESI-MS spectra of palmitic acid methyl ester in F1 fraction from ethyl acetate extract of <i>C. militaris</i>	111
Figure 20.	Mass-spectra of palmitic acid (Rt = 17.09) in F1 fraction from ethyl acetate extract of <i>C. militaris</i> detected by GC-MS.....	113
Figure 21.	ESI-MS spectra of palmitic acid in F1 fraction from ethyl acetate extract of <i>C. militaris</i>	113
Figure 22.	Mass-spectra of 9,12-Octadecadienoic acid (Z, Z) (Rt = 18.73) in F1 fraction from ethyl acetate extract of <i>C. militaris</i> detected by GC-MS.....	115
Figure 23.	ESI-MS spectra of 9,12-Octadecadienoic acid (Z, Z) in F1 fraction from ethyl acetate extract of <i>C. militaris</i>	115
Figure 24.	GC-MS chromatogram of F2 fraction from ethyl acetate extract of <i>C. militaris</i>	116
Figure 25.	Mass-spectra of palmitic acid methyl ester (Rt = 16.72) in F2 fraction from ethyl acetate extract of <i>C. militaris</i> detected by GC-MS	117
Figure 26.	ESI-MS spectra of palmitic acid methyl ester in F2 fraction from ethyl acetate extract of <i>C. militaris</i>	117
Figure 27.	Mass-spectra of palmitic acid (Rt = 17.11) in F2 fraction from ethyl acetate extract of <i>C. militaris</i> detected by GC-MS.....	119
Figure 28.	ESI-MS spectra of palmitic acid in F2 fraction from ethyl acetate extract of <i>C. militaris</i>	119
Figure 29.	Mass-spectra of 9,12-Octadecadienoic acid (Z, Z) (Rt = 18.76) in F2 fraction from ethyl acetate extract of <i>C. militaris</i> detected by GC-MS.....	121
Figure 30.	ESI-MS spectra of 9,12-Octadecadienoic acid (Z, Z) in F2	

	fraction from ethyl acetate extract of <i>C. militaris</i>	121
Figure 31.	Mass-spectra of ergosta-4,6,8(14),22-tetraen-3-one (Rt = 29.12) in F2 fraction from ethyl acetate extract of <i>C. militaris</i> detected by GC-MS.....	123
Figure 32.	ESI-MS spectra of ergosta-4,6,8(14),22-tetraen-3-one in F2 fraction from ethyl acetate extract of <i>C. militaris</i>	124
Figure 33.	GC-MS chromatogram of F3 fraction from ethyl acetate extract of <i>C. militaris</i>	124
Figure 34.	Mass-spectra of pentadecanal (Rt = 14.56) in F3 fraction from ethyl acetate extract of <i>C. militaris</i> detected by GC-MS.....	126
Figure 35.	ESI-MS spectra of pentadecanal in F3 fraction from ethyl acetate extract of <i>C. militaris</i>	126
Figure 36.	Mass-spectra of 2-oxopalmitic acid methyl ester (Rt = 17.41) in F3 fraction from ethyl acetate extract of <i>C. militaris</i> detected by GC-MS.....	127
Figure 37.	ESI-MS spectra of 2-oxopalmitic acid methyl ester in F3 fraction from ethyl acetate extract of <i>C. militaris</i>	128
Figure 38.	Mass-spectra of octadecanal (Rt = 22.11) in F3 fraction from ethyl acetate extract of <i>C. militaris</i> detected by GC-MS.....	129
Figure 39.	ESI-MS spectra of octadecanal in F3 fraction from ethyl acetate extract of <i>C. militaris</i>	130
Figure 40.	Mass-spectra of dodecanamide (Rt = 25.55) in F3 fraction from ethyl acetate extract of <i>C. militaris</i> detected by GC-MS.....	131
Figure 41.	ESI-MS spectra of dodecanamide in F3 fraction from ethyl acetate extract of <i>C. militaris</i>	131
Figure 42.	GC-MS chromatogram of F4 fraction from ethyl acetate extract of <i>C. militaris</i>	132
Figure 43.	Mass-spectra of pentadecanal (Rt = 14.56) in F4 fraction from ethyl acetate extract of <i>C. militaris</i> detected by GC-MS.....	133
Figure 44.	ESI-MS spectra of pentadecanal in F4 fraction from ethyl acetate extract of <i>C. militaris</i>	133

Figure 45.	Mass-spectra of 2-oxopalmitic acid methyl ester (Rt = 17.40) in F4 fraction from ethyl acetate extract of <i>C. militaris</i> detected by GC-MS.....	134
Figure 46.	ESI-MS spectra of 2-oxopalmitic acid methyl ester in F4 fraction from ethyl acetate extract of <i>C. militaris</i>	135
Figure 47.	Mass-spectra of octadecanal (Rt = 22.11) in F4 fraction from ethyl acetate extract of <i>C. militaris</i> detected by GC-MS.....	136
Figure 48.	ESI-MS spectra of octadecanal in F4 fraction from ethyl acetate extract of <i>C. militaris</i>	137
Figure 49.	GC-MS chromatogram of F5 fraction from ethyl acetate extract of <i>C. militaris</i>	137
Figure 50.	Mass-spectra of pentadecanal (Rt = 14.56) in F5 fraction from ethyl acetate extract of <i>C. militaris</i> detected by GC-MS.....	138
Figure 51.	ESI-MS spectra of pentadecanal in F5 fraction from ethyl acetate extract of <i>C. militaris</i>	139
Figure 52.	Mass-spectra of hexadecanal (Rt = 15.65) in F5 fraction from ethyl acetate extract of <i>C. militaris</i> detected by GC-MS.....	140
Figure 53.	ESI-MS spectra of hexadecanal in F5 fraction from ethyl acetate extract of <i>C. militaris</i>	141
Figure 54.	Mass-spectra of 2-oxopalmitic acid methyl ester (Rt = 17.41) in F4 fraction from ethyl acetate extract of <i>C. militaris</i> detected by GC-MS.....	142
Figure 55.	ESI-MS spectra of 2-oxopalmitic acid methyl ester in F5 fraction from ethyl acetate extract of <i>C. militaris</i>	142
Figure 56.	Mass-spectra of octadecanal (Rt = 22.11) in F5 fraction from ethyl acetate extract of <i>C. militaris</i> detected by GC-MS.....	144
Figure 57.	ESI-MS spectra of octadecanal in F5 fraction from ethyl acetate extract of <i>C. militaris</i>	144
Figure 58.	GC-MS chromatogram of F6 fraction from ethyl acetate extract of <i>C. militaris</i>	145
Figure 59.	Mass-spectra of 1,6-anhydro- β -D-glucopyranose (Rt = 11.82) in	

	F6 fraction from ethyl acetate extract of <i>C. militaris</i> detected by GC-MS.....	146
Figure 60.	ESI-MS spectra of 1,6-anhydro- β -D-glucopyranose in F6 fraction from ethyl acetate extract of <i>C. militaris</i>	146
Figure 61.	Mass-spectra of pentadecanal (Rt = 14.56) in F6 fraction from ethyl acetate extract of <i>C. militaris</i> detected by GC-MS.....	148
Figure 62.	ESI-MS spectra of pentadecanal in F6 fraction from ethyl acetate extract of <i>C. militaris</i>	148
Figure 63.	Mass-spectra of palmitic acid (Rt = 17.07) in F6 fraction from ethyl acetate extract of <i>C. militaris</i> detected by GC-MS.....	149
Figure 64.	ESI-MS spectra of palmitic acid in F6 fraction from ethyl acetate extract of <i>C. militaris</i>	150
Figure 65.	Mass-spectra of 1-heneicosanol (Rt = 26.33) in F6 fraction from ethyl acetate extract of <i>C. militaris</i> detected by GC-MS.....	151
Figure 66.	ESI-MS spectra of 1-heneicosanol in F6 fraction from ethyl acetate extract of <i>C. militaris</i>	151
Figure 67.	GC-MS chromatogram of F7 fraction from ethyl acetate extract of <i>C. militaris</i>	152
Figure 68.	Mass-spectra of 1,6-anhydro- β -D-glucopyranose (Rt = 11.76) in F7 fraction from ethyl acetate extract of <i>C. militaris</i> detected by GC-MS.....	153
Figure 69.	ESI-MS spectra of 1,6-anhydro- β -D-glucopyranose in F7 fraction from ethyl acetate extract of <i>C. militaris</i>	153
Figure 70.	Mass-spectra of pentadecanal (Rt = 14.52) in F7 fraction from ethyl acetate extract of <i>C. militaris</i> detected by GC-MS.....	155
Figure 71.	ESI-MS spectra of pentadecanal in F6 fraction from ethyl acetate extract of <i>C. militaris</i>	155
Figure 72.	Mass-spectra of palmitic acid (Rt = 17.03) in F7 fraction from ethyl acetate extract of <i>C. militaris</i> detected by GC-MS.....	156
Figure 73.	ESI-MS spectra of palmitic acid in F7 fraction from ethyl acetate extract of <i>C. militaris</i>	157

Figure 74.	Mass-spectra of 2-oxopalmitic acid methyl ester (Rt = 17.40) in F9 fraction from ethyl acetate extract of <i>C. militaris</i> detected by GC-MS.....	158
Figure 75.	ESI-MS spectra of 2-oxopalmitic acid methyl ester in F9 fraction from ethyl acetate extract of <i>C. militaris</i>	158
Figure 76.	Mass-spectra of Octanamide, N-(2-hydroxyethyl) (Rt = 18.77) in F7 fraction from ethyl acetate extract of <i>C. militaris</i> detected by GC-MS.....	159
Figure 77.	ESI-MS spectra of Octanamide, N-(2-hydroxyethyl) in F7 fraction from ethyl acetate extract of <i>C. militaris</i>	160
Figure 78.	GC-MS chromatogram of F8 fraction from ethyl acetate extract of <i>C. militaris</i>	160
Figure 79.	Mass-spectra of 1,6-anhydro- β -D-glucopyranose (Rt = 11.76) in F8 fraction from ethyl acetate extract of <i>C. militaris</i> detected by GC-MS.....	161
Figure 80.	ESI-MS spectra of 1,6-anhydro- β -D-glucopyranose in F8 fraction from ethyl acetate extract of <i>C. militaris</i>	162
Figure 81.	Mass-spectra of pentadecanal (Rt = 14.52) in F8 fraction from ethyl acetate extract of <i>C. militaris</i> detected by GC-MS.....	163
Figure 82.	ESI-MS spectra of pentadecanal in F8 fraction from ethyl acetate extract of <i>C. militaris</i>	164
Figure 83.	Mass-spectra of cordycepin (Rt = 21.98) in F8 fraction from ethyl acetate extract of <i>C. militaris</i> detected by GC-MS.....	165
Figure 84.	ESI-MS spectra of cordycepin in F8 fraction from ethyl acetate extract of <i>C. militaris</i>	166
Figure 85.	GC-MS chromatogram of F9 fraction from ethyl acetate extract of <i>C. militaris</i>	166
Figure 86.	Mass-spectra of pentadecanal (Rt = 14.55) in F9 fraction from ethyl acetate extract of <i>C. militaris</i> detected by GC-MS.....	168
Figure 87.	ESI-MS spectra of pentadecanal in F9 fraction from ethyl acetate extract of <i>C. militaris</i>	168

Figure 88.	Mass-spectra of 2-oxopalmitic acid methyl ester (Rt = 17.40) in F9 fraction from ethyl acetate extract of <i>C. militaris</i> detected by GC-MS.....	169
Figure 89.	ESI-MS spectra of 2-oxopalmitic acid methyl ester in F9 fraction from ethyl acetate extract of <i>C. militaris</i>	170
Figure 90.	Mass-spectra of cordycepin (Rt = 21.97) in F9 fraction from ethyl acetate extract of <i>C. militaris</i> detected by GC-MS.....	172
Figure 91.	ESI-MS spectra of cordycepin in F9 fraction from ethyl acetate extract of <i>C. militaris</i>	172
Figure 92.	GC-MS chromatogram of F10 fraction from ethyl acetate extract	173
Figure 93.	Mass-spectra of tetradecanal (Rt = 13.39) in F10 fraction from ethyl acetate extract of <i>C. militaris</i> detected by GC-MS.....	174
Figure 94.	ESI-MS spectra of tetradecanal in F10 fraction from ethyl acetate extract of <i>C. militaris</i>	174
Figure 95.	Mass-spectra of pentadecanal (Rt = 14.56) in F10 fraction from ethyl acetate extract of <i>C. militaris</i> detected by GC-MS.....	177
Figure 96.	ESI-MS spectra of pentadecanal in F10 fraction from ethyl acetate extract of <i>C. militaris</i>	178
Figure 97.	Mass-spectra of cordycepin (Rt = 21.95) in F10 fraction from ethyl acetate extract of <i>C. militaris</i> detected by GC-MS.....	179
Figure 98.	ESI-MS spectra of cordycepin in F10 fraction from ethyl acetate extract of <i>C. militaris</i>	180
Figure 99.	GC-MS chromatogram of F11 fraction from ethyl acetate extract	180
Figure 100.	Mass-spectra of malic acid (Rt = 6.18) in F11 fraction from ethyl acetate extract of <i>C. militaris</i> detected by GC-MS.....	181
Figure 101.	ESI-MS spectra of malic acid in F11 fraction from ethyl acetate extract of <i>C. militaris</i>	182
Figure 102.	Mass-spectra of palmitic acid (Rt = 17.03) in F11 fraction from ethyl acetate extract of <i>C. militaris</i> detected by GC-MS.....	183
Figure 103.	ESI-MS spectra of palmitic acid in F11 fraction from ethyl acetate extract of <i>C. militaris</i>	183

-
- Figure 104.** Mass-spectra of 2-palmitoylglycerol (Rt = 21.89) in F11 fraction from ethyl acetate extract of *C. militaris* detected by GC-MS.....184
- Figure 105.** ESI-MS spectra of 2-palmitoylglycerol in F11 fraction from ethyl acetate extract of *C. militaris*.....185
- Figure 106.** GC-MS chromatogram of F12 fraction from ethyl acetate extract of *C. militaris*.....185
- Figure 107.** Mass-spectra of palmitic acid (Rt = 17.03) in F12 fraction from ethyl acetate extract of *C. militaris* detected by GC-MS.....186
- Figure 108.** ESI-MS spectra of palmitic acid in F12 fraction from ethyl acetate extract of *C. militaris*.....187
- Figure 109.** Mass-spectra of 1, E-11, Z-13-octadecatriene (Rt = 17.68) in F12 fraction from ethyl acetate extract of *C. militaris* detected by GC-MS188
- Figure 110.** ESI-MS spectra of 1, E-11, Z-13-octadecatriene in F12 fraction from ethyl acetate extract of *C. militaris*.....189
- Figure 111.** Mass-spectra of 1-n-hexadecylindan (Rt = 21.74) in F12 fraction from ethyl acetate extract of *C. militaris* detected by GC-MS.....190
- Figure 112.** ESI-MS spectra of 1-n-hexadecylindan in F12 fraction from ethyl acetate extract of *C. militaris*.....190
- Figure 113.** GC-MS chromatogram of F13 fraction from ethyl acetate extract of *C. militaris*.....191
- Figure 114.** Mass-spectra of palmitic acid (Rt = 17.02) in F13 fraction from ethyl acetate extract of *C. militaris* detected by GC-MS.....192
- Figure 115.** ESI-MS spectra of palmitic acid in F13 fraction from ethyl acetate extract of *C. militaris*.....192
- Figure 116.** Mass-spectra of 1, E-11, Z-13-octadecatriene (Rt = 18.67) in F13 fraction from ethyl acetate extract of *C. militaris* detected by GC-MS193
- Figure 117.** ESI-MS spectra of 1, E-11, Z-13-octadecatriene in F13 fraction from ethyl acetate extract of *C. militaris*.....194
- Figure 118.** GC-MS chromatogram of F14 fraction from ethyl acetate extract

	of <i>C. militaris</i>	194
Figure 119.	Mass-spectra of carbamic acid (3-methylphenyl) methyl ester (Rt = 7.00) in F14 fraction from ethyl acetate extract of <i>C. militaris</i> detected by GC-MS	195
Figure 120.	ESI-MS spectra of carbamic acid (3-methylphenyl) methyl ester in F14 fraction from ethyl acetate extract of <i>C. militaris</i>	196
Figure 121.	Mass-spectra of palmitic acid (Rt = 17.03) in F14 fraction from ethyl acetate extract of <i>C. militaris</i> detected by GC-MS.....	197
Figure 122.	ESI-MS spectra of palmitic acid in F14 fraction from ethyl acetate extract of <i>C. militaris</i>	197
Figure 123.	Mass-spectra of 1, E-11, Z-13-octadecatriene (Rt = 18.67) in F14 fraction from ethyl acetate extract of <i>C. militaris</i> detected by GC-MS	198
Figure 124.	ESI-MS spectra of 1, E-11, Z-13-octadecatriene in F14 fraction from ethyl acetate extract of <i>C. militaris</i>	199
Figure 125.	GC-MS chromatogram of CM4 fraction from ethyl acetate extract of <i>C. militaris</i>	201
Figure 126.	Mass-spectra of cordycepin (Rt = 21.98) in CM4 fraction from ethyl acetate extract of <i>C. militaris</i> detected by GC-MS.....	202
Figure 127.	Total ion chromatogram and mass spectra of standard cordycepin by LC-ESI-MS	203
Figure 128.	HPLC standard curve of cordycepin	204
Figure 129.	HPLC chromatogram of cordycepin in CM4 fraction from ethyl acetate extract of <i>C. militaris</i>	204

List of tables

Table 1.	Xanthine oxidase inhibitory and antioxidant activities of different crude extracts from <i>C. militaris</i>	14
Table 2.	Xanthine oxidase inhibitory activity of 14 fractions isolated from EtOAc extract of <i>C. militaris</i>	15
Table 3.	Identification of principal compounds of 14 EtOAc fractions from <i>C. militaris</i>	17
Table 4.	Antibacterial activities of crude extracts of <i>C. militaris</i>	27
Table 5.	Antibacterial activity of 14 fractions from EtOAc extract of <i>C. militaris</i>	28
Table 6.	Chemical constituents of the most active fractions in antibacterial activity by GC-MS.....	29
Table 7.	Different extractions for comparing cordycepin content.....	38
Table 8.	Inhibition capacities of different crude extracts of <i>C. militaris</i> on germination, root and shoot of radish.....	39
Table 9.	Inhibition of different fractions from EtOAc extract of <i>C. militaris</i> on germination, root length and shoot height of radish.....	40
Table 10.	Identification of bioactive compounds in CM4 fraction from <i>C. militaris</i> by GC-MS analysis.....	41
Table 11.	Identification of the most active fraction by GC-MS and LC-ESI-MS.....	43
Table 12.	Effects of cordycepin, CM4 fraction, BA, paraquat and glyphosate on the germination and emergence of radish.....	52
Table 13.	Effects of CM4 fraction, BA, cordycepin and glyphosate on the germination and growth of barnyard grass.....	53
Table 14.	Description of types of enzyme inhibition of inhibitor.....	66
Table 15.	Structure of allopurinol and different purine-based compounds for xanthine oxidase inhibition.....	67
Table 16.	Fragmentation pattern of palmitic acid methyl ester (retention time = 16.72) in F1 fraction from ethyl acetate extract of <i>C. militaris</i>	

	detected by GC-MS	110
Table 17.	Fragmentation pattern of palmitic acid (retention time = 17.09) in F1 fraction from ethyl acetate extract of <i>C. militaris</i> detected by GC-MS.....	112
Table 18.	Fragmentation pattern of 9,12-Octadecadienoic acid (Z, Z) (retention time = 18.73) in F1 fraction from ethyl acetate extract of <i>C. militaris</i> detected by GC-MS	114
Table 19.	Fragmentation pattern of palmitic acid methyl ester (retention time = 16.72) in F2 fraction from ethyl acetate extract of <i>C. militaris</i> detected by GC-MS	116
Table 20.	Fragmentation pattern of palmitic acid (retention time = 17.11) in F2 fraction from ethyl acetate extract of <i>C. militaris</i> detected by GC-MS.....	118
Table 21.	Fragmentation pattern of 9,12-Octadecadienoic acid (Z, Z) (retention time = 18.76) in F2 from EtOAc extract of <i>C. militaris</i> detected by GC-MS	120
Table 22.	Fragmentation pattern of ergosta-4,6,8(14),22-tetraen-3-one (retention time = 29.12) in F2 fraction from ethyl acetate extract of <i>C. militaris</i> detected by GC-MS	122
Table 23.	Fragmentation pattern of pentadecanal (retention time = 14.56) in F3 fraction from ethyl acetate extract of <i>C. militaris</i> detected by GC-MS.....	125
Table 24.	Fragmentation pattern of 2-oxopalmitic acid methyl ester (retention time = 17.41) in F3 fraction from ethyl acetate extract of <i>C. militaris</i> detected by GC-MS	127
Table 25.	Fragmentation pattern of octadecanal (retention time = 22.11) in F3 fraction from ethyl acetate extract of <i>C. militaris</i> detected by GC-MS.....	128
Table 26.	Fragmentation pattern of dodecanamide (retention time = 25.55) in F3 fraction from ethyl acetate extract of <i>C. militaris</i> detected by GC-MS.....	130

Table 27.	Fragmentation pattern of pentadecanal (retention time = 14.56) in F4 fraction from ethyl acetate extract of <i>C. militaris</i> detected by GC-MS.....	132
Table 28.	Fragmentation pattern of 2-oxopalmitic acid methyl ester (retention time = 17.40) in F4 fraction from ethyl acetate extract of <i>C. militaris</i> detected by GC-MS.....	134
Table 29.	Fragmentation pattern of octadecanal (retention time = 22.11) in F4 fraction from ethyl acetate extract of <i>C. militaris</i> detected by GC-MS.....	135
Table 30.	Fragmentation pattern of pentadecanal (retention time = 14.56) in F5 fraction from ethyl acetate extract of <i>C. militaris</i> detected by GC-MS.....	137
Table 31.	Fragmentation pattern of hexadecanal (retention time = 15.65) in F5 fraction from ethyl acetate extract of <i>C. militaris</i> detected by GC-MS.....	139
Table 32.	Fragmentation pattern of 2-oxopalmitic acid methyl ester (retention time = 17.41) in F4 fraction from ethyl acetate extract of <i>C. militaris</i> detected by GC-MS.....	141
Table 33.	Fragmentation pattern of octadecanal (retention time = 22.11) in F5 fraction from ethyl acetate extract of <i>C. militaris</i> detected by GC-MS.....	143
Table 34.	Fragmentation pattern of 1,6-anhydro- β -D-glucopyranose (retention time = 11.82) in F6 fraction from ethyl acetate extract of <i>C. militaris</i> detected by GC-MS.....	145
Table 35.	Fragmentation pattern of pentadecanal (retention time = 14.56) in F6 fraction from ethyl acetate extract of <i>C. militaris</i> detected by GC-MS.....	147
Table 36.	Fragmentation pattern of palmitic acid (retention time = 17.07) in F6 fraction from ethyl acetate extract of <i>C. militaris</i> detected by GC-MS.....	149
Table 37.	Fragmentation pattern of 1-heneicosanol (retention time = 26.33)	

	in F6 fraction from ethyl acetate extract of <i>C. militaris</i> detected by GC-MS.....	150
Table 38.	Fragmentation pattern of 1,6-anhydro- β -D-glucopyranose (retention time = 11.76) in F7 fraction from ethyl acetate extract of <i>C. militaris</i> detected by GC-MS	152
Table 39.	Fragmentation pattern of pentadecanal (retention time = 14.52) in F7 fraction from ethyl acetate extract of <i>C. militaris</i> detected by GC-MS.....	154
Table 40.	Fragmentation pattern of palmitic acid (retention time = 17.03) in F7 fraction from ethyl acetate extract of <i>C. militaris</i> detected by GC-MS.....	156
Table 41.	Fragmentation pattern of 2-oxopalmitic acid methyl ester (retention time = 17.40) in F9 fraction from ethyl acetate extract of <i>C. militaris</i> detected by GC-MS	157
Table 42.	Fragmentation pattern of Octanamide, N-(2-hydroxyethyl) (retention time = 18.77) in F7 fraction from ethyl acetate extract of <i>C. militaris</i> detected by GC-MS	159
Table 43.	Fragmentation pattern of 1,6-anhydro- β -D-glucopyranose (retention time = 11.76) in F8 fraction from ethyl acetate extract of <i>C. militaris</i> detected by GC-MS	161
Table 44.	Fragmentation pattern of pentadecanal (retention time = 14.52) in F8 fraction from ethyl acetate extract of <i>C. militaris</i> detected by GC-MS.....	162
Table 45.	Fragmentation pattern of cordycepin (retention time = 21.98) in F8 fraction from ethyl acetate extract of <i>C. militaris</i> detected by GC-MS	164
Table 46.	Fragmentation pattern of pentadecanal (retention time = 14.55) in F9 fraction from ethyl acetate extract of <i>C. militaris</i> detected by GC-MS.....	166
Table 47.	Fragmentation pattern of 2-oxopalmitic acid methyl ester (retention time = 17.40) in F9 fraction from ethyl acetate extract of	

	<i>C. militaris</i> detected by GC-MS.....	169
Table 48.	Fragmentation pattern of cordycepin (retention time = 21.97) in F9 fraction from ethyl acetate extract of <i>C. militaris</i> detected by GC-MS	170
Table 49.	Fragmentation pattern of tetradecanal (retention time = 13.39) in F10 fraction from ethyl acetate extract of <i>C. militaris</i> detected by GC-MS.....	173
Table 50.	Fragmentation pattern of pentadecanal (retention time = 14.56) in F10 fraction from ethyl acetate extract of <i>C. militaris</i> detected by GC-MS.....	175
Table 51.	Fragmentation pattern of cordycepin (retention time = 21.95) in F10 fraction from ethyl acetate extract of <i>C. militaris</i> detected by GC-MS.....	178
Table 52.	Fragmentation pattern of malic acid (retention time = 6.18) in F11 fraction from ethyl acetate extract of <i>C. militaris</i> detected by GC-MS	181
Table 53.	Fragmentation pattern of palmitic acid (retention time = 17.03) in F11 fraction from ethyl acetate extract of <i>C. militaris</i> detected by GC-MS.....	182
Table 54.	Fragmentation pattern of 2-palmitoylglycerol (retention time = 21.89) in F11 fraction from ethyl acetate extract of <i>C. militaris</i> detected by GC-MS	184
Table 55.	Fragmentation pattern of palmitic acid (retention time = 17.03) in F12 fraction from ethyl acetate extract of <i>C. militaris</i> detected by GC-MS.....	186
Table 56.	Fragmentation pattern of 1, E-11, Z-13-octadecatriene (retention time = 17.68) in F12 fraction from ethyl acetate extract of <i>C. militaris</i> detected by GC-MS.....	187
Table 57.	Fragmentation pattern of 1-n-hexadecylindan (retention time = 21.74) in F12 fraction from ethyl acetate extract of <i>C. militaris</i> detected by GC-MS	189

Table 58.	Fragmentation pattern of palmitic acid (retention time = 17.02) in F13 fraction from ethyl acetate extract of <i>C. militaris</i> detected by GC-MS.....	191
Table 59.	Fragmentation pattern of 1, E-11, Z-13-octadecatriene (retention time = 18.67) in F13 fraction from ethyl acetate extract of <i>C. militaris</i> detected by GC-MS.....	193
Table 60.	Fragmentation pattern of carbamic acid (3-methylphenyl) methyl ester (retention time = 7.00) in F14 fraction from ethyl acetate extract of <i>C. militaris</i> detected by GC-MS.....	195
Table 61.	Fragmentation pattern of palmitic acid (retention time = 17.03) in F14 fraction from ethyl acetate extract of <i>C. militaris</i> detected by GC-MS.....	196
Table 62.	Fragmentation pattern of 1, E-11, Z-13-octadecatriene (retention time = 18.67) in F14 fraction from ethyl acetate extract of <i>C. militaris</i> detected by GC-MS.....	198
Table 63.	Fragmentation pattern of cordycepin (retention time = 21.98) in CM4 fraction from ethyl acetate extract of <i>C. militaris</i> detected by GC-MS.....	201

List of appendixes

Appendix A. Identification of the most active fraction of <i>C. militaris</i> on xanthine oxidase inhibitory, antioxidant, and antibacterial activities	109
Appendix B. Identification of the most active fraction and cordycepin of <i>C. militaris</i> on allelopathic activity	200

Abstract

Cordyceps militaris (L.) is an edible fungus with fruiting body containing an excellent source of secondary metabolites. Recently, this fungus has entered a large-scale artificial cultivation in Southeast Asia countries, especially in Vietnam. *C. militaris* is more widely used because it contains a wide range of various bioactive compounds as well as possesses a broad spectrum of medicinal and pharmaceutical properties. However, the xanthine oxidase inhibitory and herbicidal activities of this fungus have not comprehensively examined. Besides, methanolic (MeOH) extract of *C. militaris* has been reported to have potential antibacterial activity but bioactive components responsible for this property have not been elaborated. Moreover, utilization of phytochemicals from fungi for nature-based alternatives for disputed commercial herbicides in agricultural production has received increasing attention. Therefore, isolation and identification of the bioactive constituents from fungal secondary metabolites warrant further efforts.

This study evaluates biological properties and identifies the chemical compounds of fruiting body of *C. militaris* produced in Vietnam. Different fractions of ethyl acetate (EtOAc) extract from column chromatography were examined for anti-hyperuricemic, antioxidant, antibacterial, and allelopathic activities. Besides, bioactive compounds from fractions were also identified and quantified by several modern analytical techniques such as thin layer chromatography (TLC), gas chromatography - mass spectrometry (GC-MS), high performance liquid chromatography (HPLC), liquid chromatography-electrospray ionization - mass spectrometry (LC-ESI-MS). The thesis is divided into 6 chapters.

Chapter 1 gives a general review of the thesis. Background of dissertation, research objectives, scientific contributions, and structure of dissertation are also illustrated in this chapter.

Chapter 2 examines *in vitro* anti-hyperuricemic and antioxidant activities of fractions from EtOAc extract of *C. militaris* fruiting body. Fourteen fractions

obtained from *C. militaris* were assessed for anti-gout and antioxidant properties. Among the test fractions, the F8 and F10 fractions possessed the most potential anti-hyperuricemia ($IC_{50} = 62.82 \mu\text{g/mL}$, $IC_{50} = 68.04 \mu\text{g/mL}$, respectively), while in both DPPH and ABTS assays, fraction F7 ($IC_{50} = 0.40$ and 0.70 mg/mL), F8 ($IC_{50} = 0.62$ and 1.03 mg/mL), and F9 ($IC_{50} = 0.68$ and 0.85 mg/mL) showed greater antioxidant capacities than other fractions. From GC-MS analysis, cordycepin (a purine nucleoside) appeared as the major component in F8, F9, and F10 fractions. Therefore, the results of fraction F8, F9, F10 and standard cordycepin demonstrated that cordycepin possesses strong xanthine oxidase inhibition capacity. Thus, this is the first study highlighted that cordycepin isolated from *C. militaris* played a crucial role in xanthine oxidase inhibition *in vitro* assay. Additionally, the presence of cordycepin and fatty acids found in F7, F8, F9 and F10 fractions suggested that these compounds are responsible for significant antioxidant property as previous reports.

Chapter 3 aims to evaluate antibacterial activity and determine the bioactive constituents from methanolic extract of *C. militaris* that are responsible for this activity. The methanolic extract of *C. militaris* was fractioned and assayed on antimicrobial property. Among the isolated fractions, F9, F11 and F12 showed the most effective inhibition against the growth of four bacterial strains including *Staphylococcus aureus*, *Escherichia coli*, *Bacillus subtilis* and *Proteus mirabilis*. In particular, fraction F9 and F11 share the same highest inhibition zone diameter (10.17 mm) on *P. mirabilis* and *E. coli*. From GC-MS analysis, fatty acids and fatty acid esters were detected in F9, F11 and F12 fractions. The fatty acids and their derivatives with a chain length of more than 10 carbon atoms may cause membrane-destabilizing and interfere important processes involved in cellular protection and functions of bacteria. Therefore, the presence of palmitic acid (F11, F12), 2-palmitoylglycerol (F11) and 2-oxopalmitic acid methyl ester (F9) suggested that they are responsible for potential antibacterial activity as previous studies. Additionally, cordycepin also appeared as the dominant component (58.04%) in fraction F9 and strongly inhibited the growth of *E. coli* and *B. subtilis*. However, it is necessary to check these bioactive compounds on

multidrug-resistant bacteria in hospital and community to increase potential value of this medicinal fungus.

Chapter 4 investigates the allelopathic activity of *C. militaris* on the germination and growth of radish (*Raphanus sativus*) and identifies allelochemical compounds from this fungus. Besides, the uses of different extraction methods to get high yield of cordycepin have been applied. Eight fractions separated from *C. militaris* were examined for the germination and growth bioassays of radish. As a result, fraction CM4 showed the strongest inhibition on germination, root elongation and shoot height ($IC_{50} = 0.078, 0.053$ and 0.052 mg/mL, respectively). Detection and identification from GC-MS, HPLC and LC-ESI-MS revealed that the dominant chemical component in fraction CM4 was cordycepin (a purine nucleoside). Besides, MeOH extraction gave the maximum yield of cordycepin (6.166 mg/g DW) as compared to the use of the 100 °C temperature for 30 min and the 70 °C temperature combined with ultrasonic for 30 min (3.548 and 4.248 mg/g DW, respectively). This is the first study to reveal that cordycepin isolated from *C. militaris* functions as an allelochemical, effectively inhibits germination and emergence of radish and may be a promising natural source to develop plant-based herbicides.

Chapter 5 explains the herbicidal potential of *C. militaris* on *Raphanus sativus* and *Echinochloa crus-galli* (barnyard grass) and compares with benzoic acid to search for nature-based alternatives for disputed commercial herbicides, paraquat and glyphosate. As compared to benzoic acid in herbicidal property, cordycepin and fraction CM4 both gave strong inhibition on the germination of radish from 4.6- to 5.9-fold. Similarly, they also showed much greater suppression on the root length (3.5- to 4.5-fold) and the shoot height (3.5- to 3.8-fold) than benzoic acid. Besides, cordycepin evidenced the stronger inhibition than paraquat by 3.3- to 3.2-fold on the germination and > 4.8-fold on shoot of radish, and glyphosate by 3.3- to 3.7-fold on the germination and emergence of radish. In case of barnyard grass, fraction CM4 and cordycepin presented effective inhibition on the germination (5.7- to 8.3-fold), root length (4.9- to 5.9-fold), shoot height (7.3- to 8.6-fold) as compared to benzoic acid. Additionally, cordycepin was stronger

than paraquat (1.8-fold) and glyphosate (>3.5-fold) on the germination of barnyard grass as compared to previous research. Therefore, cordycepin is more phytotoxic and has a greater inhibition on indicator plants. With respect to the mode of action, cordycepin acts as an herbicidal component reduced photosynthetic capacity, increased electrolyte leakage, lipid peroxidation, promoted total phenolic, total flavonoid and proline contents compared to benzoic acid. Therefore, cordycepin, a purine nucleoside is a potent plant growth inhibitor should encourage the development of plant-based herbicides for environmentally friendly agricultural production. However, further studies are needed to evaluate the mechanism of cordycepin as well as its synthesized derivatives compared with paraquat and glyphosate against the physiological and biochemical responses of principal weeds. Especially, investigations on cordycepin are also required to exclude any human health risks and to carefully evaluate the benefit to risk ratio of cordycepin use. This would help clarify under what conditions cordycepin could safely and effectively be used as a natural herbicide.

Finally, Chapter 6 discusses about basic mechanisms of biological assays and gives the key findings of the dissertation. This study is successful to investigate biological activities of *C. militaris* and to identify bioactive compounds by GC-MS, HPLC and LC-ESI-MS analyses. It was found that this fungus possesses anti-hyperuricemic, antioxidant, antibacterial and allelopathic activities. Among detected and identified components, cordycepin, a purine nucleoside analog was responsible for anti-gout and herbicidal properties. Additionally, cordycepin, fatty acid and their derivatives also contributed to treat oxidative stress and bacterial infection diseases. In case of xanthine oxidase inhibition, cordycepin has a purine ring and active sites like allopurinol, therefore, it may inhibit the enzyme xanthine oxidase by substrate competition mechanism as allopurinol. With the antibacterial activity, fatty acids and their derivatives disrupt the membrane enzyme activity, the electron transport chain, uncoupling oxidative phosphorylation and increase membrane permeability and leakage leading to inhibition of cell growth and eventually cell death. Finally, depending upon the specific mode of action, herbicides or allelochemicals may

inhibit plant enzyme or biological system leading to injuring or disrupting plant growth and consequently plant death. Basically, glyphosate inhibit the enzyme 5-enolpyruvylshikimate-3-phosphate synthase (EPSPS) that is essential for the biosynthesis of aromatic amino acids (phenylalanine, tryptophan, and tyrosine) on the shikimate pathway in plant. In the different way, paraquat interferes photosynthesis process and produces reactive oxygen species (ROS) which cause lipid peroxidation and membrane breakdown of plants. In case of cordycepin, it inhibits photosynthetic pigments, promotes electrolyte leakage, lipid peroxidation, and stimulates total phenolic, total flavonoid and proline accumulations. Findings of this study suggested that *C. militaris* is a promising natural source to develop foods and beverages to treat anti-gout, oxidative stress, bacterial infections and plant-based herbicides on agricultural production.

Acknowledgments

I would like to express my deepest gratitude to my academic supervisor, Associate Professor Tran Dang Xuan, for his valuable and practical guidance and constant encouragement for me to do research, revise scientific papers and complete this thesis. I am most grateful for his advices and help, not only for my study but also for my student life in Japan.

I am extremely thankful to my thesis committee members, Professors Tsudzuki Masaoki and Maeda Teruo, Associate Professors Hosaka Tetsuro and Morimoto Masanori for their efforts in making worthwhile suggestions for the revision of the dissertation. My sincere appreciation goes to Professor Rolf Teschke for his help in writing as well as revising scientific papers. I am also grateful to Mrs. Amimoto Tomoko (Natural Science Center for Basic Research and Development) for training and generous support in analyzing GC-MS and LC-ESI-MS.

I am deeply indebted to the Vietnamese Government and Hiroshima University for financial support (Hiroshima-VIED joint scholarship) during three-year study at Hiroshima University. Similarly, I wish to thanks to Truc Anh company (Bac Lieu city, Vietnam) kindly provides samples for my research. I would also like to take this opportunity to thank all staff of IDEC office for their assistances.

My sincere thank to all members of the Xuan lab (Laboratory of Plant Physiology and Biochemistry) for their support and collaboration in conducting experiments and revising paper manuscripts during the time I have studied at Hiroshima University.

Finally, I would like to express my earnest gratitude to my mother, my sisters and brothers, my lovely wife, relatives and dear friends who continuously support precious counsels and mentally encouragements in every circumstance as well as positive motivations for me to fulfill this dissertation.

TRAN NGOC QUY

January, 2020

1 Introduction

1.1 Background

Edible fungi have long been an important part of human civilization and used as functional foods and medicines in the world since at least 5000 BC (Panda and Swain, 2011). They are the second largest group after insects with 1.5 million fungi existing in nature (Chiu *et al.*, 2016). Among them, *Cordyceps* has historically been used for the maintenance of health, prevention and treatment various diseases worldwide (Kim *et al.*, 2010).

Cordyceps, a kind of caterpillar-shape entomopathogenic fungus is classified in phylum Ascomycota, class Ascomycetes, order Hypocreales, family Clavicipitaceae and parasitic mainly on body of insects or other arthropods (Pathania *et al.*, 2015). It is the largest and most diverse genus with over 750 identified species (Kim *et al.*, 2010; Olatunji *et al.*, 2018).

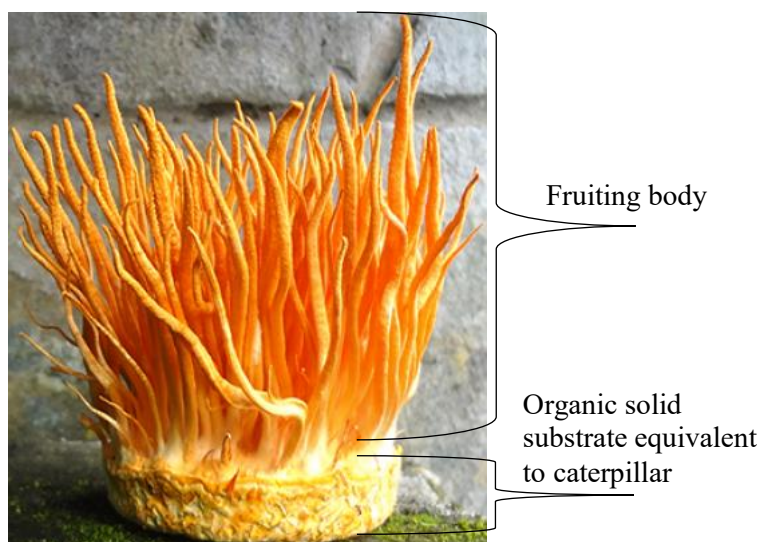
The name *Cordyceps* was obtained from Latin words, “cord” meaning “club”, and “ceps” meaning “head”. The Latin conjugation accurately describes the shape of “club fungi” with fruiting body and stroma formation from the mummified carcasses of insect larvae (Caihong *et al.*, 2015; Pathania *et al.*, 2015).

In nature, *Cordyceps* species exist dormant in the soil until they get in contact with a host (Olatunji *et al.*, 2018). They typically inhabit inside or over the surface of the host body in the winters, leading to emerging of stroma (fruiting body) in the summers (Shrestha and Sung, 2005; Adnan *et al.*, 2017). All *Cordyceps* species have similar life cycle and mechanisms to infect different stages of their host insects from larva to adult. *Cordyceps* create highly specific and sophisticated mechanisms to avoid the host immune system and harmonize their life cycle parameter for the purpose of survival and multiplication (Hajek and Leger, 1994). The mechanisms for existence have resulted in the production many secondary metabolites in response to the host defense which are promising natural sources for new medicine discovery (Olatunji *et al.*, 2018).

Most of *Cordyceps* species thrives at humid temperate and tropical forest, with a vast distribution in North America, Europe, Southeast Asia, especially

China, Korea, Japan, Nepal and Vietnam (Holliday and Cleaver, 2008; Panda and Swain, 2011; Olatunji *et al.*, 2018). Two out of these species namely *Cordyceps sinensis* and *Cordyceps militaris* are the most prominent used and widely explored species of this genus (Hui *et al.*, 2006; Xiong *et al.*, 2010).

In natural environment, both fungus species are parasitic of certain species of moth larvae and have similar compound profile. Although both *C. sinensis* and *C. militaris* have some similarities, they differ in their color and appearance. *C. sinensis* grows singly from the larval head with dark brown or black stroma (fruiting body), cylindrical stipe and slightly swollen head (sterile apex), while *C. militaris* arises from the buried larvae and pupae of insects with orange fruiting body, club or clavate shaped. Stipe is 1~1.5 mm wide with head being slightly broader than stipe (Shrestha and Sung, 2005; Xiong *et al.*, 2010).



(Source: <http://dongtrunghathaotrucanh.com.vn>)

Figure 1. The figure of *C. militaris* cultivating in artificial solid medium.

In recent years, both fungi materials can be obtained from two main sources, natural collection and artificial culture (Figure 1). Comparing to the harsh growth conditions of *C. sinensis*, *C. militaris* has short production cycle, low cost requirements and much easier to cultivate in solid state culture (SSC) and liquid state culture (SLC) with a variety of carbon and nitrogen sources (Shrestha *et al.*, 2012; Lu *et al.*, 2018). Therefore, *C. militaris* has entered a large-scale artificial

cultivation and much more widely distributed in the world.

Fruiting body of *C. militaris* is well-known for its medicinal properties with several important bioactive components such as cordycepin, polysaccharides, fatty acids, amino acids, mannitol, trace elements, fiber, ash and other chemical compositions (Hur, 2008; Liu *et al.*, 2016; Zhou *et al.*, 2016; Zhu *et al.*, 2016; Chiang *et al.*, 2017; Cho and Kang, 2018; Jin *et al.*, 2018).

In a comparative study of metabolites, *C. militaris* (292 metabolites) has more kind of metabolites than *C. sinensis* (118 metabolites) (Wen *et al.*, 2019). In addition, the extract of *C. militaris* were reported to possess higher antioxidant efficiency, higher cordycepin, polyphenolic and flavonoid contents than *C. sinensis* (Li *et al.*, 2001; Hui *et al.*, 2006; Lei *et al.*, 2009).

C. militaris exhibited several health benefits including antifatigue and anti-stress (Koh *et al.*, 2003); anti-angiogenetic (Yoo *et al.*, 2004); anti-inflammatory activity (Yu *et al.*, 2004; Jeong *et al.*, 2010; Smiderle *et al.*, 2014); antiviral (Hta *et al.*, 2007); antifungal and anticancer (Bizarro *et al.*, 2015; Park *et al.*, 2017; Cho and Kang, 2018); HIV-1 protease inhibiting (Jiang *et al.*, 2011); antioxidant activity (Reis *et al.*, 2013; Chen *et al.*, 2013; Zhu *et al.*, 2016; Liu *et al.*, 2016); anti-microbial (Reis *et al.*, 2013; Dong *et al.*, 2014; Tuli *et al.*, 2014; Zhou *et al.*, 2016); inhibition high-fat diet metabolic disorders (Kim *et al.*, 2014); and immunomodulatory activity (Tuli *et al.*, 2013; Liu *et al.*, 2016).

Furthermore, several studies have demonstrated that the fermented broth of *C. militaris* has a number of medicinal functions such as the prevention of alcohol-induced hepatotoxicity (Cha *et al.*, 2013), hyperglycemia in alloxan-induced diabetic (Ma *et al.*, 2015), traumatic brain injury-induced brain impairments of blood-brain barrier integrity (Yuan *et al.*, 2016), anti-tumor and anti-metastatic (Wada *et al.*, 2017; Jin *et al.*, 2018), induce apoptotic cell death for human brain cancer cells and inhibitory the proliferation (Chaicharoenaudomrung *et al.*, 2018), and the inhibition of LPS-induced acute lung injury (Lei *et al.*, 2018).

However, other biological activities, for example, xanthine oxidase inhibitory and herbicidal activities of *C. militaris* have not been comprehensively examined. Additionally, methanolic extract of this fungus was found to possess

potential antibacterial activity but bioactive components responsible for this property have not been elaborated (Reis *et al.*, 2013; Dong *et al.*, 2014). Therefore, this study was conducted to exploit new biological activities and identify bioactive compounds as well as increase value addition of this fungus.

1.2 Research objectives

The main objectives of this study were to evaluate biological activities and identify the chemical constituents of fruiting body of *C. militaris* produced in Vietnam. The achievements from the main objectives is based on the following specific objectives:

1. To examine anti-hyperuricemic and antioxidant activities of *C. militaris*.
2. To identify active compounds responsible for xanthine oxidase inhibitory and antioxidant properties.
3. To evaluate antibacterial property and analyze of bioactive constituents from methanolic extract of *C. militaris* that responsible for this activity.
4. To investigate the allelopathic activity of *C. militaris* on the germination, root length and shoot height of radish (*Raphanus sativus*).
5. To identify the active herbicidal compounds from *C. militaris*.
6. To explain the phytotoxic potential of cordycepin from *C. militaris* on radish and barnyard grass (*Echinochloa crus-galli*) compared with benzoic acid to search for nature-based alternative to disputed herbicides, paraquat and glyphosate.

1.3 Scientific contributions of the present study

In regard to the scientific consideration and responsibility, there are two scientific papers and one oral presentation (two journal papers and one oral presentation) become the backbone of the dissertation as follows:

1. Quy, T.N. and Xuan, T.D., 2019. Xanthine Oxidase Inhibitory Potential, Antioxidant and Antibacterial Activities of *Cordyceps militaris* (L.) Link Fruiting Body. Medicines, 6, 20 (Chapter 2 and Chapter 3).
2. Quy, T.N., Xuan, T.D., Andriana, Y., Teschke, R., Khanh, T.D. and Tran,

- H.D., 2019. Cordycepin Isolated from *Cordyceps militaris*: Its Newly Discovered Herbicidal Property and Potential Plant-Based Novel Alternative to Glyphosate. *Molecules*, 24, 2901 (Chapter 4 and Chapter 5).
3. Quy, T.N., Andriana, Y., Xuan, T.D. 2019. Allelopathic activity and identification of allelochemicals from fruiting body of *Cordyceps militaris* (L.) Link, has been presented in 54th Japan Society for Bioscience, Biotechnology, and Agrochemistry (JBBA) Meeting, June 1st, 2019, Okayama, Japan (Section of Chapter 4).

1.4 Dissertation structure

This dissertation outline can be divided into six chapters:

- Chapter 1 - gives an overview including thesis background, problem statements, research objectives of the present research work.
- Chapter 2 - examines xanthine oxidase inhibitory and antioxidant activities, and identifies bioactive compounds responsible for the above activities.
- Chapter 3 - aims to evaluate antibacterial property and analyze active constituents from methanolic extract of *C. militaris* that responsible for this activity.
- Chapter 4 - investigates the allelopathic activity of *C. militaris* on the germination and emergence of radish and identifies the active herbicidal compounds from this fungal.
- Chapter 5 - explains the herbicidal potential of cordycepin from *C. militaris* on radish and barnyard grass compared with benzoic acid to search for nature-based alternative to disputed commercial herbicides, paraquat and glyphosate.
- Chapter 6 - discusses about basic mechanisms of biological assays and gives key findings of the thesis.

2 Xanthine oxidase (XO) inhibitory and antioxidant activities of *Cordyceps militaris* (L.) Link fruiting body

2.1 Introduction

Nowadays, hyperuricemia phenomenon, a predisposing factor of gouty arthritis, has been recognized as a lifestyle disease that affects the adult population in the developing as well as developed countries (Kapoor and Saxena, 2016). Gout is common in the elderly and management of this disease is frequently complicated by the presence of co-morbid conditions and medications prescribed for other conditions. When people's living standard is improved, the incidence of gout rate will continue to increase, especially emerge at younger age (Liu *et al.*, 2017).

Gout disease is a purine metabolic disorder, induced by overproduction or under-excretion of uric acid in blood. It caused by a high dietary intake of foods containing high amounts of nucleic acids, such as some types of seafood, meats (especially organ meats) and yeasts (Nguyen *et al.*, 2004). It happens as a result of increased uric acid production, impaired renal uric acid excretion, or a combination of them resulting in deposition of uric acid in the form of monosodium urate crystals in joints, kidneys, causing reoccurring inflammation or gouty arthritis and nephrolithiasis. The precipitation of needle shaped monosodium urate crystals in the synovial fluid of the major joints induced an extremely painful acute arthritis with repeated attacks of gout (Saag and Choi, 2006; Umamaheswari *et al.*, 2007; Yong *et al.*, 2016).

Xanthine oxidase (XO) has reported as a key enzyme that catalyzes the oxidation of hypoxanthine to xanthine and then xanthine form into uric acid. This enzyme is responsible for producing gout and causing oxidative damage to living tissues (Dong *et al.*, 2016). Its structure is a homodimer commonly distributed in mammalian tissues with a molecular mass of 290 KDa. Each subunit of XO contains one molybdenum molybdopterin (Mo-pt), the oxidation process occurs with one flavinadenine dinucleotide (FAD) and two distinct (2Fe-2S) center (Santi

et al., 2018). XO is highly localized in the liver and gastrointestinal tract (GI) and situated at the final reactions in the metabolism of purine bases (Abdullahi *et al.*, 2012). It also generates reactive oxygen species (ROS) as well as superoxide anion radicals (O_2^-) during oxidation of substrates, subsequently involves in various pathological states such as inflammatory, hepatitis, interstitial nephritis, eosinophilia, ischemia-reperfusion, tissue and vascular injuries, chronic heart failure, atherosclerosis, carcinogenesis and aging (Umamaheswari *et al.*, 2007; Nguyen and Nguyen, 2012), hypertension, hyperlipidaemia, obesity, diabetes and cancer (Azmi *et al.*, 2012; Kapoor and Saxena, 2016).

The therapeutic strategy for treatment of chronic gout and hyperuricemia in clinical is to decrease the uric acid to pre-established level by uricosuric drug and xanthine oxidase inhibitors (Liu *et al.*, 2017).

Uricosurics (sulfapyrazone, benzbromarone, probenecid) are drugs interact directly with renal transporters (renal urate transporter 1; URAT1) to elevate excretions of uric acid for anti-gout, but they are sometimes limited by the associated adverse effects such as allergic, hypersensitivity reaction and enhancement of 6-mercaptopurine toxicity (Yong *et al.*, 2018).

While uricosuric drugs enhance the urinary excretion of uric acid, XO inhibitors block the terminal step of uric acid biosynthesis from purine in the body and this reaction is believed that either by increasing the excretion of uric acid or reducing the uric acid formation helps to decrease the risk of gout and hyperuricemia (Azmi *et al.*, 2012; Kapoor and Saxena, 2014). Thus, effective XO inhibitors against XO enzyme might be beneficial not only to treat gout but also to combat various other diseases (Ngoc *et al.*, 2012; Ouyang *et al.*, 2017).

Until now, only allopurinol (1,5-dihydropyrazolo[3,4-d]pyrimidin-4-one, an analogue of hypoxanthine) is the most common clinically used as XO inhibitor prescribed for the treatment of hyperuricemia and gout (Figure 9). However, there are varied degrees of undesirable effects such as hypersensitivity syndrome, hepatitis, nephropathy, vasculitis, allergic, Stevens-Johnson syndrome, renal toxicity and even fatal liver necrosis (Nguyen *et al.*, 2004; Dong *et al.*, 2016; Liu *et al.*, 2017; Santi *et al.*, 2018).

Moreover, febuxostat (2-[3-cyano-4-(2-methylpropoxy)phenyl]-4-methyl-1,3-thiazole-5-carboxylic acid) was also the first synthetic nonpurine based XO inhibitor approved by the Food and Drug Administration (FDA or USFDA) in 2009 for people suffering from allopurinol syndrome. It acts for an alternative therapy for patients with contraindications or intolerance to allopurinol. However, febuxostat has also been associated with side effect, taking as cardiovascular complications, liver function abnormalities, diarrhea and skin rash (Dong *et al.*, 2016; Liu *et al.*, 2017; Duong *et al.*, 2017).

At the present, the undesirable adverse effects of anti-gout drugs are becoming more and more prominent (Ragab *et al.*, 2017). So, it is necessary to require more efforts in finding novel XO inhibitors with greater effectiveness, minimal undesirable side-effects as well as a better safety profile (Duong *et al.*, 2017). A number of research groups have conducted screening for XO inhibitors from medicinal fungi and this approach was shown to be effective (Duong *et al.*, 2017). *In vitro* screening studies for pharmacological property may lead to identify new medicines or dietary recommendations for treatment and prevention of various ailments (Havlik *et al.*, 2010). Thus, several herbal plants have been discovered and used for the prevention and treatment of gout and related oxidative stress, but the isolation and characterization of the bioactive compounds have not been completed yet (Lin *et al.*, 2013).

Recently, Yong *et al.* (2016) reported that hot water of *C. militaris* may decrease the serum uric acid levels of the hyperuricemic mice, but active components for this activity was unclear. Hence, the present study was conducted to evaluate *in vitro* xanthine oxidase inhibitory and antioxidant potential of fractions from *C. militaris* fruiting body. The identification of bioactive compounds from this medicinal fungus was also conducted.

2.2 Materials and methods

2.2.1 Chemicals

Methanol, ethanol, ethyl acetate, hexane and chloroform were supplied from Junsei Chemical Co., Ltd., Tokyo, Japan. Reagents including 2,2'-azinobis

(3-ethylbenzothiazoline-6-sulfonic acid) (ABTS), 1,1-diphenyl-2-picrylhydrazyl (DPPH), acetic acid, sodium acetate, dibutyl hydroxytoluene (BHT) and potassium peroxydisulfate were purchased by Kanto Chemical Co. InC., Tokyo, Japan. Cordycepin standard, allopurinol, hydrochloric acid, xanthine oxidase, xanthine, potassium phosphate monobasic and dibasic were obtained from Sigma-Aldrich Corp., St. Louis, MO USA.

2.2.2 Plant materials



(Source: <http://dongtrunghathaotrucanh.com.vn>)

Figure 2. The fruiting-bodies of *C. militaris* (L.) from Truc Anh company.

The fruiting bodies of *C. militaris* were prepared by Truc Anh Company, Bac Lieu city, Vietnam. *C. militaris* fruiting bodies were dried and sterilized by freeze-drying machine (Mactech MSL1000, 15 °C) and packaged (Figure 2). The samples were deposited to the Laboratory of Plant Physiology and Biochemistry, Graduate School for International Development and Cooperation (IDEC), Hiroshima University, Higashi-Hiroshima, Japan for further analysis.

2.2.3 Preparation of fungus extract

The sample was immersed in water for 12 h at ambient temperature and dried in a convection oven (MOV - 212F, Sanyo, Japan) at 50 °C for 2 d before pulverized into powder. The powder (1.0 kg) of *C. militaris* was soaked in 15 L methanol (MeOH) for two weeks at ambient temperature. After that, the filtrate from powder-methanol dispersion was evaporated under vacuum at 45°C by using

a rotary evaporator (SB-350-EYELA, Tokyo Rikakikai Co., Ltd., Tokyo, Japan) to produce 126.14 g of methanol extract. The methanol extract was suspended in distilled water (500 mL) and successively fractionated with hexane, chloroform and ethyl acetate to produce 10.24, 19.25, 50.21, and 20.17 g crude extracts, respectively. The extract with the highest xanthine oxidase inhibitory and antioxidant properties was applied for further isolation by column chromatography (Figure 3).

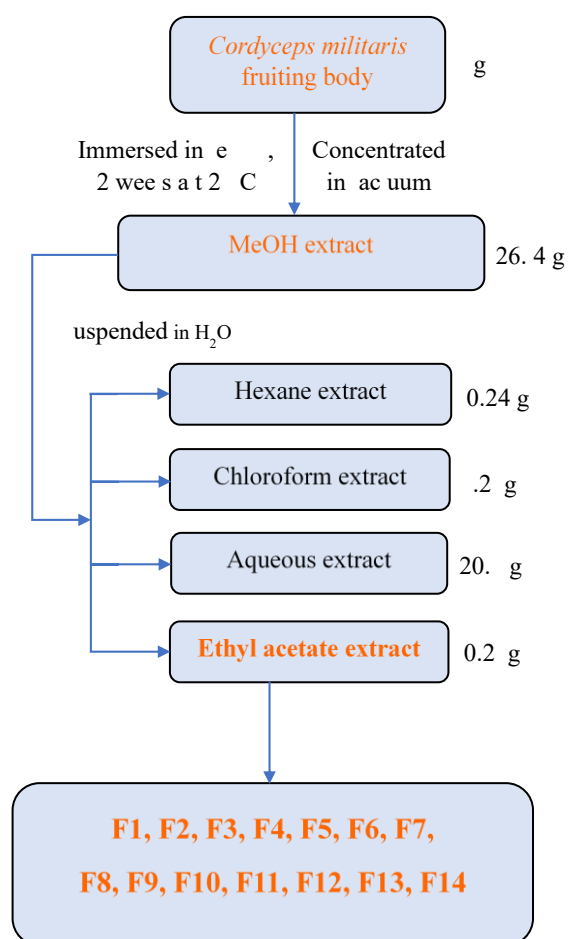


Figure 3. Process of extraction and fractionation of *C. militaris* fruiting-bodies (F: fraction).

2.2.4 Fractionation of ethyl acetate extract

The ethyl acetate extract (EtOAc, 16.28 g) showed the highest xanthine oxidase inhibitory and antioxidant activities on a preliminary test was subjected to a normal-phase of column chromatography (40 mm diameter × 600 mm height,

Climbing G2, Mixell, Tokyo, Japan) filled with silica gel (size Å 60, 200–400 mesh particle size, Sigma-Aldrich, Tokyo, Japan). This separation got 14 fractions by increasing the polarity by CHCl₃ with MeOH of the following eluents: F1 in CHCl₃, F2 in CHCl₃: MeOH (9.9:0.1), F3 in CHCl₃: MeOH (9.8: 0.2), F4 in CHCl₃: MeOH (9.6:0.4), F5 in CHCl₃: MeOH (9.4:0.6), F6 in CHCl₃: MeOH (9.2:0.8), F7 in CHCl₃: MeOH (9:1), F8 in CHCl₃: MeOH (8.8:1.2), F9 in CHCl₃: MeOH (8.6:1.4), F10 in CHCl₃: MeOH (8.4:1.6), F11 in CHCl₃: MeOH (8:2), F12 in CHCl₃: MeOH (7:3), F13 in CHCl₃: MeOH (1:1), and F14 in CHCl₃: MeOH (4:6) - MeOH. Each of fractions was assayed for anti-gout and antioxidant activities and the active fractions were run by GC-MS to identify their chemical compounds.

2.2.5 Xanthine oxidase (XO) inhibitory activity

The xanthine oxidase inhibitory property was tested spectrophotometrically in aerobic conditions as described previously (Umamaheswari *et al.*, 2007) with some adjustments. The test mixture consisted of 50 µL of tests solution (6.25 - 100.00 µg/mL), 30 µL of 70 mM phosphate buffer (pH = 7.5) and 30 µL of enzyme solution (0.01 units/mL in 70 mM phosphate buffer, pH = 7.5), which was prepared immediately before using. After pre-incubation at 25 °C for 15 min, assay reaction was initiated by putting of 60 µL of substrate solution (150 µM xanthine in buffer). After that, the mixture reaction was placed at 25 °C for 30 min. The reaction was stopped by addition 25 µL of 1 N hydrochloric acid (HCl) and the absorbance was read at 290 nm by using a microplate reader. A blank was applied in similar ways but the enzyme solution was put to the assay mixture after the solution of 1 N HCl added. One unit of XO was defined as the amount of enzyme that required to produce 1 µmol of uric acid per min at 25 °C.

The xanthine oxidase inhibitory activity was evaluated by this formula:

$$\% \text{ (XO) Inhibition} = \left\{ \frac{(A-B)-(C-D)}{(A-B)} \right\} * 100$$

Where A was the activity of the enzyme without extracts or fractions, B

was the control of A without extracts or fractions and enzyme. C and D were the activities of the test solutions with and without xanthine oxidase enzyme. The values of IC₅₀ were expressed from the means of the spectrophotometric data of the sample trials repeated 5 times. The sample solutions were dissolved in dimethyl sulfoxide (DMSO) followed by dilution with buffer. The final concentration of DMSO was less than 0.25%. Allopurinol at 6.25, 12.5, 25, 50, 100 µg/mL dilutions were applied as a positive control.

2.2.6 DPPH radical scavenging activity

The antioxidant property of the sample was measured by using 2,2-Diphenyl-1-picrylhydrazyl (DPPH) free radical scavenging method as reported previously (Elzaawely *et al.*, 2007) with some adjustments. Briefly, an amount of 100 µL test solutions were mixed with 0 µL of 0.1 mM DPPH and 100 µL of 0.1 M acetate buffer (pH 5.5). After mixing, the mixtures were put in the dark at room temperature for 30 min. The reduction of the DPPH radical was recorded at 517 nm by using a microplate reader. BHT standard solutions (0.001 - 0.05 mg/mL) were applied as positive controls.

$$\text{DPPH (\%)} = \left[\frac{A_{\text{control}} - (A_{\text{sample}} - A_{\text{blank sample}})}{A_{\text{control}}} \right] * 100$$

Where A_{control} was the absorbance of DPPH solution without test solution. A_{sample} was the absorbance of test solution with DPPH and $A_{\text{blank sample}}$ was the absorbance of test solution without DPPH solution. Lower absorbance indicated higher DPPH radical scavenging property. The IC₅₀ (inhibitory concentration) value was calculated as the concentration required to reduce the initial DPPH radical concentration by 50%. Therefore, the lower IC₅₀ value presented higher DPPH radical scavenging property.

2.2.7 ABTS radical scavenging activity

The ABTS radical cation decolorization assay was conducted as reported previously (Mikulic-Petkovsek *et al.*, 2015) with some modifications. Briefly, the ABTS radical solution was prepared by mixing 2.45 mM potassium persulfate and

7 mM ABTS [2,2-azinobis(3-ethylbenzothiazoline-6-sulfonic acid)] in water. Then, this solution was put in the dark at ambient temperature for 16 h and diluted with methanol to get an absorbance of 0.70 ± 0.05 at 734 nm. An aliquot of 120 μL of the ABTS solution was mixed with 24 μL of test solution and the mixture reaction was placed at the dark at room temperature for 30 min. The absorbance of reaction was read at 734 nm by using a microplate reader. BHT standard (0.01 - 0.25 mg/mL) was used as a reference. The percentage inhibition was evaluated according to the formula:

$$\text{ABTS (\%)} = [\{A_{\text{control}} - (A_{\text{sample}} - A_{\text{blank sample}})\} / A_{\text{control}}] * 100$$

The A_{control} was the absorbance of ABTS radical solution without test solution. A_{sample} was the absorbance of ABTS with test solution and $A_{\text{blank sample}}$ was the absorbance of test solution without ABTS. A lower absorbance showed higher ABTS radical scavenging property. The IC_{50} (inhibitory concentration) value was expressed as the concentration needed to scavenge 50% of ABTS. As a result, lower IC_{50} value presented higher antioxidant activity.

2.2.8 Identification of chemical constituents by gas chromatography-mass spectrometry (GC-MS)

A volume of 1 μL aliquot of each sample was injected into a GC-MS system. The column employed in this identification was DB-5MS column (length 30 m, thickness 0.25 μm , internal diameter 0.25 mm). The system uses helium as a carrier gas and the split ratio was 5.0/1.0. The temperature program was provided in the GC oven as follows: the initial temperature at 50 $^{\circ}\text{C}$ without hold time, the programmed rate by 10 $^{\circ}\text{C}/\text{min}$ up to a final temperature of 300 $^{\circ}\text{C}$ with 20 min for hold time. The injector and detector temperatures were put at 300 $^{\circ}\text{C}$ and 320 $^{\circ}\text{C}$, respectively. The mass range scanned from 29 to 800 amu. The peak data set was collected using the JEOL's GC-MS Mass Center System version 2.65a (JEOL Ltd., Tokyo, Japan) and comparing detected peaks with National Institute of Standards and Technology (NIST) MS library (Andriana *et al.*, 2018).

2.2.9 Statistical analysis

Data were statistically analyzed by using the Minitab 16.2.3 (Minitab Inc., State College, PA, USA) and expressed as means \pm standard deviations (SD). One-way ANOVA was used to analyze the data. The mean differences were determined by using Tukey's test with a confidence level of 95% ($p < 0.05$). All experiments were conducted in triplicate.

2.3 Results

2.3.1 Xanthine oxidase inhibitory activity of crude extracts and fractions of *C. militaris*

XO inhibition from a decrease of uric acid production, was evaluated spectrophotometrically at 290 nm. The ethyl acetate (EtOAc) extract presented a XO inhibition by 31.66% at 100 $\mu\text{g/mL}$ concentration, whereas other crude extracts showed negligible inhibitions (Table 1).

Fourteen fractions obtained from the EtOAc extract were examined for their XO inhibitory ability. Of them, eight fractions had the presence of XO inhibition activity (Table 2). Furthermore, the percentage of XO inhibition of F6 (61.70%), F7 (52.72%), F8 (52.58%), and F10 (56.56%) fractions were found to be more stronger than other fractions at 100 $\mu\text{g/mL}$.

Table 1. Xanthine oxidase inhibitory and antioxidant activities of different crude extracts from *C. militaris*

Crude extracts	% XO inhibition at 100 $\mu\text{g/mL}$	Antioxidant properties	
		DPPH (IC ₅₀ mg/mL)	ABTS (IC ₅₀ mg/mL)
Hexane	-	3.07 \pm 0.04 ^a	4.45 \pm 0.06 ^a
Chloroform	-	1.65 \pm 0.15 ^b	2.52 \pm 0.19 ^b
EtOAc	31.66 \pm 2.86	0.60 \pm 0.03 ^c	1.03 \pm 0.02 ^d
Aqueous residue	-	1.35 \pm 0.07 ^b	1.65 \pm 0.07 ^c

Data were presented as means \pm standard deviations (SD). Values with different superscript letters (a, b, c d) in a column indicated a significant difference at $p < 0.05$ according to Tukey's test. -: not detected.

The XO inhibition were expressed by IC₅₀ value and the lower IC₅₀ showed the higher XO inhibition property. As a result, the fraction F8 was the most potential XO inhibition (IC₅₀ = 62.82 µg/mL), followed by F10 (IC₅₀ = 68.04 µg/mL), F7 (IC₅₀ = 86.8 µg/mL), and F6 (IC₅₀ = 87.3 µg/mL) fractions. Other isolated fractions possessed trivial inhibitory activities which were not considerable enough to evaluate IC₅₀ values. Besides, cordycepin standard showed strong anti-hyperuricemic activity (IC₅₀ = 10.67 µg/mL), but it was weaker than allopurinol (IC₅₀ = 4.85 µg/mL).

Table 2. Xanthine oxidase inhibitory activity of 14 fractions isolated from EtOAc extract of *C. militaris*

Fractions	% XO inhibition at 100 µg/mL	IC ₅₀ value (µg/mL)
F1	-	-
F2	-	-
F3	-	-
F4	21.88 ± 0.78 ^g	-
F5	39.57 ± 0.56 ^e	-
F6	61.70 ± 0.64 ^c	87.73 ± 0.81 ^a
F7	52.72 ± 0.74 ^d	86.78 ± 1.20 ^a
F8	52.58 ± 1.55 ^d	62.82 ± 4.48 ^b
F9	31.12 ± 3.71 ^f	-
F10	56.56 ± 2.95 ^c	68.04 ± 5.85 ^b
F11	-	-
F12	11.92 ± 1.79 ^h	-
F13	-	-
F14	-	-
Cordycepin	74.95 ± 0.68 ^b	10.67 ± 0.31 ^c
Allopurinol	90.20 ± 6.19 ^a	4.85 ± 2.19 ^c

Data were presented as means ± standard deviations (SD). Values with different superscript letters (a, b, c, d, e, f, g, h) in a column indicated a significant difference at $p < 0.05$ according to Tukey's test. -: not detected.

2.3.2 Antioxidant activities of 14 fractions from EtOAc extract of *C. militaris*

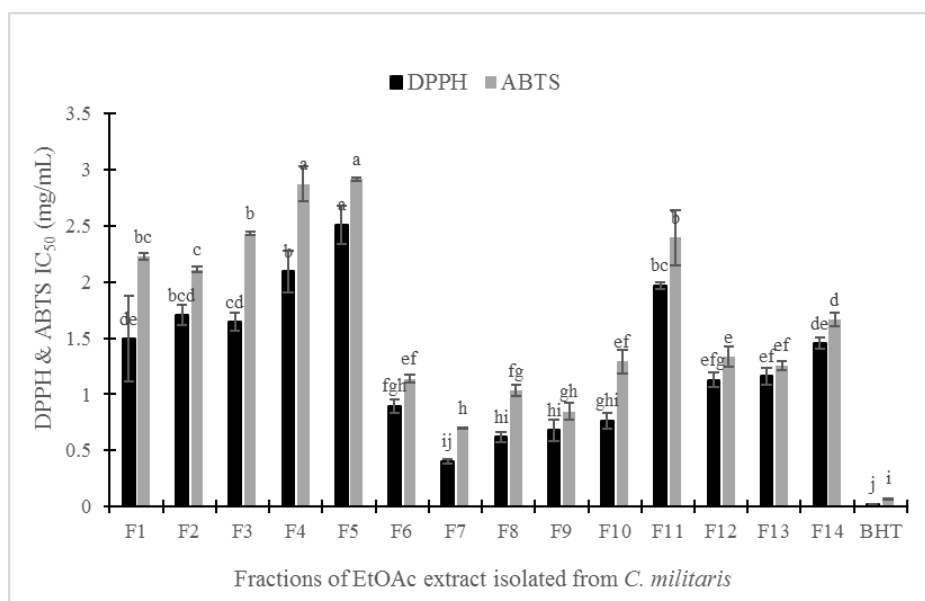


Figure 4. ABTS and DPPH radical scavenging activities of EtOAc fractions from *C. militaris* and antioxidant butylated hydroxytoluene (BHT) standard. Values with different superscript letters (a, b, c, d, e, f, g, h, i, j) in a column indicated a significant difference at $p < 0.05$ according to Tukey's test.

The antioxidant properties of 14 fractions from EtOAc extract of *C. militaris* were measured by using DPPH and ABTS assays, compared with the standard BHT in Figure 4. The antioxidant activities of them were evaluated by IC₅₀ value and the lower IC₅₀ showed the higher radical scavenging property. Fourteen isolated fractions presented various levels of DPPH and ABTS scavenging ability (Figure 4), of which the F7 fraction was the strongest antioxidant activities in both ABTS and DPPH assays. Meanwhile, the antioxidant capacity of fraction F5 was the lowest performance in Figure 4.

In the ABTS assay, the F7 and F9 fractions showed the highest effective properties (IC₅₀ = 0.702 mg/mL and 0.845 mg/mL, respectively), followed by the F8 (IC₅₀ = 1.032 mg/mL) and F6 (IC₅₀ = 1.138 mg/mL). In DPPH scavenging activity, the F8 was also potential but this fraction was statistically similar to that of the F9 and F10 fractions. Overall, it was found the fraction F7, F8, F9 and F10 showed greater antioxidant activities than other fractions.

2.3.3 GC-MS of analysis of *C. militaris* fractions from EtOAc extract

Gas chromatographic-mass spectrometry (GC-MS) is an effective and reliable analytical analysis to identify the presence of components in complex mixtures (Xuan *et al.*, 2018). The major bioactive constituents of the 14 isolated fractions were detected and identified by GC-MS and showed in Table 3. Principal compounds from EtOAc extract of *C. militaris* included cordycepin (3'-deoxyadenosine), hexadecenoic acid, and pentadecanal.

Cordycepin was found as the major compound that was identified in F8, F9 and F10 fractions, while pentadecanal appeared in most of isolated fractions (F3 - F10). Additionally, fatty acids and their derivatives (palmitic acid; palmitic acid, methyl ester; and palmitic acid, 2-oxo-, methyl ester) were detected in the F1, F2, F6, F7, F11, F12, F13 and F14 fractions (Table 3).

Table 3. Identification of principal compounds of 14 EtOAc fractions from *C. militaris*

No.	Major constituents	Retention	Peak	Fractions
		Times (min)	Area (%)	
1	1) Palmitic acid methyl ester	16.72	5.95	F1
	2) Palmitic acid	17.09	17.08	
	3) 9,12-Octadecadienoic acid (Z, Z)	18.73	29.54	
2	1) Palmitic acid methyl ester	16.72	2.23	F2
	2) Palmitic acid	17.11	20.64	
	3) 9,12-Octadecadienoic acid (Z, Z)	18.76	32.16	
	4) Ergosta-4,6,8(14),22-tetraen-3-one	29.12	6.25	
3	1) Pentadecanal	14.56	16.02	F3
	2) 2-Oxopalmitic acid methyl ester	17.41	3.04	
	3) Octadecanal	22.11	34.91	
	4) Dodecanamide	25.55	2.73	
4	1) Pentadecanal	14.56	10.38	F4
	2) 2-Oxopalmitic acid methyl ester	17.40	3.20	
	3) Octadecanal	22.11	30.13	

5	1) Pentadecanal	14.56	7.11	F5
	2) Hexadecanal	15.65	1.30	
	3) 2-Oxopalmitic acid methyl ester	17.41	3.22	
	4) Octadecanal	22.11	25.85	
6	1) 1,6-Anhydro- β -D-glucopyranose	11.82	5.65	F6
	2) Pentadecanal	14.56	53.80	
	3) Palmitic acid	17.07	1.33	
	4) 2-Palmitoylglycerol	20.30	1.25	
	5) 1-Heneicosanol	26.33	1.99	
7	1) 1,6-Anhydro- β -D-glucopyranose	11.76	1.92	F7
	2) Pentadecanal	14.52	21.35	
	3) Palmitic acid	17.03	1.75	
	4) N-(2-Hydroxyethyl) octanamide	18.77	2.73	
8	1) 1,6-Anhydro- β -D-glucopyranose	11.76	0.54	F8
	2) Pentadecanal	14.52	19.79	
	3) Cordycepin	21.98	55.38	
9	1) Pentadecanal	14.55	19.90	F9
	2) 2-Oxopalmitic acid methyl ester	17.40	0.77	
	3) Cordycepin	21.97	58.04	
10	1) Tetradecanal	13.39	0.83	F10
	2) Pentadecanal	14.56	45.00	
	3) Cordycepin	21.95	18.61	
11	1) Malic Acid	6.18	1.89	F11
	2) Palmitic acid	17.03	1.90	
	3) 1, E-11, Z-13-Octadecatriene	18.67	0.72	
	4) 2-Palmitoylglycerol	21.89	3.79	
12	1) Palmitic acid	17.03	1.41	F12
	2) 1, E-11, Z-13-Octadecatriene	18.67	1.27	

	3) 1-n-Hexadecylindan	21.74	2.62	
13	1) Palmitic acid	17.02	4.18	F13
	2) 1, E-11, Z-13-Octadecatriene	18.67	15.71	
14	1) Carbamic acid (3-methylphenyl) methyl ester	7.03	10.26	
	2) Palmitic acid	17.03	9.95	F14
	3) 1, E-11, Z-13-Octadecatriene	18.67	25.50	

2.4 Discussion

It was found that the significant increase of gout and hyperuricemia principally caused by unusual habits of diet and exercise regimen (Nile and Park, 2015). The food and drinks with high content of nucleic acids such as seafood and meat gave rise to the risk of gout disease. Hyperuricemia is a biochemical abnormality or metabolic disorder phenomenon that caused development of gout and related oxidative stress-related diseases such as hypertension, cardiovascular disease, diabetes, cancer, and a variety of other disorders (Kapoor and Saxena, 2014; Ouyang *et al.*, 2017). Therefore, the lowering serum uric acid concentration within normal range is important and can be achieved by blocking the biosynthesis of uric acid (Kapoor and Saxena, 2016).

Xanthine oxidase is a form of xanthine oxidoreductase enzyme, which has been found for decades. Natural xanthine oxidase inhibitors from plants are used in traditional herbal medicines for the prevention and treatment of gout or diseases associated with symptoms such as arthritis and inflammation (Nguyen *et al.*, 2004). From this fact, screening of xanthine oxidase inhibitory property from medicinal plants might be an effective method to find new potential inhibitors for these major disease treatments. In this study, the XO inhibitory and antioxidant property of *C. militaris* fungus were determined. It was found that this fungus possessed potent XO inhibitory and antioxidant activities and contained rich bioactive compounds which were identified by column chromatography and GC-MS analysis (Tables 1-3).

Several previous studies showed that the majority of natural bioactive

compounds that possessed xanthine oxidase inhibition belonged to flavonoids (Dong *et al.*, 2016; Santi *et al.*, 2018), phenolics (Gawlik-Dziki *et al.*, 2017), and lanostanoids (Lin *et al.*, 2013). Besides, chemical compound with purine ring was found to have remarkably potent inhibitor of xanthine oxidase such as 6-(N-benzoylamino)purine ($IC_{50} = 0.45 \mu\text{M}$) (Tamta *et al.*, 2005), 2-amino-6-purine thiol ($IC_{50} = 16.38 \mu\text{M}$), and 2-amino-6-hydroxy-8-mercaptapurine ($IC_{50} = 17.71 \mu\text{M}$) (Kalra *et al.*, 2007). These results indicate that purine ring structure may play an important role in the inhibition of xanthine oxidase enzyme. Earlier study indicated that cordycepin isolated from *C. militaris* may interact with uric acid transporter 1 (URAT1) to lower serum uric acid levels in an *in vivo* model (Yong *et al.*, 2018). From GC-MS results, cordycepin (a purine nucleoside) appeared as the major bioactive constituents in F8, F9, and F10 fractions obtained by column chromatography. Therefore, the results of fraction F8, F9, F10 and cordycepin standard confirmed that cordycepin possessed strong xanthine oxidase inhibition capacity. Thus, this study highlighted that cordycepin isolated from *C. militaris* played a crucial role in inhibition of XO by an *in vitro* model. Recently, it was found that cordycepin played a role in the regulation of sleep which might be a promising tranquilizer contributing to the treatment of sleep disturbance (Hu *et al.* 2013; Hulpia *et al.* 2019).

Additionally, most of the healing therapies require a qualitative sleep that may help the body quickly recuperate. And, the prescription of sedatives together with specific medicines is no longer strange in some common disease treatments. Besides, Tsai *et al.* (2010) reported that cordycepin is rapidly degraded by adenosine deaminase in the endogenous nucleoside metabolic pathway. The discovery of cordycepin with a sleep improvement, quickly degradation and a diverse beneficial health effect suggests that this precious natural compound is really feasible in the future therapeutics. However, the most effective dose of the substance should be recognized by further clinical trials.

Oxidative stress results in human disease development or an abnormal immune response (Liu *et al.*, 2016). Additionally, it was found that free radicals caused oxidative damage to biomolecules and are responsible for progression of

several diseases such as inflammatory, metabolic disorders, aging, atherosclerosis, diabetes, cancer, and cardiovascular diseases (Ouyang *et al.*, 2017). As a result, XO acted as a biological source of oxygen-derived free radical leading to cell and tissue damage (Lin *et al.*, 2013). Obviously, the xanthine oxidase inhibitory activity of *C. militaris* was attributed to their survival strategy to the oxidative stress. Recently, several studies revealed that polysaccharides from aqueous extracts of this fungus possessed antioxidant activities (Yu *et al.*, 2007; Fengyao *et al.*, 2011; Chen *et al.*, 2013), but there was little polysaccharide quantity detected in methanolic extracts (Dong *et al.*, 2014). Furthermore, the *in vitro* antioxidant property was found to be correlated to cordycepin (Olatunji *et al.*, 2016; Lei *et al.*, 2018) and fatty acids (Karimi *et al.*, 2015). Therefore, the considerable amounts of cordycepin and fatty acids observed in fraction F7, F8, F9, and F10 by this study indicated that these components obtained in *C. militaris* might be responsible for significant antioxidant capacity (Table 1; Figure 1) as found in previous reports (Hui *et al.*, 2006; Reis *et al.*, 2013).

This study has successfully isolated fractions from *C. militaris* actives on xanthine oxidase inhibitory, and antioxidant properties separated by column chromatography and identified potent bioactive compounds by GC-MS technique. It was proposed that there were some components other than cordycepin and fatty acids in this fungus can also be potential for medicinal properties and needed further analyses.

2.5 Conclusion

This is the first study revealed that *C. militaris* possessed strong XO inhibition in an *in vitro* model which may be potential for gout treatment, although further *in vivo* trial is required. From effective separation techniques of column chromatography and GC-MS analyses, cordycepin, fatty acids and their derivatives appeared as the major constituents that may be responsible for antioxidant, and anti-hyperuricemic properties as observed by this research. Findings of this study highlighted that *C. militaris* is potential to develop foods and drinks potential for prevention and treatment of gout.

3 Antibacterial activity of *Cordyceps militaris* (L.) Link fruiting body

3.1 Introduction

Bacterial infection is considered as the most common reason for illness and death worldwide (Dzotam *et al.*, 2016; Mostafa *et al.*, 2018). In 2011, the World Health Organization reported that 22 million people died with one-third of the deaths owing to infectious diseases (Liu *et al.*, 2017).

Bacteria cause disease are called pathogenic bacteria with producing poisonous substances called endotoxins and exotoxins. These substances are responsible for the symptoms that occur with bacteria related diseases (Spilak *et al.*, 2015; Cavaillon, 2018).

The urinary tract infections (UTI) and gastroenteritis have become a more serious problem today because of multidrug resistance to *Escherichia coli* (E), *Staphylococcus aureus* (S), *Proteus mirabilis* (P) and *Bacillus subtilis* (B) infection (Chimnoi *et al.*, 2018; Mostafa *et al.*, 2018; Kakian *et al.*, 2019). *E. coli* and *P. mirabilis*, two Gram-negative bacteria are the most commonly isolated pathogen of urinary tract infections. These infections are often caused by anatomical or physiological malformations of the urinary tract, catheterised patients or due to medical care mistakes (Jacobsen *et al.*, 2008; Kwiecińska-Piróg *et al.*, 2013). Besides, the majority of researches reported that pathogenesis of gastroenteritis caused by two Gram-positive bacteria, *S. aureus* and *B. subtilis*. They commonly contaminate raw foods and food materials, particularly foods in contact with the soil or of vegetable origin such as sliced meats, vegetable, cold salads, tuna, chicken, macaroni, cream-filled pastries, puddings, sandwiches or seafood dishes (Kadariya *et al.*, 2014; Elshaghabee *et al.*, 2017; Kim *et al.*, 2019).

An UTI is an infection that develop in the urinary tract, which includes the kidneys, ureters, urethra, and bladder. Women have a lifetime risk of over 50 percent of developing a UTI. It is common among emergency department patients, causing conditions ranging from the relatively benign and easily treatable

to threaten fertility and life (Sarah *et al.*, 2019; Sheerin and Glover, 2019). The infecting bacteria normally constitutes the faecal flora and the urine flow in an individual is obstructed by several reasons such as, tumours, prostatic hypertrophy, strictures, calculi, vesicourethral reflux, diabetes and anal disease (Mishra *et al.*, 2017).

Besides, gastroenteritis is caused by infection of the stomach or intestines. It is a cause for hospitalisation in children and a major cause of mortality with young children, particularly under 5 years of age being disproportionately affected (Onyon and Dawson, 2018). The symptoms of gastroenteritis include diarrhea, stomach cramps, fever, headache, blood in feces, bloating, loss of appetite, and body aches (Chimnoi *et al.*, 2018).

Less than a century ago, a wide range of synthetic and semi-synthetic antibacterial agents was discovered to inhibit bacterial enzymes and other proteins necessary for bacterial cell function as well as treatment bacterial infections (Yoon *et al.*, 2018). However, despite numerous benefits, the antibacterial agents also cause various adverse drug reactions such as hyper-sensitivity and immunosuppression (Tanović *et al.*, 2016). Furthermore, with increasing exposure to antibiotics and fighting selective pressure, bacteria have evolved to form many antibiotic-resistant bacteria. The spread of antibiotic resistance bacteria in hospital and community settings continue to be a widely unresolved problem to challenge the healthcare services in both developing and developed countries. Therefore, there is an urgent need to find newer antimicrobial agents effective against bacteria and less harmful to the human body (Valle *et al.*, 2015).

In ancient times, people have used natural plant materials to prevent or treat infectious diseases and scientific investigations have clearly demonstrated the therapeutic efficacy of them over time (Sharma *et al.*, 2017). Today, thousands of plants or their components are used as folk medicines in many countries to treat various infectious diseases such as urinary tract infections, gastroenteritis, bronchitis, diarrhea, cutaneous abscesses and parasitic diseases (Yasunaka *et al.*, 2005; Sharma *et al.*, 2017). According to World Health Organization (WHO), 60% of the world's population relies on traditional medicine and about

80% of the population in developing countries depends almost entirely on it for their primary health care needs (Paul *et al.*, 2015). According to the literature, many plants have been examined *in vitro* against many bacterial strains, and a good number of medicinal plant and fungus extracts and pure constituents have been proven to be active against Gram-positive and Gram-negative bacteria (Sharma *et al.*, 2017). Thus, medicinal fungi and plant extracts have been found as nutritionally safe and easily degradable source of antibacterial agents against human pathogens (Olatunji *et al.*, 2016; Liu *et al.*, 2017; Choong *et al.*, 2018).

The exploration of naturally obtaining antibacterial is increasing attention because of consumers' awareness of natural food products and the emergence of multidrug resistance in both human and plant pathogenic microorganisms. In recent years, it has been considerable interest in extracts and fractions from edible fungi with antibacterial activity (Dong *et al.*, 2014). *C. militaris* is a rare medicinal higher fungus and contains many biological active components, such as cordycepin, polysaccharides, fatty acids, amino acid, fiber, ash and trace elements (Wang *et al.*, 2012; Zhu *et al.*, 2016; Tongmai *et al.*, 2018). It has been used widely as a crude drug and a folk tonic food in Southeast Asia (Das *et al.*, 2010; Shrestha *et al.*, 2012; Pathania *et al.*, 2015). Recent researches indicated that *C. militaris* had multiple pharmacological activities such as antitumor, antioxidant, anti-angiogenic, anti-fatigue, anti-inflammation, anticancer, antifungal, antiviral, hepatoprotective, hypoglycemic, hypolipidemic, and immunomodulatory benefits (Chen *et al.*, 2013; Chen *et al.*, 2014; Liu *et al.*, 2016; Wada *et al.*, 2017; Jin *et al.*, 2018; Zhang *et al.*, 2019).

Furthermore, many previous studies have been found that methanolic extract of this fungus possess potential antibacterial activity but bioactive compounds responsible for this property have not been elaborated (Reis *et al.*, 2013; Dong *et al.*, 2014). Therefore, the aims of the current study are to examine the potential antibacterial activity, as well as to determine the bioactive constituents from fruiting body of *C. militaris*.

3.2 Materials and methods

3.2.1 Chemicals

Four bacteria strains including *Staphylococcus aureus*, *Escherichia coli*, *Bacillus subtilis*, and *Proteus mirabilis* were provided by Sigma-Aldrich Corp., St. Louis, MO USA. Methanol, ethanol, hexane, ethyl acetate and chloroform were bought from Junsei Chemical Co., Ltd., Tokyo, Japan. Dimethyl sulfoxide (DMSO), streptomycin, ampicillin, agar, filter paper discs, bacterial culture tubes were purchased from by Kanto Chemical Co. Inc., Tokyo, Japan. All chemicals used were of analytical grade.

3.2.2 Plant materials and fractions preparation

The fruiting bodies of *C. militaris* were obtained from Truc Anh Company, 53F/5, Ton Duc Thang street, Bac Lieu city, Vietnam. The samples were dried and sterilized before packaging and depositing at Laboratory of Plant Physiology and Biochemistry, Graduate School for International Development and Cooperation (IDEC), Hiroshima University, Higashi-Hiroshima, Japan for further analysis.

An amount of 1.0 kg of *C. militaris* powder was soaked in 15 L methanol for two weeks, then evaporated to produce 126.14 g of MeOH extract. The MeOH extract was fractionated using hexane, chloroform and ethyl acetate (EtOAc). The EtOAc extract (16.28 g) possessed the highest antibacterial property and was subjected to column chromatography to obtain 14 fractions (F1 - F14). Each of separated fractions was examined for antimicrobial activity and effective fractions were analyzed by GC-MS to identified bioactive compounds.

3.2.3 Antibacterial activity

The evaluation of antibacterial property was based on a method reported previously (Fukuta *et al.*, 2007). All bacteria were cultured in a Luria-Bertani (LB) medium for 24 h at 37 °C. The four bacterial strains assayed in this experiment included *Escherichia coli*, *Staphylococcus aureus*, *Proteus mirabilis* and *Bacillus subtilis*. The final population density was standardized to be 1.45×10^6 CFU/mL (*E. coli*), 1.29×10^6 CFU/mL (*S. aureus*), 2.87×10^6 CFU/mL

(*P. mirabilis*) and 1.63×10^6 CFU/mL (*B. subtilis*). An amount of 0.1 mL of the bacterial suspension was spread over the surface of the solid LB agar broth in Petri dish (9 cm in diameter). After that, filter paper discs (6 mm diameter) loaded with 20 μ L of each test solution (with a concentration 40 mg/mL in DMSO) were placed on the surface of the LB broth plates. The Petri dishes were placed at 37 °C for 24 h and then the inhibition zone was recorded. Streptomycin and ampicillin were used as the positive controls and DMSO was used as a negative control.

3.2.4 Identification of chemical constituents of active fractions by gas chromatography-mass spectrometry (GC-MS)

GC-MS technique was performed to elucidate chemical name and structure of identified compounds. One μ L aliquot of active fractions was injected into a GC-MS system using DB-5MS column, 30 m in length, 0.25 μ m in thickness, and internal diameter 0.25 mm (Agilent Technologies, J & W Scientific Products, Folsom, CA, USA). The data were measured by using helium for the carrier gas, and the split ratio was 5.0/1.0. At the beginning of program, the temperature of GC oven was set up at 50 °C without hold time, then up to a final temperature of 300 °C at a rate of 10 °C/min with 20 minutes for hold time at 300 °C. The injector and detector temperatures were set at 300 °C and 320 °C, respectively with the mass range scanned from 29 to 800 amu. The component identification were conducted by comparing the mass spectral fragmentation patterns of active fractions with the mass spectral libraries of the JEOL's GC-MS Mass Center System version 2.65a and standards {National Institute of Standards and Technology (NIST) MS library} (Van *et al.*, 2018).

3.2.5 Statistical analysis

The statistical analyses were conducted by using the Minitab 16.2.3 (Minitab Inc., State College, PA, USA). The means and standard deviations of test samples were calculated by one-way ANOVA. Tukey's test were implemented to compare significant differences between means with the confidence level of 95% ($p < 0.05$). All experiments were carried out in triplicate and expressed as mean \pm standard deviation (SD).

3.3 Results

3.3.1 Antibacterial activities of crude extracts of *C. militaris*

The *in vitro* antibacterial activity of different crude extracts of *C. militaris* against the tested microorganisms (two Gram-positive and two Gram-negative) was evaluated and expressed by the inhibition zones (mm) in Table 4. It was found that the antibacterial activity varied among bacterial strains and extractions. Among them, only the ethyl acetate extract (EtOAc) inhibited the growth of all bacterial strains, *B. subtilis*, *S. aureus*, *E. coli*, and *P. mirabilis*. The EtOAc extract possessed the highest antibacterial capacity with inhibition zone larger than 11 mm diameter at *E. coli*, and followed by *P. mirabilis* (> 10 mm), whereas aqueous residue extract exhibited negligible inhibition at all four bacterial strains. This results suggest that the EtOAc extract contains more potent antibacterial compounds than other extracts.

Table 4. Antibacterial activity of crude extracts of *C. militaris*

Extracts	Antibacterial Activities			
	<i>B. subtilis</i> (+)	<i>S. aureus</i> (+)	<i>E. coli</i> (-)	<i>P. mirabilis</i> (-)
Hexane	7.50 ± 0.50 ^b	-	-	-
Chloroform	7.83 ± 0.29 ^{ab}	-	6.67 ± 0.29 ^b	-
Ethyl acetate	8.17 ± 0.29 ^a	7.7 ± 0.31	11.67 ± 1.53 ^a	10.70 ± 0.67
Aqueous residue	-	-	-	-

Data presented means ± standard deviation (SD). Values in a column with similar superscript letters (a, b) are not significantly different by Tukey's test ($p < 0.05$). -: not detected.

3.3.2 Antibacterial activity of fractions from EtOAc extract of *C. militaris*

Fourteen fractions from the EtOAc extract showed various antibacterial inhibition ability (Table 5). As compared to the standards including streptomycin and ampicillin, the inhibitory level can be ranked as follows: *E. coli* > *P. mirabilis* > *B. subtilis* > *S. aureus*.

In case of different fractions, F9, F11 and F12 indicated the most effective inhibition at all tested bacterial strains, followed by F2, F7 and F1. Especially, F9

and F11 fractions share the same highest inhibition zone diameter (10.17 mm). In other fractions, F6, F8, F10, F13 and F14 were the least effective as they only inhibited to one or two tested bacterial strains, whereas the activity of F4 fraction remained unknown, as it did not give inhibition on *E. coli*, *P. mirabilis*, *B. subtilis*, *S. aureus*.

Table 5. Antibacterial activity of 14 fractions from EtOAc extract of *C. militaris*

Fractions	Zone of Inhibition (mm)			
	<i>B. subtilis</i> (+)	<i>S. aureus</i> (+)	<i>E. coli</i> (-)	<i>P. mirabilis</i> (-)
F1	7.50 ± 0.50 ^e	7.33 ± 0.58 ^{cde}	7.67 ± 0.58 ^{efg}	7.50 ± 0.50 ^{de}
F2	6.83 ± 0.29 ^e	8.67 ± 0.58 ^c	8.00 ± 0.00 ^{ef}	6.67 ± 0.29 ^e
F3	6.67 ± 0.29 ^e	-	7.33 ± 0.58 ^{efg}	6.83 ± 0.29 ^{de}
F4	-	-	-	-
F5	6.50 ± 0.00 ^e	6.83 ± 0.29 ^{de}	6.83 ± 0.29 ^{fg}	-
F6	7.33 ± 0.58 ^e	8.33 ± 0.58 ^c	-	-
F7	7.83 ± 0.29 ^{de}	6.67 ± 0.29 ^e	8.33 ± 0.29 ^{de}	7.00 ± 0.00 ^{de}
F8	-	6.83 ± 0.29 ^{de}	9.33 ± 0.58 ^{cd}	-
F9	9.33 ± 0.58 ^c	7.33 ± 0.58 ^{cde}	8.33 ± 0.58 ^{de}	10.17 ± 0.76 ^c
F10	-	6.67 ± 0.29 ^e	6.67 ± 0.29 ^g	-
F11	9.67 ± 0.29 ^c	7.33 ± 0.58 ^{cde}	10.17 ± 0.76 ^c	8.00 ± 0.50 ^d
F12	9.00 ± 1.00 ^{cd}	8.17 ± 0.29 ^{cd}	9.33 ± 0.58 ^{cd}	7.17 ± 0.29 ^{de}
F13	-	8.33 ± 0.29 ^c	-	-
F14	-	7.67 ± 0.58 ^{cde}	-	-
DMSO	-	-	-	-
Streptomycin	23.33 ± 1.16 ^b	24.67 ± 0.58 ^b	17.33 ± 0.58 ^b	23.00 ± 1.00 ^b
Ampicillin	27.33 ± 0.58 ^a	36.00 ± 1.00 ^a	24.33 ± 0.58 ^a	24.33 ± 0.58 ^a

The data presented the means ± SD (standard deviation). Values in a column with similar superscript letters (a, b, c, d, e, f, g) are not significantly different by Tukey's test ($p < 0.05$). -: not detected.

Among the individual bacteria, the F9 fraction showed the strongest antibacterial activity on *P. mirabilis* (10.17 mm), followed by F11, F1, F12, F7, F3 and F2. In the case of *E. coli*, F11 were the best candidate to inhibit growth of the

bacteria, but it was statistically similar to F8 and F12 fractions. In *S. aureus*, fraction F2, F6 and F13 possessed the strongest inhibition. In *B. subtilis*, F9, F11, and F12 fraction exerted the maximum inhibition, while the other fractions showed similar antibacterial ability (Table 5).

In general, fractions from EtOAc extract of *C. militaris* showed strong inhibition on *B. subtilis*, *S. aureus*, *E. coli*, and *P. mirabilis*, but lower than streptomycin and ampicillin as the positive control.

3.3.3 Compounds identification by GC-MS of active fractions from EtOAc extract of *C. militaris*

The identification of the most active fractions in antibacterial activity was analyzed by using GC-MS technique.

Table 6. Chemical constituents of the most active fraction in antibacterial activity by GC-MS

No	Compounds	Chemical Formula	MW (g/mol)	Chemical Classification	GC-MS		Fractions
					Rt (min)	Area (%)	
1	Pentadecanal	C ₁₅ H ₃₀ O	226.40	Fatty aldehydes	14.55	19.90	
2	2-Oxopalmitic acid methyl ester	C ₁₇ H ₃₂ O ₃	284.4	Fatty acid ester	17.40	0.77	F9
3	Cordycepin	C ₁₀ H ₁₃ N ₅ O ₃	251.24	Nucleosides	21.97	58.04	
4	Malic acid	C ₄ H ₆ O ₅	134.09	Dicarboxylic acid	6.18	1.89	
5	Palmitic acid	C ₁₆ H ₃₂ O ₂	256.43	Fatty acid	17.03	1.90	F11
6	2-Palmitoylglycerol	C ₁₉ H ₃₈ O ₄	330.5	Fatty acid ester	21.89	3.79	
7	Palmitic acid	C ₁₆ H ₃₂ O ₂	256.43	Fatty acid	17.03	1.41	F12
8	1-n-Hexadecylindan	C ₂₅ H ₄₂	342.6	Hexadecane	21.74	2.62	

The results were shown in Table 6. Chemicals belong to fatty acids and fatty acid esters were detected in all fractions (F9, F11 and F12).

Among the identified components in F9 fraction, the main compound was cordycepin (58.04%) followed by pentadecanal (19.9%) and 2-oxopalmitic acid methyl ester (0.77%). Three constituents were identified in F11 fraction, of which 2-palmitoylglycerol was the most major compound (3.79%), followed by palmitic acid (1.9%) and malic acid (1.89%). Besides, 1-n-hexadecylindan (2.62%) and palmitic acid (1.41%) were detected in F12 fraction (Table 6).

3.4 Discussion

The urinary tract infection and gastroenteritis have become a more serious problem today because of multidrug resistance to *E. coli*, *S. aureus*, *P. mirabilis* and *B. subtilis* infection (Mishra *et al.*, 2017; Chimnoi *et al.*, 2018). This problem associate with global medical crisis and require constant surveillance, which continuously challenges community of scientific researchers. Scientists need to screening more natural or organic materials for solutions. Traditional medicine has been used worldwide for centuries, particularly the application of herbal plants or fungi for therapeutic purposes (Valle *et al.*, 2015).

In recent years, it was documented that methanolic extract of *C. militaris* had potential antibacterial activity (Joshi *et al.*, 2019). In this study, the fractions exhibited a broad spectrum of activity against both Gram-positive and Gram-negative bacteria, and the results confirm the use of *C. militaris* in traditional medicine for the treatment of infections. To date, thousands of phytochemicals derived from plant extracts with various mechanisms of action have been identified as antibacterial compounds (Barbieri *et al.*, 2017). From GC-MS analysis, cordycepin appeared as the key component antibacterial activity, especially in *E. coli* and *B. subtilis* although further *in vitro* trial was needed. This study highlighted that *C. militaris* obtained potential substances which may be beneficial for the treatments of urinary tract infections (UTI) and gastroenteritis infection.

Several previous studies also indicated that fatty acids and their derivative methyl, ethyl esters exhibited antibacterial activities (Huang *et al.*, 2011; Karimi *et al.*, 2015). The fatty acids with a chain length of more than 10 carbon atoms induced lysis of bacterial protoplasts. This mechanism could further distress the expression of bacterial virulence which played an important role in establishing infection (Mohy El-Din and El-Ahwany, 2016). Therefore, the presence of palmitic acid; 2-palmitoylglycerol; and 2-oxopalmitic acid methyl ester suggested that these components may be responsible for potent antibacterial activity of this medicinal fungus as reported by previous studies (Eleazu, 2016; Al-Abd *et al.*, 2017). However, it is necessary to check these compounds on multidrug-resistant bacteria in hospital and community to increase potential value of this fungus.

Thus, isolated fractions from *C. militaris* possessed significant antibacterial activity separated by column chromatography and identified potent constituents by GC-MS analysis. It was proposed that there were some compounds other than cordycepin and fatty acids in *C. militaris* can also be potential for pharmaceutical properties and needed further analyses.

3.5 Conclusion

This study provides new concerning in isolation and chemical characterization of bioactive compounds of *C. militaris*. These results resolutely established the efficacy of cordycepin, fatty acid and their esters against both Gram-positive and Gram-negative bacterial strains and *C. militaris* can produces compounds that are able to combat the bacterial infections. Finding of this study provide important values and scientifically supports the effectiveness of medicinal fungi in the case of an increasing number of bacteria resistance to commercial antibiotics. However, effectiveness must need to evaluate via *in vivo* studies in order to determine new promising antibacterial mixtures or compounds. Additional studies are also required to concern the application of different extraction methods, bioassay-guided isolation, purification and quantification of bioactive compounds, including the detection of side effects and pharmacokinetic properties in preparation for its *in vivo* assessment.

4 Allelopathic activity and identification of allelochemicals from fruiting body of *Cordyceps militaris* (L.) Link fruiting body

4.1 Introduction

Modern agriculture is dependent on the use of herbicides, a powerful tool to suppress the growth of weeds that are a persistent threat to crop productivity (Dennis *et al.*, 2018; Kraus and Stout, 2019). However, these chemicals may affect ecosystems as well as human health (Bonnet *et al.*, 2007; Gonzalo *et al.*, 2011; Hagner *et al.*, 2019).

In settings of agriculture, botany, politics, and medicine, much controversy has emerged on the overuse and risks of herbicides in agricultural production, and discussions have recently focused on the development of biological controls using an allelopathy approach. The term “allelopathy” was formed from the Greek-derived compounds “allelo” and “pathy”, “allelo” meaning “mutual harm” and “pathy” meaning “suffering” and was first used in 1937 by plant physiologist Molisch (Tesio and Ferrero, 2010).

Allelopathy is a biological phenomenon where an organism produces phytochemicals that affect the growth and development of other nearby plant organisms (Xuan *et al.*, 2005). These chemical components, also called allelochemicals, are produced primarily as secondary metabolites of plants and microorganisms (Trezzi *et al.*, 2016). So far, several allelochemicals have been isolated and identified from many different plant species (Kong *et al.*, 2019). Allelochemicals are various chemical families and classified into the following 14 categories based on chemical similarity: (1) water-soluble organic acids, aliphatic aldehydes, straight-chain alcohols, and ketones; (2) long-chain fatty acids and polyacetylenes; (3) simple unsaturated lactones; (4) anthraquinone and complex quinones, benzoquinone; (5) benzoic acid and its derivatives, simple phenols; (6) cinnamic acid and its derivatives; (7) flavonoids; (8) tannins; (9) coumarin; (10) steroids and terpenoids; (11) alkaloids and cyanohydrins; (12) amino acids and

peptides; (13) glucosinolate and sulfide; and (14) purines and nucleosides (Cheng and Cheng, 2015).

As natural toxins, allelochemicals inhibit target plant by morphological, cytological, biochemical and physiological changes in the plant roots and aerial parts (Ladhari *et al.*, 2014). They affect cellular processes in susceptible plants such as membrane permeability, stomatal closure, cell division, absorption of nutrients, photosynthesis, metabolic processes, ATP synthesis and gene expression (Omezzine *et al.*, 2014). Recently, the allelopathic compounds has been used as an alternative tool to the use of commercial herbicides as well as the chemical control application for weed plants suppression in agroecosystems (Albuquerque *et al.*, 2011; Spiassi *et al.*, 2015).

Several secondary metabolites produced by fungi are also allelochemicals (Brown, 1967; Vikrant *et al.*, 2006; Idrees, 2008; Cimmino *et al.*, 2014; Osivand *et al.*, 2018). The phytochemicals of fungi are dependent on the strength, quantity, and variety of allelochemicals (Xuan *et al.*, 2005). Some kinds of fungi containing herbicidal components inhibited the growth of target plants and might be a promising natural tool to combat the environmental pollution challenges and the development of herbicide resistance (Xuan *et al.*, 2005). Utilization of phytotoxicity from fungi to control weeds in agricultural field has received increasing attention (Khanh *et al.*, 2008). Therefore, isolation and identification of the active phytotoxic substances from fungal metabolites need to have more efforts.

C. militaris is a fungus belonging to the class Ascomycetes (Dong *et al.*, 2013). The fruiting body of *C. militaris* contains various active constituents such as cordycepin, polysaccharides, adenosine, fatty acids, and other chemicals (Quy *et al.*, 2019). Among of them, cordycepin, a nucleoside analog (3'-deoxyadenosine), exhibited the most biological and pharmaceutical functions such as antineoplastic, anti-inflammatory, and a decrease in tumor cell proliferation (Wu *et al.*, 2007; Lee *et al.*, 2012; Wang *et al.*, 2014). Thus, *C. militaris* possessed a wide spectrum of medicinal properties including anti-stress, antifatigue (Koh *et al.*, 2003), antioxidant (Liu *et al.*, 2016), antifungal, and anticancer (Cho and

Kang, 2018). However, the allelopathic activity of this fungus has not been comprehensively investigated.

The present study evaluates the phytotoxic effects of *C. militaris* on radish (*Raphanus sativus*) and identify the active herbicidal compounds from this fungus. Besides, the use of different extraction methods to get a maximum yield of cordycepin have been conducted.

4.2 Materials and methods

4.2.1 Reagents

Methanol plus and methanol were obtained from Junsei Chemical Co., Ltd., Tokyo, Japan. Ethyl acetate, chloroform, hexane, and acetone were provided by Kanto Chemical Co. Inc., Tokyo, Japan. Radish seed was bought from Sakata Seed Co. Inc., Yokohama, Japan.

4.2.2 Plant materials

C. militaris fruiting-bodies were obtained by Truc Anh Company, Vietnam. The sample was harvested and dried by freeze-drying machine (Mactech MSL1000, Mactech, Hanoi, Vietnam) at 15 °C. Then, the sample was sterilized and packaged in a sealed container and deposited at Laboratory of Plant Physiology and Biochemistry, Hiroshima University, Japan for further analysis.

4.2.3 Preparation of plant extract

The fruiting-bodies of *C. militaris* were soaked in water at ambient temperature for 12 h and dried at 50 °C for two days before pulverized to powder by using a grinding machine. The powder (1.0 kg) was immersed in 15 L methanol (MeOH) for 2 weeks at room temperature. The MeOH extract (126.14 g) was mixed with distilled water (500 mL) and then fractionated with hexane, chloroform and ethyl acetate (EtOAc). The fractionation process resulted in 10.24 g of hexane (10.25%), 19.25 g of chloroform (19.28%), 50.21 g of EtOAc (50.27%), and 20.17 g of water residue (20.20%) crude extracts, respectively. The crude extract with the highest herbicidal property was used for further separation using column chromatography.

4.2.4 Fractionation of ethyl acetate extract

The ethyl acetate extract (16.28 g) showed the highest phytotoxic activity on a preliminary assay was isolated in a normal phase of column chromatography (40 mm diameter × 600 mm height) filled with silica gel (size Å 60, 200-400 mesh particle size, Sigma-Aldrich, Tokyo, Japan) (Figure 5). This process yielded eight fractions by the following eluents: CM1 in CHCl₃, CM2 in CHCl₃:MeOH (9.5:0.5), CM3 in CHCl₃:MeOH (9:1), CM4 in CHCl₃:MeOH (8.5:1.5), CM5 in CHCl₃:MeOH (7.5:2.5), CM6 in CHCl₃:MeOH (7:3), CM7 in CHCl₃:MeOH (6:4), CM8 in CHCl₃:MeOH (5:5) - MeOH.

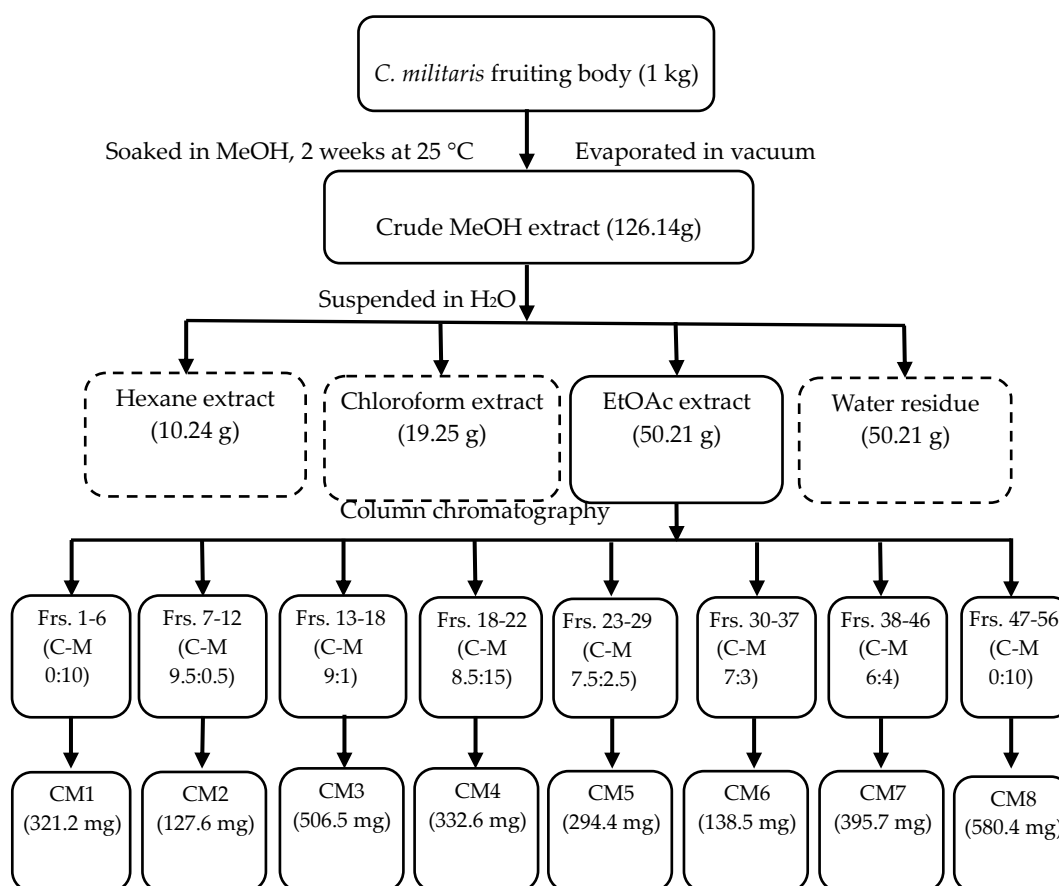


Figure 5. Process of extraction and fractionation of the fruiting-bodies of *C. militaris*.

4.2.5 Germination and growth bioassays

The herbicidal property was evaluated using the protocol described by (Andriana *et al.*, 2018) (Figure 6). An aliquot 300 µL of sample was pipetted in a

plate with 12 wells (22.1 mm diameter × 35 mm height). After methanol solution was evaporated within 5 h at ambient temperature, a total of 10 seeds of radish were placed in each well and added 300 μ L of distilled water. Then, plate was put in a growth chamber. The photoperiod of chamber was day/night 12/12h with a 28/25 $^{\circ}$ C cycle. After 5 days, germinated seeds, root length and shoot height were recorded. The percentages of germination, root, and shoot over the control were evaluated as the inhibition percentage (%). The inhibitions on germination and emergence of radish were expressed by the IC_{50} value, which was the amount to inhibit 50% of the germination, shoot and root of radish, therefore a lower IC_{50} showed a higher herbicidal activity.

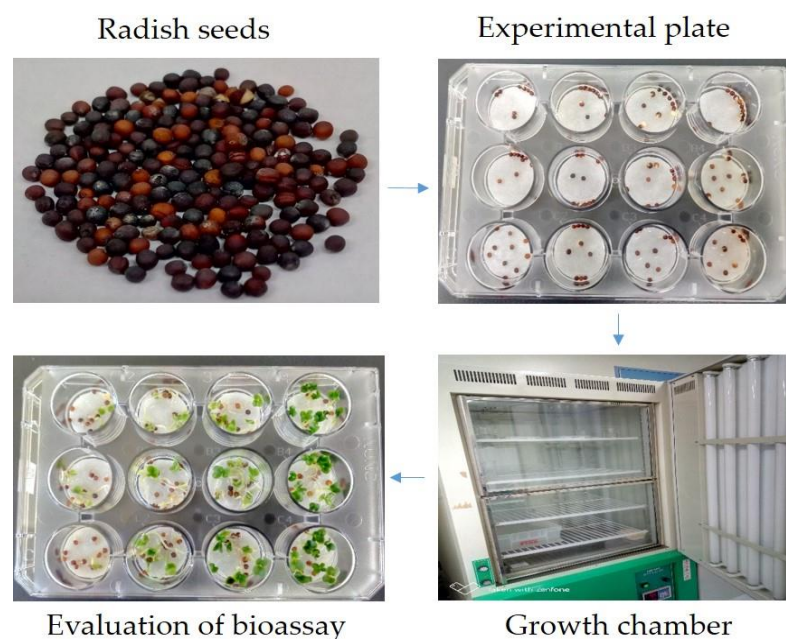


Figure 6. Germination and growth bioassays on radish.

4.2.6 Identification of chemical constituents by gas chromatography-mass spectrometry (GC-MS)

An aliquot of 1 μ L of fraction was injected into a GC-MS system with DB-5MS column, 30 m in length, 0.25 μ m in thickness and 0.25 mm internal diameter (Agilent Technologies, J&W Scientific Products, Folsom, CA, USA). Helium was chosen as the carrier gas with the split ratio 5.0/1.0. The GC oven temperature was began at 50 $^{\circ}$ C without hold time, then increased to 300 $^{\circ}$ C with

a rate 10 °C/min and finally kept for 20 min at 300 °C. The temperatures of injector and detector were set at 300 °C and 320 °C, respectively, with the mass ranges scanned from 29 to 800 amu. The identification of bioactive components was conducted by comparing the mass spectral fragmentation patterns of fractions with the mass spectral libraries of the JEOL's GC-MS Mass Center System version 2.65a software (Van *et al.*, 2018).

4.2.7 Quantification of cordycepin by HPLC

Cordycepin in the fraction CM4 was quantified according to a method reported previously (Zhou *et al.*, 2016). It was measured at 260 nm wavelength by using the system (LC-Net II/ADC, UV-4075 Plus and PU-4180 Plus, Jasco, Tokyo, Japan). A column, J-Pak Symphonia C18 was used with a 250 mm length, 4.6 mm internal diameter and 5 µm thickness. The mobile phase was acetonitrile (A) 10%: water (B) 90%. A gradient elution was applied at 0.8 mL/min of flow-rate with 1 µL of fraction injection volume. Quantification of cordycepin was conducted by evaluating the peak area based on a cordycepin standard curve (5, 10, 50, 100 and 250 µg/mL). Cordycepin in CM4 fraction was identified and quantified by comparing the retention time and peak area of corresponding standard cordycepin.

4.2.8 Determination identification of cordycepin by LC-ESI-MS

The bioactive constituents in the fraction CM4 were identified by LC-ESI-MS technique. The identification was conducted by a positive/negative ion mode by using the system (Thermo Fisher Scientific TM, LTQ XLTM, Ion Trap Mass Spectrometer, Tokyo, Japan). The J-Pak Symphonia C18 column (5 µm, 4.6 mm x 250 mm internal diameter) and mobile phase, acetonitrile (10%): water (90%) was used in the LC phase. One aliquot 1 µL of fraction was injected to the system and the operation time was 30 min with a flow rate of 0.5 mL/min. ESI system conditions were sheath gas flow rate, 60 arb; ion spray voltage, 4.5 kV; aux gas flow rate, 20 arb, capillary voltage, 50V; capillary temperature, 350 °C; tube lens, 80V. MS condition analyses were conducted by using a positive (*m/z* 100-1000) fourier transform mass spectrometer (FTMS) with a resolution of 60000 and

negative (m/z 115-1000) ion trap mass spectrometry (ITMS). Peak processing was measured by using Thermo Xcalibur Qual Browser software (Thermo scientific™, Tokyo, Japan) equipped with library, NIST MS (Minh *et al.*, 2019). The presence of cordycepin in CM4 fraction was identified by comparing its total ion chromatograms (TEC) and mass spectra with those of cordycepin standard.

4.2.9 Cordycepin content in different extractions

Several extraction methods were conducted to obtain maximum yields of cordycepin. Water and methanol were used because of the polarity of these solvents, as cordycepin is a polar component. Different temperatures, times, and ultrasonic conditions were also implemented to get optimal yield of cordycepin from *C. militaris* fruiting body (Table 7).

Table 7. Different extractions for comparing cordycepin content

No.	Fungus Part	Extraction Methods			
		Solvents	Extraction Time	Temperature	Ultrasonic
1	Fruiting body	Methanol	two weeks	Room temperature	-
2	Fruiting body	Water	30 min	100 °C	-
3	Fruiting body	Water	30 min	70 °C	40 Hz, 30 min

-: not employed.

4.2.10 Statistical analysis

All data were analyzed by one-way ANOVA using the Minitab 16.2.3 software (Minitab Inc., Philadelphia, PA, USA). The results were shown as means \pm standard deviations (SD). Tukey's test was used to compare significant differences between control, treatments and standard at the confidence level of 95% ($p < 0.05$).

4.3 Results

4.3.1 Inhibitory effects of crude extracts of *C. militaris*

The effect of four crude extracts fractionated from various solvents are shown in Table 8. In general, all crude extracts inhibit germination, root length

and shoot height of radish, however, the EtOAc extract shows the highest inhibition of germination, root length and shoot height of radish ($IC_{50} = 0.235$, 0.127 and 0.096 mg/mL, respectively). The inhibition capacities of four crude extracts followed the order EtOAc > aqueous > chloroform > hexane, suggesting that the EtOAc extract contains more potent allelochemicals than other crude extracts. So, this extract was thus selected for further fractionation by column chromatography.

Table 8. Inhibition capacities of different crude extracts of *C. militaris* on germination, root and shoot of radish

Extracting Solvents	IC_{50} (mg/mL)		
	Germination	Root	Shoot
Hexane	1.388 ± 0.170^a	1.022 ± 0.132^a	0.794 ± 0.043^a
Chloroform	1.250 ± 0.126^b	0.795 ± 0.033^b	0.641 ± 0.436^a
EtOAc	0.235 ± 0.030^d	0.127 ± 0.008^d	0.096 ± 0.006^b
Aqueous	0.849 ± 0.082^c	0.410 ± 0.042^c	0.556 ± 0.029^a

Data were presented as means \pm standard deviations (SD). Values with different superscript letters (a, b, c, d) in a column indicated a significant difference at $p < 0.05$ according to Tukey's test.

4.3.2 Effects of fractions from the EtOAc extract of *C. militaris*

The isolation of fractions from *C. militaris* fruiting body was conducted following the process illustrated in Figure 19. Finally, the EtOAc extract was isolated by column chromatography (CC) to obtain 8 fractions with their corresponding yields (CM1 to CM8).

The herbicidal property of the obtained fractions, which was evaluated on the germination and emergence of radish, are presented in Table 9. Eight fractions separated from the EtOAc extract possessed various levels of inhibitions. The fraction CM4 shows the strongest inhibitory levels in germination, roots and shoots (IC_{50} values = 0.078 , 0.053 and 0.052 mg/mL, respectively) (Table 9, Figure 7). Overall, the greater effect of CM4 fraction indicates that it preferentially contains strong allelochemicals, more so than the other fractions.

Table 9. Inhibition of different fractions from EtOAc extract of *C. militaris* on germination, root length and shoot height of radish

Fractions	IC ₅₀ (mg/mL)		
	Germination	Root	Shoot
CM1	2.865 ± 0.247 ^a	2.137 ± 0.100 ^a	1.291 ± 0.183 ^{ab}
CM2	2.438 ± 0.108 ^{ab}	0.561 ± 0.213 ^b	1.780 ± 0.350 ^a
CM3	2.090 ± 0.300 ^{bc}	0.467 ± 0.156 ^b	1.682 ± 0.204 ^a
CM4	0.078 ± 0.013 ^d	0.053 ± 0.004 ^c	0.052 ± 0.015 ^d
CM5	1.402 ± 0.121 ^c	0.382 ± 0.030 ^{bc}	0.611 ± 0.019 ^c
CM6	1.442 ± 0.126 ^c	0.368 ± 0.205 ^{bc}	0.862 ± 0.113 ^{bc}
CM7	2.982 ± 0.449 ^a	0.466 ± 0.175 ^b	0.521 ± 0.092 ^{cd}
CM8	2.463 ± 0.449 ^{ab}	0.580 ± 0.076 ^b	0.523 ± 0.165 ^{cd}

Data presented means ± standard deviations (SD). Values with different superscript letters (a, b, c, d) in a column were significantly different according to Tukey's test ($p < 0.05$).

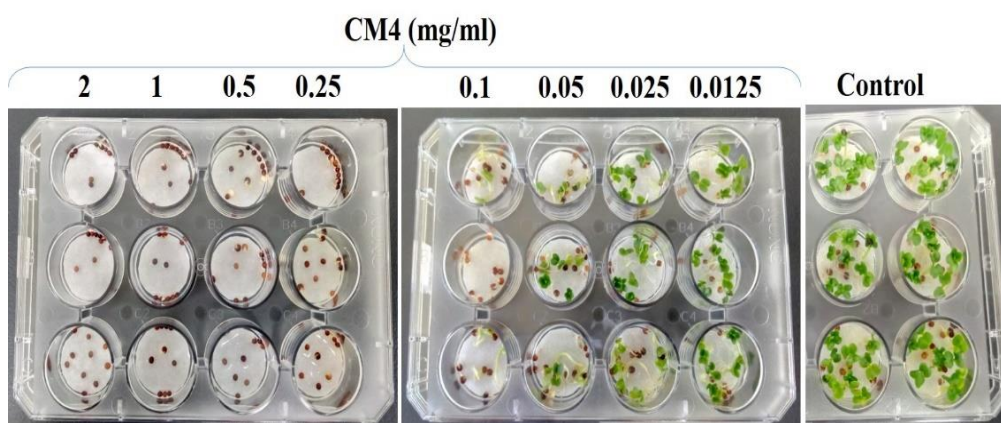


Figure 7. Figure of inhibition on radish of CM4 fraction and control.

4.3.3 Identification chemical compounds in CM4 fraction

The phytochemical constituents in the fraction CM4 (crystal mixture) was analysed by gas chromatographic-mass spectrometry (GC-MS). Among the identified components, cordycepin (a purine nucleoside) appeared as the major compound with 55.38 % of peak area, while pentadecanal and 1,6-anhydro- β -D-glucopyranose were also detected with lower peak area percentages (19.79% and 0.54%, respectively) (Table 10).

Table 10. Identification of bioactive compounds in CM4 fraction from *C. militaris* by GC-MS analysis

No	Compounds	Chemical Formula	MW (g/mol)	Chemical Classification	GC-MS		Fraction
					Rt (min)	Area (%)	
	β -D-						
1	Glucopyranose, 1,6-anhydro	C ₆ H ₁₀ O ₅	162.14	Anhydrohexose	11.76	0.54	
2	Pentadecanal	C ₁₅ H ₃₀ O	226.40	Fatty aldehydes	14.52	19.79	CM4
3	Cordycepin	C ₁₀ H ₁₃ N ₅ O ₃	251.24	Purine Nucleoside	21.98	55.38	

4.3.4 Determination and quantification of cordycepin by high-performance liquid chromatography (HPLC)

The HPLC chromatograms of standard cordycepin and fraction CM4 are shown in Figures 8 a, b. Cordycepin was determined at 9.78 min in the HPLC profile of both standard cordycepin and the CM4 fraction. By HPLC quantification, the yield of cordycepin in fraction CM4 was 0.226 g.

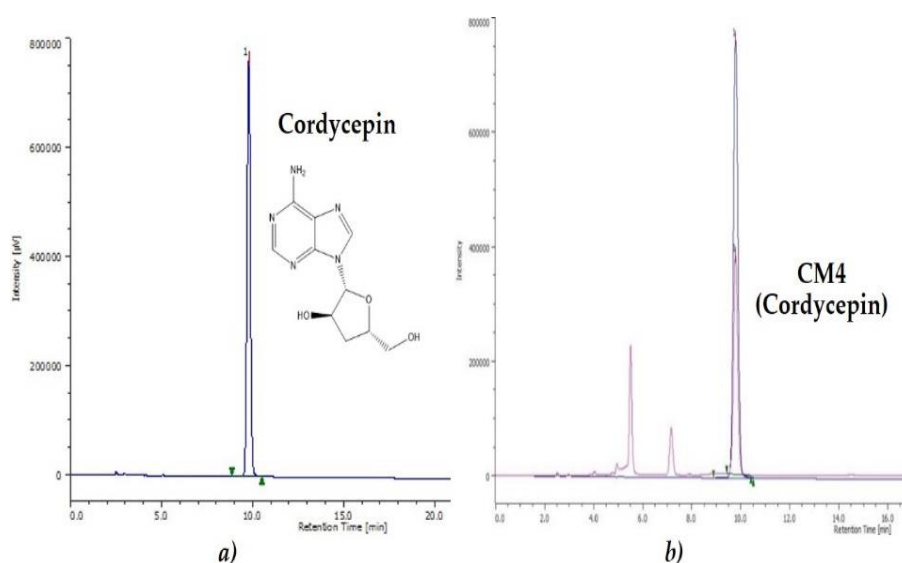


Figure 8. (a) HPLC chromatogram of cordycepin standard, (b) HPLC chromatogram of cordycepin in the fraction CM4 compared with the cordycepin standard (0.5 mg/mL).

4.3.5 Cordycepin detection by liquid chromatography-electrospray ionization-mass spectrometry (LC-ESI-MS)

The LC-ESI-MS results from Figure 9 determined the presence of cordycepin in the fraction CM4 (13.7 min; $[M+H]^+$ m/z : 252.1; $[M + Na]^+$ m/z : 274.1). Positive fourier transform mass spectrometry (FTMS) mode was used and certain mass range scans resulted in a total ion chromatogram (TIC) of the CM4 fraction, which showed major peaks. The retention time and fragmentation patterns from the peak in the fraction CM4 were identified as cordycepin, which coincided with that of the cordycepin standard (Appendix B, Figure 127).

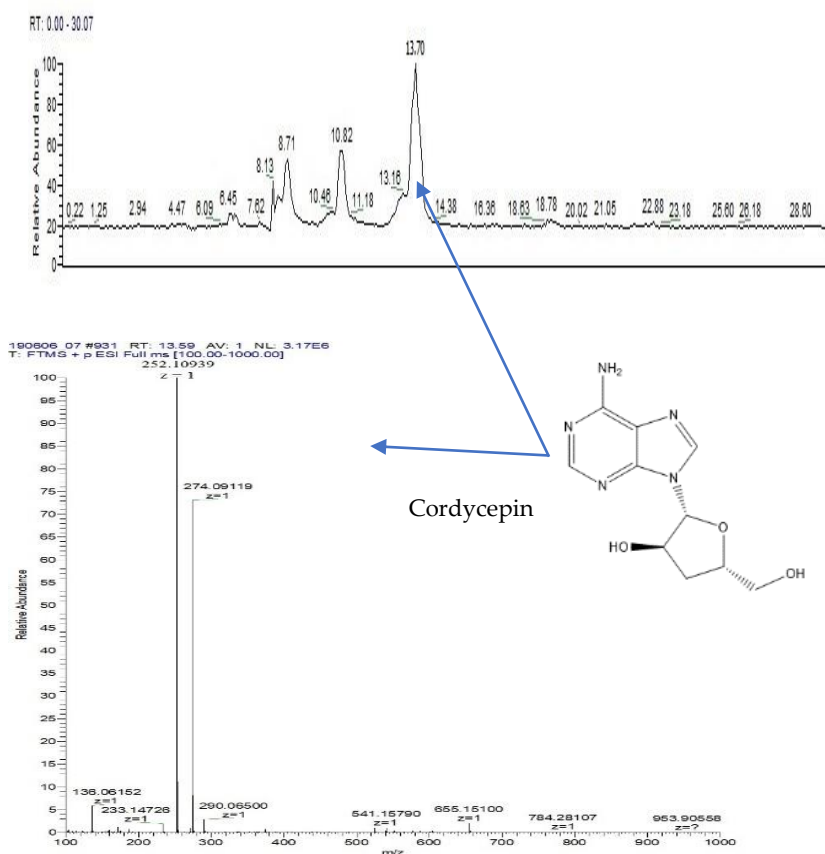


Figure 9. Total ion chromatogram and mass of cordycepin detected in the CM4 fraction by LC-ESI-MS.

4.3.6 Comparison of cordycepin yields in different extractions

Table 11 presented a comparison of the cordycepin yields obtained by three extraction methods. Methanol extraction provided the maximum amount of

cordycepin (6.166 mg/g DW) as compared to other extractions, while the use of a temperature of 70 °C combined with ultrasonic for 30 min obtained greater amounts of cordycepin than using a temperature of 100 °C in 30 min (Table 11). In general, the use of methanol solvent was more effective than water extraction of cordycepin.

Table 11. Comparison of cordycepin yield in different extractions

No.	Fungus Part	Extraction Methods				Cordycepin (mg/g DW)
		Solvents	Extraction Times	Temperatures	Ultrasonic	
1	Fruiting body	Methanol	two weeks	Room temperature	-	6.166 ± 0.021 ^a
2	Fruiting body	Water	30 min	100 °C	-	3.548 ± 0.012 ^b
3	Fruiting body	Water	30 min	70 °C	40 KHz, 30 min	4.248 ± 0.027 ^b

Data were presented as means ± standard deviations (SD). Values with different superscript letters (a, b) in a column indicated a significant difference at $p < 0.05$ according to Tukey's test. -: not employed; DW: dry weight.

4.4 Discussion

Allelopathy is a common biological phenomenon in nature. This phenomenon has been defined as any process involving secondary metabolites produced by plants, fungi and micro-organisms that influence the growth and development of agricultural and biological systems (Soltys *et al.*, 2013; Achatz *et al.*, 2014). Allelochemicals are active biomolecules that can be detected in leaves, fruits, roots, flowers or stems and also be found in the surrounding soils released by organisms. The production of these phytochemicals depends on various factors such as the stage of growth, species, abiotic and biotic stresses (Cheema *et al.*, 2013).

Due to their natural origin, allelochemicals will not only be biodegradable but also less polluting than herbicides because most of them have short half lives compared to synthetic pesticides (Qian *et al.*, 2009a; Trezzi *et al.*, 2016). Therefore, allelopathy can become a promising tool for the sustainable

development of agricultural production because of the inhibition of weed growth associated with the prevention of weed resistance to commercial herbicides (Xuan *et al.*, 2001; Cheng and Cheng, 2015). Released from allelopathic plants, allelochemicals such as momilactones, phenolics, alkaloids, carbohydrates, amino acids, purines and nucleosides are important sources for natural herbicide development (Cheng and Cheng, 2015; Van *et al.*, 2018; Tzvetkova *et al.*, 2019). Thus, natural phytotoxic compounds from herbal plants and medicinal fungi may help decrease the use of synthetic herbicides for weed control, reducing pollution, and providing safer agricultural products of high quality (Sodaeizadeh *et al.*, 2010).

The present study revealed that EtOAc extract of *C. militaris* had the maximum inhibitory effects on the germination and emergence of radish, as compared to hexane, chloroform, and aqueous extracts (Table 8). This result suggests that EtOAc extract of *C. militaris* fruiting body might contain more principal allelochemicals. In fact, extraction with various suitable solvents can also obtain high yields of potent allelochemicals (Van *et al.*, 2018). Among fractions isolated by column chromatography eluted by chloroform and methanol (10:0 to 0:10 v/v), CM4 was the most active fraction to inhibit the germination, root length and shoot height of radish (Table 9). The analyses of GC-MS, HPLC and LC-ESI-MS confirmed that cordycepin, a purine nucleoside was the major component in fraction CM4 (55.38%) (Table 10).

Additionally, purine alkaloids were reported to inhibit 90% of root growth of lettuce at 1.5 mM concentration (Cho *et al.*, 1980), 50% of root growth of maize at 0.5 mg/mL (Anaya *et al.*, 2006), and completely inhibited root growth of coffee at 10 mM (Friedman and Waller, 1983). In particular, nebularine, a purine nucleoside inhibited 50% of shoot growth of wheat at 1.0 mM dose (Brown and Konuk, 1994), reduced cell division and chromosome contraction of onion at 0.01% (Löfgren *et al.*, 1954). Therefore, cordycepin as well as purine nucleoside play an important role in plant growth inhibition as previous report (Cheng *et al.*, 2015; Rice *et al.*, 1984). Besides, methanol extraction for two weeks provided more cordycepin than hot water extraction (70-100 °C) (Table 11), and it was

found that repeat boiling of the fruiting bodies of *C. militaris* combined with ultrasonic apparently provided greater yields of cordycepin than a single boil. Commonly, cordycepin is isolated and separated from a liquid medium of *C. militaris*. In this study, cordycepin from the fruiting body of *C. militaris* was isolated. Compared with the previous study that isolated cordycepin from *C. militaris* fruiting body (Zhang *et al.*, 2016) by high-speed countercurrent chromatography, the present technique is more simple and obtains a higher yield.

Several factors, such as the temperature, type of solvents, extraction time and sonication affect the yield of bioactive constituents isolated from plant and fungi (Mokrani and Madani, 2016). In the present study, extraction time and solvent polarity may affect the yield of cordycepin in *C. militaris* fruiting body. Additional solvents combined with different extracting methods should be examined to obtain maximum yields of cordycepin from *C. militaris*. This research shows that *C. militaris*, with cordycepin as its active component, effectively controls the germination and growth of radish *in vitro* experiment.

4.5 Conclusion

The current study investigated the inhibitory potential of *C. militaris* on the germination, root length and shoot height of radish. Among isolation fractions from the fruiting body of *C. militaris*, CM4 was the most active fraction to inhibit the germination and emergence of radish. GC-MS, HPLC, and LC-ESI-MS analyses found that the major phytotoxic compound in fraction CM4 was cordycepin (a purine nucleoside). This is the first study to reveal that cordycepin isolated from *C. militaris* acts as an allelochemical, effectively inhibits plant growth and may be a promising natural source to develop plant-based herbicides in agricultural production.

5 Cordycepin isolated from *Cordyceps militaris*: Its newly discovered herbicidal property and potential plant-based novel alternative to glyphosate and paraquat

5.1 Introduction

During the last decades, a significant number of synthetic herbicides have been used in agricultural, urban, or domestic applications (Bonnet *et al.*, 2007). Although commercial herbicides are a highly effective tools to control weeds, they have led to a change in the phytosociological composition of weeds and to a selection of herbicide-resistant weeds. In particular, they also cause impacts in the environment and human health (Aparecida *et al.*, 2013; Jugulam and Chandrima, 2019).

Benzoic acid (BA) is one of phytotoxic compound belongs to phenolic group which the most studied (Sunaina and Singh, 2015). BA is used as a commercial herbicide (Bhowmik and Inderjit, 2003) and is reported to modify in susceptible plants physiological processes such as the net photosynthetic rate, nutrient uptake, stomatal conductance, and resulted in growth inhibition (Yu *et al.*, 2003; Kaur *et al.*, 2005; Gao *et al.*, 2018). Recently, Andriana *et al.* (2018) reported that BA totally inhibited the germination of radish (*Raphanus sativus*) at a concentration of 1.0 mg/mL in the germination and growth bioassays. However, benzoic acid or dicamba herbicide is often responsible for injury to non target organisms such as delaying flowering and reducing the number of flowers of plant species, especially affecting beneficial insect communities in agricultural landscapes (Egan *et al.*, 2014; Bohnenblust *et al.*, 2016).

Besides, glyphosate and paraquat are the most commonly herbicides used upon by farmers around the world (Annett *et al.*, 2014; Kongtip *et al.*, 2017; Kniss, 2017). Glyphosate, N-(phosphonomethyl) glycine is a broad spectrum, nonselective and post emergence herbicide in agricultural production field since

1970 (Bruggen *et al.*, 2018; Hagner *et al.*, 2019). Due to its effectiveness against most annual and perennial weeds, glyphosate has become one of the most popularly used herbicide in agricultural and non-agricultural cultivation systems (Tzvetkova *et al.*, 2019). This herbicide is not only known for its effectiveness but also for its indirect impacts on non-target organisms (Slaby *et al.*, 2019). In March 2015, the US Environmental Protection Agency (EPA) and the International Agency for Research on Cancer (IARC) has classified glyphosate in the group 2A as a probable carcinogen to humans (Tarazona *et al.*, 2017).

Paraquat (PQ, 1,1'-dimethyl-4,4'-bipyridinium dichloride) is an extensively used herbicide in more than 100 countries (Huang *et al.*, 2019). It can quickly kill green plant tissue upon contact with non-selective action (Santos *et al.*, 2013). PQ is used against many kinds of annual or perennial weeds, but it is also a highly toxic chemical for humans and animals (Frimpong *et al.*, 2018). In fact, the greatest weed management challenge for safe and sustainable agriculture is the lack of effective natural product herbicides. Their suppression of weeds can reduce the use of synthetic herbicides (David *et al.*, 2003) and natural phytotoxic compounds may be the next-generation herbicides (Dayan and Duke, 2014).

The present study evaluates the phytotoxic potential of *C. militaris* on *R. sativus* (radish), *Echinochloa crus-galli* (barnyard grass) compared with BA in a search for nature-based alternatives for disputed herbicides, such as paraquat and glyphosate. More specifically, the inhibition of cordycepin on biochemical and physiological responses of radish seedlings including total flavonoid contents (TFC), total phenolic contents (TPC), chlorophyll and carotenoid contents, lipid peroxidation, electrolyte leakage, and proline contents were also evaluated in this study.

5.2 Materials and methods

5.2.1 Chemicals

Folin-Ciocalteu's phenol, proline, cordycepin, trichloroacetic acid (TCA), thiobarbituric acid (TBA), glacial acetic acid, ninhydrin, sulfosalicylic acid and toluene were provided by Sigma-Aldrich Japan K.K., Tokyo, Japan. Methanol

plus, methanol, and sodium carbonate and aluminum (III) chloride hexahydrate were bought from Junsei Chemical Co., Ltd., Tokyo, Japan. Ethyl acetate, hexane, chloroform, and acetone were purchased from Kanto Chemical Co. Inc., Tokyo, Japan. Radish seed was bought from Sakata Seed Co. Inc., Yokohama, Japan.

5.2.2 *Plant materials and CM4 fraction*

The *C. militaris* fruiting body of were provided by Truc Anh Company, Bac Lieu city, Vietnam. The samples were harvested and dried by freeze-drying machine at 15 °C (Mactech MSL1000, Mactech, Hanoi, Vietnam). The dried and sterilized samples were packaged in a sealed container and deposited at 4 °C for further analysis.

C. militaris fruiting-bodies powder (1 kg) was soaked in 15 L methanol, evaporated by vacuum machine, and fractionated using hexane, chloroform, ethyl acetate, and water to get 50.21 g of ethyl acetate extract. This extract (16.28 g) was then fractionated by using column chromatography with chloroform and methanol as the solvent system to get eight fractions. Among isolated fractions, CM4 from using CHCl₃:EtOAc, 8.5:1.5 as an eluent showed the most effective inhibition in herbicidal property, was then used for physiological and biochemical responses evaluations.

5.2.3 *Germination and growth bioassays*

The germination and growth bioassays were conducted by filter paper according to using the protocol previously reported (Andriana *et al.*, 2018). The radish seeds were sterilized with sodium hypochlorite (5 %) for 5 min then rinsed with distilled water four times. There were ten seeds were sowed in in a growth chamber. The test solutions (300 µL) were added to each 12 well-plate (22.1 mm diameter × 35 mm height) lined with filter papers. After methanol in the wells was allowed to evaporate within 6 h at room temperature, a total of 10 healthy seeds of radish were placed in each well and then added 300 µL of distilled water. The plate was put in a growth chamber (Biotron NC system, Nippon Medical & Chemical Instrument, Co. Ltd, Osaka, Japan). An additional volume of 100 µL distilled water was added subsequently at the 2nd, 3rd, and 4th days. The

photoperiod of growth chamber was day/night with a 28/25 °C cycle. Methanol was used as control. The bioassay was replicated three times. After five days, germination rate, shoot height and root length were evaluated. The percentages of germination, shoot height and root length over the control were expressed as the inhibition percentage (%). Concentration in reducing 50% of germination, shoot height and root length (IC₅₀) were also calculated and expressed.

5.2.4 *Physiological responses*

5.2.4.1 *Chlorophyll and carotenoid contents*

Chlorophyll (a, b), total chlorophylls, and carotenoid contents of radish seedlings were evaluated following the protocol described previously (Ladhari *et al.*, 2014). Briefly, 100 mg fresh weight (FW) of radish seedling leaves was put in a test tube, ground, and pipetted 1.5 mL of acetone solution (80%). The tube with mixture was centrifuged at 15,000 rpm and supernatant absorbance was read at 663, 645 and 440 nm wavelength by a microplate reader. The applied concentration of cordycepin, the CM4 fraction, as well as BA was 0.04 mg/mL (40 ppm). This dose was applied because it was close to the IC₅₀ value of the most inhibitory CM4 fraction (Table 2). The contents of all pigments were evaluated as µg/g FW with according to the formulas:

$$\text{Chlorophyll a } (\mu\text{g/g}) = 12.7 \times A_{663} - 2.69 \times A_{645}$$

$$\text{Chlorophyll b } (\mu\text{g/g}) = 22.9 \times A_{645} - 4.68 \times A_{663}$$

$$\text{Total chlorophylls } (\mu\text{g/g}) = 20.2 \times A_{645} + 8.02 \times A_{663}$$

$$\text{Total carotenoid } (\mu\text{g/g}) = (4.7 \times A_{440} - (1.38 \times A_{663} + 5.48 \times A_{645}))$$

5.2.4.2 *Electrolyte leakage*

The electrolyte leakage of radish seedlings was determined based on the protocol reported previously (Jaballah *et al.*, 2017). An amount of 100 mg freshly roots or aerial parts was put in the test tube with 15 mL of distilled water. Then, the tubes were placed at room temperature for 24 h, 48 h and the initial electrical conductivity (EC1) was evaluated by an electrical conductivity meter. The micro

tube was then autoclaved for 20 min at 121 °C to completely release all electrolytes and quickly reduced to 25 °C. The second electrical conductivity (EC2) was measured. The applied concentration of cordycepin, the fraction CM4 as well as BA was 0.04 mg/mL (40 ppm). The electrolyte leakage (EL) percentage was determined following the equation:

$$\% \text{ Electrolyte leakage (EL) } = \left(\frac{EC_1}{EC_2} \right) \times 100$$

5.2.4.3 Lipid peroxidation

Lipid peroxidation was measured as malondialdehyde (MDA) by using thiobarbituric acid (TBA) following the previous report (Farooq *et al.*, 2016). Fresh samples of aerial parts or roots from 5th day (100 mg) were homogenized in 1.5 mL 0.1% trichloroacetic acid (TCA) and then centrifuged at 15,000 rpm for 20 min at 4 °C. An aliquot of 250 µL of the supernatant was transferred to a microtube, and pipetted 750 µL thiobarbituric acid (TBA, 0.5%) in TCA (20%). The test tube was heated for 10 min at 90 °C in a dry bath incubator. The tube with mixture was cooled down for 5 min in an ice bath. After centrifugation at 10,000 rpm at 4 °C for 5 min, the absorbance of the supernatant was recorded at 532 and 600 nm wavelength by a microplate reader. The MDA quantity was calculated by using an extinction coefficient ($\epsilon = \text{ m} / \text{cm}$). The applied dose of cordycepin, the CM4 fraction as well as BA was 0.04 mg/mL. The results were expressed as nmol MDA/g FW using the formula:

$$\text{MDA (mM/L)} = (A_{532} - A_{600}) / \epsilon$$

5.2.5 Biochemical responses

5.2.5.1 Quantification of total phenolic contents

The total phenolic contents (TPC) were determined according to the protocol described by Quan *et al.* (2019). Briefly, 100 mg of fresh samples of roots or aerial parts was extracted in 24 h with 1.5 mL of MeOH and centrifuged at 15,000 rpm at 4 °C for 15 min. Then, the supernatant was applied for the total phenolic assay. Briefly, 20 µL of the test solution was homogenized 100 µL of the Folin-Ciocalteu's reagent and 80 µL sodium carbonate (10% and 7.5%,

respectively). The absorbance was read at 765 nm wavelength after 30 min of incubation at room temperature. The TPC was expressed as mg gallic acid equivalent per g of fresh weight of roots or aerial parts (mg GAE/g FW).

5.2.5.2 Quantification of total flavonoid contents

The flavonoid contents were measured according to a previous report (Rayee *et al.*, 2018). In brief, a volume of 100 μ L of the MeOH extract (roots or aerial parts) was mixed with 100 μ L aluminum (III) chloride hexahydrate (2% w/v in MeOH) in a microplate. The absorbance of mixture was recorded at 430 nm wavelength after 30 min incubation at room temperature. The total flavonoid contents (TFC) was presented as mg quercetin equivalent per g fresh weight of roots or aerial parts (mg QE/g FW).

5.2.5.3 Proline content

Proline content was evaluated as reported by Hodaei *et al.* (2018). Briefly, an amount of 10 mg of sample powder (roots or aerial parts) was homogenized with 1.5 mL of sulfosalicylic acid 3% and centrifuged at 15,000 rpm for 10 min. Then, a volume of 250 μ L of the supernatant was mixed with 250 μ L of glacial acetic acid and 250 μ L ninhydrin reagent (40 mL 6 M H_3PO_4 and 2.5 g ninhydrin in 60 mL glacial acetic) in a micro-tube. It was incubated at 100 $^{\circ}C$ in a water bath for 1 h and quickly cooled down in an ice bath to stop the reaction. After addition of 500 μ L toluene, the upper phase was read at 520 nm against toluene blank. L-proline (2.5-50 μ g/mL) was applied as a standard and proline determination was evaluated as μ mol/g FW.

5.2.6 Statistical analysis

The statistical analysis was analyzed by one-way ANOVA by using the Minitab software (Minitab Inc., Philadelphia, PA, USA). The values of treatments, controls, and standards were shown as means \pm standard deviations (SD). The significant differences between means were determined by using Tukey's test at confidence level of 95% ($p < 0.05$).

5.3 Results

5.3.1 Effects of cordycepin, CM4 fraction, BA, glyphosate and paraquat on radish and barnyard grass.

The inhibitory effects of cordycepin, the fraction CM4, BA, glyphosate and paraquat were shown in Table 12. The CM4 fraction and cordycepin both shows strong suppression of the germination of radish from 4.6- to 5.9-fold as compared to benzoic acid. Similarly, They also presented much greater inhibition on the root length (3.5- to 4.5-fold) and shoot height (3.5- to 3.8-fold) than benzoic acid. Overall, it was concluded that the inhibition capacities of CM4 fraction and cordycepin were both greater than that of benzoic acid, by 3.5- to 5.9-fold on the germination and growth of radish. The inhibition of cordycepin was found to be greater than that of fraction CM4, but they were not statistically significant difference (Table 12).

Table 12. Effects of cordycepin, CM4 fraction, BA, paraquat and glyphosate on the germination and emergence of radish

Treatments	IC ₅₀ (mg/mL)			References
	Germination	Root	Shoot	
Benzoic acid	0.357 ± 0.052 ^a	0.183 ± 0.017 ^a	0.180 ± 0.004 ^a	present study
CM4	0.078 ± 0.013 ^b	0.053 ± 0.004 ^b	0.052 ± 0.015 ^b	present study
Cordycepin	0.061 ± 0.001 ^b	0.041 ± 0.003 ^b	0.047 ± 0.004 ^b	present study
Paraquat *	0.197	0.046	> 0.224	(Tzvetkova <i>et al.</i> , 2019)
Glyphosate *	0.226	0.137	0.161	(Tzvetkova <i>et al.</i> , 2019)

Data expressed means ± standard deviation (SD). Means with different superscript letters (a, b) in a column were significantly different according to Tukey's test ($p < 0.05$). * Germination and growth bioassays of paraquat and glyphosate on radish were conducted in a petri dish assay (Tzvetkova *et al.*, 2019).

Besides, compared to the previous report (Tzvetkova *et al.*, 2019), cordycepin was stronger than paraquat by 3.2-fold on the germination and over 4.8-fold on the shoot of radish, but nearly similar at root inhibition. Additionally, cordycepin also exhibited phytotoxicity on radish more effective than glyphosate by 3.3- to 3.7-fold on the germination and emergence of radish (Table 12).

Table 13. Effects of CM4 fraction, BA, cordycepin and glyphosate on the germination and growth of barnyard grass

Treatments	IC ₅₀ (mg/mL)			References
	Germination	Root	Shoot	
Benzoic acid	0.598 ± 0.102 ^a	0.305 ± 0.020 ^a	0.402 ± 0.057 ^a	present study
CM4	0.105 ± 0.015 ^b	0.062 ± 0.007 ^b	0.055 ± 0.002 ^b	present study
Cordycepin	0.072 ± 0.018 ^b	0.052 ± 0.008 ^b	0.056 ± 0.002 ^b	present study
Paraquat *	0.126			(Egley & Williams, 1978)
Glyphosate *	> 0.250			(Egley & Williams, 1978)

Data express means ± standard deviation (SD). Means with different superscript letters (a, b) in a column were significantly different according to Tukey's test ($p < 0.05$).

* Germination and growth bioassays of paraquat and glyphosate on barnyard grass were conducted in a petri dish assay (Egley and Williams, 1978).

The herbicidal property on barnyard grass of cordycepin, fraction CM4, BA, paraquat and glyphosate are presented in Table 13. Cordycepin and fraction CM4 gave strong inhibition on the germination (5.7- to 8.3-fold), root length (4.9- to 5.9-fold), shoot height (7.2- to 7.3-fold) of barnyard grass as compared to benzoic acid. Similar to the results on radish, the phytotoxicity of cordycepin on *Echinochloa crus-galli* was stronger than that of CM4, but statistical analysis was not different. In particular, cordycepin was also stronger than paraquat (1.8-fold) and glyphosate (>3.5-fold) on the germination as compared to previous study (Egley and Williams, 1978) (Table 13).

5.3.2 Physiological responses to cordycepin, CM4 fraction and benzoic acid

5.3.2.1 Chlorophyll and carotenoid contents

Cordycepin, CM4 fraction, and benzoic acid reduced the chlorophyll and carotenoid contents of radish by 40 ppm, although the inhibitory capacities varied (Figure 10). The fraction CM4 significantly decreases chlorophylls (a, b, and total chlorophylls) and carotenoid accumulations by 80.65%, 80%, 80.43%, and 70%, respectively, as compared to the control. Besides, cordycepin reduces chlorophylls and carotenoids concentrations remarkably higher than both CM4 and BA.

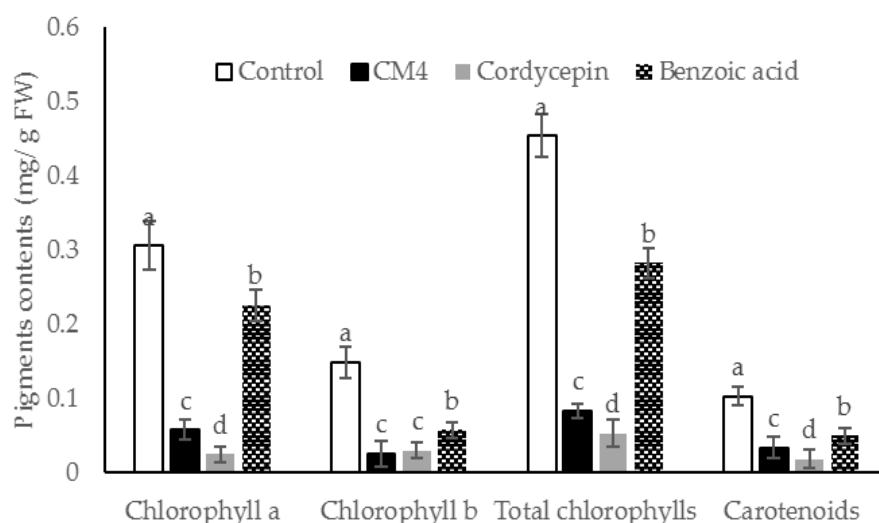


Figure 10. Chlorophylls and carotenoids contents of radish treated by cordycepin, CM4 fraction and BA at 40 ppm. Values with similar superscript letters (a, b, c, d) in bars were not significantly different according to Tukey's test ($p < 0.05$).

Overall, the reduction of accumulation levels is as follows: cordycepin > CM4 > BA. Findings from Table 12, 13 and Figure 25 indicate that cordycepin acts as an herbicidal compound, which strongly inhibits germination and emergence of radish, as well as the contents of chlorophylls a and b and carotenoids. Both cordycepin and CM4 caused significantly stronger inhibition than benzoic acid.

5.3.2.2 Electrolyte leakage

Compared to controls, the levels of electrolyte leakage of the aerial parts and roots of radish caused by cordycepin, fraction CM4, and BA are variable (Figure 11); with all treatments and after 24 and 48 h, values of electrolyte leakage (EL) are significantly higher as compared to controls. Additionally, the EL value provoked by cordycepin was remarkably greater than the one caused by fraction CM4 and benzoic acid, while fraction CM4 caused markedly higher EL than benzoic acid (Figure 11). The conclusion is reached that treatment of cordycepin, fraction CM4 and benzoic acid promoted electrolyte leakage values of radish, substantiating their potential herbicidal property.

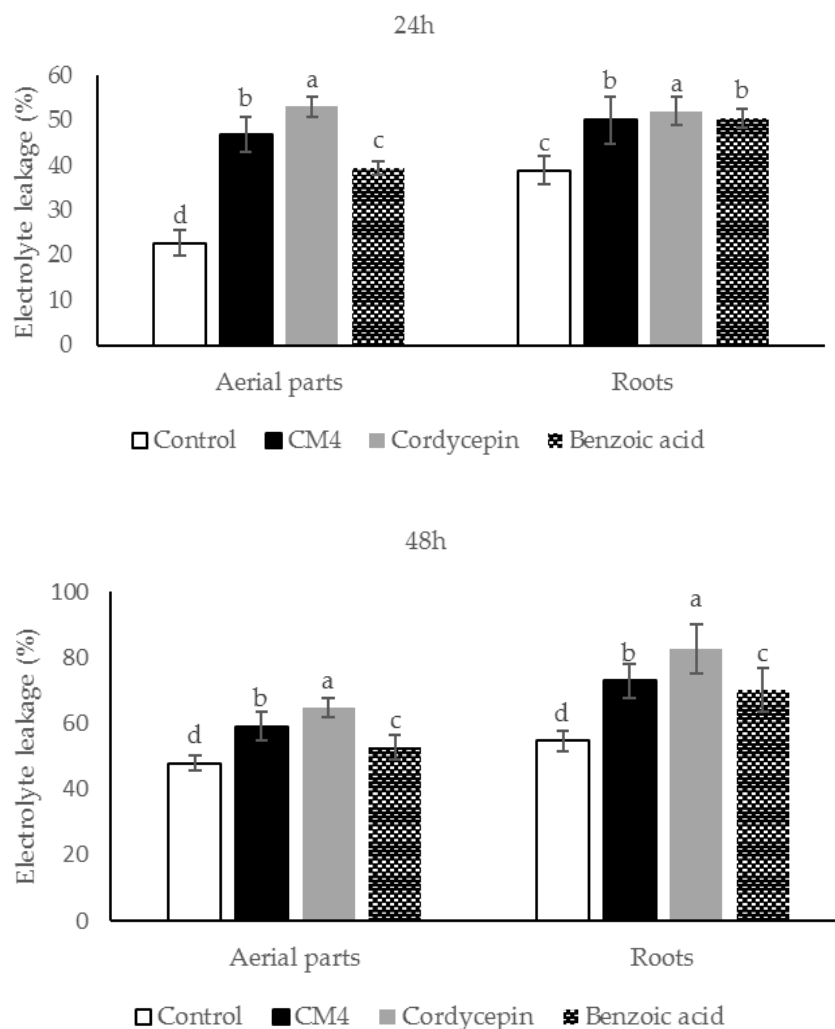


Figure 11. Electrolyte leakage of radish treated by cordycepin, CM4 fraction and BA at 40 ppm. Values with similar superscript letters (a, b, c, d) in bars were not significantly different according to Tukey's test ($p < 0.0$).

5.3.2.3 Lipid peroxidation

The responses of radish to cordycepin, fraction CM4, and benzoic acid in malondialdehyde (MDA) content are illustrated in Figure 12.

All treatments significantly promote lipid peroxidation in both the roots and aerial parts. The fraction CM4 remarkably increases the MDA accumulation of radish by 2.26- and 3.28-fold in the roots and aerial parts as compared to controls (Figure 12).

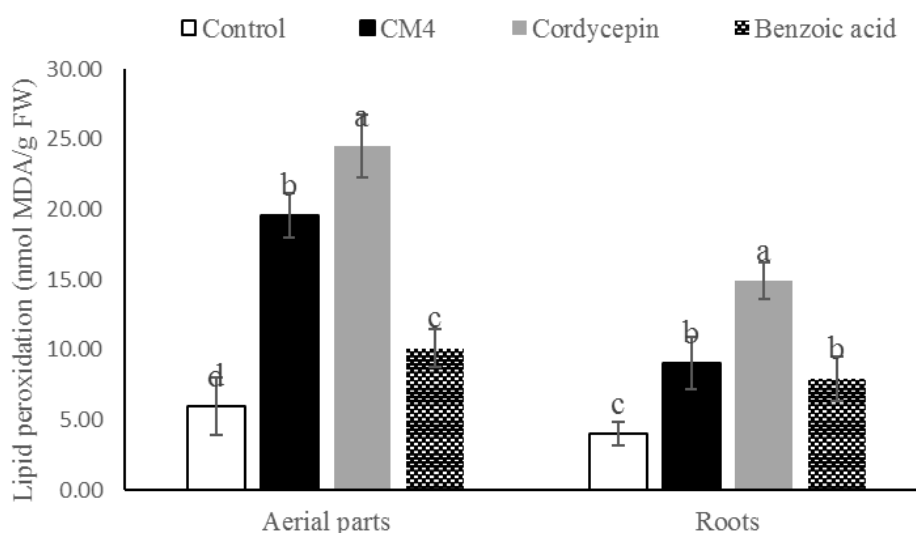


Figure 12. Lipid peroxidation accumulation in radish among control and treatments (cordycepin, CM4 fraction and BA) at 40 ppm. Values with similar superscript letters (a, b, c, d) in bars were not significantly different according to Tukey's test ($p < 0.05$).

Furthermore, the MDA accumulation in the radish by the fraction CM4 is higher than accumulation by benzoic acid in the aerial parts. However, cordycepin causes maximum capacity of lipid peroxidation as compared with either fraction CM4 or BA (Figure 12).

5.3.3 Biochemical responses to the CM4 Fraction, cordycepin and benzoic acid

5.3.3.1 Total phenolic contents

The effects of cordycepin, fraction CM4, and benzoic acid on the total phenolic contents of radish are variable (Figure 13). Fraction CM4 treatment significantly enhanced the TPC in the aerial parts and roots of the radish by 42.95% and 87.69%, respectively, as compared with controls. The total phenolic contents by fraction CM4 is similar to cordycepin and benzoic acid in the aerial parts, however, the total phenolic contents in the roots of the radish caused by cordycepin is remarkably higher than that caused by benzoic acid (Figure 13).

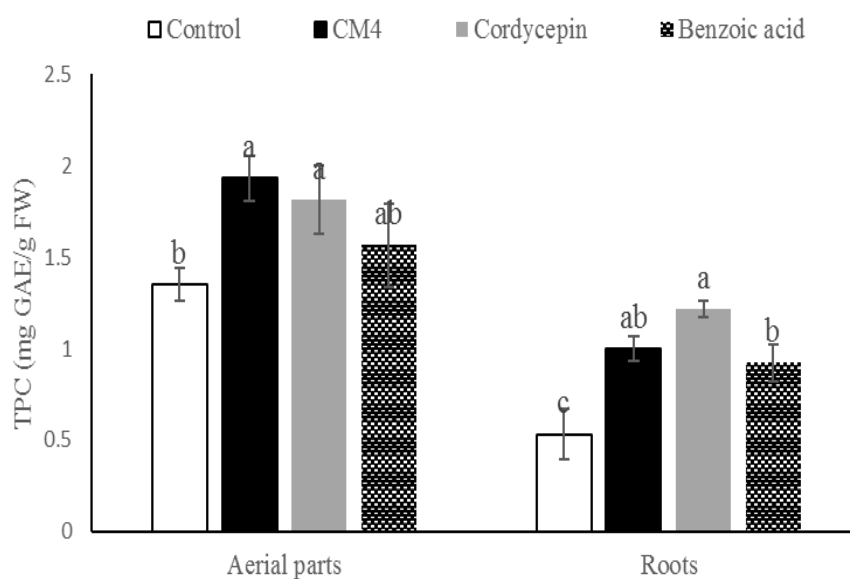


Figure 13. Total phenolic contents in the roots and aerial parts of radish among cordycepin, CM4 fraction and BA at 40 ppm. Values with similar superscript letters (a, b, c) in bars were not significantly different according to Tukey's test ($p < 0.05$).

5.3.3.2 Total flavonoid contents

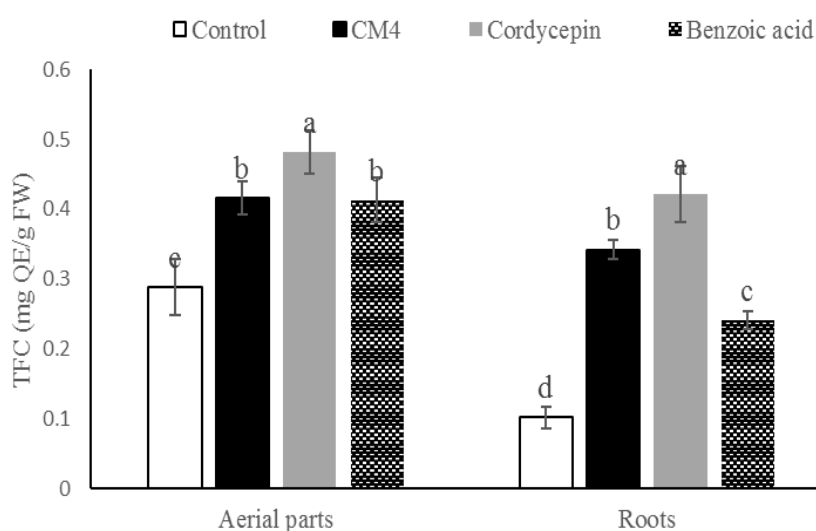


Figure 14. Total flavonoid contents in the roots and aerial parts of radish among cordycepin, CM4 fraction, and BA at 40 ppm. Values with similar superscript letters (a, b, c, d) in bars were not significantly different according to Tukey's test ($p < 0.05$).

Figure 14 shows the accumulation in the total flavonoid contents (TFC) of the roots and aerial parts of radish seedlings by treatments with cordycepin, fraction CM4, and benzoic acid. The TFC values in both roots and aerial parts are significantly increases as compared to the controls. The TFC in the roots is promoted in greater levels compared to the aerial parts. In every treatment, cordycepin causes the highest TFC, as compared to either fraction CM4 or BA (Figure 14).

5.3.3.3 Proline contents

The responses of proline content in radish due to cordycepin, fraction CM4, and benzoic acid are presented in detail (Figure 15). All treatments remarkably stimulate the proline accumulation in both the roots and aerial parts, as compared with the controls. Treatment by cordycepin shows significantly higher proline quantities than either fraction CM4 or benzoic acid. Additionally, the proline accumulation in aerial parts is higher than in roots for all chemical treatments (Figure 15).

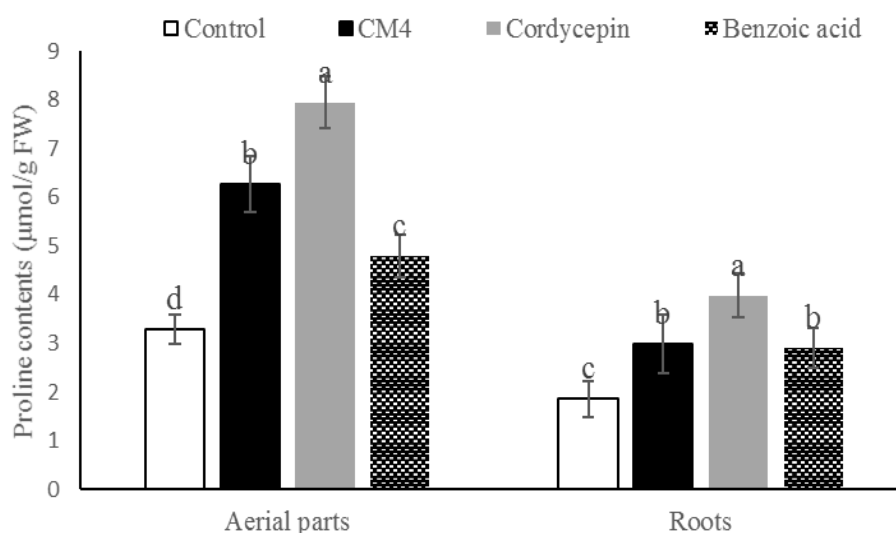


Figure 15. Proline contents in root and aerial parts of radish treated by cordycepin, CM4 fraction, and BA at 40 ppm. Values with similar superscript letters (a, b, c, d) in bars were not significantly different according to Tukey's test ($p < 0.05$).

5.4 Discussion

Public awareness of worldwide increase in the use of commercial herbicides, their undesirable effects on environment, human health, and the evolution of herbicide-resistant weed has been increasing over the past decades (Gonzalo *et al.*, 2011). So, weed management needs a significant focus shifted to the development of eco-friendly methods to reduce reliance on commercial herbicides (Chauhan *et al.*, 2017). The structural diversity and herbicidal property of natural phytotoxic compounds can bring opportunities for development of both directly used natural phytotoxins and synthetic herbicides (Morimoto *et al.*, 2009; Dayan and Duke, 2014). The application of natural herbicide would avoid the use of common herbicides such as glyphosate, paraquat which have serious effects on the environment as well as on human health (Thiour-Mauprivez *et al.*, 2019; Tsai, 2019).

The current study investigated plant-derived alternatives for globally used agrochemicals, including commercial herbicides such as paraquat, glyphosate which have recently been debated and removed from the market in some countries (Kongtip *et al.*, 2017; Dennis *et al.*, 2018; Tzvetkova *et al.*, 2019). The focus is on cordycepin, and details were shown on a variety of herbicidal characteristics (Figures 25-30). This research thereby expands previous reports and experience in the area of botanical science including herbicide properties of plants (Xuan *et al.*, 2005). Consensus exists among agricultural researchers that herbicides should help provide the world population with enough foods that are free of toxic residues and well tolerated by consumers without causing any health risks. Under these premises, natural phytotoxins or allelochemicals may be a source for the next-generation herbicides (Sodaeizadeh *et al.*, 2010; Dayan and Duke, 2014).

Allelochemicals inhibit indicator plants directly by affecting their physiology, biochemistry, and morphology (Omezzine *et al.*, 2014). In this research, cordycepin, the CM4 fraction containing cordycepin and benzoic acid significantly decreased the amount of chlorophyll (a, b, total chlorophylls) and carotenoid contents of radish as compared with control (Figure 10). Kaya *et al.* (2013) found that benzoic acid reduced pigment accumulations and reduced the

photosynthesis rate. In this experiment, cordycepin reduced 2.0- to 9.5-fold the pigment accumulations of radish compared to benzoic acid (Figure 10). These findings suggest that cordycepin has stronger phytotoxic activity than benzoic acid. Similar to other allelochemicals, both cordycepin and benzoic acid may inhibit porphyrin, a precursor for chlorophyll biosynthesis (Bano *et al.*, 2017). Reduction of chlorophylls content under allelochemical stress may be caused by impairing chlorophyll biosynthesis, promoting of pigment degradation, or both (Batish *et al.*, 2006).

There are many biochemical and physiological indicators that can be implemented to understand how allelochemicals affect the receiver plant. (Jaballah *et al.*, 2017) mentioned that pigments accumulations, lipid peroxidation, electrolyte leakage, total phenolic, total flavonoid and proline contents are common indicators in response to allelochemical stresses. Electrolyte leakage is one of the strongest indicators of membrane damage that inhibited by allelochemical stress (Sunaina and Singh, 2015). Increasing membrane permeability of indicator plants could be due to peroxidation of polyunsaturated fatty acids in the bio-membranes, resulted in a variety of products including malondialdehyde (Jaballah *et al.*, 2017). In this study, electrolyte leakage and lipid peroxidation of radish were increased in both the aerial parts and roots when treated with the fraction CM4 containing cordycepin, as well as benzoic acid (Figure 11). Chen *et al.* (1991) reported that benzoic acid destructs the cell membrane's integrity of plants due to the formation of free radicals. Generally, cordycepin increased the electrolyte leakage percentage and lipid peroxidation of radish more than benzoic acid (Figures 11 and 12).

Total flavonoid and total phenolic contents as well as the proline accumulation in radish, was significantly promoted as compared to the control by cordycepin, fraction CM4, and benzoic acid (Figures 28-30). Secondary metabolites from plants, such as total flavonoids and phenolics, are structural components of cell walls and participate in defense mechanisms of plants against biotic and abiotic stressors (Taïbi *et al.*, 2016). Ladhari *et al.* (2014) found that allelochemicals from methanolic and aqueous extracts increase the content of

proline in the leaves and roots of lettuce. Flavonoids are the predominant phenolic components with important roles as potential inhibitors of the lipoxygenase enzyme, that converts polyunsaturated fatty acids to oxygen-containing derivatives. They accumulate in organs of plants and may help reduce the process of lipid peroxidation in plants under stresses (Taïbi *et al.*, 2016). Similarly, the aerial parts of radish accumulated more proline content than the root parts. These results are in line with previous study, which reported that the water extract of corn leaves augmented the proline accumulation in wheat leaves (Ibrahim *et al.*, 2013). In addition, benzoic acid promoted the proline accumulation in leaves of tomato seedlings (Sunaina and Singh, 2015) and wheat seedlings (Amist and Singh, 2018). Similarly, in this study cordycepin increased proline content more than benzoic acid in both the aerial parts and roots (Figure 15). Proline synthesis is regulated by various kinds of stress to allow for the accumulation of proline, a common solute compatible with protective properties (Zegaoui *et al.*, 2017). Therefore, increasing the proline level in radish may be due to the phytotoxic effects of cordycepin, as well as benzoic acid (Figure 15).

Phytotoxic capacity, biochemical and physiological responses of radish, barnyard grass and some different indicator plants to glyphosate and paraquat have been reported. In a study (Grzesiuk *et al.*, 2018) treating radish plants at 2 mM concentration for 4 days exposure, glyphosate stimulated the shoot height by 20% as compared to the control, but when the concentration of glyphosate was increased, this herbicide had a strong inhibition. Compared to the present results, cordycepin inhibited 50% of the shoot of radish at 0.188 mM concentration. Additionally, in the greenhouse experiment, glyphosate required more than 600 g/ha to reduce chlorophyll a and b of radish from 81.6% to 86.28%, compared to the control (Silva *et al.*, 2014). In other susceptible plants and at a 10 mM concentration, glyphosate had a negligible effect on proline content in maize, but electrolyte leakage and lipid peroxidation promoted notably (Sergiev *et al.*, 2006). Besides, glyphosate concentration 0.5% (v/v) presented ineffective inhibition of cogongrass (Huang *et al.*, 2012). Moreover, paraquat inhibited barnyard grass emergence at 9.0 kg/ha, while glyphosate did not inhibit at the same dose with this

weed when applied at greenhouse experiment (Egley and Williams, 1987). Compared to the present results, cordycepin inhibited 50% of the germination of barnyard grass at 0.222 mM dose. Therefore, cordycepin is more phytotoxic and has a greater inhibition on the biochemical and physiological processes of receiver plants. With respect to the mode of action, cordycepin acts as an allelochemical compound by inhibiting the germination and emergence of barnyard grass and radish, reducing pigment synthesis (chlorophylls and carotenoids), stimulating electrolyte leakage, lipid peroxidation, total phenolic, total flavonoid, and proline accumulation of radish as compared to benzoic acid. However, evaluating additional activities of cordycepin, including its functional groups -NH₂, -OH, and the presence of N on the C4, 7, and 9 of its chemical structure (Figure 9) is required, and respective studies are in the progress.

C. militaris is a valuable edible fungus. It is in use as a tonic and medicinal food in the US and elsewhere, belongs to the large group of medicinal fungi, and has likely been used safely for centuries in many countries, particularly in China and Southeast Asia (Kang *et al.*, 2017). Among its bioactive components, cordycepin has been well characterized in animal experiments regarding an *in vivo* subacute toxicity test and Ames test (Aramwit *et al.*, 2015), and it is characterized also by rapid decomposition in humans through adenosine deaminase enzyme, as evidenced by a short half-life of about 1 min (Aramwit *et al.*, 2015). Thus, this test likely decreased the possible risk of toxicity and tumor initiation. Besides, cordycepin with the chemical structure is very similar to adenosine, with the absence of hydroxyl group on carbon number 3 (Aramwit *et al.*, 2015). Therefore, cordycepin can easily be synthesized from adenosine, a natural chemical present in all living cells (Huang *et al.*, 2018).

The isolation of cordycepin has been reported in the literature using various techniques (Wang *et al.*, 2014; Masuda *et al.*, 2015; Zhang *et al.*, 2016; Sari *et al.*, 2016; Huang *et al.*, 2018). The present study improved the isolation process, provided a rapid separation method, and conducted bioassay-guided isolation and identification of phytotoxic compound from *C. militaris* (Figure 5; Table 11), resulting in a detailed description of the herbicidal property of this

fungus with its active cordycepin (Table 9). Presently, it is unclear whether cordycepin can outperform currently used herbicides as paraquat and glyphosate. Further examination on the effect of this component on the growth of different and common weeds in agricultural production and other fields are needed.

This study indicates that *C. militaris*, with cordycepin as its active component, effectively inhibits plant growth and may be a promising natural source to develop plant-based herbicides. Cordycepin shows at 0.04 ppm greater inhibitory efficacy as compared with benzoic acid and is thereby basically a promising phytochemical compound. To clarify the mode of action of this allelochemical, different concentrations as well as its synthesized derivatives, should be evaluated to detail the biochemical and physiological responses of susceptible plants as well as agricultural weeds. The correlation between the phytotoxicity of cordycepin on indicator plants with the corresponding levels of chlorophylls, carotenoids, electrolyte leakage, lipid peroxidation, total phenolic, total flavonoid and proline content should be addressed. In particular, it is necessary to check whether cordycepin is selective or non-selective herbicidal compound and how they eliminate or control weeds on the fields. This would help clarify under what conditions cordycepin and its derivatives could effectively and safely be used as an herbicide.

5.5 Conclusion

This research focused on cordycepin successfully separated from *C. militaris* and on the discovery of its strong inhibitory capacity, which was greater than paraquat and glyphosate on the germination and growth of *Raphanus sativus* and *Echinochloa crus-galli*, as evaluated by a variety of laboratory bioassays. Cordycepin, a purine nucleoside (3'-deoxyadenosine) caused phytotoxicity as an allelochemical compound by reducing photosynthetic pigments and promoting electrolyte leakage, lipid peroxidation, total phenolic, total flavonoid, and proline contents. It was found that cordycepin is a novel and potent plant growth inhibitor should encourage the development of plant-based herbicides for environmentally-friendly agricultural production and other fields. Further researchs are needed to

compare the mechanism of cordycepin as well as its synthesized derivatives compared to paraquat and glyphosate against the physiological and biochemical responses of indicator plants as well as principal weeds.

6 General discussion and conclusion

6.1 General discussion

C. militaris is a highly valued edible fungus which is often used as nourishing foods and effective traditional medicines in worldwide, particularly in Southeast Asia to prevent and treat various diseases (Feng *et al.*, 2018; Lu *et al.*, 2019). Nowadays, *C. militaris* is entered a large-scale artificial cultivation by using different types of media instead of obtained from natural sources (Tang *et al.*, 2018; Lee *et al.*, 2019; Lou *et al.*, 2019). *C. militaris* contains a broad range of bioactive compounds, so it is necessary to explore more biological activities as well as increase value addition of this fungus.

This study investigates bioactive compounds and biological activities of *C. militaris* (L.) Link fruiting body which is cultured in solid medium. Both medicinal and herbicidal properties of this fungus, xanthine oxidase inhibitory, antioxidant, antibacterial and allelopathic assays were performed and examined.

It is found that *C. militaris* possess significant strong antioxidant, antibacterial and anti-hyperuricemic properties in an *in vitro* model. Among isolated compounds, cordycepin, fatty acids and their derivatives show potent free radical scavenging activities against DPPH and ABTS free radicals. Thus, several previous researchs reported that cordycepin and fatty acids are free-radical scavengers (Wang *et al.*, 2015; Freitas *et al.*, 2017; Khan *et al.*, 2018; Saccà *et al.*, 2018; Kopalli *et al.*, 2019; Wang *et al.*, 2019). Besides, they also exhibit a broad spectrum of activity against both Gram-negative (*E.coli* and *P. mirabilis*) and Gram-positive (*B. subtilis* and *S. aureus*) bacterial strains. In line with previous studies, cordycepin and fatty acids possessed potent antimicrobial activities (Dhouioui *et al.*, 2016; Nguyen *et al.*, 2017; Mirani *et al.*, 2017; Ni *et al.*, 2018; Jiang *et al.*, 2019; Huang *et al.*, 2019). Moreover, cordycepin, a bioactive compound belongs to purine nucleosides presents remarkable anti-hyperuricemic or anti-gout activity. This is the first study revealed that the edible fungus *C. militaris* with cordycepin as its active component possess xanthine oxidase inhibition in an *in vitro* experiment.

In the herbicidal property, fraction CM4 from EtOAc extract of *C. militaris* shows the strong inhibition on germination, root elongation and shoot height of radish and barnyard grass. Cordycepin, a purine analog emerged as the dominant component in this fraction and gave powerful inhibition on plant growth. Its herbicidal capacity was higher than commercial herbicides, benzoic acid, paraquat, and glyphosate. Similarity, several previous studies have reported that purine nucleosides possess strong allelopathic activity (Suzuki and Waller, 1987; Sabina *et al.*, 2007; Peneva, 2007; Sasamoto *et al.*, 2015; Tanti *et al.*, 2016; Thanh *et al.*, 2019). Thus, cordycepin may reduce photosynthetic pigments (chlorophyll a, b, total chlorophyll and carotenoid) and promote electrolyte leakage, lipid peroxidation, total phenolic, total flavonoid and proline accumulations in the aerial parts and roots of radish seedlings. The study investigated that cordycepin is a novel and potent plant growth inhibitor should encourage the development of plant-based herbicides for environmentally friendly agricultural production and other fields.

6.2 Xanthine oxidase inhibition

Table 14. Description of types of enzyme inhibition of inhibitor

No	Types of inhibition	Description
1	Competitive	A competitive inhibitor binds only to free enzyme. This binding most often occurs on the active site of the target at the precise location where substrate or cofactor also binds.
2	Noncompetitive	A noncompetitive inhibitor binds equally well to both free enzyme and the enzyme-substrate complex. These binding events occur at a site distinct from the precise active site occupied by substrate.
3	Uncompetitive	An uncompetitive inhibitor binds only to the enzyme-substrate complex yielding an inactive enzyme-substrate-inhibitor complex. Uncompetitive inhibition needs to form enzyme-substrate complex.

There are three main kinds of inhibition (competitive, noncompetitive, and uncompetitive) that are commonly used to describe the binding of an inhibitor to a target enzyme (Strelow *et al.*, 2012; Rodriguez and Towns, 2019; Ouertani *et al.*, 2019) (Table 14).

Allopurinol is known as an effective inhibitor that block the action of the enzyme xanthine oxidase by substrate competition mechanism (Pacher *et al.*, 2006; Lin *et al.*, 2015; Osman *et al.*, 2016; Alvionita *et al.*, 2019).

The allopurinol can bind to the xanthine oxidase and this binding will prevent the binding of the true substrate. Allopurinol acts by locking the biosynthesis of uric acid and relates to actions of purine ring (Tamta *et al.*, 2005; Tamta *et al.*, 2006; Kalra *et al.*, 2007; Kostić *et al.*, 2015) (Table 15).

Table 15. Structure of allopurinol and different purine-based compounds for xanthine oxidase inhibition

No	Xanthine oxidase Inhibitors	IC ₅₀ (μ M)	References
1	Adenine	75.61	(Tamta <i>et al.</i> , 2005)
2	4-amino-6-mercaptopyrazolo-3,4-d-pyrimidine	0.06	(Tamta <i>et al.</i> , 2006)
3	4-mercapto-1H-pyrazolo-3,4-d-pyrimidine	1.33	(Tamta <i>et al.</i> , 2006)
4	4-aminopyrazolo- 3,4-d-pyrimidine	7.44	(Tamta <i>et al.</i> , 2006)
5	4,6-dihydroxy- pyrazolo-3,4-d- pyrimidine	6.29	(Tamta <i>et al.</i> , 2006)
6	8-azaguanine	5.46	(Tamta <i>et al.</i> , 2006)
7	2-amino-6-hydroxy-8-mercaptapurine	5.08	(Kalra <i>et al.</i> , 2007)
8	2-amino-6-purine thiol	7.28	(Kalra <i>et al.</i> , 2007)
9	4-amino-6-hydroxypyrazolo-3,4-d-pyrimidine	6.79	(Kalra <i>et al.</i> , 2007)

The structure of allopurinol is very similar to substrate-xanthine, so allopurinol becomes a competitive inhibitor binding to the active site of the xanthine oxidase enzyme as xanthine. Cordycepin has a purine ring and sites like allopurinol, therefore, it may play a role to inhibit the xanthine oxidase as mechanism of allopurinol (Figure 16).

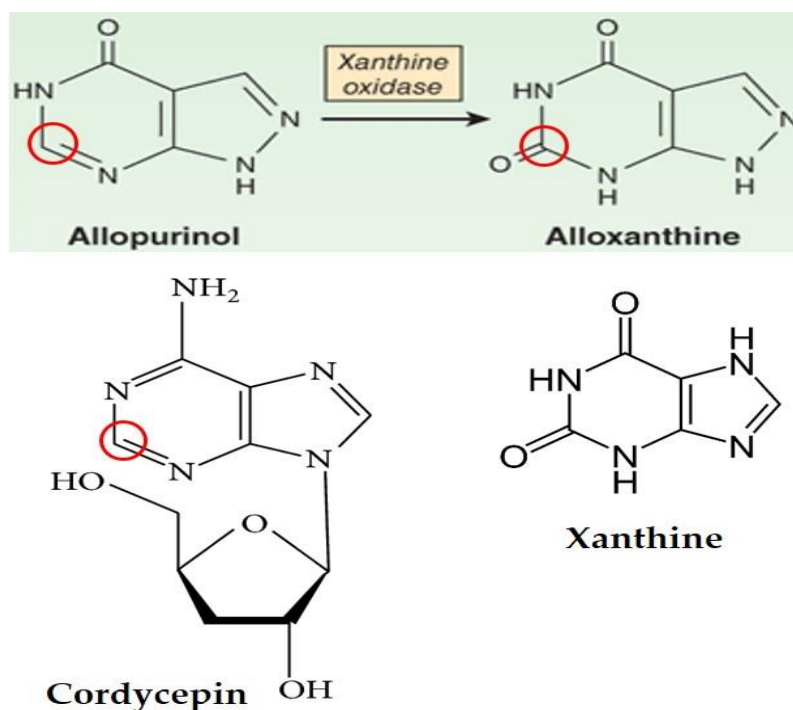


Figure 16. Comparison structure of cordycepin, allopurinol and xanthine.

6.3 Antibacterial activity

The mechanism of antibacterial property of fatty acids and their derivatives is through disrupting the bacterial membrane enzyme activity, the electron transport chain, uncoupling oxidative phosphorylation and increasing membrane permeability and leakage (McGaw *et al.*, 2002; Desbois and Smith, 2010; Yoon *et al.*, 2018).

Fatty acids directly bind to the carriers of electron transport chain or insert into inner membrane to move or displace electron carriers from cell membrane. As a result, the ability of electron transport chain to transfer electrons is impaired leading to reducing the proton (H^+) gradient and membrane potential (Peters and Chin, 2003). Thus, entering of the proton (H^+) into the cytosol reduce electron

transport chain to convert ADP to ATP as well as prevent oxidative phosphorylation (Boyaval *et al.*, 1995; Beck *et al.*, 2007). This process can reduce ATP synthesis as an essential energy source leading to inhibition of cell growth and ultimately cell death (Borst *et al.*, 1962; Sheu and Freese, 1972).

Besides, they inhibit the activity of membrane-associated enzymes and fatty acid biosynthesis of bacterial cells (Zheng *et al.*, 2005; Hamel, 2009; Sado-Kamdem *et al.*, 2009; Zhou *et al.*, 2018). Thus, they can directly inhibit membrane enzymes because their molecular structures are very similar to small molecular inhibitors (Kurihara *et al.*, 1999; Won *et al.*, 2007). Especially, fatty acids and their derivatives inhibit bacterial enoyl-acyl carrier protein reductase which plays an important role in the fatty acid elongation process (Zheng *et al.*, 2005; Sado-Kamdem *et al.*, 2009).

In addition, fatty acids can insert into the bacterial inner membrane to increase membrane permeability and fluidity due to small molecular structures, (Greenway and Dyke, 1979; Chamberlain *et al.*, 1991; Cybulski *et al.*, 2002; Kenny *et al.*, 2009). If this phenomenon increases excessively, the membrane can destabilize and the bacterial cell will lyse which can cause growth inhibition or lead to cell death (Speert *et al.*, 1979; Carson and Daneo-Moore, 1980; Thompson *et al.*, 1994; Shin *et al.*, 2007).

The antibacterial mechanism of cordycepin also disrupts cell bio-membranes which caused bacteria to lose ability to maintain cytoplasm macromolecules. Additionally, cordycepin binds to bacterial genomic DNA to affect the structure and function of nucleic acids, eventually leading to cell death. These mechanisms may be related to the electronic delocalization of the N group on the aromatic ring from the chemical structure of cordycepin (Jiang *et al.*, 2019).

6.4 Allelopathic activity

The mechanism of action of herbicides are variable and based on their chemical compositions to control weeds through various biochemical means (Duke, 1990; Forouzesh *et al.*, 2015). Depending upon the specific mode of action, they may interrupt a plant enzyme or a biological system leading to injuring or

disrupting plant growth and consequently cell death (Westwood *et al.*, 2018; Dayan, 2019).

The mode of action of glyphosate (*N*-phosphonomethyl glycine) acts by inhibiting the amino acid synthesis (Sammons and Gaines, 2014; Mesnage and Antoniou, 2017). Glyphosate inhibits the enzyme 5-enolpyruvylshikimate-3-phosphate synthase (EPSPS) that catalyses the reaction of shikimate-3-phosphate and phosphoenolpyruvate to yield 5-enolpyruvylshikimate-3-phosphate (Yi *et al.*, 2016; Wicke *et al.*, 2019). This enzyme is essential for the biosynthesis of aromatic amino acids (phenylalanine, tryptophan, and tyrosine) on the shikimate pathway that is localized in the stroma of chloroplasts of plants (Tohge *et al.*, 2013; Dor *et al.*, 2017; Yanniccari *et al.*, 2017). Aromatic amino acids have important roles such as antioxidants, pigments, signaling agents, electron transport, the structural element lignan, communication and defense mechanism (Tzin and Galili, 2010; Polimova *et al.*, 2011; Maeda and Dudareva, 2012; Yoo *et al.*, 2013; He *et al.*, 2018; Parthasarathy *et al.*, 2018; De and Chakraborty, 2019). Thus, they are depleted after EPSPS inhibition. In consequence, several physiological processes and biosynthetic metabolic pathways are affected leading to eventually plant death (Zulet *et al.*, 2013; Martinez *et al.*, 2018; Fernández-Escalada *et al.*, 2019).

The mechanism of paraquat (PQ) interferes photosynthesis process at the chloroplasts (Qian *et al.*, 2009b; Sedigheh *et al.*, 2011; Liu *et al.*, 2013). The active ingredient of paraquat is methyl viologen which cause a deviation of electron flow from Photosystem I (PSI), leading to reduce oxidation of nicotinamide adenine dinucleotide phosphate (NADP⁺) during photosynthesis (Dinis-Oliveira *et al.*, 2008; Brunharo and Hanson, 2017). Paraquat accepts photosynthetic electrons from PSI and transfers these electrons to oxygen producing toxic oxygen species which cause lipid peroxidation and membrane breakdown (Upham and Hatzios, 1987; Wang *et al.*, 2014; Hajji *et al.*, 2019). Therefore, this process will produce toxic reactive oxygen species (ROS) and induced plant cell death (Li *et al.*, 2013; Cui *et al.*, 2019).

Allelochemicals as natural phytotoxins offer new opportunities for the development next-generation herbicides with new target sites based on the structures of natural compounds (Duke *et al.*, 2000; Dayan and Duke, 2014; Lebecque *et al.*, 2019). However, due to their diverse chemical nature, interactive natures and multiple target sites in higher plants, it is often difficult to determine their accurate roles and mechanisms of allelochemical action in susceptible plants (Zeng, 2014).

Although, their mode of action is not fully understood, using appropriate assays for screening with different mechanisms of actions may confirm specific assessment at the site of action such as photosynthesis, membrane permeability, protein and nucleic acid synthesis, water and nutrient uptake, respiration, and growth regulation in indicator plants (Macias *et al.*, 2004). In this study, cordycepin are such allelochemical, a natural phytotoxins extracted from *C. militaris* and able to inhibit the germination and growth of radish and barnyard grass. The action of cordycepin reduces photosynthesis and promotes electrolyte leakage, lipid peroxidation, total phenolic, total flavonoid and proline contents of radish. Thus, the effects of cordycepin as well as allelochemicals in plant physiological, molecular and morphological parameters were illustrated on cell biology (Gomes *et al.*, 2017).

Allelochemicals reduced the plasma membrane H⁺-ATPase (active transport system), so the plant cells can not maintain cell turgor, membrane ion transport and osmoregulation leading to morphological disturbances and decreased growth (Lovett *et al.*, 1989; Cheng and Cheng, 2015). Furthermore, they can also cause oxidative damage and activate antioxidant mechanisms (Gomes *et al.*, 2017). When increasing in antioxidant enzyme activities will increase in reactive oxygen species (ROS) production (Zhang *et al.*, 2010). The excessive ROS levels are related to several cell-damaging processes such as enzyme inactivation, DNA and protein losses, and lipid peroxidation. In addition, allelochemicals can inhibit electron transport chains in chloroplasts (effects on photosynthesis) and mitochondria. As a results, they deprive energy sources of cells (NAD[P]H, FAD and ATP), intermediary metabolic products, and generate

ROS that would make the seedlings more vulnerable to cellular dysfunctions and ultimately cell death (Dayan *et al.*, 2009).

6.5 Conclusion

The study found that *C. militaris* possessed strong anti-hyperuricemic, antioxidant, antibacterial and allelopathic activities. From several modern analyses (HPLC, GC-MS, LC-ESI-MS) confirmed cordycepin, fatty acid and their derivatives as the active components of this fungus. In particular, cordycepin (a purine nucleoside) plays a crucial role in the inhibition of enzyme xanthine oxidase as well as the germination and growth of radish and barnyard grass. Besides, the presence of fatty acids and their derivatives were suggested to be responsible for antioxidant and antibacterial properties. This is the first study revealed that cordycepin from *C. militaris* had remarkably anti-gout and herbicidal activities *in vitro* assays. Findings of this study suggest that *C. militaris* is a promising natural source to develop foods and beverages to treat hyperuricemia, oxidative stress, bacterial infections and plant-based herbicides on agricultural production.

References

- Abdullahi, A., Hamzah, R., Jigam, A., Yahya, A., Kabiru, A., Muhammad, H., Sakpe, S., Adefolalu, F., Isah, M., Kolo, M., 2012. Inhibitory activity of xanthine oxidase by fractions *Crateva adansonii*. *J. Acute Dis.* 1, 126–129. [https://doi.org/10.1016/S2221-6189\(13\)60029-3](https://doi.org/10.1016/S2221-6189(13)60029-3)
- Achatz, M., Morris, E.K., Müller, F., Hilker, M., Rillig, M.C., 2014. Soil hypha-mediated movement of allelochemicals: Arbuscular mycorrhizae extend the bioactive zone of juglone. *Funct. Ecol.* 28, 1020-1029. <https://doi.org/10.1111/1365-2435.12208>
- Adnan, M., Ashraf, S.A., Khan, S., Alshammari, E., Awadelkareem, A.M., 2017. Effect of pH, temperature and incubation time on cordycepin production from *Cordyceps militaris* using solid-state fermentation on various substrates. *CyTA - J. Food.* 15, 617–621. <https://doi.org/10.1080/19476337.2017.1325406>
- Al-Abd, N.M., Nor, Z.M., Mansor, M., Zajmi, A., Hasan, M.S., Azhar, F., Kassim, M., 2017. Phytochemical constituents, antioxidant and antibacterial activities of methanolic extract of *Ardisia elliptica*. *Asian Pac. J. Trop. Biomed.* 7, 569–576. <https://doi.org/10.1016/j.apjtb.2017.05.010>
- Albuquerque, M.B., Dos Santos, R.C., Lima, L.M., Melo Filho, P.D.A., Nogueira, R.J.M.C., Da Camara, C.A.G., Ramos, A.D.R., 2011. Allelopathy, an alternative tool to improve cropping systems. *A review. Agron. Sustain. Dev.* 31, 379–395. <https://doi.org/10.1051/agro/2010031>
- Alvionita, M., Oktavia, I., Subandi, S., Muntholib, 2019. Bioactivity of flavonoid in ethanol extract of *Annona squamosa* L. fruit as xanthine oxidase inhibitor. *IOP Conf. Ser. Mater. Sci. Eng.* 546, 1-10. <https://doi.org/10.1088/1757-899X/546/6/062003>
- Amist, N., Singh, N.B., 2018. Comparative effects of benzoic acid and water stress on wheat seedlings. *Russ. J. Plant Physiol.* 65, 709–716. <https://doi.org/10.1134/s1021443718050023>
- Anaya, A.L.; Cruz-Ortega, R.; Waller, G.R., 2006. Metabolism and ecology of

- purine alkaloids. *Front. Biosci.* 11, 2354-2370. <https://doi.org/10.2741/1975>
- Andriana, Y., Xuan, T.D., Quan, N. V., Quy, T.N., 2018. Allelopathic potential of *Tridax procumbens* L. on radish and identification of allelochemicals. *Allelopath. J.* 43, 223–238. <https://doi.org/10.26651/allelo.j/2018-43-2-1143>
- Annett, R., Habibi, H.R., Hontela, A., 2014. Impact of glyphosate and glyphosate-based herbicides on the freshwater environment. *J. Appl. Toxicol.* 34, 458–479. <https://doi.org/10.1002/jat.2997>
- Aparecida, M., Campos Ventura-Camargo, B., Miyuki, M., 2013. Toxicity of herbicides: impact on aquatic and soil biota and human health. *Herbic. Curr. Res. Case Stud. Use.* 16, 401-443. <https://doi.org/10.5772/55851>
- Aramwit, P., Porasuphatana, S., Srichana, T., Nakpheng, T., 2015. Toxicity evaluation of cordycepin and its delivery system for sustained *in vitro* anti-lung cancer activity. *Nanoscale Res. Lett.* 152, 1-10 <https://doi.org/10.1186/s11671-015-0851-1>
- Azmi, S.M.N., Jamal, P., Amid, A., 2012. Xanthine oxidase inhibitory activity from potential Malaysian medicinal plant as remedies for gout. *Int. Food Res. J.* 19, 159–165.
- Bano, C., Amist, N., Sunaina, Singh, N.B., 2017. UV-B radiation escalate allelopathic effect of benzoic acid on *Solanum lycopersicum* L. *Sci. Hortic.* 220, 199-205. (Amsterdam). <https://doi.org/10.1016/j.scienta.2017.03.052>
- Barbieri, R., Coppo, E., Marchese, A., Daglia, M., Sobarzo-Sánchez, E., Nabavi, S.F., Nabavi, S.M., 2017. Phytochemicals for human disease: An update on plant-derived compounds antibacterial activity. *Microbiol. Res.* 196, 44–68. <https://doi.org/10.1016/j.micres.2016.12.003>
- Batish, D.R., Singh, H.P., Rana, N., Kohli, R.K., 2006. Assessment of allelopathic interference of *Chenopodium album* through its leachates, debris extracts, rhizosphere and amended soil. *Arch. Agron. Soil Sci.* 52, 705–715. <https://doi.org/10.1080/03650340601037119>
- Bec, V., Jabure, ., Demina, T., Rupprecht, A., Porter, R.K., Ježe, P., Pohl, E.E., 2007. Polyunsaturated fatty acids activate human uncoupling proteins 1 and 2 in planar lipid bilayers. *FASEB J.* 21, 1137–1144.

- <https://doi.org/10.1096/fj.06-7489com>
- Bhowmik, P.C., Inderjit, 2003. Challenges and opportunities in implementing allelopathy for natural weed management. *Crop Prot.* 22, 661–671. [https://doi.org/10.1016/S0261-2194\(02\)00242-9](https://doi.org/10.1016/S0261-2194(02)00242-9)
- Bizarro, A., Ferreira, I., o o íc, ., Griens e n, L., ousa, D., Vasconcelos, M., Lima, R., 2015. *Cordyceps militaris* (L.) Link fruiting body reduces the growth of a non-small cell lung cancer cell line by increasing cellular levels of p53 and p21. *Molecules.* 20, 13927–13940. <https://doi.org/10.3390/molecules200813927>
- Bohnenblust, E.W., Vaudo, A.D., Egan, J.F., Mortensen, D.A., Tooker, J.F., 2016. Effects of the herbicide dicamba on nontarget plants and pollinator visitation. *Environ. Toxicol. Chem.* 35, 144–151. <https://doi.org/10.1002/etc.3169>
- Bonnet, J.L., Bonnemoy, F., Dusser, M., Bohatier, J., 2007. Assessment of the potential toxicity of herbicides and their degradation products to nontarget cells using two microorganisms, the bacteria vibrio fischeri and the ciliate *Tetrahymena pyriformis*. *Environ Toxicol.* 22, 79-81. <https://doi.org/10.1002/tox.20237>
- Borst, P., Loos, J.A., Christ, E.J., Slater, E.C., 1962. Uncoupling activity of long-chain fatty acids. *BBA - Biochim. Biophys. Acta* 62, 509–518. [https://doi.org/10.1016/0006-3002\(62\)90232-9](https://doi.org/10.1016/0006-3002(62)90232-9)
- Boyaval, P., Corre, C., Dupuis, C., Roussel, E., 1995. Effects of free fatty acids on propionic acid bacteria. *Lait.* 75, 17–29. <https://doi.org/10.1051/lait:199512>
- Brown, E.G.; Konuk, M., 1994. Plant cytotoxicity of nebularine (purine riboside). *Phytochemistry.* 37, 1589-1592. [https://doi.org/10.1016/S0031-9422\(00\)89572-2](https://doi.org/10.1016/S0031-9422(00)89572-2)
- Brown, R.T., 1967. Influence of naturally occurring compounds on germination and growth of Jack Pine. *Ecological Society of America.* 48, 542–546. <https://doi.org/10.2307/1936497>
- Bruggen, A.H.C., He, M.M., Shin, K., Mai, V., Jeong, K.C., Finckh, M.R., Morris, J.G., 2018. Environmental and health effects of the herbicide glyphosate. *Sci. Total Environ.* 616–617, 255–268.

- <https://doi.org/10.1016/j.scitotenv.2017.10.309>
- Brunharo, C.A.C.G., Hanson, B.D., 2017. Vacuolar sequestration of paraquat is involved in the resistance mechanism in *Lolium perenne* L. *spp. multiflorum*. *Front. Plant Sci.* 8, 1–9. <https://doi.org/10.3389/fpls.2017.01485>
- Caihong, D., Suping, G., Wenfeng W., Xingzhong, L., 2015. *Cordyceps* industry in China. *Mycology.* 6, 121-129. <https://doi.org/10.1080/21501203.2015.1043967>
- Carson, D.D., Daneo-Moore, L., 1980. Effects of fatty acids on lysis of *Streptococcus faecalis*. *J. Bacteriol.* 141, 1122–1126.
- Cavaillon, J.M., 2018. Exotoxins and endotoxins: Inducers of inflammatory cytokines. *Toxicon.* 149, 45-53. <https://doi.org/10.1016/j.toxicon.2017.10.016>
- Cha, J.Y., Ahn, H.Y., Cho, Y.S., Je, J.Y., 2013. Protective effect of cordycepin-enriched *Cordyceps militaris* on alcoholic hepatotoxicity in Sprague-Dawley rats. *Food Chem. Toxicol.* 60, 52–57. <https://doi.org/10.1016/j.fct.2013.07.033>
- Chaicharoenaudomrung, N., Jaroonwichawan, T., Noisa, P., 2018. Cordycepin induces apoptotic cell death of human brain cancer through the modulation of autophagy. *Toxicol. Vitr.* 46, 113–121. <https://doi.org/10.1016/j.tiv.2017.10.002>
- Chamberlain, N.R., Mehrtens, B.G., Xiong, Z., Kapral, F.A., Boardman, J.L., Rearick, J.I., 1991. Correlation of carotenoid production, decreased membrane fluidity, and resistance to oleic acid killing in *Staphylococcus aureus* 18Z. *Infect. Immun.* 59, 4332–4337.
- Chauhan, B.S., Matloob, A., Mahajan, G., Aslam, F., Florentine, S.K., Jha, P., 2017. Emerging challenges and opportunities for education and research in weed science. *Front. Plant Sci.* 8, 1–13. <https://doi.org/10.3389/fpls.2017.01537>
- Cheema, Z.A., Farooq, M., Wahid, A., 2013. Allelopathy: Current trends and future applications. *Allelopath. Curr. Trends Futur. Appl.* ISBN: 978-3-642-30594-8. <https://doi.org/10.1007/978-3-642-30595-5>
- Chen, C.T., Li, C.C., Kao, C.H., 1991. Senescence of rice leaves XXXI. Changes of chlorophyll, protein, and polyamine contents and ethylene production

- during senescence of a chlorophyll-deficient mutant. *J. Plant Growth Regul.* 10, 201–205. <https://doi.org/10.1007/BF02279335>
- Chen, R., Jin, C., Li, H., Liu, Z., Lu, J., Li, S., Yang, S., 2014. Ultrahigh pressure extraction of polysaccharides from *Cordyceps militaris* and evaluation of antioxidant activity. *Sep. Purif. Technol.* 134, 90–99. <https://doi.org/10.1016/j.seppur.2014.07.017>
- Chen, X., Wu, G., Huang, Z., 2013. Structural analysis and antioxidant activities of polysaccharides from cultured *Cordyceps militaris*. *Int. J. Biol. Macromol.* 58, 18–22. <https://doi.org/10.1016/j.ijbiomac.2013.03.041>
- Cheng, F., Cheng, Z., 2015. Research progress on the use of plant allelopathy in agriculture and the physiological and ecological mechanisms of allelopathy. *Front. Plant Sci.* 6, 1-16. <https://doi.org/10.3389/fpls.2015.01020>
- Chiang, S.-S., Liang, Z.C., Wang, Y.C., Liang, C.H., 2017. Effect of light-emitting diodes on the production of cordycepin, mannitol and adenosine in solid-state fermented rice by *Cordyceps militaris*. *J. Food Compos. Anal.* 60, 51–56. <https://doi.org/10.1016/j.jfca.2017.03.007>
- Chimnoi, N., Reuk-ngam, N., Chuysinuan, P., Khlaychan, P., Khunnawutmanotham, N., Chokchaichamnankit, D., Thamniyom, W., Klayraung, S., Mahidol, C., Techasakul, S., 2018. Characterization of essential oil from *Ocimum gratissimum* leaves: Antibacterial and mode of action against selected gastroenteritis pathogens. *Microb. Pathog.* 118, 290–300. <https://doi.org/10.1016/j.micpath.2018.03.041>
- Chiu, C.P., Hwang, T.L., Chan, Y., El-Shazly, M., Wu, T.Y., Lo, I.W., Hsu, Y.M., Lai, K.H., Hou, M.F., Yuan, S.S., Chang, F.R., Wu, Y.C., 2016. Research and development of *Cordyceps* in Taiwan. *Food Sci. Hum. Wellness* 5, 177–185. <https://doi.org/10.1016/j.fshw.2016.08.001>
- Cho, S.H., Kang, I.C., 2018. The inhibitory effect of cordycepin on the proliferation of cisplatin-resistant A549 lung cancer cells. *Biochem. Biophys. Res. Commun.* 498, 431–436. <https://doi.org/10.1016/j.bbrc.2018.02.188>
- Chou, C. H; Waller, G. R., 1980. Possible allelopathic constituents of *Coffea arabica*. *J. Chem. Ecol.* 6, 643-654. <https://doi.org/10.1007/BF00987675>

- Choong, V., Ong Gaik Ai, L., Kim Suan, T., 2018. Synthesis of silver nanoparticles mediated by endophytic fungi associated with orchids and its antibacterial activity. *Mater. Today Proc.* 5, 22093–22100. <https://doi.org/10.1016/j.matpr.2018.07.074>
- Cimmino, A., Andolfi, A., Evidente, A., 2014. Phytotoxic terpenes produced by phytopathogenic fungi and allelopathic plants. *Nat. Prod. Commun.* 9, 401–408. <https://doi.org/10.1177/1934578x1400900330>
- Cui, F., Brosché, M., Shapiguzov, A., He, X.Q., Vainonen, J.P., Leppälä, J., Trotta, A., Kangasjärvi, S., Salojärvi, J., Kangasjärvi, J., Overmyer, K., 2019. Interaction of methyl viologen-induced chloroplast and mitochondrial signalling in *Arabidopsis*. *Free Radic. Biol. Med.* 134, 555–566. <https://doi.org/10.1016/j.freeradbiomed.2019.02.006>
- Cybulski, L.E., Albanesi, D., Mansilla, M.C., Altabe, S., Aguilar, P.S., De Mendoza, D., 2002. Mechanism of membrane fluidity optimization: Isothermal control of the *Bacillus subtilis* acyl-lipid desaturase. *Mol. Microbiol.* 45, 1379–1388. <https://doi.org/10.1046/j.1365-2958.2002.03103.x>
- Das, S.K., Masuda, M., Sakurai, A., Sakakibara, M., 2010. Medicinal uses of the mushroom *Cordyceps militaris*: Current state and prospects. *Fitoterapia.* 81, 961–968. <https://doi.org/10.1016/j.fitote.2010.07.010>
- David, R. G., Eric J. W., Leopoldo E. E., Rebacca, S.C.C., 2003. Rice cultivar differences in suppression of barnyardgrass (*Echinochloa crus-galli*) and economics of reduced propanil rates. *Weed Sci.* 51, 601–609. [https://doi.org/10.1614/0043-1745\(2003\)051](https://doi.org/10.1614/0043-1745(2003)051)
- Dayan, F.E., 2019. Current status and future prospects in herbicide discovery. *Plants.* 8, 1-18. <https://doi.org/10.3390/plants8090341>
- Dayan, F.E., Duke, S.O., 2014. Natural compounds as next-generation herbicides. *Plant Physiol.* 166, 1090–1105. <https://doi.org/10.1104/pp.114.239061>
- Dayan, F.E., Howell, J., Weidenhamer, J.D., 2009. Dynamic root exudation of sorgoleone and its in planta mechanism of action. *J. Exp. Bot.* 60, 2107–2117. <https://doi.org/10.1093/jxb/erp082>
- De, S.K., Chakraborty, A., 2019. Interaction of monomeric and self-assembled

- aromatic amino acids with model membranes. *Chem Commun (Camb)*. 55, 15109–15112. <https://doi.org/10.1039/c9cc08495a>
- Dennis, P.G., Kukulies, T., Forstner, C., Orton, T.G., Pattison, A.B., 2018. The effects of glyphosate, glufosinate, paraquat and paraquat-diquat on soil microbial activity and bacterial, archaeal and nematode diversity. *Sci. Rep.* 8, 1–9. <https://doi.org/10.1038/s41598-018-20589-6>
- Desbois, A.P., Smith, V.J., 2010. Antibacterial free fatty acids: Activities, mechanisms of action and biotechnological potential. *Appl. Microbiol. Biotechnol.* 85, 1629–1642. <https://doi.org/10.1007/s00253-009-2355-3>
- Dhouioui, M., Boulila, A., Jemli, M., Schiets, F., Casabianca, H., Zina, M.S., 2016. Fatty acids composition and antibacterial activity of *Aristolochia longa* L. and *Bryonia dioica* Jacq. Growing wild in Tunisia. *J. Oleo Sci.* 65, 655–661. <https://doi.org/10.5650/jos.ess16001>
- Dill, G.M., 2005. Glyphosate-resistant crops: History, status and future. *Pest Manag. Sci.* 61, 219–224. <https://doi.org/10.1002/ps.1008>
- Dinis-Oliveira, R.J., Duarte, J.A., Sánchez-Navarro, A., Remião, F., Bastos, M.L., Carvalho, F., 2008. Paraquat poisonings: Mechanisms of lung toxicity, clinical features, and treatment. *Crit. Rev. Toxicol.* 38, 13–71. <https://doi.org/10.1080/10408440701669959>
- Dong, C.H., Yang, T., Lian, T., 2014. A Comparative study of the antimicrobial, antioxidant, and cytotoxic activities of methanol extracts from fruit bodies and fermented mycelia of caterpillar medicinal mushroom *Cordyceps militaris* (Ascomycetes). *Int. J. Med. Mushrooms*. 16, 485–495. <https://doi.org/10.1615/IntJMedMushrooms.v16.i5.70>
- Dong, J.Z., Wang, S.H., Ai, X.R., Yao, L., Sun, Z.W., Lei, C., Wang, Y., Wang, Q., 2013. Composition and characterization of cordyxanthins from *Cordyceps militaris* fruit bodies. *J. Funct. Foods*. 5, 1450–1455. <https://doi.org/10.1016/j.jff.2013.06.002>
- Dong, Y., Huang, H., Zhao, M., Sun-Waterhouse, D., Lin, L., Xiao, C., 2016. Mechanisms underlying the xanthine oxidase inhibitory effects of dietary flavonoids galangin and pinobanksin. *J. Funct. Foods*. 24, 26–36.

- <https://doi.org/10.1016/j.jff.2016.03.021>
- Dor, E., Galili, S., Smirnov, E., Hacham, Y., Amir, R., Hershenhorn, J., 2017. The effects of herbicides targeting aromatic and branched chain amino acid biosynthesis support the presence of functional pathways in broomrape. *Front. Plant Sci.* 8, 1–15. <https://doi.org/10.3389/fpls.2017.00707>
- Duke, S.O., 1990. Overview of herbicide mechanisms of action. *Environ. Health Perspect.* 87, 263–271. <https://doi.org/10.1289/ehp.9087263>
- Duke, S.O., Romagni, J.G., Dayan, F.E., 2000. Natural products as sources for new mechanisms of herbicidal action. *Crop Prot.* 19, 583–589. [https://doi.org/10.1016/S0261-2194\(00\)00076-4](https://doi.org/10.1016/S0261-2194(00)00076-4)
- Duong, N.T., Vinh, P.D., Thuong, P.T., Hoai, N.T., Thanh, L.N., Bach, T.T., Nam, N.H., Anh, N.H., 2017. Xanthine oxidase inhibitors from *Archidendron clypearia* (Jack.) I.C. Nielsen: Results from systematic screening of Vietnamese medicinal plants. *Asian Pac. J. Trop. Med.* 10, 549–556. <https://doi.org/10.1016/j.apjtm.2017.06.002>
- Dzotam, J.K., Touani, F.K., Kuete, V., 2016. Antibacterial activities of the methanol extracts of *Canarium schweinfurthii* and four other Cameroonian dietary plants against multi-drug resistant Gram-negative bacteria. *Saudi J. Biol. Sci.* 23, 565–570. <https://doi.org/10.1016/j.sjbs.2015.06.006>
- Egan, J.F., Bohnenblust, E., Goslee, S., Mortensen, D., Tooker, J., 2014. Herbicide drift can affect plant and arthropod communities. *Agric. Ecosyst. Environ.* 185, 77–87. <https://doi.org/10.1016/j.agee.2013.12.017>
- Egley, G., Williams, R., 1978. Glyphosate and paraquat effects on weed seed germination and seedling emergence. *Weed Sci.* 26, 249–251. <https://doi.org/10.1017/S004317450004981X>
- Eleazu, C.O., 2016. Characterization of the natural products in cocoyam (*Colocasia esculenta*) using GC-MS. *Pharm. Biol.* 54, 2880–2885. <https://doi.org/10.1080/13880209.2016.1190383>
- Elshagabee, F.M.F., Rokana, N., Gulhane, R.D., Sharma, C., Panwar, H., 2017. *Bacillus* as potential probiotics: Status, concerns, and future perspectives. *Front. Microbiol.* 8, 1–15. <https://doi.org/10.3389/fmicb.2017.01490>

- Elzaawely, A.A., Xuan, T.D., Tawata, S., 2007. Essential oils, kava pyrones and phenolic compounds from leaves and rhizomes of *Alpinia zerumbet* (Pers.) B.L. Burtt. & R.M. Sm. and their antioxidant activity. *Food Chem.* 103, 486–494. <https://doi.org/10.1016/j.foodchem.2006.08.025>
- Farooq, M.A., Ali, S., Hameed, A., Bharwana, S.A., Rizwan, M., Ishaque, W., Farid, M., Mahmood, K., Iqbal, Z., 2016. Cadmium stress in cotton seedlings: Physiological, photosynthesis and oxidative damages alleviated by glycinebetaine. *South African J. Bot.* 104, 61–68. <https://doi.org/10.1016/j.sajb.2015.11.006>
- Feng, Y.J., Zhu, Y., Li, Y.M., Li, J., Sun, Y.F., Shen, H.T., Wang, A.Y., Lin, Z.P., Zhu, J.B., 2018. Effect of strain separated parts, solid-state substrates and light condition on yield and bioactive compounds of *Cordyceps militaris* fruiting bodies. *CYTA - J. Food.* 16, 916–922. <https://doi.org/10.1080/19476337.2018.1498130>
- Fengyao, W., Hui, Y., Xiaoning, M., Junqing, J., Guozheng, Z., Xijie, G., Zhongzheng, G., 2011. Structural characterization and antioxidant activity of purified polysaccharide from cultured *Cordyceps militaris*. *African J. Microbiol. Res.* 5, 2743–2751. <https://doi.org/10.5897/AJMR11.548>
- Fernández-Escalada, M., Zulet-González, A., Gil-Monreal, M., Royuela, M., Zabalza, A., 2019. Physiological performance of glyphosate and imazamox mixtures on *Amaranthus palmeri* sensitive and resistant to glyphosate. *Sci. Rep.* 9, 1–14. <https://doi.org/10.1038/s41598-019-54642-9>
- Forouzesh, A., Zand, E., Soufizadeh, S., Samadi F. S., 2015. Classification of herbicides according to chemical family for weed resistance management strategies-an update. *Weed Res.* 55, 334–358. <https://doi.org/10.1111/wre.12153>
- Freitas, H.R., Ferreira, G.D.C., Trevenzoli, I.H., Oliveira, K.D.J., Reis, R.A.D.M., 2017. Fatty acids, antioxidants and physical activity in brain aging. *Nutrients.* 9, 1–23. <https://doi.org/10.3390/nu9111263>
- Friedman, J.; Waller, G.R., 1983. Caffeine hazards and their prevention in germinating seeds of coffee (*Coffea arabica* L.). *J. Chem. Ecol.* 9, 1099–

1106. <https://doi.org/10.1007/BF00982214>
- Frimpong, J.O., Ofori, E.S.K., Yeboah, S., Marri, D., Offei, B.K., Apaatah, F., Sintim, J.O., Ofori-Ayeh, E., Osae, M., 2018. Evaluating the impact of synthetic herbicides on soil dwelling macrobes and the physical state of soil in an agro-ecosystem. *Ecotoxicol. Environ. Saf.* 156, 205–215. <https://doi.org/10.1016/j.ecoenv.2018.03.034>
- Fukuta, M., Xuan, T.D., Deba, F., Tawata, S., Khanh, T.D., Chung, I.M., 2007. Comparative efficacies *in vitro* of antibacterial, fungicidal, antioxidant, and herbicidal activities of momilatonones A and B. *J. Plant Interact.* 2, 245–251. <https://doi.org/10.1080/17429140701713811>
- Gao, Y., Liu, W., Wang, X., Yang, L., Han, S., Chen, S., Strasser, R.J., Valverde, B.E., Qiang, S., 2018. Comparative phytotoxicity of usnic acid, salicylic acid, cinnamic acid and benzoic acid on photosynthetic apparatus of *Chlamydomonas reinhardtii*. *Plant Physiol. Biochem.* 128, 1–12. <https://doi.org/10.1016/j.plaphy.2018.04.037>
- Gawlik-Dzi i , U., Dzi i , D., Świeca, M., Nowak, R., 2017. Mechanism of action and interactions between xanthine oxidase inhibitors derived from natural sources of chlorogenic and ferulic acids. *Food Chem.* 225, 138–145. <https://doi.org/10.1016/j.foodchem.2017.01.016>
- Gomes, M.P., Garcia, Q.S., Barreto, L.C., Pimenta, L.P.S., Matheus, M.T., Figueredo, C.C., 2017. Allelopathy: An overview from micro-to macroscopic organisms, from cells to environments, and the perspectives in a climate-changing world. *Biol.* 72, 113–129. <https://doi.org/10.1515/biolog-2017-0019>
- Gonzalo, L. P., María, S.V., Leandro, A.M., 2011. Effects of herbicide glyphosate and glyphosate-based formulations on aquatic ecosystems. *Herbic. Environ.* 16, 343-368. <https://doi.org/10.5772/12877>
- Greenway, D.L.A., Dyke, K.G.H., 1979. Mechanism of the inhibitory action of linoleic acid on the growth of *Staphylococcus aureus*. *J. Gen. Microbiol.* 115, 233–245. <https://doi.org/10.1099/00221287-115-1-233>
- Grzesiu , A., Dębs i , ., nińs a , K., Kocz oda j, D., zwed, ., or bowicz, M., 2018. Effect of root-zone glyphosate exposure on growth and

- anthocyanins content of radish seedlings. *Acta Sci. Pol. Hortorum Cultus*. 17, 3–10. <https://doi.org/10.24326/asphc.2018.2.1>
- Hagner, M., Mikola, J., Saloniemi, I., Saikkonen, K., Helander, M., 2019. Effects of a glyphosate-based herbicide on soil animal trophic groups and associated ecosystem functioning in a northern agricultural field. *Sci. Rep.* 9, 1–13. <https://doi.org/10.1038/s41598-019-44988-5>
- Hajek, A.E., St Leger, R.J., 1994. Interactions between fungal pathogens and insect hosts. *Annu. Rev. Entomol.* 39, 293–322. <https://doi.org/10.1146/annurev.ento.39.1.293>
- Hajji, K., Mteyrek, A., Sun, J., Cassar, M., Mezghani, S., Leprince, J., Vaudry, D., Masmoudi-Kouki, O., Birman, S., 2019. Neuroprotective effects of PACAP against paraquat-induced oxidative stress in the *Drosophila* central nervous system. *Hum. Mol. Genet.* 28, 1905–1918. <https://doi.org/10.1093/hmg/ddz031>
- Hamel, F.G., 2009. Preliminary report: inhibition of cellular proteasome activity by free fatty acids. *Metabolism*. 58, 1047–1049. <https://doi.org/10.1016/j.metabol.2009.04.005>
- Havlik, J., de la Huebra, R.G., Hejtmankova, K., Fernandez, J., Simonova, J., Melich, M., Rada, V., 2010. Xanthine oxidase inhibitory properties of Czech medicinal plants. *J. Ethnopharmacol.* 132, 461–465. <https://doi.org/10.1016/j.jep.2010.08.044>
- He, F., Wu, C., Li, P., Li, N., Zhang, D., Zhu, Q., Ren, W., Peng, Y., 2018. Functions and signaling pathways of amino acids in intestinal inflammation. *Biomed Res. Int.* 3, 1-13. <https://doi.org/10.1155/2018/9171905>
- Hodaei, M., Rahimmalek, M., Arzani, A., Talebi, M., 2018. The effect of water stress on phytochemical accumulation, bioactive compounds and expression of key genes involved in flavonoid biosynthesis in *Chrysanthemum morifolium* L. *Ind. Crops Prod.* 120, 295–304. <https://doi.org/10.1016/j.indcrop.2018.04.073>
- Holliday, J.C., Cleaver, M., 2008. Medicinal value of the caterpillar fungi species of the genus *Cordyceps* (Fr.) link (*Ascomycetes*). A review. *Int. J. Med.*

- Mushrooms*. 10, 219–234. <https://doi.org/10.1615/IntJMedMushr.v10.i3.30>.
- Hu, Z., Lee, C. Il., Shah, V.K., Oh, E.H., Han, J.Y., Bae, J.R., Lee, K., Chong, M.S., Hong, J.T., Oh, K.W., 2013. Cordycepin increases nonrapid eye movement sleep via adenosine receptors in rats. *Evidence-based Complement. Altern. Med.* 2013, 8. <https://doi.org/10.1155/2013/840134>.
- Huang, C.B., Alimova, Y., Myers, T.M., Ebersole, J.L., 2011. Short- and medium-chain fatty acids exhibit antimicrobial activity for oral microorganisms. *Arch. Oral Biol.* 56, 650–654. <https://doi.org/10.1016/j.archoralbio.2011.01.011>
- Huang, F., Li, W., Xu, H., Qin, H., He, Z.G., 2019. Cordycepin kills *Mycobacterium tuberculosis* through hijacking the bacterial adenosine kinase. *PLoS One* 14, 1–19. <https://doi.org/10.1371/journal.pone.0218449>
- Huang, J., Silva, E.N., Shen, Z., Jiang, B., Lu, H., 2012. Effects of glyphosate on photosynthesis, chlorophyll fluorescence and physicochemical properties of cogongrass (*Imperata cylindrical* L.). *Plant Omics*. 5, 177–183.
- Huang, S., Liu, H., Sun, Y., Chen, J., Li, X., Xu, J., Hu, Y., Li, Y., Deng, Z., Zhong, S., 2018. An effective and convenient synthesis of cordycepin from adenosine. *Chem. Pap.* 72, 149–160. <https://doi.org/10.1007/s11696-017-0266-9>
- Huang, Y., Zhan, H., Bhatt, P., Chen, S., 2019. Paraquat degradation from contaminated environments: Current achievements and perspectives. *Front. Microbiol.* 10, 1–9. <https://doi.org/10.3389/fmicb.2019.01754>
- Hui, M.Y., Wang, B. Sen, Shiow, C.H., Duh, P. D., 2006. Comparison of protective effects between cultured *Cordyceps militaris* and natural *Cordyceps sinensis* against oxidative damage. *J. Agric. Food Chem.* 54, 3132–3138. <https://doi.org/10.1021/jf053111w>
- Hulpia, F., Mabile, D., Campagnaro, G.D., Schumann, G., Maes, L., Roditi, I., Hofer, A., Koning, H.P., Caljon, G., Calenbergh, S. V., 2019. Combining tubercidin and cordycepin scaffolds results in highly active candidates to treat late-stage sleeping sickness. *Nat. Commun.* 1–11. <https://doi.org/10.1038/s41467-019-13522-6>.
- Hur, H., 2008. Chemical Ingredients of *Cordyceps militaris*. *Mycobiology* 36,

- 233–5. <https://doi.org/10.4489/MYCO.2008.36.4.233>
- Hussain, M., Farooq, M., Basra, S.M.A., Lee, D.J., 2013. Application of moringa allelopathy in crop sciences. *Allelopath. Curr. Trends Futur. Appl.* 20, 469–484. https://doi.org/10.1007/978-3-642-30595-5_20
- Ibrahim, M., Ahmed, N., Ullah, F., Shinwari, Z.K., Bano, A., 2013. Comparative impact of genetically modified and non modified maize (*Zea mays* L.) on succeeding crop and associated weed. *Toxicol. Ind. Health.* 32, 614–624. <https://doi.org/10.1177/0748233713505125>
- Idrees, H., Javaid, A., 2008. Screening of some pathogenic fungi for their herbicidal potential against parthenium weed. *Pak. J. Phytopathol.* 20, 150–155.
- Jaballah, S. B., Zribi, I., Haouala, R., 2017. Physiological and biochemical responses of two lentil varieties to chickpea (*Cicer arietinum* L.) aqueous extracts. *Sci. Hortic. (Amsterdam)*. 225, 74–80. <https://doi.org/10.1016/j.scienta.2017.06.069>
- Jacobsen, S.M., Stickler, D.J., Mobley, H.L.T., Shirtliff, M.E., 2008. Complicated catheter-associated urinary tract infections due to *Escherichia coli* and *Proteus mirabilis*. *Clin. Microbiol. Rev.* 21, 26–59. <https://doi.org/10.1128/CMR.00019-07>
- Jeong, J.W., Jin, C.Y., Kim, G.Y., Lee, J.D., Park, C., Kim, G. Do, Kim, W.J., Jung, W.K., Seo, S.K., Choi, I.W., Choi, Y.H., 2010. Anti-inflammatory effects of cordycepin via suppression of inflammatory mediators in BV2 microglial cells. *Int. Immunopharmacol.* 10, 1580–1586. <https://doi.org/10.1016/j.intimp.2010.09.011>
- Jiang, Q., Lou, Z., Wang, H., Chen, C., 2019. Antimicrobial effect and proposed action mechanism of cordycepin against *Escherichia coli* and *Bacillus subtilis*. *J. Microbiol.* 57, 288–297. <https://doi.org/10.1007/s12275-019-8113-z>
- Jiang, Y., Wong, J.H., Fu, M., Ng, T.B., Liu, Z.K., Wang, C.R., Li, N., Qiao, W.T., Wen, T.Y., Liu, F., 2011. Isolation of adenosine, iso-sinensetin and dimethylguanosine with antioxidant and HIV-1 protease inhibiting activities

- from fruiting bodies of *Cordyceps militaris*. *Phytomedicine*. 18, 189–193. <https://doi.org/10.1016/j.phymed.2010.04.010>
- Jin, Y., Meng, X., Qiu, Z., Su, Y., Yu, P., Qu, P., 2018. Anti-tumor and anti-metastatic roles of cordycepin, one bioactive compound of *Cordyceps militaris*. *Saudi J. Biol. Sci.* 25, 991–995. <https://doi.org/10.1016/j.sjbs.2018.05.016>
- Joshi, M., Sagar, A., Kanwar, S., Singh, S., 2019. Anticancer, antibacterial and antioxidant activities of *Cordyceps militaris*. *Indian J. Exp. Biol.* 57, 15–20.
- Jugulam, M., Shyam, C., 2019. Non-target-site resistance to herbicides: Recent developments. *Plants (Basel)*. 8, 1-16. <https://doi.org/10.3390/plants8100417>
- Kadariya, J., Smith, T.C., Thapaliya, D., 2014. *Staphylococcus aureus* and Staphylococcal food-borne disease: An ongoing challenge in public health. *Biomed Res. Int.* 2014. 1-9 <https://doi.org/10.1155/2014/827965>
- Kakian, F., Shahini Shams Abadi, M., Gholipour, A., Fadaie, M., Zamanzad, B., Khairi, S., Parchami, S., Damavandi, M.S., 2019. Evaluating the prevalence of virulence genes of *Escherichia coli* in patients affected by urinary tract infection. *Gene Reports*. 16, 1-4. <https://doi.org/10.1016/j.genrep.2019.100433>
- Kalra, S., Jena, G., Tikoo, K., Mukhopadhyay, A.K., 2007. Preferential inhibition of xanthine oxidase by 2-amino-6-hydroxy-8-mercaptapurine and 2-amino-6-purine thiol. *BMC Biochem.* 8, 1–11. <https://doi.org/10.1186/1471-2091-8-8>
- Kang, N., Lee, H.H., Park, I., Seo, Y.S., 2017. Development of high cordycepin-producing *Cordyceps militaris* strains. *Mycobiology*. 45, 31–38. <https://doi.org/10.5941/MYCO.2017.45.1.31>
- Kapoor, N., Saxena, S., 2016. Xanthine oxidase inhibitory and antioxidant potential of Indian *Muscodor* species. *3 Biotech.* 6, 1-6. <https://doi.org/10.1007/s13205-016-0569-5>
- Kapoor, N., Saxena, S., 2014. Potential xanthine oxidase inhibitory activity of endophytic *Lasiodiplodia pseudotheobromae*. *Appl. Biochem. Biotechnol.* 173, 1360–1374. <https://doi.org/10.1007/s12010-014-0927-x>

- Karimi, E., Ze Jaafar, H., Ghasemzadeh, A., Ebrahimi, M., 2015. Fatty acid composition, antioxidant and antibacterial properties of the microwave aqueous extract of three varieties of *Labisia pumila* Benth. *Biol. Res.* 48, 1–6. <https://doi.org/10.1186/0717-6287-48-9>
- Kaur, H., Inderjit, Kaushik, S., 2005. Cellular evidence of allelopathic interference of benzoic acid to mustard (*Brassica juncea* L.) seedling growth. *Plant Physiol. Biochem.* 43, 77-81. <https://doi.org/10.1016/j.plaphy.2004.12.007>
- Kaya, C., Ashraf, M., Dikilitas, M., Tuna, A.L., 2013. Alleviation of salt stress-induced adverse effects on maize plants by exogenous application of indoleacetic acid (IAA) and inorganic nutrients - A field trial. *Aust. J. Crop Sci.* 7, 249–254.
- Kenny, J.G., Ward, D., Josefsson, E., Jonsson, I.M., Hinds, J., Rees, H.H., Lindsay, J.A., Tarkowski, A., Horsburgh, M.J., 2009. The *Staphylococcus aureus* response to unsaturated long chain free fatty acids: Survival mechanisms and virulence implications. *PLoS One.* 4, 1-29. <https://doi.org/10.1371/journal.pone.0004344>
- Khan, I.T., Nadeem, M., Imran, M., Ajmal, M., Ali, S., 2018. Antioxidant activity, fatty acids characterization and oxidative stability of Gouda cheese fortified with mango (*Mangifera indica* L.) kernel fat. *J. Food Sci. Technol.* 55, 992–1002. <https://doi.org/10.1007/s13197-017-3012-y>
- Khanh, T.D., Cong, L.C., Xuan, T.D., Lee, S.J., Kong, D.S., Chung, I.M., 2008. Weed-suppressing potential of dodder (*Cuscuta hygrophilae*) and its phytotoxic constituents. *Weed Sci.* 56, 119–127. <https://doi.org/10.1614/ws-07-102.1>
- Kim, H.G., Song, H., Yoon, D.H., Song, B.W., Park, S.M., Sung, G.H., Cho, J.Y., Park, H. Il, Choi, S., Song, W.O., Hwang, K.C., Kim, T.W., 2010. *Cordycepspruinosa* extracts induce apoptosis of HeLa cells by a caspase dependent pathway. *J. Ethnopharmacol.* 128, 342–351. <https://doi.org/10.1016/j.jep.2010.01.049>
- Kim, S.B., Ahn, B., Kim, M., Ji, H.J., Shin, S.K., Hong, I.P., Kim, C.Y., Hwang, B.Y., Lee, M.K., 2014. Effect of *Cordyceps militaris* extract and active

- constituents on metabolic parameters of obesity induced by high-fat diet in C58BL/6J mice. *J. Ethnopharmacol.* 151, 478–484. <https://doi.org/10.1016/j.jep.2013.10.064>
- Kim, Y.J., Park, K.H., Park, D.A., Park, J., Bang, B.W., Lee, S.S., Lee, E.J., Lee, H.J., Hong, S.K., Kim, Y.R., 2019. Guideline for the antibiotic use in acute gastroenteritis. *Infect. Chemother.* 51, 217–243. <https://doi.org/10.3947/ic.2019.51.2.217>
- Kniss, A.R., 2017. Long-term trends in the intensity and relative toxicity of herbicide use. *Nat. Commun.* 8, 1–7. <https://doi.org/10.1038/ncomms14865>
- Koh, J.H., Kim, K.M., Kim, J.M., Song, J.C., Suh, H.J., 2003. Antifatigue and antistress effect of the hot-water fraction from mycelia of *Cordyceps sinensis*. *Biol. Pharm. Bullin* 26, 691–694. <https://doi.org/10.1248/bpb.26.84>
- Kong, C.H., Xuan, T.D., Khanh, T.D., Tran, H.D., Trung, N.T., 2019. Allelochemicals and signaling chemicals in plants. *Molecules.* 24, 1-19. <https://doi.org/10.3390/molecules24152737>
- Kongtip, P., Nankongnab, N., Phupancharoensuk, R., Palarach, C., Sujirarat, D., Sangprasert, S., Sermsuk, M., Sawattrakool, N., Woskie, S.R., 2017. Glyphosate and paraquat in maternal and fetal serums in Thai women. *J. Agromedicine.* 22, 282–289. <https://doi.org/10.1080/1059924X.2017.1319315>
- Kopalli, S.R., Cha, K.M., Lee, S.H., Hwang, S.Y., Lee, Y.J., Koppula, S., Kim, S.K., 2019. Cordycepin, an active constituent of nutrient powerhouse and potential medicinal mushroom *Cordyceps militaris* Linn., Ameliorates Age-related testicular dysfunction in rats. *Nutrients.* 11, 1-24. <https://doi.org/10.3390/nu11040906>
- Kostić, D.A., Dimitrijević, D., tojano ić, G., Palić, I.R., Dorde i ć, A., Ickovski, J.D., 2015. Xanthine oxidase: Isolation, assays of activity, and inhibition. *J. Chem.* 2015, 1-8. <https://doi.org/10.1155/2015/294858>
- Kraus, E.C., Stout, M.J., 2019. Direct and indirect effects of herbicides on insect herbivores in rice, *Oryza sativa*. *Sci. Rep.* 9, 1–13. <https://doi.org/10.1038/s41598-019-43361-w>

- Kurihara, H., Goto, Y., Aida, M., Hosokawa, M., Takahashi, K., 1999. Antibacterial activity against cariogenic bacteria and inhibition of insoluble glucan production by free fatty acids obtained from dried *Gloiopeltis furcata*. *Fish. Sci.* 65, 129–132. <https://doi.org/10.2331/fishsci.65.129>
- Kwiecińska -Piróg, J., Skowron, K., Zniszczol, K., Gospodarek, E., 2013. The assessment of *Proteus mirabilis* susceptibility to ceftazidime and ciprofloxacin and the impact of these antibiotics at subinhibitory concentrations on *Proteus mirabilis* biofilms. *Biomed Res. Int.* 2013, 1-8. <https://doi.org/10.1155/2013/930876>
- Ladhari, A., Omezzine, F., Haouala, R., 2014. The impact of Tunisian *Capparidaceae* species on cytological, physiological and biochemical mechanisms in lettuce. *South African J. Bot.* 93, 222–230. <https://doi.org/10.1016/j.sajb.2014.04.014>
- Lebecque, S., Lins, L., Dayan, F.E., Fauconnier, M.L., Deleu, M., 2019. Interactions between natural herbicides and lipid bilayers mimicking the plant plasma membrane. *Front. Plant Sci.* 10, 1–11. <https://doi.org/10.3389/fpls.2019.00329>
- Lee, H.J., Burger, P., Vogel, M., Friese, K., Brüning, A., 2012. The nucleoside antagonist cordycepin causes DNA double strand breaks in breast cancer cells. *Invest. New Drugs.* 30, 1917–1925. <https://doi.org/10.1007/s10637-012-9859-x>
- Lee, S.K., Lee, Ju Hun, Kim, H.R., Chun, Y., Lee, Ja Hyun, Yoo, H.Y., Park, C., Kim, S.W., 2019. Improved cordycepin production by *Cordyceps militaris* KYL05 using casein hydrolysate in submerged conditions. *Biomolecules.* 9, 1-11. <https://doi.org/10.3390/biom9090461>
- Lei Huang, Qizhang Li, Yiyuan Chen, X.W. and X.Z., 2009. Determination and analysis of cordycepin and adenosine in the products of *Cordyceps* spp. *African J. Microbiol. Res.* 3, 957-961.
- Lei, J., Wei, Y., Song, P., Li, Y., Zhang, T., Feng, Q., Xu, G., 2018. Cordycepin inhibits LPS-induced acute lung injury by inhibiting inflammation and oxidative stress. *Eur. J. Pharmacol.* 818, 110–114.

- <https://doi.org/10.1016/j.ejphar.2017.10.029>
- Li, J., Mu, J., Bai, J., Fu, F., Zou, T., An, F., Zhang, J., Jing, H., Wang, Q., Li, Z., Yang, S., Zuo, J., 2013. Paraquat resistant 1, a Golgi-localized putative transporter protein, is involved in intracellular transport of paraquat. *Plant Physiol.* 162, 470–483. <https://doi.org/10.1104/pp.113.213892>
- Li, S.P., Li, P., Dong, T.T.X., Tsim, K.W.K., 2001. Anti-oxidation activity of different types of natural *Cordyceps sinensis* and cultured *Cordyceps mycelia*. *Phytomedicine.* 8, 207–212. <https://doi.org/10.1078/0944-7113-00030>
- Lin, K.W., Chen, Y.T., Yang, S.C., Wei, B.L., Hung, C.F., Lin, C.N., 2013. Xanthine oxidase inhibitory lanostanoids from *Ganoderma tsugae*. *Fitoterapia.* 89, 231–238. <https://doi.org/10.1016/j.fitote.2013.06.006>
- Lin, S., Zhang, G., Liao, Y., Pan, J., Gong, D., 2015. Dietary flavonoids as xanthine oxidase inhibitors: Structure-affinity and structure-activity relationships. *J. Agric. Food Chem.* 63, 7784–7794. <https://doi.org/10.1021/acs.jafc.5b03386>
- Liu, F., Deng, C., Cao, W., Zeng, G., Deng, X., Zhou, Y., 2017. Phytochemicals of *Pogostemon cablin* (Blanco) Benth. aqueous extract: Their xanthine oxidase inhibitory activities. *Biomed. Pharmacother.* 89, 544–548. <https://doi.org/10.1016/j.biopha.2017.01.040>
- Liu, J.Y., Feng, C.P., Li, X., Chang, M.C., Meng, J.L., Xu, L.J., 2016. Immunomodulatory and antioxidative activity of *Cordyceps militaris* polysaccharides in mice. *Int. J. Biol. Macromol.* 86, 594–598. <https://doi.org/10.1016/j.ijbiomac.2016.02.009>
- Liu, L., Zhao, J., Guan, L., 2013. Tracking photosynthetic injury of paraquat-treated crop using chlorophyll fluorescence from hyperspectral data. *Eur. J. Remote Sens.* 46, 459–473. <https://doi.org/10.5721/EuJRS20134627>
- Liu, Q., Meng, X., Li, Y., Zhao, C.N., Tang, G.Y., Li, H. Bin, 2017. Antibacterial and antifungal activities of spices. *Int. J. Mol. Sci.* 18, 1–62. <https://doi.org/10.3390/ijms18061283>
- Lou, H.W., Zhao, Y., Tang, H.B., Ye, Z.W., Wei, T., Lin, J.F., Guo, L.Q., 2019. Transcriptome analysis of *Cordyceps militaris* reveals genes associated with

- carotenoid synthesis and identification of the function of the *Cmtns* gene. *Front. Microbiol.* 10, 1–10. <https://doi.org/10.3389/fmicb.2019.02105>
- Lovett, J. V., Ryuntyu, M.Y., Liu, D.L., 1989. Allelopathy, chemical communication, and plant defense. *J. Chem. Ecol.* 15, 1193–1202. <https://doi.org/10.1007/BF01014822>
- Löfgren, N.; Lüning, B.; Hedström, H.; Burriss, R.H., 1954. The isolation of nebularine and the determination of its structure. *Acta Chem. Scand.* 8, 670–680. <https://doi.org/10.3891/acta.chem.scand.08-0670>
- Lu, L., Yang, C., Qing, L., Ning, X., Mengzhou, Z., Bing, G., Chao, W., Yong, S., 2018. Fermenting liquid vinegar with higher taste, flavor and healthy value by using discarded *Cordyceps militaris* solid culture medium. *LWT-Food Sci Technol.* 98, 654-660.pdf.
- Lu, Y., Zhi, Y., Miyakawa, T., Tanokura, M., 2019. Metabolic profiling of natural and cultured *Cordyceps* by NMR spectroscopy. *Sci. Rep.* 9, 1–11. <https://doi.org/10.1038/s41598-019-44154-x>
- Ma, L., Zhang, S., Du, M., 2015. Cordycepin from *Cordyceps militaris* prevents hyperglycemia in alloxan-induced diabetic mice. *Nutr. Res.* 35, 431–439. <https://doi.org/10.1016/j.nutres.2015.04.011>
- Macias, F.A., Galindo, J.C.G., Molinillo, J.M.G., Cutler, H. G., 2004. Allelopathy: Chemistry and mode of action of allelochemicals. CRC, 2004, 217-227. <https://doi.org/10.1002/cbf.1140>
- Maeda, H., Dudareva, N., 2012. The shikimate pathway and aromatic amino acid biosynthesis in plants. *Annu. Rev. Plant Biol.* 63, 73–105. <https://doi.org/10.1146/annurev-arplant-042811-105439>
- Martinez, D.A., Loening, U.E., Graham, M.C., 2018. Impacts of glyphosate-based herbicides on disease resistance and health of crops: a review. *Environ. Sci. Eur.* 30, 1-14. <https://doi.org/10.1186/s12302-018-0131-7>
- Masuda, M., Hatashita, M., Fujihara, S., Suzuki, Y., Sakurai, A., 2015. Simple and efficient isolation of cordycepin from culture broth of a *Cordyceps militaris* mutant. *J. Biosci. Bioeng.* 120, 732–735. <https://doi.org/10.1016/j.jbiosc.2015.04.008>

- McGaw, L.J., Jäger, A.K., Van Staden, J., 2002. Antibacterial effects of fatty acids and related compounds from plants. *South African J. Bot.* 68, 417–423. [https://doi.org/10.1016/S0254-6299\(15\)30367-7](https://doi.org/10.1016/S0254-6299(15)30367-7)
- Mesnager, R., Antoniou, M.N., 2017. Facts and fallacies in the debate on glyphosate toxicity. *Front. Public Heal.* 5, 1–7. <https://doi.org/10.3389/fpubh.2017.00316>
- Mikulic-Petkovsek, M., Samoticha, J., Eler, K., Stampar, F., Veberic, R., 2015. Traditional elderflower beverages: A rich source of phenolic compounds with high antioxidant activity. *J. Agric. Food Chem.* 63, 1477–1487. <https://doi.org/10.1021/jf506005b>
- Minh, T.N., Xuan, T.D., Tran, H.D., Van, T.M., Andriana, Y., Khanh, T.D., Van Quan, N., Ahmad, A., 2019. Isolation and purification of bioactive compounds from the stem bark of *Jatropha podagrica*. *Molecules.* 24, 1-15 <https://doi.org/10.3390/molecules24050889>
- Mirani, Z.A., Naz, S., Khan, F., Aziz, M., Asadullah, Khan, M.N., Khan, S.I., 2017. Antibacterial fatty acids destabilize hydrophobic and multicellular aggregates of biofilm in *S. aureus*. *J. Antibiot. (Tokyo).* 70, 115–121. <https://doi.org/10.1038/ja.2016.76>
- Mishra, M.P., Rath, S., Swain, S.S., Ghosh, G., Das, D., Padhy, R.N., 2017. *In vitro* antibacterial activity of crude extracts of 9 selected medicinal plants against UTI causing MDR bacteria. *J. King Saud Univ. - Sci.* 29, 84–95. <https://doi.org/10.1016/j.jksus.2015.05.007>
- Mohy El-Din, S.M., El-Ahwany, A.M.D., 2016. Bioactivity and phytochemical constituents of marine red seaweeds (*Jania rubens*, *Corallina mediterranea* and *Pterocladia capillacea*). *J. Taibah Univ. Sci.* 10, 471–484. <https://doi.org/10.1016/j.jtusci.2015.06.004>
- Mokrani, A., Madani, K., 2016. Effect of solvent, time and temperature on the extraction of phenolic compounds and antioxidant capacity of peach (*Prunus persica* L.) fruit. *Sep. Purif. Technol.* 162, 68–76. <https://doi.org/10.1016/j.seppur.2016.01.043>
- Morimoto, M., Cantrell, C.L., Libous-Bailey, L., Duke, S.O., 2009. Phytotoxicity

- of constituents of glandular trichomes and the leaf surface of camphorweed, *Heterotheca subaxillaris*. *Phytochemistry*. 70, 69–74. <https://doi.org/10.1016/j.phytochem.2008.09.026>
- Mostafa, A.A., Al-Askar, A.A., Almaary, K.S., Dawoud, T.M., Sholkamy, E.N., Bakri, M.M., 2018. Antimicrobial activity of some plant extracts against bacterial strains causing food poisoning diseases. *Saudi J. Biol. Sci.* 25, 253–258. <https://doi.org/10.1016/j.sjbs.2017.02.004>
- Ngoc, T.M., Khoi, N.M., Ha, D.T., Nhiem, N.X., Tai, B.H., Don, D.V., Luong, H.V., Son, D.C., Bae, K., 2012. Xanthine oxidase inhibitory activity of constituents of *Cinnamomum cassia* twigs. *Bioorganic Med. Chem. Lett.* 22, 4625–4628. <https://doi.org/10.1016/j.bmcl.2012.05.051>
- Nguyen, M.T.T., Awale, S., Tezuka, Y., Tran, Q.L., Watanabe, H., Kadota, S., 2004. Xanthine oxidase inhibitory activity of Vietnamese medicinal plants. *Biol. Pharm. Bull.* 27, 1414–1421. <https://doi.org/10.1248/bpb.27.1414>
- Nguyen, M.T.T., Nguyen, N.T., 2012. Xanthine oxidase inhibitors from Vietnamese *Blumea balsamifera* L. *Phyther. Res.* 26, 1178–1181. <https://doi.org/10.1002/ptr.3710>
- Nguyen, V.T.A., Le, T.D., Phan, H.N., Tran, L.B., 2017. Antibacterial activity of free fatty acids from hydrolyzed virgin coconut oil using lipase from *Candida rugosa*. *J. Lipids*. 2017, 1–7. <https://doi.org/10.1155/2017/7170162>
- Ni, H., Hao, R.L., Li, X.F., Raikos, V., Li, H.H., 2018. Synergistic anticancer and antibacterial activities of cordycepin and selected natural bioactive compounds. *Trop. J. Pharm. Res.* 17, 1621–1627. <https://doi.org/10.4314/tjpr.v17i8.22>
- Nile, S.H., Park, S.W., 2015. Chromatographic analysis, antioxidant, anti-inflammatory, and xanthine oxidase inhibitory activities of ginger extracts and its reference compounds. *Ind. Crops Prod.* 70, 238–244. <https://doi.org/10.1016/j.indcrop.2015.03.033>
- Ohta, Y., Ee, Lee, J.B., Hayashi, K., Fujita, A., Park, D.K., Hayashi, T., 2007. *In vivo* anti-influenza virus activity of an immunomodulatory acidic polysaccharide isolated from *Cordyceps militaris* grown on germinated

- soybeans. *J. Agric. Food Chem.* 55, 10194–10199. <https://doi.org/10.1021/jf721287>
- Olatunji, O.J., Feng, Y., Olatunji, O.O., Tang, J., Ouyang, Z., Su, Z., 2016. Cordycepin protects PC12 cells against 6-hydroxydopamine induced neurotoxicity via its antioxidant properties. *Biomed. Pharmacother.* 81, 7–14. <https://doi.org/10.1016/j.biopha.2016.03.009>
- Olatunji, O.J., Tang, J., Tola, A., Auberon, F., Oluwaniyi, O., Ouyang, Z., 2018. The genus *Cordyceps*: An extensive review of its traditional uses, phytochemistry and pharmacology. *Fitoterapia.* 129, 293-316. <https://doi.org/10.1016/j.fitote.2018.05.010>
- Omezzine, F., Ladhari, A., Haouala, R., 2014. Physiological and biochemical mechanisms of allelochemicals in aqueous extracts of diploid and mixoploid *Trigonella foenum-graecum* L. *South African J. Bot.* 93, 167–178. <https://doi.org/10.1016/j.sajb.2014.04.009>
- Onyon, C., Dawson, T., 2018. Gastroenteritis. *Paediatr. Child Heal. (United Kingdom)* 28, 527–532. <https://doi.org/10.1016/j.paed.2018.08.010>
- Osivand, A., Araya, H., Appiah, K.S., Mardani, H., Ishizaki, T., Fujii, Y., 2018. Allelopathy of wild mushrooms-An important factor for assessing forest ecosystems in Japan. *Forests* 9, 1–15. <https://doi.org/10.3390/f9120773>
- Osman, N.I., Sidik, N.J., Awal, A., Adam, N.A.M., Rezali, N.I., 2016. *In vitro* xanthine oxidase and albumin denaturation inhibition assay of *Barringtonia racemosa* L. and total phenolic content analysis for potential anti-inflammatory use in gouty arthritis. *J. Intercult. Ethnopharmacol.* 5, 343–349. <https://doi.org/10.5455/jice.20160731025522>
- Ouertani, A., Neifar, M., Ouertani, R., Masmoudi, A.S., Cherif, A., 2019. Effectiveness of enzyme inhibitors in biomedicine and pharmacotherapy. *Adv Tissue Eng Regen Med Open Access.* 5, 85-90. <https://doi.org/10.15406/atroa.2019.05.00104>
- Ouyang, H., Hou, K., Peng, W., Liu, Z., Deng, H., 2017. Antioxidant and xanthine oxidase inhibitory activities of total polyphenols from onion. *Saudi J. Biol. Sci.* 25, 1509-1513. <https://doi.org/10.1016/j.sjbs.2017.08.005>

- Pacher, P., Nivorozhkin, A., Szabó, C., 2006. Therapeutic effects of xanthine oxidase inhibitors: Renaissance half a century after the discovery of allopurinol. *Pharmacol. Rev.* 58, 87–114. <https://doi.org/10.1124/pr.58.1.6>
- Panda, A.K., Swain, K.C., 2011. Traditional uses and medicinal potential of *Cordyceps sinensis* of Sikkim. *J. Ayurveda Integr. Med.* 2, 9–13. <https://doi.org/10.4103/0975-9476.78183>
- Park, J.G., Son, Y.-J., Lee, T.H., Baek, N.J., Yoon, D.H., Kim, T.W., Aravinthan, A., Hong, S., Kim, J.-H., Sung, G.-H., Cho, J.Y., 2017. Anticancer efficacy of *Cordyceps militaris* ethanol extract in a xenografted leukemia model. *Evidence-Based Complement. Altern. Med.* 2017, 1–7. <https://doi.org/10.1155/2017/8474703>
- Parthasarathy, A., Cross, P.J., Dobson, R.C.J., Adams, L.E., Savka, M.A., Hudson, A.O., 2018. A three-ring circus: Metabolism of the three proteogenic aromatic amino acids and their role in the health of plants and animals. *Front. Mol. Biosci.* 5, 1–30. <https://doi.org/10.3389/fmolb.2018.00029>
- Pathania, P., Joshi, M., Sagar, A., 2015. Morphological, physiological and molecular studies on wildy collected *Cordyceps militaris* from North West Himalayas, India. 3, 53–62.
- Paul, C.C., Okey, A.O., 2015. Herbal medicine: Yesterday, today and tomorrow. *Altern. Integr. Med.* 4, 1-5. <https://doi.org/10.4172/2327-5162.1000195>
- Peneva, A., 2007. Allelopathic effect of seed extracts and powder of coffee (*Coffea arabica* L.) on common cocklebur (*Xanthium strumarium* L.). *Bulg.J.Agric.Sci.* 13, 205–211.
- Peters, J.S., Chin, C.K., 2003. Inhibition of photosynthetic electron transport by palmitoleic acid is partially correlated to loss of thylakoid membrane proteins. *Plant Physiol. Biochem.* 41, 117–124. [https://doi.org/10.1016/S0981-9428\(02\)00014-1](https://doi.org/10.1016/S0981-9428(02)00014-1)
- Polimova, A.M., Vladimirova, G.A., Proskurnina, E. V., Vladimirov, Y.A., 2011. Aromatic amino acid oxidation products as antioxidants. *Biophysics (Oxf).* 56, 585–589. <https://doi.org/10.1134/S000635091104021X>
- Qian, H., Chen, W., Sun, L., Jin, Y., Liu, W., Fu, Z., 2009a. Inhibitory effects of

- paraquat on photosynthesis and the response to oxidative stress in *Chlorella vulgaris*. *Ecotoxicology*. 18, 537–543. <https://doi.org/10.1007/s10646-009-0311-8>
- Qian, H., Xu, X., Chen, W., Jiang, H., Jin, Y., Liu, W., Fu, Z., 2009b. Allelochemical stress causes oxidative damage and inhibition of photosynthesis in *Chlorella vulgaris*. *Chemosphere*. 75, 368-375. <https://doi.org/10.1016/j.chemosphere.2008.12.040>
- Quan, N.V., Xuan, T.D., Tran, H.D., Thuy, N.T.D., Trang, L.T., Huong, C.T., Andriana, Y., Tuyen, P.T., 20 . Antioxidant, α -Amylase and α -Glucosidase Inhibitory Activities and Potential Constituents of *Canarium tramdenum* Bark. *Molecules* 24. 1-14. <https://doi.org/10.3390/molecules24030605>
- Quy, T.N., Xuan, T.D., Andriana, Y., Khanh, T.D., Teschke, R., 2019. Cordycepin isolated from *Cordyceps militaris*: Its newly discovered herbicidal property and potential plant-based novel alternative to glyphosate. *Molecules*. 24, 1-18. <https://doi.org/10.3390/molecules24162901>
- Ragab, G., Elshahaly, M., Bardin, T., 2017. Gout: An old disease in new perspective – A review. *J. Adv. Res.* 8, 495–511. <https://doi.org/10.1016/j.jare.2017.04.008>
- Rayee, R., Tran, H.D., Xuan, T.D., Khanh, T.D., 2018. Imposed water deficit after anthesis for the improvement of macronutrients, quality, phytochemicals, and antioxidants in rice grain. *Sustain.* 10, 1-12. <https://doi.org/10.3390/su10124843>
- Reis, F. ., Barros, L., Calhella, R.C., Ćirić, A., Griens e n, L.J.L.D., o o íć, ., Ferreira, I.C.F.R., 2013. The methanolic extract of *Cordyceps militaris* (L.) Link fruiting body shows antioxidant, antibacterial, antifungal and antihuman tumor cell lines properties. *Food Chem. Toxicol.* 62, 91–98. <https://doi.org/10.1016/j.fct.2013.08.033>
- Rice, E.L. (1984) Allelopathy. 2nd Edition, Academic Press, New York, 422.
- Rodriguez, J.M.G., Towns, M.H., 2019. Analysis of student reasoning about Michaelis-Menten enzyme kinetics: Mixed conceptions of enzyme inhibition. *Chem. Educ. Res. Pract.* 20, 428–442. <https://doi.org/10.1039/c8rp00276b>

- Saag, K.G., Choi, H., 2006. Epidemiology, risk factors, and lifestyle modifications for gout. *Arthritis Res. Ther.* 8, 1–7. <https://doi.org/10.1186/ar1907>
- Sabina, R.L., Paul, A.L., Ferl, R.J., Laber, B., Lindell, S.D., 2007. Adenine nucleotide pool perturbation is a metabolic trigger for AMP deaminase inhibitor-based herbicide toxicity. *Plant Physiol.* 143, 1752–1760. <https://doi.org/10.1104/pp.107.096487>
- Saccà, S.C., Cutolo, C.A., Ferrari, D., Corazza, P., Traverso, C.E., 2018. The eye, oxidative damage and polyunsaturated fatty acids. *Nutrients* 10, 1–15. <https://doi.org/10.3390/nu10060668>
- Sado-Kamdem, S.L., Vannini, L., Guerzoni, M.E., 2009. Effect of α -linolenic, capric and lauric acid on the fatty acid biosynthesis in *Staphylococcus aureus*. *Int. J. Food Microbiol.* 129, 288–294. <https://doi.org/10.1016/j.ijfoodmicro.2008.12.010>
- Sammons, R.D., Gaines, T.A., 2014. Glyphosate resistance: State of knowledge. *Pest Manag. Sci.* 70, 1367–1377. <https://doi.org/10.1002/ps.3743>
- Santi, M.D., Paulino Zunini, M., Vera, B., Bouzidi, C., Dumontet, V., Abin-Carriquiry, A., Grougnet, R., Ortega, M.G., 2018. Xanthine oxidase inhibitory activity of natural and hemisynthetic flavonoids from *Gardenia oudiepe* (Rubiaceae) *in vitro* and molecular docking studies. *Eur. J. Med. Chem.* 143, 577–582. <https://doi.org/10.1016/j.ejmech.2017.11.071>
- Santos, M.S.F., Schaule, G., Alves, A., Madeira, L.M., 2013. Adsorption of paraquat herbicide on deposits from drinking water networks. *Chem. Eng. J.* 229, 324–333. <https://doi.org/10.1016/j.cej.2013.06.008>
- Sarah, B.D., Sarah, K.S., 2019. Evaluation and management of urinary tract infection in the emergency department. *Emerg. Med. Clin. North. Am.* 37, 707–723. <https://doi.org/10.1016/j.emc.2019.07.007>
- Sari, N., Suparmin, A., Kato, T., Park, E.Y., 2016. Improved cordycepin production in a liquid surface culture of *Cordyceps militaris* isolated from wild strain. *Biotechnol. Bioprocess Eng.* 21, 595–600. <https://doi.org/10.1007/s12257-016-0405-0>
- Sarmah, A.K., Kookana, R.S., Alston, A.M., 1998. Fate and behaviour of

- triasulfuron, metsulfuron-methyl, and chlorsulfuron in the Australian soil environment: A review. *Aust. J. Agric. Res.* 49, 775–790. <https://doi.org/10.1071/A97131>
- Sasamoto, H., Fujii, Y., Ashihara, H., 2015. Effect of purine alkaloids on the proliferation of lettuce cells derived from protoplasts. *Nat. Prod. Commun.* 10, 751–754. <https://doi.org/10.1177/1934578x1501000513>
- Sedigheh, H.G., Mortazavian, M., Norouzian, D., Atyabi, M., Akbarzadeh, A., Hasanpoor, K., Ghorbani, M., 2011. Oxidative stress and leaf senescence. *BMC Res. Notes* 4, 477. <https://doi.org/10.1186/1756-0500-4-477>
- Sergiev, I.G., Alexieva, V.S., Ivanov, S. V., Moskova, I.I., Karanov, E.N., 2006. The phenylurea cytokinin 4PU-30 protects maize plants against glyphosate action. *Pestic. Biochem. Physiol.* 85, 139–146. <https://doi.org/10.1016/j.pestbp.2006.01.001>
- Sharma, A., Flores-Vallejo, R. del C., Cardoso-Taketa, A., Villarreal, M.L., 2017. Antibacterial activities of medicinal plants used in Mexican traditional medicine. *J. Ethnopharmacol.* 208, 264–329. <https://doi.org/10.1016/j.jep.2016.04.045>
- Sheerin, N.S., Glover, E.K., 2019. Urinary tract infection. *Med. (United Kingdom)*. 47, 546–550. <https://doi.org/10.1016/j.mpmed.2019.06.008>
- Sheu, C.W., Freese, E., 1972. Effects of fatty acids on growth and envelope proteins of *Bacillus subtilis*. *J. Bacteriol.* 111, 516–524.
- Shin, S.Y., Bajpai, V.K., Kim, H.R., Kang, S.C., 2007. Antibacterial activity of eicosapentaenoic acid (EPA) against foodborne and food spoilage microorganisms. *LWT - Food Sci. Technol.* 40, 1515–1519. <https://doi.org/10.1016/j.lwt.2006.12.005>
- Shrestha, B., Sung, J.M., 2005. Notes on *Cordyceps* species collected from the central region of Nepal. *Mycobiology.* 33, 235–239. <https://doi.org/10.4489/myco.2005.33.4.235>
- Shrestha, B., Zhang, W., Zhang, Y., Liu, X., 2012. The medicinal fungus *Cordyceps militaris*: Research and development. *Mycol. Prog.* 11, 599–614. <https://doi.org/10.1007/s11557-012-0825-y>

- Silva, F.B., Costa, A.C., Alves, R.R., Megguer, C.A., 2014. Chlorophyll fluorescence as an indicator of cellular damage by glyphosate herbicide in *Raphanus sativus* L. plants. *Am. J. Plant Sci.* 05, 2509–2519. <https://doi.org/10.4236/ajps.2014.516265>
- Slaby, S., Titran, P., Marchand, G., Hanotel, J., Lescuyer, A., Leprêtre, A., Bodart, J.F., Marin, M., Lemiere, S., 2019. Effects of glyphosate and a commercial formulation Roundup® exposures on maturation of *Xenopus laevis* oocytes. *Environ. Sci. Pollut. Res. Int.* 2019, 1-9. <https://doi.org/10.1007/s11356-019-04596-2>
- Smiderle, F.R., Baggio, C.H., Borato, D.G., Santana-Filho, A.P., Sasaki, G.L., Iacomini, M., Van Griensven, L.J.L.D., 2014. Anti-inflammatory properties of the medicinal mushroom *Cordyceps militaris* might be related to its linear ($\rightarrow 3$)- β -D-glucan. *PLoS One.* 9, 1-11. <https://doi.org/10.1371/journal.pone.0110266>
- Sodaeizadeh, H., Rafieiohossaini, M., Van Damme, P., 2010. Herbicidal activity of a medicinal plant, *Peganum harmala* L., and decomposition dynamics of its phytotoxins in the soil. *Ind. Crops Prod.* 31, 385–394. <https://doi.org/10.1016/j.indcrop.2009.12.006>
- Soltys, D., Krasuska, U., Bogatek, R., Gniazdowski, A., 2013. Allelochemicals as bioherbicides -present and perspectives. *Herbic. - Curr. Res. Case Stud. Use.* 20, 517-542. <https://doi.org/10.5772/56185>
- Speert, D.P., Wannamaker, L.W., Gray, E.D., Clawson, C.C., 1979. Bactericidal effect of oleic acid on group A streptococci: Mechanism of action. *Infect. Immun.* 26, 1202–1210.
- Spiassi, A., Nóbrega, L.H.P., Rosa, D.M., Pacheco, F.P., Senem, J., Piccolo De Lima, G., 2015. Allelopathic effects of pathogenic fungi on weed plants of soybean and corn crops. *Biosci. J.* 31, 1037–1048. <https://doi.org/10.14393/BJ-v31n4a2015-26142>
- Spilak, M.P., Madsen, A.M., Knudsen, S.M., Kolarik, B., Hansen, E.W., Frederiksen, M., Gunnarsen, L., 2015. Impact of dwelling characteristics on concentrations of bacteria, fungi, endotoxin and total inflammatory potential

- in settled dust. *Build. Environ.* 93, 64–71.
<https://doi.org/10.1016/j.buildenv.2015.03.031>
- tan o ić , N., ihaji lo -Krstev, T., Zlat o ić, B., tan o -Jo a no ić, V., it ić, V., Jo ić, J., Čomić, L., Kocić, B., Bernstein, N., 20 6. Antibacterial and antioxidant activity of traditional medicinal plants from the *Balkan peninsula*. *NJAS - Wageningen J. Life Sci.* 78, 21–28.
<https://doi.org/10.1016/j.njas.2015.12.006>
- Strelow, J., Dewe, W., Iversen, P.W., Brooks, H.B., Radding, J.A., Mcgee, J., Weidner, J., 2012. Mechanism of action assays for enzymes. *Assay Guid. Man.* 2012, 1–22. <https://doi.org/10.1016/j.tics.2014.04.003>
- Sunaina, D., Singh, N.B., 2015. Alleviation of allelopathic stress of benzoic acid by indole acetic acid in *Solanum lycopersicum*. *Sci. Hortic. (Amsterdam)*. 192, 211–217. <https://doi.org/10.1016/j.scienta.2015.06.013>
- Suzuki, T., Waller, G.R., 1987. Allelopathy due to purine alkaloids in tea seeds during germination. *Plant Soil.* 98, 131–136.
<https://doi.org/10.1007/BF02381733>
- Taïbi, K., Taïbi, F., Ait Abderrahim, L., Ennajah, A., Belkhodja, M., Mulet, J.M., 2016. Effect of salt stress on growth, chlorophyll content, lipid peroxidation and antioxidant defence systems in *Phaseolus vulgaris* L. *South African J. Bot.* 105, 306–312. <https://doi.org/10.1016/j.sajb.2016.03.011>
- Tamta, H., Kalra, S., Mukhopadhyay, A.K., 2006. Biochemical characterization of some pyrazolopyrimidine-based inhibitors of xanthine oxidase. *Biochem.* 71, 2–7. <https://doi.org/10.1134/S0006297906130086>
- Tamta, H., Thilagavathi, R., Chakraborti, A.K., Mukhopadhyay, A.K., 2005. 6-(N-benzoylamino)purine as a novel and potent inhibitor of xanthine oxidase: Inhibition mechanism and molecular modeling studies. *J. Enzyme Inhib. Med. Chem.* 20, 317–324. <https://doi.org/10.1080/14756360500112326>
- Tang, J., Qian, Z., Wu, H., 2018. Enhancing cordycepin production in liquid static cultivation of *Cordyceps militaris* by adding vegetable oils as the secondary carbon source. *Bioresour. Technol.* 268, 60–67.
<https://doi.org/10.1016/j.biortech.2018.07.128>

- Tanti, A., Bhattacharyya, P., Sandilya, S., Dutta, P., 2016. Allelopathic potential of caffeine as growth and germination inhibitor to popular tea weed, *Borreria hispida* L. *Curr. Life Sci.* 2, 114–117. <https://doi.org/10.5281/zenodo.163671>
- Tarazona, J. V., Court-Marques, D., Tiramani, M., Reich, H., Pfeil, R., Istace, F., Crivellente, F., 2017. Glyphosate toxicity and carcinogenicity: a review of the scientific basis of the European Union assessment and its differences with IARC. *Arch. Toxicol.* 91, 2723–2743. <https://doi.org/10.1007/s00204-017-1962-5>
- Tesio, F., Ferrero, A., 2010. Allelopathy, a chance for sustainable weed management. *Int. J. Sustain. Dev. World Ecol.* 17, 377-389. <https://doi.org/10.1080/13504509.2010.507402>
- Thanh, P.T.V., Ismail, T., Mishyna, M., Appiah, S.K., Oikawa, Y., Fuji, Y., 2019. Caffeine: The allelochemical responsible for the plant growth inhibitory activity of Vietnamese tea (*Camellia sinensis* L. Kuntze). *Agronomy.* 9, 1-15. <https://doi.org/10.3390/agronomy9070396>
- Thiour-Mauprivez, C., Martin-Laurent, F., Calvayrac, C., Barthelmebs, L., 2019. Effects of herbicide on non-target microorganisms: Towards a new class of biomarkers? *Sci. Total Environ.* 684, 314–325. <https://doi.org/10.1016/j.scitotenv.2019.05.230>
- Thompson, L., Cockayne, A., Spiller, R.C., 1994. Inhibitory effect of polyunsaturated fatty acids on the growth of *Helicobacter pylori*: A possible explanation of the effect of diet on peptic ulceration. *Gut* 35, 1557–1561. <https://doi.org/10.1136/gut.35.11.1557>
- Tohge, T., Watanabe, M., Hoefgen, R., Fernie, A.R., 2013. Shikimate and phenylalanine biosynthesis in the green lineage. *Front. Plant Sci.* 4, 1–13. <https://doi.org/10.3389/fpls.2013.00062>
- Tongmai, T., Maketon, M., Chumnanpuen, P., 2018. Prevention potential of *Cordyceps militaris* aqueous extract against cyclophosphamide-induced mutagenicity and sperm abnormality in rats. *Agric. Nat. Resour.* 52, 419–423. <https://doi.org/10.1016/j.anres.2018.11.005>
- Trezzi, M.M., Vidal, R.A., Junior, A.A.B., Hertwig Bittencourt, H., Silva Souza

- Filho, A.P., 2016. Allelopathy: Driving mechanisms governing its activity in agriculture. *J. Plant Interact.* 11, 53-60. <https://doi.org/10.1080/17429145.2016.1159342>
- Tsai, W.T., 2019. Trends in the use of glyphosate herbicide and its relevant regulations in Taiwan: A water contaminant of increasing concern. *Toxics*.7, 1-9. <https://doi.org/10.3390/toxics7010004>
- Tsai, Y.J., Lin, L.C., Tsai, T.H., 2010. Pharmacokinetics of adenosine and cordycepin, a bioactive constituent of *Cordyceps sinensis* in rat. *J. Agric. Food Chem.* 58, 4638–4643. <https://doi.org/10.1021/jf100269g>
- Tuli, H.S., Sandhu, S.S., Sharma, A.K., 2014. Pharmacological and therapeutic potential of *Cordyceps* with special reference to Cordycepin. *3 Biotech.* 4, 1–12. <https://doi.org/10.1007/s13205-013-0121-9>
- Tuli, H.S., Sharma, A.K., Sandhu, S.S., Kashyap, D., 2013. Cordycepin: A bioactive metabolite with therapeutic potential. *Life Sci.* 93, 863–869. <https://doi.org/10.1016/j.lfs.2013.09.030>
- Tzin, V., Galili, G., 2010. The Biosynthetic pathways for shikimate and aromatic amino acids in *Arabidopsis thaliana*. *Arab. B.* 8, 1-18. <https://doi.org/10.1199/tab.0132>
- Tzvetkova, P., Lyubenova, M., Boteva, S., Todorovska, E., Tsonev, S., Kalcheva, H., 2019. Effect of herbicides paraquat and glyphosate on the early development of two tested plants. *IOP Conf. Ser. Earth Environ. Sci.* 221, 1-16. <https://doi.org/10.1088/1755-1315/221/1/012137>
- Umamaheswari, M., AsokKumar, K., Somasundaram, A., Sivashanmugam, T., Subhadradevi, V., Ravi, T.K., 2007. Xanthine oxidase inhibitory activity of some Indian medical plants. *J. Ethnopharmacol.* 109, 547–551. <https://doi.org/10.1016/j.jep.2006.08.020>
- Upham, B.L., Hatzios, K.K., 1987. Counteraction of paraquat toxicity at the chloroplast level. *Zeitschrift fur Naturforsch. - Sect. C J. Biosci.* 42, 824–828. <https://doi.org/10.1515/znc-1987-0631>
- Valle, D.L., Andrade, J.I., Puzon, J.J.M., Cabrera, E.C., Rivera, W.L., 2015. Antibacterial activities of ethanol extracts of Philippine medicinal plants

- against multidrug-resistant bacteria. *Asian Pac. J. Trop. Biomed.* 5, 532–540.
<https://doi.org/10.1016/j.apjtb.2015.04.005>
- Van, T.M., Xuan, T.D., Minh, T.N., Quan, N.V., 2018. Isolation and purification of potent growth inhibitors from *Piper methysticum* root. *Molecules* 23, 1–13.
<https://doi.org/10.3390/molecules23081907>
- Vikrant, P., Verma, K.K., Rajak, R.C., Pandey, A.K., 2006. Characterization of a phytotoxin from *Phoma herbarum* for management of *Parthenium hysterophorus* L. *J. Phytopathol.* 154, 461–468.
<https://doi.org/10.1111/j.1439-0434.2006.01129.x>
- Wada, T., Sumardika, I.W., Saito, S., Ruma, I.M.W., Kondo, E., Shibukawa, M., Sakaguchi, M., 2017. Identification of a novel component leading to anti-tumor activity besides the major ingredient cordycepin in *Cordyceps militaris* extract. *J. Chromatogr. B Anal. Technol. Biomed. Life Sci.* 1061–1062, 209–219. <https://doi.org/10.1016/j.jchromb.2017.07.022>
- Wang, F., Yin, P., Lu, Y., Zhou, Z., Jiang, C., Liu, Y., Yu, X., 2015. Cordycepin prevents oxidative stress-induced inhibition of osteogenesis. *Oncotarget.* 6, 35496–35508. <https://doi.org/10.18632/oncotarget.6072>
- Wang, H.J., Pan, M.C., Chang, C.K., Chang, S.W., Hsieh, C.W., 2014. Optimization of ultrasonic-assisted extraction of cordycepin from *Cordyceps militaris* using orthogonal experimental design. *Molecules.* 19, 20808–20820. <https://doi.org/10.3390/molecules191220808>
- Wang, M., Meng, X.Y., Yang, R. Le, Qin, T., Wang, X.Y., Zhang, K.Y., Fei, C.Z., Li, Y., Hu, Y.L., Xue, F.Q., 2012. *Cordyceps militaris* polysaccharides can enhance the immunity and antioxidation activity in immunosuppressed mice. *Carbohydr. Polym.* 89, 461–466.
<https://doi.org/10.1016/j.carbpol.2012.03.029>
- Wang, X., Luo, F., Zhao, H., 2014. Paraquat-induced reactive oxygen species inhibit neutrophil apoptosis via a p38 MAPK/NF- κ B-IL-6/TNF- α positive feedback circuit. *PLoS One.* 9, 1–7.
<https://doi.org/10.1371/journal.pone.0093837>
- Wang, Z., Chen, Z., Jiang, Z., Luo, P., Liu, L., Huang, Y., Wang, H., Wang, Yu,

- Long, L., Tan, X., Liu, D., Jin, T., Wang, Yawei, Wang, Yang, Liao, F., Zhang, C., Chen, L., Gan, Y., Liu, Y., Yang, F., Huang, C., Miao, H., Chen, J., Cheng, T., Fu, X., Shi, C., 2019. Cordycepin prevents radiation ulcer by inhibiting cell senescence via NRF2 and AMPK in rodents. *Nat. Commun.* 10, 1-16. <https://doi.org/10.1038/s41467-019-10386-8>
- Wen, Z., Du, X., Meng, N., Li, Y., Mi, R., Li, X., Sun, Y., Ma, S., Li, S., 2019. Tussah silkworm pupae improve anti-tumor properties of *Cordyceps militaris* (L.) Link by increasing the levels of major metabolite cordycepin. *RSC Adv.* 9, 5480-5491. <https://doi.org/10.1039/c8ra09491h>
- Westwood, J.H., Charudattan, R., Duke, S.O., Fennimore, S.A., Marrone, P., Slaughter, D.C., Swanton, C., Zollinger, R., 2018. Weed management in 2050: Perspectives on the future of weed science. *Weed Sci.* 66, 275–285. <https://doi.org/10.1017/wsc.2017.78>
- Wicke, D., Schulz, L.M., Lentjes, S., Scholz, P., Poehlein, A., Gibhardt, J., Daniel, R., Ischebeck, T., Commichau, F.M., 2019. Identification of the first glyphosate transporter by genomic adaptation. *Environ. Microbiol.* 21, 1287–1305. <https://doi.org/10.1111/1462-2920.14534>
- Won, S.R., Hong, M.J., Kim, Y.M., Li, C.Y., Kim, J.W., Rhee, H.I., 2007. Oleic acid: An efficient inhibitor of glucosyltransferase. *FEBS Lett.* 581, 4999–5002. <https://doi.org/10.1016/j.febslet.2007.09.045>
- Wu, W.C., Hsiao, J.R., Lian, Y.Y., Lin, C.Y., Huang, B.M., 2007. The apoptotic effect of cordycepin on human OEC-M1 oral cancer cell line. *Cancer Chemother. Pharmacol.* 60, 103–111. <https://doi.org/10.1007/s00280-006-0354-y>
- Xiong, C., Xia, Y., Zheng, P., Shi, S., Wang, C., 2010. Developmental stage-specific gene expression profiling for a medicinal fungus *Cordyceps militaris*. *Mycology.* 1, 25-66. <https://doi.org/10.1080/21501201003674581>
- Xuan, T.D., Yulianto, R., Andriana, Y., Khanh, T.D., Khanh, T.D., Anh, T.T.T., Kakar, K., Haqani, M.S., 2018. Chemical profile, antioxidant activities and allelopathic potential of liquid waste from germinated brown rice. *Allelopath. J.* 45, 89-100. <https://doi.org/10.13140/RG.2.2.16579.71208>

- Xuan, T.D., Shinkichi, T., Khanh, T.D., Chung, I.M., 2005. Biological control of weeds and plant pathogens in paddy rice by exploiting plant allelopathy: An overview. *Crop Prot.* 24, 197–206. <https://doi.org/10.1016/j.cropro.2004.08.004>
- Xuan, T. D., Tawata, S., Khanh, T.D., Chung, I.M., 2005. Decomposition of allelopathic plants in soil. *J. Agron. Crop Sci.* 191, 162–171. <https://doi.org/10.1111/j.1439-037X.2005.00170.x>
- Xuan, T.D., Tsuzuki, E., Uematsu, H., Terao, H., 2001. Weed control with alfalfa pellets in transplanting rice. *Weed Biol. Manag.* 1, 231–235. <https://doi.org/10.1046/j.1445-6664.2001.00034.x>
- Yannicari, M., Gómez-Lobato, M.E., Istilart, C., Natalucci, C., Giménez, D.O., Castro, A.M., 2017. Mechanism of resistance to glyphosate in *Lolium perenne* from Argentina. *Front. Ecol. Evol.* 5, 1–8. <https://doi.org/10.3389/fevo.2017.00123>
- Yasunaka, K., Abe, F., Nagayama, A., Okabe, H., Lozada-Pérez, L., López-Villafranco, E., Muñiz, E.E., Aguilar, A., Reyes-Chilpa, R., 2005. Antibacterial activity of crude extracts from Mexican medicinal plants and purified coumarins and xanthenes. *J. Ethnopharmacol.* 97, 293–299. <https://doi.org/10.1016/j.jep.2004.11.014>
- Yi, S.Y., Cui, Y., Zhao, Y., Liu, Z.D., Lin, Y.J., Zhou, F., 2016. A novel naturally occurring class I 5-Enolpyruvylshikimate-3-Phosphate Synthase from *Janibacter* sp. confers high glyphosate tolerance to rice. *Sci. Rep.* 6, 1–11. <https://doi.org/10.1038/srep19104>
- Yong, T., Chen, S., Xie, Y., Chen, D., Su, J., Shuai, O., Jiao, C., Zuo, D., 2018. Cordycepin, a characteristic bioactive constituent in *Cordyceps militaris*, ameliorates hyperuricemia through URAT1 in hyperuricemic mice. *Front. Microbiol.* 9, 1–12. <https://doi.org/10.3389/fmicb.2018.00058>
- Yong, T., Zhang, M., Chen, D., Shuai, O., Chen, S., Su, J., Jiao, C., Feng, D., Xie, Y., 2016. Actions of water extract from *Cordyceps militaris* in hyperuricemic mice induced by potassium oxonate combined with hypoxanthine. *J. Ethnopharmacol.* 194, 403–411. <https://doi.org/10.1016/j.jep.2016.10.001>

- Yoo, H., Shin, J., Cho, J., Son, C., Lee, Y., Park, S., Cho, C., 2004. Effects of *Cordyceps militaris* extract on angiogenesis and tumor growth. *Acta. Pharmacol. Sin.* 25, 657-665.
- Yoo, H., Widhalm, J.R., Qian, Y., Maeda, H., Cooper, B.R., Jannasch, A.S., Gonda, I., Lewinsohn, E., Rhodes, D., Dudareva, N., 2013. An alternative pathway contributes to phenylalanine biosynthesis in plants via a cytosolic tyrosine:phenylpyruvate aminotransferase. *Nat. Commun.* 4, 1-11. <https://doi.org/10.1038/ncomms3833>
- Yoon, B.K., Jackman, J.A., Valle-González, E.R., Cho, N.J., 2018. Antibacterial free fatty acids and monoglycerides: Biological activities, experimental testing, and therapeutic applications. *Int. J. Mol. Sci.* 19, 1-40. <https://doi.org/10.3390/ijms19041114>
- Yu, J.Q., Ye, S.F., Zhang, M.F., Hu, W.H., 2003. Effects of root exudates and aqueous root extracts of cucumber (*Cucumis sativus*) and allelochemicals, on photosynthesis and antioxidant enzymes in cucumber. *Biochem. Syst. Ecol.* 31, 129–139. [https://doi.org/10.1016/S0305-1978\(02\)00150-3](https://doi.org/10.1016/S0305-1978(02)00150-3)
- Yu, R., Song, L., Zhao, Y., Bin, W., Wang, L., 2004. Isolation and biological properties of polysaccharide CPS-1 from cultured *Cordyceps militaris*. *Fitoterapia.* 75, 465-472. <https://doi.org/10.1016/j.fitote.2004.04.003>
- Yu, R., Yang, W., Song, L., Yan, C., Zhang, Z., Zhao, Y., 2007. Structural characterization and antioxidant activity of a polysaccharide from the fruiting bodies of cultured *Cordyceps militaris*. *Carbohydr. Polym.* 70, 430–436. <https://doi.org/10.1016/j.carbpol.2007.05.005>
- Yuan, J., Wang, A., He, Y., Si, Z., Xu, S., Zhang, S., Wang, K., Wang, D., Liu, Y., 2016. Cordycepin attenuates traumatic brain injury-induced impairments of blood-brain barrier integrity in rats. *Brain Res. Bull.* 127, 171–176. <https://doi.org/10.1016/j.brainresbull.2016.09.010>
- Zegaoui, Z., Planchais, S., Cabassa, C., Djebbar, R., Belbachir, O.A., Carol, P., 2017. Variation in relative water content, proline accumulation and stress gene expression in two cowpea landraces under drought. *J. Plant Physiol.* 218, 26–34. <https://doi.org/10.1016/j.jplph.2017.07.009>

- Zeng, R. S., 2014. Allelopathy - The solution is indirect. *J. Chem. Ecol.* 40, 515–516. <https://doi.org/10.1007/s10886-014-0464-7>
- Zhang, D. ju, Zhang, J., Yang, W. qin, Wu, F. zhong, 2010. Potential allelopathic effect of *Eucalyptus grandis* across a range of plantation ages. *Ecol. Res.* 25, 13–23. <https://doi.org/10.1007/s11284-009-0627-0>
- Zhang, J., Wen, C., Duan, Y., Zhang, H., Ma, H., 2019. Advance in *Cordyceps militaris* (Linn) Link polysaccharides: Isolation, structure, and bioactivities: A review. *Int. J. Biol. Macromol.* 132, 906–914. <https://doi.org/10.1016/j.ijbiomac.2019.04.020>
- Zhang, Z., Tudi, T., Liu, Y., Zhou, S., Feng, N., Yang, Y., Tang, C., Tang, Q., Zhang, J., 2016. Preparative isolation of cordycepin, N6-(2-hydroxyethyl)-adenosine and adenosine from *Cordyceps militaris* by macroporous resin and purification by recycling high-speed counter-current chromatography. *J. Chromatogr. B Anal. Technol. Biomed. Life Sci.* 1033–1034, 218–225. <https://doi.org/10.1016/j.jchromb.2016.08.025>
- Zheng, C.J., Yoo, J.S., Lee, T.G., Cho, H.Y., Kim, Y.H., Kim, W.G., 2005. Fatty acid synthesis is a target for antibacterial activity of unsaturated fatty acids. *FEBS Lett.* 579, 5157–5162. <https://doi.org/10.1016/j.febslet.2005.08.028>
- Zhou, X., Cai, G., He, Y.I., Tong, G., 2016. Separation of cordycepin from *Cordyceps militaris* fermentation supernatant using preparative HPLC and evaluation of its antibacterial activity as an NAD⁺-dependent DNA ligase inhibitor. *Exp. Ther. Med.* 12, 1812–1816. <https://doi.org/10.3892/etm.2016.3536>
- Zhou, X., Stevens, M.J.A., Neuenschwander, S., Schwarm, A., Kreuzer, M., Bratus-Neuenschwander, A., Zeitz, J.O., 2018. The transcriptome response of the ruminal methanogen *Methanobrevibacter ruminantium* strain M1 to the inhibitor lauric acid. *BMC Res. Notes.* 11, 1–10. <https://doi.org/10.1186/s13104-018-3242-8>
- Zhu, Z.Y., Liu, F., Gao, H., Sun, H., Meng, M., Zhang, Y.M., 2016. Synthesis, characterization and antioxidant activity of selenium polysaccharide from *Cordyceps militaris*. *Int. J. Biol. Macromol.* 93, 1090–1099.

<https://doi.org/10.1016/j.ijbiomac.2016.09.076>

Zulet, A., Gil-Monreal, M., Villamor, J.G., Zabalza, A., van der Hoorn, R.A.L., Royuela, M., 2013. Proteolytic pathways induced by herbicides that inhibit amino acid biosynthesis. *PLoS One.* 8, 1-9.
<https://doi.org/10.1371/journal.pone.0073847>

Appendix A: Identification of the most active fraction of *C. militaris* on xanthine oxidase inhibitory, antioxidant, and antibacterial activities

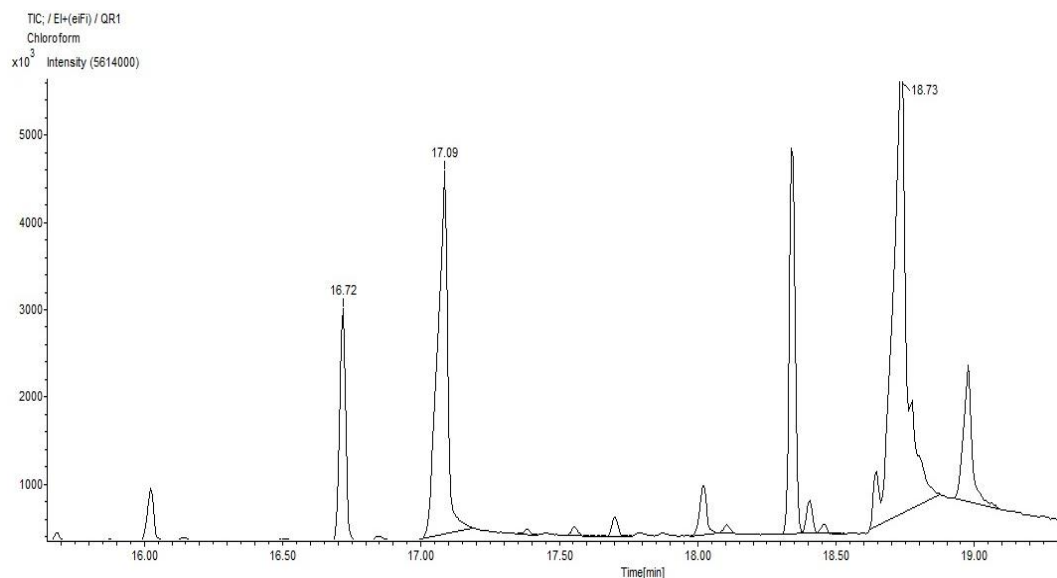


Figure 17. GC-MS chromatogram of F1 fraction from ethyl acetate extract of *C. militaris*.

Table 16. Fragmentation pattern of palmitic acid methyl ester (retention time = 16.72) in F1 fraction from ethyl acetate extract of *C. militaris* detected by GC-MS

Peak#	m/z	Intensity	Relative Intensity (%)	Peak#	m/z	Intensity	Relative Intensity (%)
1	29.048	15495	13.69	28	76.067	1117	0.99
2	39.035	3650	3.23	29	81.095	2079	1.84
3	40.043	923	0.82	30	83.074	1856	1.64
4	41.052	33686	29.77	31	83.111	6642	5.87
5	42.059	6826	6.03	32	84.083	2477	2.19
6	43.032	8420	7.44	33	85.127	2180	1.93
7	43.068	40636	35.91	34	87.071	70581	62.37
8	44.072	1460	1.29	35	88.077	5778	5.11
9	45.048	1447	1.28	36	95.113	1272	1.12
10	53.055	1860	1.64	37	97.094	2473	2.19
11	54.063	2324	2.05	38	97.131	2958	2.61
12	55.035	4021	3.55	39	98.102	2317	2.05
13	55.072	27323	24.14	40	101.091	4483	3.96
14	56.079	5370	4.75	41	111.113	1131	1.00
15	57.051	1495	1.32	42	115.109	1513	1.34
16	57.088	17375	15.35	43	129.130	4778	4.22
17	59.031	8847	7.82	44	143.149	9587	8.47
18	59.068	4014	3.55	45	147.109	2848	2.52
19	67.075	3325	2.94	46	171.188	1969	1.74
20	68.083	1623	1.43	47	185.208	2492	2.20
21	69.092	14148	12.50	48	199.227	2126	1.88
22	70.098	2474	2.19	49	227.266	7331	6.48
23	71.108	4627	4.09	50	239.306	4846	4.28
24	73.070	11579	10.23	51	241.286	2342	2.07
25	74.059	113169	100.00	52	270.333	10196	9.01
26	74.128	2945	2.60	53	271.336	2143	1.89
27	75.067	19381	17.13				

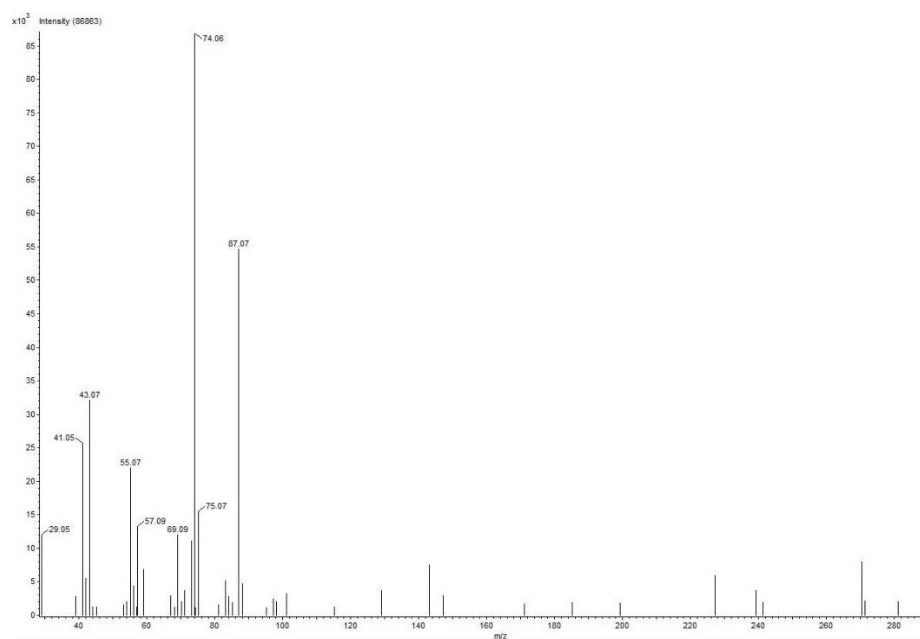


Figure 18. Mass-spectra of palmitic acid methyl ester ($R_t = 16.72$) in F1 fraction from ethyl acetate extract of *C. militaris* detected by GC-MS.

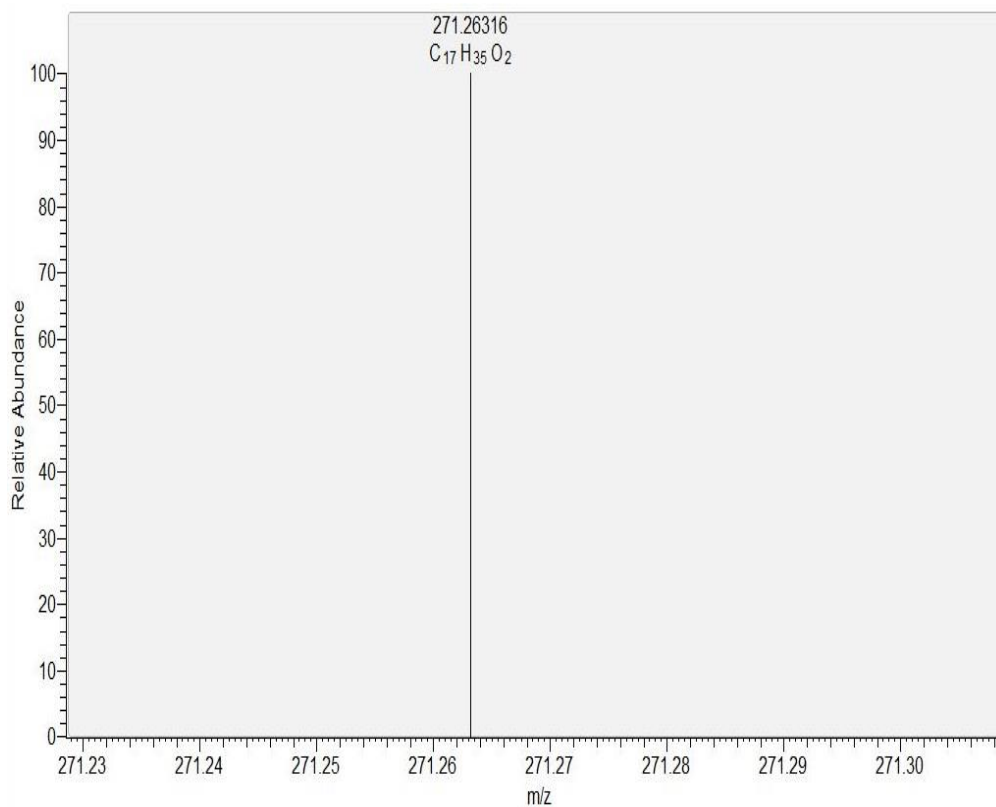


Figure 19. ESI-MS spectra of palmitic acid methyl ester in F1 fraction from ethyl acetate extract of *C. militaris*.

Table 17. Fragmentation pattern of palmitic acid (retention time = 17.09) in F1 fraction from ethyl acetate extract of *C. militaris* detected by GC-MS

Peak#	m/z	Intensity	Relative Intensity (%)	Peak#	m/z	Intensity	Relative Intensity (%)
1	29.048	24522	39.68	46	82.103	2181	3.53
2	30.052	642	1.04	47	83.075	2886	4.67
3	31.028	887	1.44	48	83.111	9524	15.41
4	31.998	696	1.13	49	84.083	2775	4.49
5	39.035	6041	9.78	50	84.118	2371	3.84
6	40.043	1511	2.44	51	85.089	512	0.83
7	41.052	50923	82.41	52	85.127	9117	14.75
8	41.086	301	0.49	53	86.131	635	1.03
9	41.103	1208	1.96	54	87.071	7102	11.49
10	42.023	1229	1.99	55	88.077	727	1.18
11	42.059	9969	16.13	56	93.098	778	1.26
12	43.032	5562	9.00	57	95.114	1442	2.33
13	43.068	61791	100.00	58	96.122	1486	2.40
14	43.121	1562	2.53	59	97.094	2938	4.75
15	44.072	2065	3.34	60	97.131	5530	8.95
16	45.012	2684	4.34	61	98.102	3473	5.62
17	45.048	4275	6.92	62	98.137	1467	2.37
18	53.056	2754	4.46	63	99.147	1987	3.22
19	54.064	3420	5.53	64	101.090	3272	5.30
20	55.035	4016	6.50	65	102.098	934	1.51
21	55.072	38744	62.70	66	110.142	685	1.11
22	55.109	303	0.49	67	111.114	1429	2.31
23	55.132	870	1.41	68	111.150	1826	2.95
24	56.079	9292	15.04	69	112.121	703	1.14
25	57.051	1327	2.15	70	112.158	775	1.25
26	57.088	37377	60.49	71	113.166	1080	1.75
27	58.092	1681	2.72	72	115.110	4881	7.90
28	59.068	2686	4.35	73	116.117	1516	2.45
29	60.040	54764	88.63	74	125.133	757	1.23
30	60.099	902	1.46	75	125.170	825	1.34
31	60.111	386	0.62	76	127.186	792	1.28
32	61.047	13045	21.11	77	129.130	12431	20.12
33	67.075	4252	6.88	78	130.134	1395	2.26
34	68.083	3074	4.97	79	143.149	1177	1.90
35	69.056	521	0.84	80	157.168	2925	4.73
36	69.092	20030	32.41	81	171.189	3092	5.00
37	70.099	5364	8.68	82	185.208	3176	5.14
38	71.071	984	1.59	83	194.260	1051	1.70
39	71.108	16105	26.06	84	199.227	1593	2.58
40	72.111	1028	1.66	85	213.247	7438	12.04
41	73.051	56317	91.14	86	214.250	1390	2.25
42	74.058	3945	6.38	87	227.267	1982	3.21
43	79.080	1202	1.94	88	256.314	13101	21.20
44	80.086	512	0.83	89	257.318	2609	4.22
45	81.095	2632	4.26				

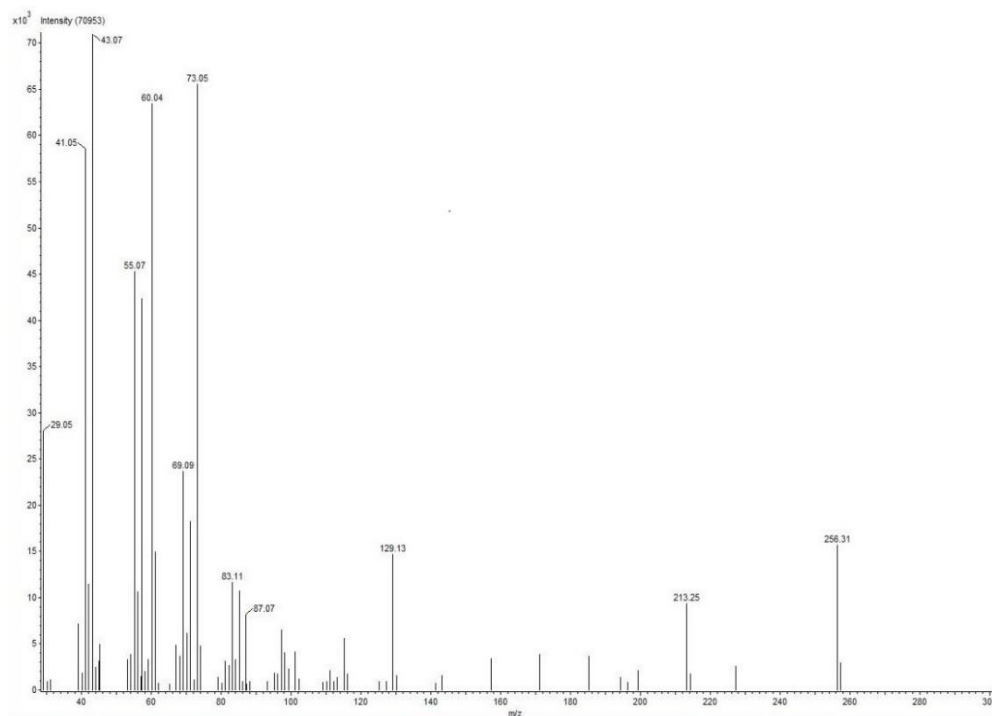


Figure 20. Mass-spectra of palmitic acid ($R_t = 17.09$) in F1 fraction from ethyl acetate extract of *C. militaris* detected by GC-MS.

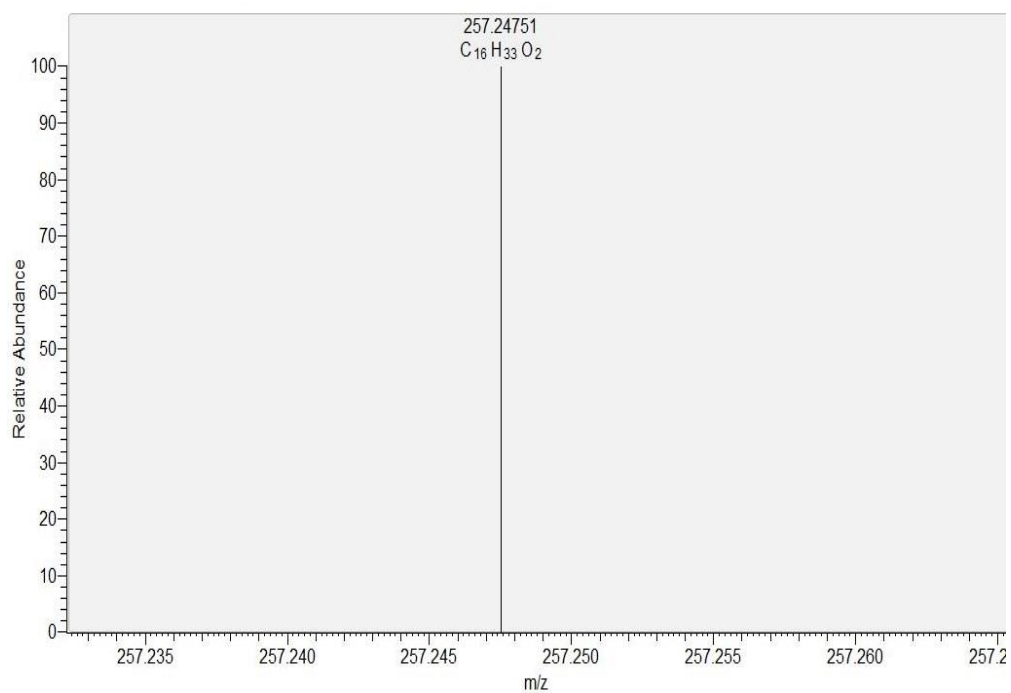


Figure 21. ESI-MS spectra of palmitic acid in F1 fraction from ethyl acetate extract of *C. militaris*.

Table 18. Fragmentation pattern of 9,12-Octadecadienoic acid (*Z, Z*) (retention time = 18.73) in F1 fraction from ethyl acetate extract of *C. militaris* detected by GC-MS

Peak#	m/z	Intensity	Relative Intensity (%)	Peak#	m/z	Intensity	Relative Intensity (%)
1	29.048	27741	28.83	61	94.106	6040	6.28
2	30.052	804	0.84	62	95.115	38981	40.51
3	31.028	1470	1.53	63	95.192	974	1.01
4	39.035	12514	13.01	64	96.087	672	0.70
5	40.043	2288	2.38	65	96.122	21965	22.83
6	41.052	74160	77.07	66	97.094	1444	1.50
7	42.024	1874	1.95	67	97.130	5551	5.77
8	42.058	6975	7.25	68	98.102	841	0.87
9	43.032	5771	6.00	69	99.073	617	0.64
10	43.068	20511	21.32	70	101.090	1175	1.22
11	44.072	804	0.84	71	105.102	1859	1.93
12	45.012	4121	4.28	72	106.110	882	0.92
13	45.048	5509	5.72	73	107.118	4203	4.37
14	51.039	1056	1.10	74	108.126	4260	4.43
15	52.047	1089	1.13	75	109.098	907	0.94
16	53.055	12080	12.55	76	109.134	15154	15.75
17	54.063	45824	47.62	77	110.142	11638	12.09
18	54.121	1043	1.08	78	111.114	635	0.66
19	55.035	4230	4.40	79	111.148	1698	1.76
20	55.072	64357	66.88	80	113.094	595	0.62
21	56.078	5732	5.96	81	119.122	1007	1.05
22	57.052	1494	1.55	82	120.129	712	0.74
23	57.088	6235	6.48	83	121.101	589	0.61
24	59.068	2269	2.36	84	121.138	2851	2.96
25	60.040	15492	16.10	85	122.109	737	0.77
26	61.046	957	0.99	86	122.145	2938	3.05
27	65.059	7069	7.35	87	123.118	1284	1.33
28	66.067	6167	6.41	88	123.154	5213	5.42
29	67.075	96225	100.00	89	124.161	4674	4.86
30	67.164	223	0.23	90	125.166	639	0.66
31	67.175	357	0.37	91	126.105	1228	1.28
32	67.194	1093	1.14	92	127.113	1090	1.13
33	68.083	41800	43.44	93	129.129	817	0.85
34	68.148	1161	1.21	94	131.124	814	0.85
35	69.055	443	0.46	95	133.141	1054	1.10
36	69.091	27322	28.39	96	135.121	1247	1.30
37	69.122	315	0.33	97	135.156	1993	2.07
38	70.097	3050	3.17	98	136.129	1622	1.69
39	71.071	2503	2.60	99	136.164	1874	1.95
40	71.107	1442	1.50	100	137.136	858	0.89
41	73.051	7766	8.07	101	137.173	2227	2.31
42	74.058	906	0.94	102	138.181	2168	2.25
43	77.063	12315	12.80	103	140.124	1252	1.30
44	78.070	2901	3.01	104	149.141	1200	1.25
45	79.079	34971	36.34	105	149.177	974	1.01
46	80.086	15991	16.62	106	150.148	2607	2.71
47	81.095	65702	68.28	107	151.154	667	0.69
48	82.103	34145	35.48	108	151.192	1174	1.22
49	82.166	305	0.32	109	152.200	793	0.82
50	82.179	459	0.48	110	153.137	462	0.48
51	83.075	1566	1.63	111	154.144	637	0.66

52	83.110	10925	11.35	112	163.161	1202	1.25
53	84.083	1108	1.15	113	164.167	1314	1.37
54	84.116	1204	1.25	114	167.156	940	0.98
55	85.091	1378	1.43	115	168.164	813	0.85
56	85.127	591	0.61	116	181.176	685	0.71
57	87.071	1512	1.57	117	182.183	1199	1.25
58	91.082	8406	8.74	118	196.202	862	0.90
59	92.088	1478	1.54	119	280.320	10835	11.26
60	93.099	8974	9.33	120	281.323	2369	2.46

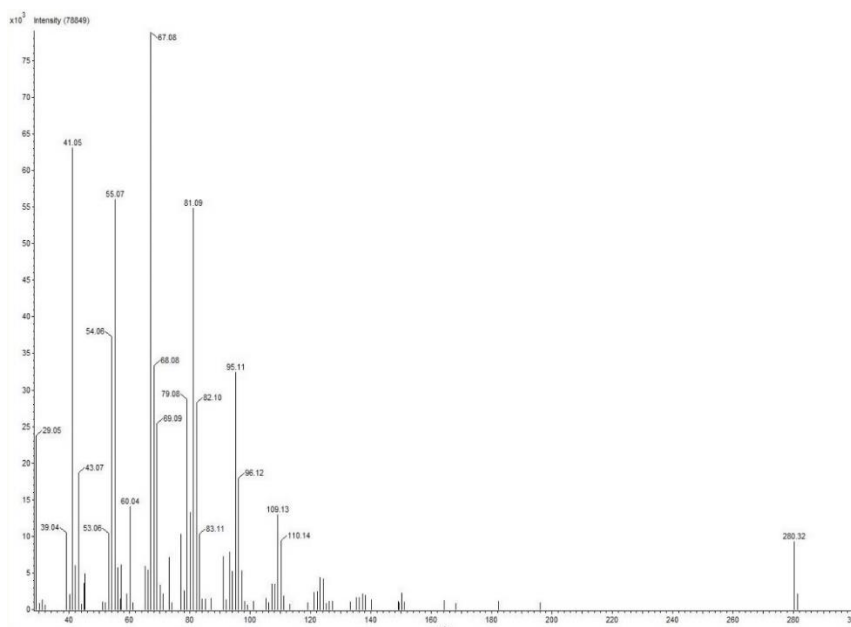


Figure 22. Mass-spectra of 9,12-Octadecadienoic acid (*Z, Z*) (*Rt* = 18.73) in F1 fraction from ethyl acetate extract of *C. militaris* detected by GC-MS.

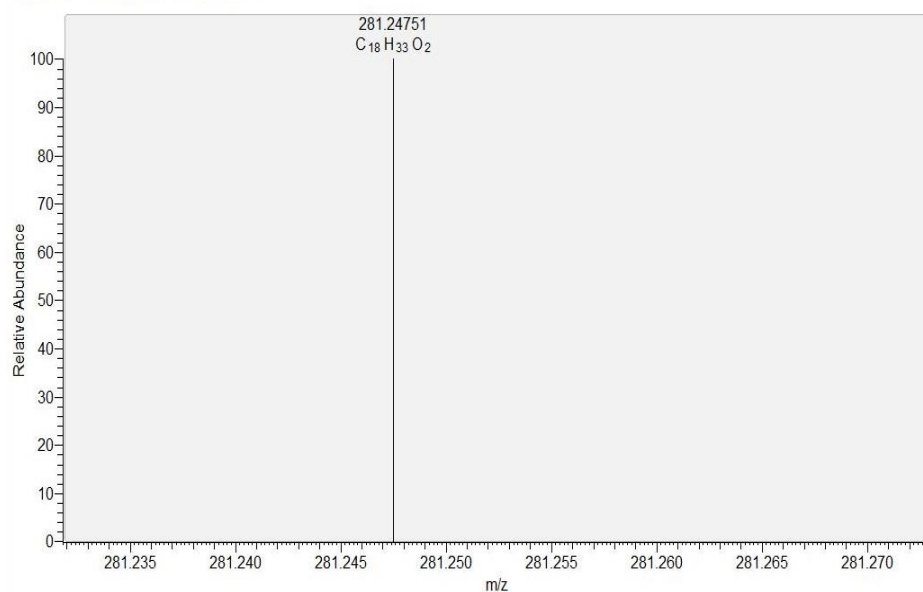


Figure 23. ESI-MS spectra of 9,12-Octadecadienoic acid (*Z, Z*) in F1 fraction from ethyl acetate extract of *C. militaris*.

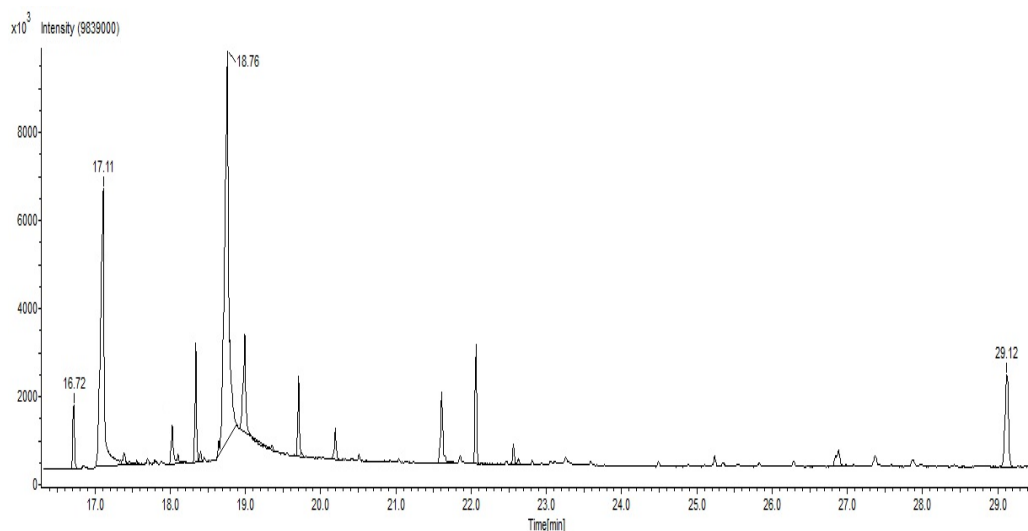


Figure 24. GC-MS chromatogram of F2 fraction from ethyl acetate extract of *C. militaris*.

Table 19. Fragmentation pattern of palmitic acid methyl ester (retention time = 16.72) in F2 fraction from ethyl acetate extract of *C. militaris* detected by GC-MS

Peak#	m/z	Intensity	Relative Intensity (%)	Peak#	m/z	Intensity	Relative Intensity (%)
1	29.048	7348	14.11	43	87.157	303	0.58
2	39.036	1661	3.19	44	87.200	203	0.39
3	40.044	463	0.89	45	88.077	2840	5.45
4	41.052	15285	29.34	46	95.113	885	1.70
5	42.024	464	0.89	47	97.094	1175	2.26
6	42.060	3184	6.11	48	97.131	1455	2.79
7	43.032	4033	7.74	49	98.103	1147	2.20
8	43.068	18685	35.87	50	101.090	2007	3.85
9	43.092	202	0.39	51	111.114	532	1.02
10	44.071	605	1.16	52	115.109	906	1.74
11	45.048	639	1.23	53	116.119	318	0.61
12	53.056	754	1.45	54	129.130	2167	4.16
13	54.063	1034	1.98	55	143.149	4453	8.55
14	55.036	1990	3.82	56	144.157	612	1.17
15	55.072	12268	23.55	57	147.109	3891	7.47
16	56.079	2626	5.04	58	148.111	583	1.12
17	57.052	711	1.36	59	171.188	949	1.82
18	57.088	7732	14.84	60	185.206	1619	3.11
19	58.060	366	0.70	61	199.228	1151	2.21
20	58.091	486	0.93	62	207.094	1056	2.03
21	59.032	4253	8.16	63	213.249	726	1.39
22	59.068	2132	4.09	64	221.149	1851	3.55
23	67.075	1275	2.45	65	222.141	177	0.34
24	68.083	825	1.58	66	222.151	231	0.44
25	69.092	6883	13.22	67	227.267	3663	7.03
26	70.098	1312	2.52	68	228.271	892	1.71
27	71.071	403	0.77	69	239.307	2476	4.75
28	71.108	2224	4.27	70	241.284	1224	2.35
29	73.070	13213	25.37	71	270.333	4757	9.13
30	74.059	52088	100.00	72	271.339	892	1.71
31	74.168	224	0.43	73	281.132	2038	3.91
32	75.067	9236	17.73	74	282.134	986	1.89

33	76.069	531	1.02	75	341.119	817	1.57
34	81.094	795	1.53	76	355.173	1532	2.94
35	82.104	576	1.11	77	356.173	780	1.50
36	83.075	902	1.73	78	415.147	419	0.81
37	83.111	3145	6.04	79	429.185	211	0.41
38	84.083	1104	2.12	80	429.210	1232	2.37
39	84.117	365	0.70	81	430.215	421	0.81
40	85.128	932	1.79	82	503.254	1292	2.48
41	87.071	32490	62.38	83	504.244	312	0.60
42	87.145	515	0.99	84	504.269	330	0.63

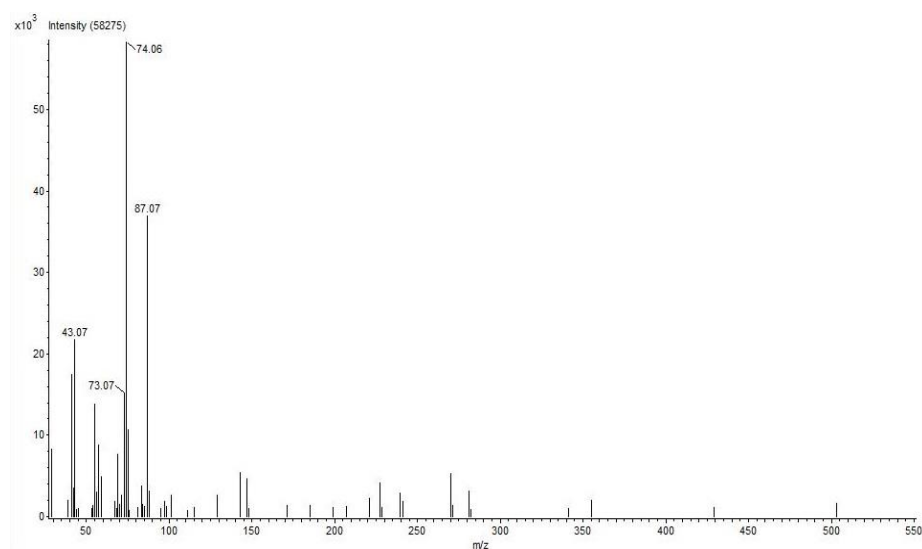


Figure 25. Mass-spectra of palmitic acid methyl ester ($R_t = 16.72$) in F2 fraction from ethyl acetate extract of *C. militaris* detected by GC-MS.

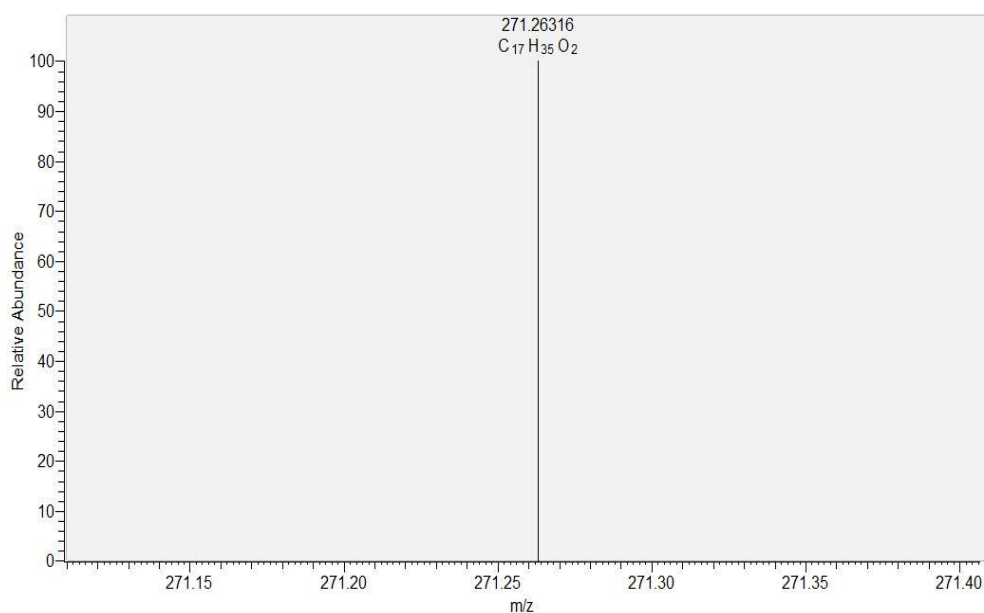


Figure 26. ESI-MS spectra of palmitic acid methyl ester in F2 fraction from ethyl acetate extract of *C. militaris*.

Table 20. Fragmentation pattern of palmitic acid (retention time = 17.11) in F2 fraction from ethyl acetate extract of *C. militaris* detected by GC-MS

Peak#	m/z	Intensity	Relative Intensity (%)	Peak#	m/z	Intensity	Relative Intensity (%)
1	29.048	32655	39.20	50	84.083	3807	4.57
2	29.068	455	0.55	51	84.118	3282	3.94
3	30.052	925	1.11	52	85.089	723	0.87
4	31.028	1215	1.46	53	85.127	12807	15.37
5	39.036	7998	9.60	54	86.131	1009	1.21
6	40.043	1905	2.29	55	87.071	9689	11.63
7	41.052	68281	81.97	56	87.107	761	0.91
8	42.024	1726	2.07	57	88.077	1005	1.21
9	42.059	13730	16.48	58	93.099	818	0.98
10	43.032	7519	9.03	59	95.115	2114	2.54
11	43.068	83300	100.00	60	96.122	1864	2.24
12	43.154	1293	1.55	61	97.095	4102	4.92
13	44.072	2835	3.40	62	97.131	7710	9.26
14	45.012	3375	4.05	63	98.103	4762	5.72
15	45.048	5809	6.97	64	98.138	1926	2.31
16	53.056	3659	4.39	65	99.147	2641	3.17
17	54.063	4450	5.34	66	101.091	4469	5.36
18	55.035	5285	6.34	67	102.098	1319	1.58
19	55.072	52153	62.61	68	107.118	589	0.71
20	55.130	1218	1.46	69	109.135	957	1.15
21	56.043	572	0.69	70	110.142	1028	1.23
22	56.079	12471	14.97	71	111.114	1801	2.16
23	57.051	1469	1.76	72	111.150	2563	3.08
24	57.088	48865	58.66	73	112.122	953	1.14
25	57.149	575	0.69	74	112.158	1028	1.23
26	58.092	2266	2.72	75	113.167	1523	1.83
27	59.068	3765	4.52	76	115.110	6650	7.98
28	60.040	73539	88.28	77	116.117	2056	2.47
29	61.047	17636	21.17	78	121.138	649	0.78
30	62.047	708	0.85	79	125.134	851	1.02
31	65.059	700	0.84	80	125.169	1177	1.41
32	67.075	5964	7.16	81	126.176	686	0.82
33	68.083	4173	5.01	82	127.186	1231	1.48
34	69.055	749	0.90	83	129.130	17154	20.59
35	69.092	27548	33.07	84	130.134	1581	1.90
36	70.063	560	0.67	85	141.206	835	1.00
37	70.099	6895	8.28	86	143.149	1792	2.15
38	71.071	1197	1.44	87	157.169	4160	4.99
39	71.108	21579	25.90	88	171.189	4516	5.42
40	72.111	1376	1.65	89	185.208	4375	5.25
41	73.051	71278	85.57	90	194.260	1630	1.96
42	73.087	5569	6.69	91	196.276	1053	1.26
43	74.058	5435	6.52	92	199.227	2250	2.70
44	79.079	1539	1.85	93	213.247	10537	12.65
45	80.087	747	0.90	94	214.252	1547	1.86
46	81.095	3509	4.21	95	227.267	2948	3.54
47	82.103	3124	3.75	96	256.314	18125	21.76
48	83.075	4027	4.83	97	257.317	3146	3.78
49	83.111	13047	15.66				

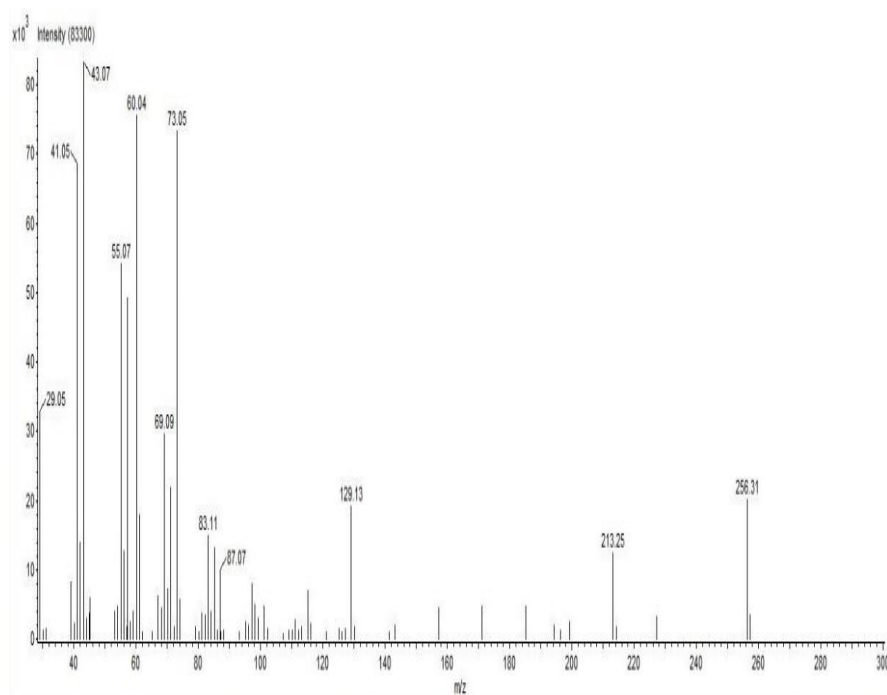


Figure 27. Mass-spectra of palmitic acid (Rt = 17.11) in F2 fraction from ethyl acetate extract of *C. militaris* detected by GC-MS.

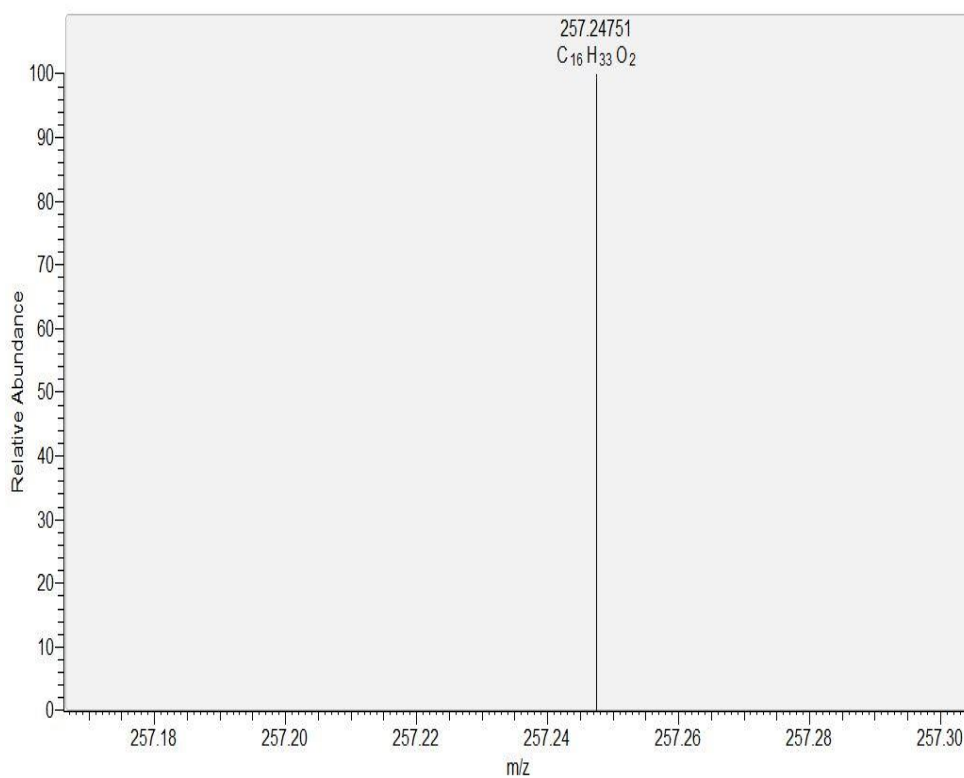


Figure 28. ESI-MS spectra of palmitic acid in F2 fraction from ethyl acetate extract of *C. militaris*.

Table 21. Fragmentation pattern of 9,12-Octadecadienoic acid (Z, Z) (retention time = 18.76) in F2 from EtOAc extract of *C. militaris* detected by GC-MS

Peak#	m/z	Intensity	Relative Intensity (%)	Peak#	m/z	Intensity	Relative Intensity (%)
1	29.048	33558	30.29	53	85.127	1031	0.93
2	30.052	894	0.81	54	87.071	1842	1.66
3	31.028	1821	1.64	55	91.082	10023	9.05
4	39.035	14969	13.51	56	92.088	1726	1.56
5	40.043	2702	2.44	57	93.098	10642	9.61
6	41.052	88539	79.92	58	94.106	7409	6.69
7	41.102	1976	1.78	59	95.115	45666	41.22
8	42.024	2325	2.10	60	96.086	1148	1.04
9	42.058	8670	7.83	61	96.122	25140	22.69
10	43.032	6978	6.30	62	97.094	2074	1.87
11	43.068	27031	24.40	63	97.130	7926	7.15
12	44.071	974	0.88	64	98.102	1460	1.32
13	45.012	5023	4.53	65	98.137	1233	1.11
14	45.048	6697	6.05	66	101.090	1575	1.42
15	51.039	1288	1.16	67	105.102	1924	1.74
16	52.047	1405	1.27	68	107.118	4662	4.21
17	53.055	14386	12.99	69	108.126	4980	4.50
18	54.063	53459	48.26	70	109.098	1192	1.08
19	55.035	5094	4.60	71	109.134	17930	16.19
20	55.072	78163	70.56	72	110.105	905	0.82
21	55.111	578	0.52	73	110.142	13157	11.88
22	55.130	1700	1.53	74	111.114	1113	1.00
23	56.078	8595	7.76	75	111.148	2650	2.39
24	57.051	2068	1.87	76	113.094	960	0.87
25	57.088	9279	8.38	77	119.121	1200	1.08
26	59.068	2763	2.49	78	121.137	3444	3.11
27	60.040	19039	17.19	79	122.109	904	0.82
28	61.046	1373	1.24	80	122.145	3580	3.23
29	65.059	8156	7.36	81	123.118	1640	1.48
30	66.067	7258	6.55	82	123.154	6163	5.56
31	67.075	110782	100.00	83	124.161	5318	4.80
32	68.083	48285	43.59	84	126.105	1417	1.28
33	69.055	897	0.81	85	127.113	1247	1.13
34	69.091	36313	32.78	86	129.129	986	0.89
35	70.098	4692	4.24	87	133.141	1299	1.17
36	71.071	2969	2.68	88	135.121	1273	1.15
37	71.107	2387	2.15	89	135.157	2256	2.04
38	73.051	8276	7.47	90	136.128	1737	1.57
39	73.087	1531	1.38	91	136.164	2042	1.84
40	74.059	1067	0.96	92	137.136	1231	1.11
41	77.063	14150	12.77	93	137.173	2753	2.49
42	78.070	3478	3.14	94	138.181	2823	2.55
43	79.079	40217	36.30	95	140.125	1288	1.16
44	80.086	17850	16.11	96	149.140	1500	1.35
45	81.095	75753	68.38	97	149.175	1176	1.06
46	81.165	1941	1.75	98	150.148	3152	2.84
47	82.102	40182	36.27	99	151.192	1283	1.16
48	83.075	1987	1.79	100	164.168	1557	1.41
49	83.110	14799	13.36	101	182.183	1271	1.15
50	84.083	1894	1.71	102	280.320	11903	10.74
51	84.117	1976	1.78	103	281.324	2266	2.05
52	85.091	1688	1.52				

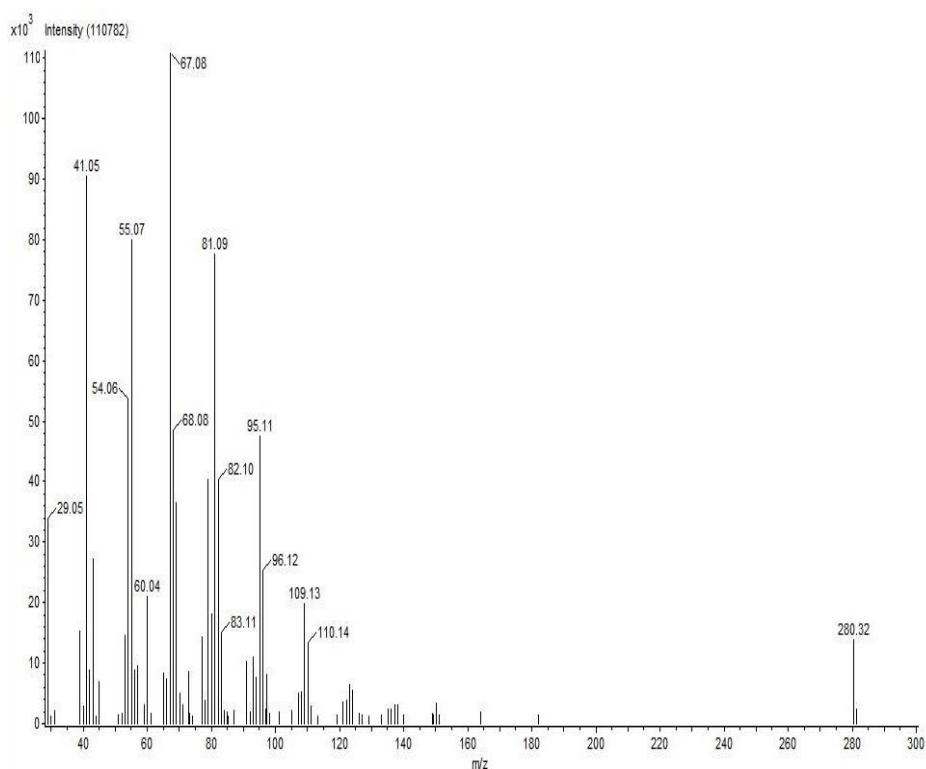


Figure 29. Mass-spectra of 9,12-Octadecadienoic acid (Z, Z) (Rt = 18.76) in F2 fraction from ethyl acetate extract of *C. militaris* detected by GC-MS.

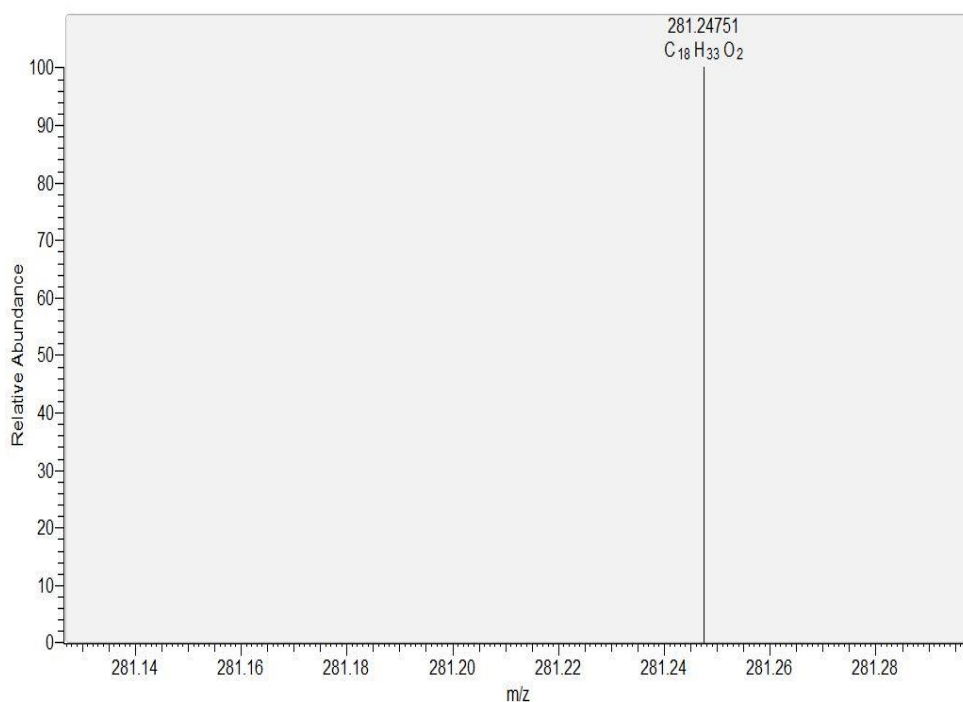


Figure 30. ESI-MS spectra of 9,12-Octadecadienoic acid (Z, Z) in F2 fraction from ethyl acetate extract of *C. militaris*.

Table 22. Fragmentation pattern of ergosta-4,6,8(14),22-tetraen-3-one (retention time = 29.12) in F2 fraction from ethyl acetate extract of *C. militaris* detected by GC-MS

Peak#	m/z	Intensity	Relative Intensity (%)	Peak#	m/z	Intensity	Relative Intensity (%)
1	29.048	2317	6.29	67	167.135	3811	10.34
2	39.035	1229	3.33	68	168.142	2044	5.55
3	41.052	13844	37.56	69	169.151	4089	11.10
4	42.058	1026	2.78	70	170.158	1531	4.15
5	43.031	1031	2.80	71	171.133	619	1.68
6	43.068	30050	81.54	72	171.167	1097	2.98
7	44.072	1012	2.75	73	173.147	7160	19.43
8	53.056	2170	5.89	74	174.152	1313	3.56
9	55.035	823	2.23	75	178.131	1568	4.26
10	55.072	22983	62.36	76	179.138	2434	6.60
11	56.076	1188	3.22	77	180.146	1510	4.10
12	57.088	4597	12.47	78	181.154	3926	10.65
13	65.059	1058	2.87	79	182.161	1831	4.97
14	67.075	6230	16.91	80	183.170	2956	8.02
15	68.081	674	1.83	81	184.177	1152	3.13
16	69.091	21855	59.30	82	185.186	1776	4.82
17	70.098	2483	6.74	83	191.142	1069	2.90
18	71.108	2568	6.97	84	192.149	1297	3.52
19	77.063	2728	7.40	85	193.158	2566	6.96
20	78.069	462	1.25	86	194.164	1425	3.87
21	79.079	4683	12.71	87	195.174	3497	9.49
22	80.085	556	1.51	88	196.179	1659	4.50
23	81.095	10155	27.56	89	197.189	3166	8.59
24	82.102	3829	10.39	90	198.195	1276	3.46
25	83.111	4265	11.57	91	205.161	991	2.69
26	91.082	4895	13.28	92	206.170	936	2.54
27	92.089	681	1.85	93	207.177	3125	8.48
28	93.098	3517	9.54	94	208.183	1596	4.33
29	94.104	757	2.05	95	209.193	3426	9.30
30	95.115	4218	11.45	96	210.198	1386	3.76
31	97.094	718	1.95	97	211.174	2089	5.67
32	103.087	847	2.30	98	212.180	1200	3.26
33	105.102	2701	7.33	99	213.189	2859	7.76
34	107.118	3059	8.30	100	214.197	7716	20.94
35	108.124	807	2.19	101	215.202	1448	3.93
36	109.134	6006	16.30	102	219.181	1781	4.83
37	110.139	755	2.05	103	221.196	948	2.57
38	115.090	3067	8.32	104	223.212	2893	7.85
39	116.096	1174	3.18	105	224.218	1894	5.14
40	117.105	2140	5.81	106	225.197	3435	9.32
41	119.121	1077	2.92	107	226.200	2402	6.52
42	121.137	969	2.63	108	227.209	1649	4.47
43	123.154	1322	3.59	109	233.200	1387	3.76
44	125.170	1132	3.07	110	235.216	1170	3.17
45	127.092	903	2.45	111	237.199	1245	3.38
46	128.101	3684	10.00	112	239.225	895	2.43
47	129.108	4800	13.02	113	239.251	601	1.63
48	130.115	1658	4.50	114	240.220	3286	8.92
49	131.124	2986	8.10	115	241.227	1076	2.92
50	141.113	3892	10.56	116	242.237	2233	6.06
51	142.119	2184	5.93	117	249.236	1826	4.96

52	143.128	3289	8.92	118	251.217	1239	3.36
53	144.134	1111	3.01	119	252.224	1590	4.32
54	145.109	622	1.69	120	253.232	9937	26.96
55	145.143	1989	5.40	121	254.235	2064	5.60
56	147.124	730	1.98	122	265.236	1234	3.35
57	152.107	1461	3.97	123	266.244	1985	5.39
58	153.116	3215	8.72	124	267.252	25264	68.55
59	154.124	2196	5.96	125	268.259	36853	100.00
60	155.131	5632	15.28	126	269.263	7238	19.64
61	156.138	1616	4.39	127	270.265	1117	3.03
62	157.113	607	1.65	128	293.274	1095	2.97
63	157.148	1858	5.04	129	349.354	1432	3.89
64	159.128	1223	3.32	130	377.397	1115	3.03
65	165.119	3515	9.54	131	392.419	8663	23.51
66	166.126	2113	5.73	132	393.423	2915	7.91

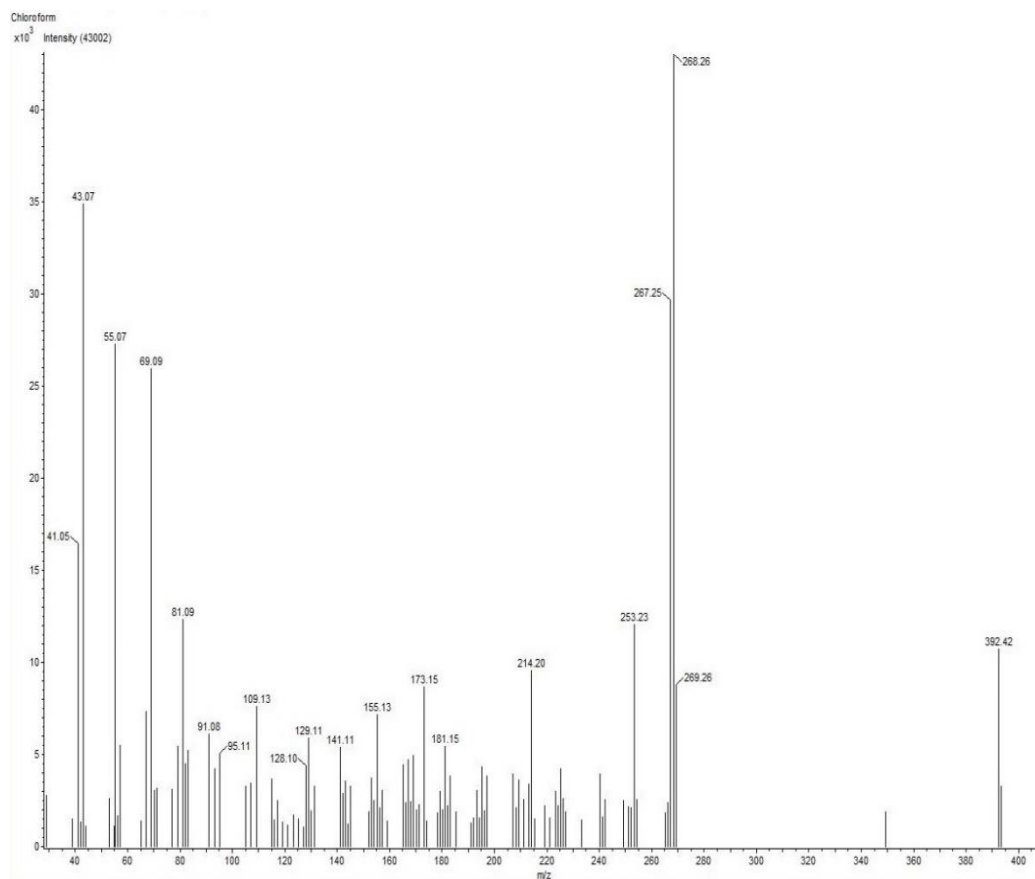


Figure 31. Mass-spectra of ergosta-4,6,8(14),22-tetraen-3-one (Rt = 29.12) in F2 fraction from ethyl acetate extract of *C. militaris* detected by GC-MS.

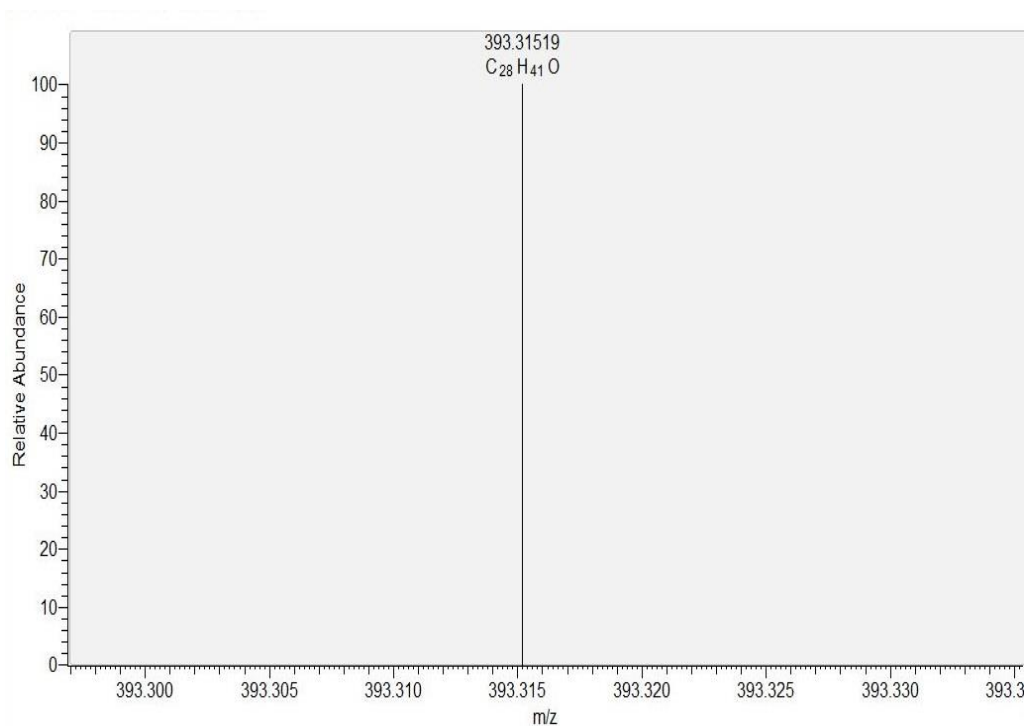


Figure 32. ESI-MS spectra of ergosta-4,6,8(14),22-tetraen-3-one in F2 fraction from ethyl acetate extract of *C. militaris*.

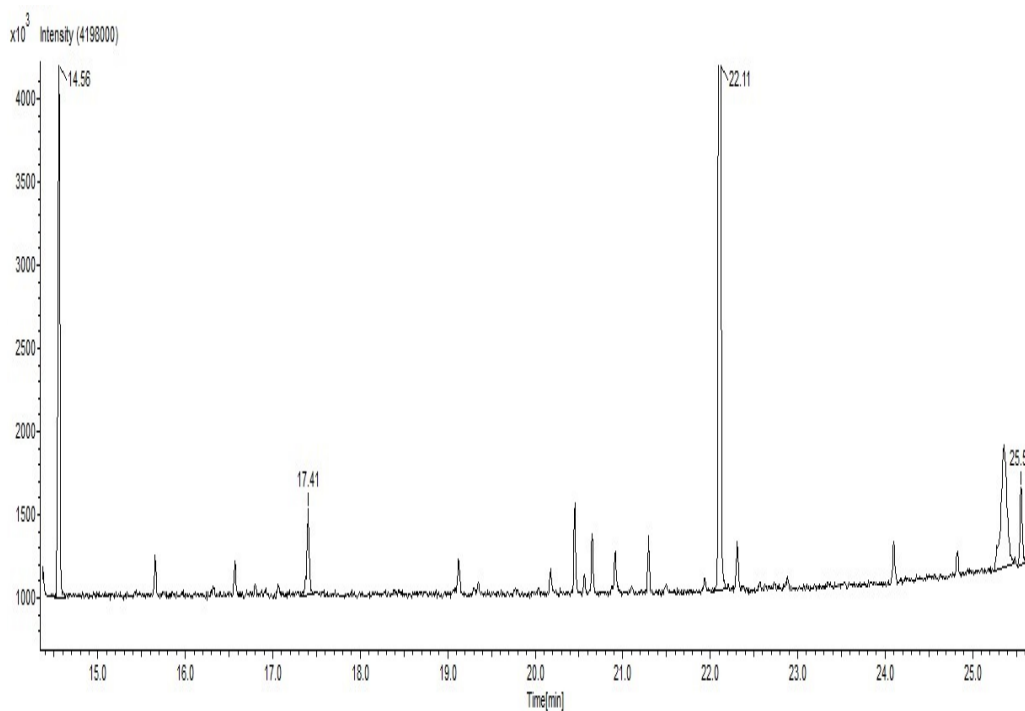


Figure 33. GC-MS chromatogram of F3 fraction from ethyl acetate extract of *C. militaris*.

Table 23. Fragmentation pattern of pentadecanal (retention time = 14.56) in F3 fraction from ethyl acetate extract of *C. militaris* detected by GC-MS

Peak#	m/z	Intensity	Relative Intensity (%)	Peak#	m/z	Intensity	Relative Intensity (%)
1	29.017	3153	5.48	42	72.092	3265	5.68
2	29.053	24694	42.93	43	72.124	889	1.55
3	30.057	649	1.13	44	79.093	2016	3.50
4	31.033	908	1.58	45	80.101	1751	3.04
5	32.003	997	1.73	46	81.109	17370	30.20
6	39.043	6325	10.99	47	82.117	36430	63.33
7	40.050	1406	2.44	48	82.149	503	0.87
8	41.059	48696	84.65	49	83.090	459	0.80
9	41.083	443	0.77	50	83.125	19605	34.08
10	41.107	426	0.74	51	84.133	6786	11.80
11	41.116	513	0.89	52	85.105	2045	3.56
12	42.067	10504	18.26	53	85.142	7260	12.62
13	43.039	2494	4.34	54	86.114	940	1.63
14	43.076	57523	100.00	55	93.115	699	1.21
15	43.100	625	1.09	56	94.123	1009	1.75
16	43.112	325	0.56	57	95.131	14846	25.81
17	43.127	1298	2.26	58	96.139	19692	34.23
18	44.048	19158	33.31	59	97.147	12146	21.11
19	44.080	2057	3.58	60	98.155	3376	5.87
20	45.056	7312	12.71	61	99.128	1125	1.96
21	53.065	3235	5.62	62	99.163	1197	2.08
22	54.073	8415	14.63	63	109.153	6405	11.13
23	55.045	1031	1.79	64	110.161	5618	9.77
24	55.081	40072	69.66	65	111.169	4477	7.78
25	55.141	951	1.65	66	112.177	1817	3.16
26	56.089	16601	28.86	67	113.186	831	1.44
27	57.062	20854	36.25	68	123.175	3107	5.40
28	57.098	36779	63.94	69	124.183	3184	5.53
29	57.159	742	1.29	70	125.191	1662	2.89
30	57.169	240	0.42	71	126.200	1367	2.38
31	58.068	2094	3.64	72	137.197	1820	3.16
32	58.102	1524	2.65	73	138.205	2077	3.61
33	65.071	582	1.01	74	139.215	689	1.20
34	66.079	4107	7.14	75	140.222	1317	2.29
35	67.087	20917	36.36	76	151.219	946	1.65
36	68.095	25261	43.91	77	152.227	2121	3.69
37	69.103	23495	40.84	78	154.244	940	1.63
38	70.075	962	1.67	79	166.252	743	1.29
39	70.112	12382	21.52	80	180.271	1978	3.44
40	71.084	6574	11.43	81	182.289	3254	5.66
41	71.120	13692	23.80	82	208.314	1235	2.15

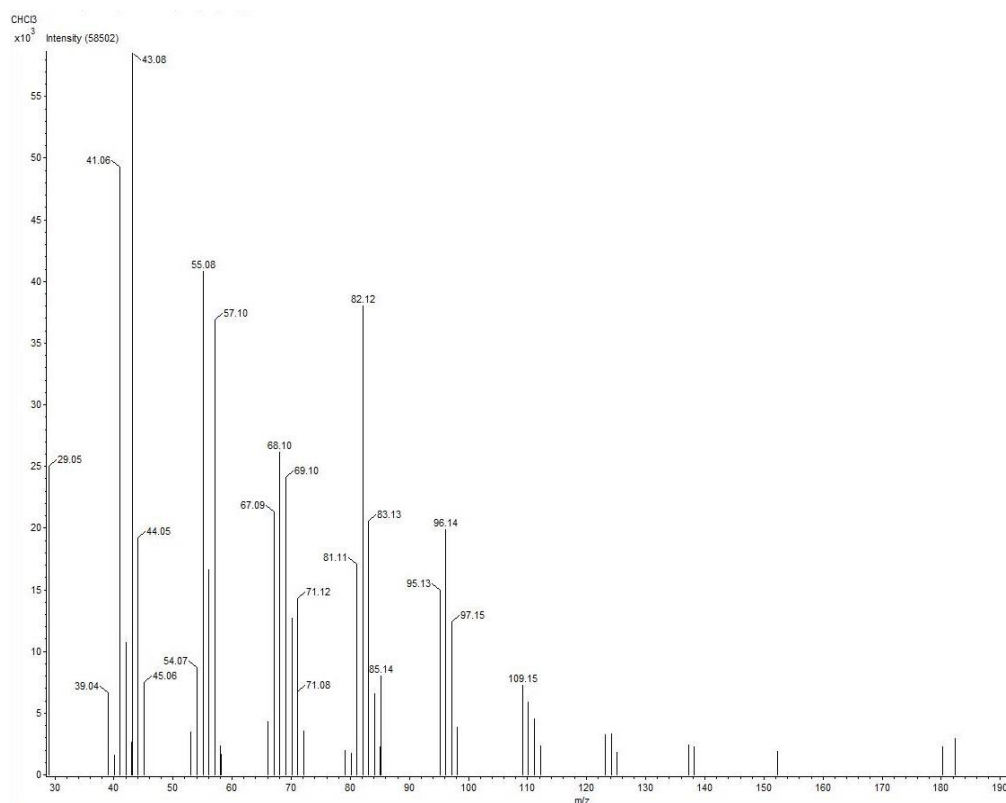


Figure 34. Mass-spectra of pentadecanal (Rt = 14.56) in F3 fraction from ethyl acetate extract of *C. militaris* detected by GC-MS.

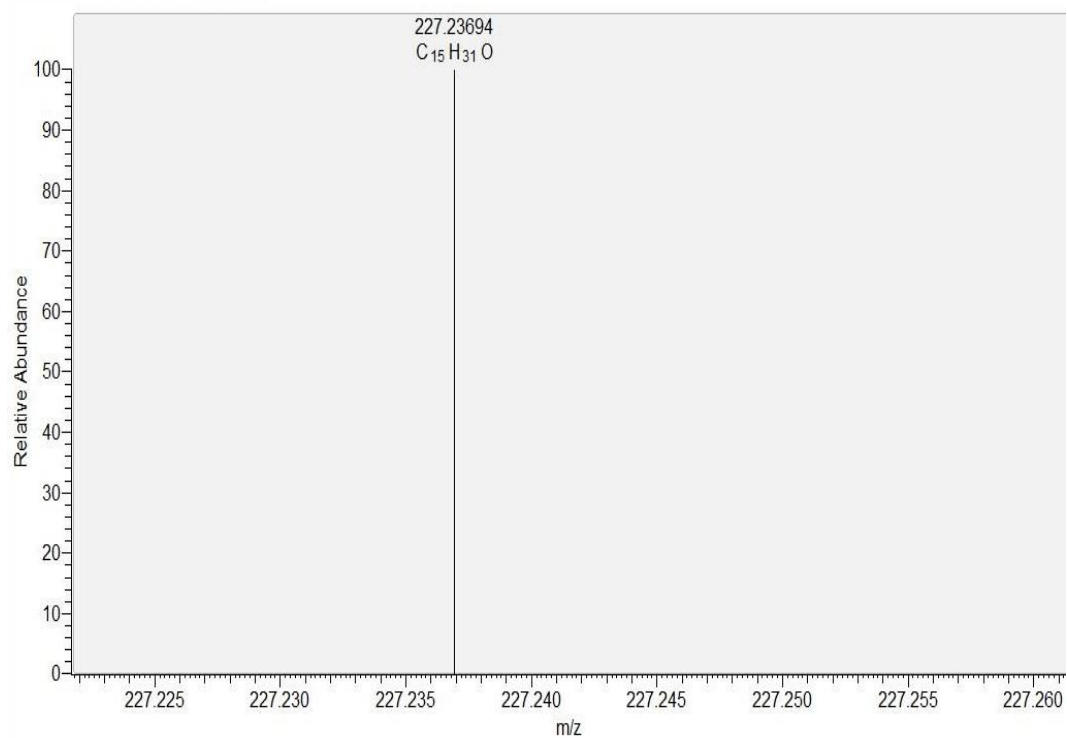


Figure 35. ESI-MS spectra of pentadecanal in F3 fraction from ethyl acetate extract of *C. militaris*.

Table 24. Fragmentation pattern of 2-oxopalmitic acid methyl ester (retention time = 17.41) in F3 fraction from ethyl acetate extract of *C. militaris* detected by GC-MS

Peak#	m/z	Intensity	Relative Intensity (%)	Peak#	m/z	Intensity	Relative Intensity (%)
1	29.053	3993	26.89	28	71.084	482	3.25
2	31.033	2115	14.25	29	71.120	7983	53.76
3	32.000	684	4.61	30	72.126	461	3.11
4	39.042	910	6.13	31	74.073	1063	7.16
5	41.059	8501	57.26	32	75.080	407	2.74
6	42.067	1726	11.63	33	79.095	274	1.84
7	43.039	634	4.27	34	81.108	1490	10.03
8	43.076	14376	96.82	35	82.115	479	3.23
9	44.079	657	4.42	36	83.090	514	3.46
10	53.064	594	4.00	37	83.125	2051	13.81
11	54.073	595	4.01	38	84.097	399	2.69
12	55.045	1431	9.64	39	85.108	212	1.43
13	55.081	6715	45.22	40	85.142	4719	31.78
14	56.049	178	1.20	41	87.081	168	1.13
15	56.054	188	1.27	42	87.088	189	1.28
16	56.089	1553	10.46	43	95.131	2281	15.37
17	57.062	890	6.00	44	96.135	543	3.66
18	57.098	14848	100.00	45	97.112	330	2.22
19	58.069	648	4.36	46	97.149	707	4.76
20	58.102	790	5.32	47	98.121	675	4.54
21	59.077	273	1.84	48	99.163	550	3.71
22	67.087	1452	9.78	49	109.152	1331	8.97
23	68.095	390	2.63	50	111.169	373	2.51
24	69.068	224	1.51	51	123.176	429	2.89
25	69.103	3750	25.25	52	225.327	9405	63.34
26	70.079	416	2.80	53	226.332	1967	13.25
27	70.109	518	3.49				

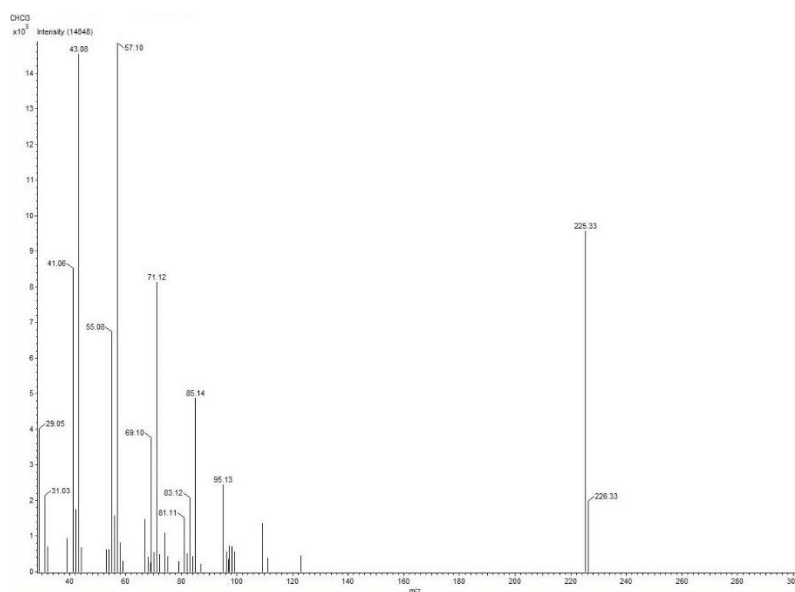


Figure 36. Mass-spectra of 2-oxopalmitic acid methyl ester (Rt = 17.41) in F3 fraction from ethyl acetate extract of *C. militaris* detected by GC-MS.

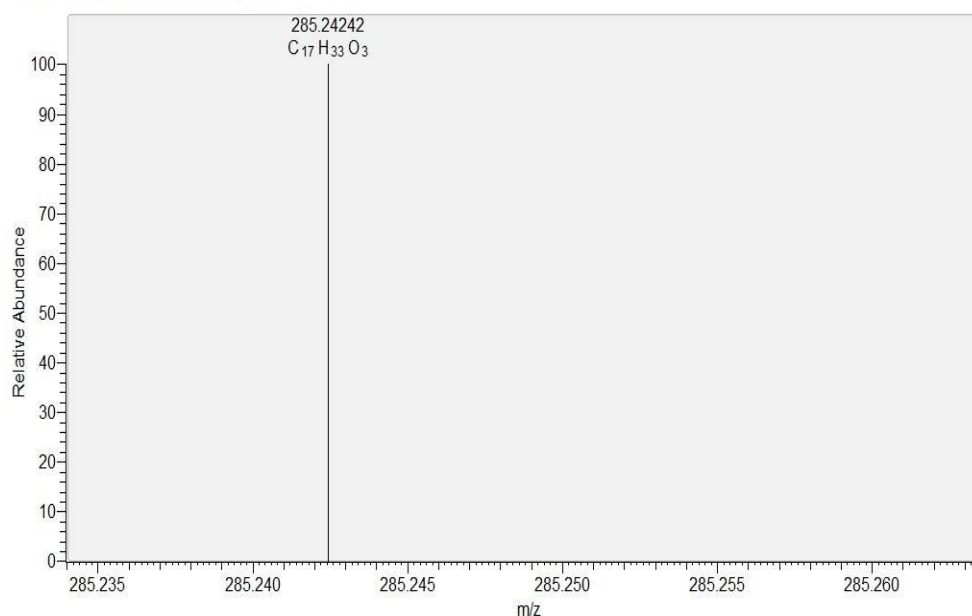


Figure 37. ESI-MS spectra of 2-oxopalmitic acid methyl ester in F3 fraction from ethyl acetate extract of *C. militaris*.

Table 25. Fragmentation pattern of octadecanal (retention time = 22.11) in F3 fraction from ethyl acetate extract of *C. militaris* detected by GC-MS

Peak#	m/z	Intensity	Relative Intensity (%)	Peak#	m/z	Intensity	Relative Intensity (%)
1	29.017	1782	1.63	59	83.090	995	0.91
2	29.053	22938	20.99	60	83.125	50610	46.30
3	30.057	659	0.60	61	83.176	242	0.22
4	31.033	550	0.50	62	83.200	1297	1.19
5	32.011	383	0.35	63	84.098	673	0.62
6	39.043	3831	3.50	64	84.133	9856	9.02
7	40.050	1271	1.16	65	85.106	3633	3.32
8	41.059	57108	52.25	66	85.142	19849	18.16
9	41.091	173	0.16	67	86.114	1640	1.50
10	41.095	262	0.24	68	86.146	1277	1.17
11	41.109	838	0.77	69	93.116	1419	1.30
12	41.119	638	0.58	70	94.124	2548	2.33
13	42.067	12552	11.48	71	95.132	31964	29.24
14	43.040	2447	2.24	72	96.139	46849	42.86
15	43.076	109305	100.00	73	96.210	155	0.14
16	43.151	532	0.49	74	96.223	374	0.34
17	43.159	269	0.25	75	97.112	721	0.66
18	43.170	1105	1.01	76	97.148	34489	31.55
19	44.048	26709	24.44	77	98.119	820	0.75
20	44.080	3972	3.63	78	98.155	5741	5.25
21	45.056	9605	8.79	79	99.129	1825	1.67
22	53.065	2682	2.45	80	99.164	2825	2.58
23	54.073	11202	10.25	81	100.136	676	0.62
24	55.046	1004	0.92	82	107.139	645	0.59
25	55.082	69539	63.62	83	108.146	1228	1.12
26	56.090	23445	21.45	84	109.154	15574	14.25
27	57.062	25322	23.17	85	110.161	13769	12.60

28	57.098	84456	77.27	86	111.170	12118	11.09
29	57.211	553	0.51	87	112.177	3036	2.78
30	58.069	2985	2.73	88	113.185	1774	1.62
31	58.102	3715	3.40	89	122.167	1164	1.07
32	59.078	684	0.63	90	123.175	8348	7.64
33	65.070	576	0.53	91	124.183	7482	6.85
34	66.079	8298	7.59	92	125.192	4276	3.91
35	67.087	35129	32.14	93	126.199	1774	1.62
36	68.095	47021	43.02	94	127.208	1036	0.95
37	68.126	760	0.69	95	137.198	4605	4.21
38	68.155	360	0.33	96	138.205	4478	4.10
39	68.163	625	0.57	97	139.213	1671	1.53
40	69.104	46295	42.35	98	140.223	1151	1.05
41	69.136	290	0.26	99	151.218	1502	1.37
42	69.148	148	0.14	100	152.227	2498	2.29
43	69.167	334	0.31	101	153.235	933	0.85
44	69.177	190	0.17	102	154.243	729	0.67
45	70.076	1696	1.55	103	165.240	753	0.69
46	70.112	16692	15.27	104	166.249	1890	1.73
47	71.084	9468	8.66	105	180.273	1113	1.02
48	71.120	35827	32.78	106	194.292	1224	1.12
49	71.152	357	0.33	107	208.316	1263	1.16
50	71.195	677	0.62	108	222.338	1070	0.98
51	72.092	4478	4.10	109	236.361	1426	1.30
52	72.124	1942	1.78	110	250.385	1154	1.06
53	73.100	1143	1.05	111	264.404	1529	1.40
54	79.093	2965	2.71	112	278.425	1347	1.23
55	80.101	3466	3.17	113	292.451	2769	2.53
56	81.109	33298	30.46	114	294.467	917	0.84
57	82.117	81766	74.81	115	320.495	6646	6.08
58	82.237	1246	1.14	116	321.498	2149	1.97

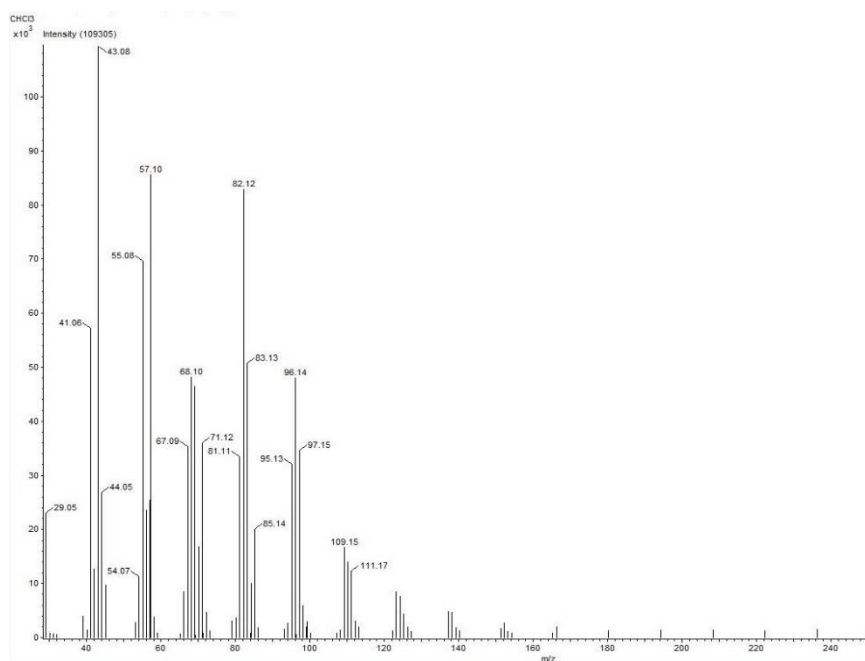


Figure 38. Mass-spectra of octadecanal (Rt = 22.11) in F3 fraction from ethyl acetate extract of *C. militaris* detected by GC-MS.

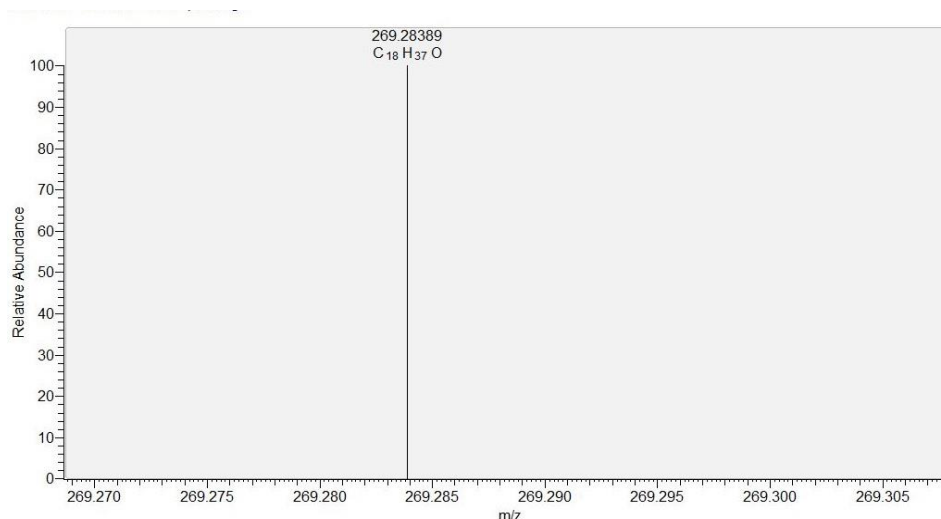


Figure 39. ESI-MS spectra of octadecanal in F3 fraction from ethyl acetate extract of *C. militaris*.

Table 26. Fragmentation pattern of dodecanamide (retention time = 25.55) in F3 fraction from ethyl acetate extract of *C. militaris* detected by GC-MS

Peak#	m/z	Intensity	Relative Intensity (%)	Peak#	m/z	Intensity	Relative Intensity (%)
1	29.053	1265	4.42	31	72.137	107	0.38
2	32.002	2413	8.44	32	72.463	262	0.92
3	39.044	191	0.67	33	73.087	1328	4.64
4	41.059	3023	10.57	34	75.066	303	1.06
5	42.067	719	2.52	35	81.105	179	0.63
6	43.076	7689	26.90	36	81.110	98	0.34
7	44.035	1942	6.79	37	83.126	1435	5.02
8	44.079	395	1.38	38	84.097	469	1.64
9	53.065	364	1.27	39	85.142	654	2.29
10	54.073	296	1.03	40	86.101	1883	6.59
11	55.044	605	2.12	41	87.109	166	0.58
12	55.081	3586	12.54	42	96.130	260	0.91
13	56.090	1036	3.62	43	97.147	832	2.91
14	57.098	4625	16.18	44	98.119	1192	4.17
15	59.066	28585	100.00	45	100.122	618	2.16
16	59.094	195	0.68	46	101.134	395	1.38
17	59.102	85	0.30	47	114.146	1450	5.07
18	59.110	326	1.14	48	115.155	682	2.39
19	59.129	278	0.97	49	128.168	1398	4.89
20	59.136	210	0.73	50	142.188	213	0.74
21	59.142	103	0.36	51	142.197	221	0.77
22	60.073	4227	14.79	52	170.233	197	0.69
23	67.084	182	0.64	53	184.256	200	0.70
24	67.088	120	0.42	54	281.184	403	1.41
25	68.092	189	0.66	55	324.486	458	1.60
26	69.104	1656	5.79	56	324.514	214	0.75
27	70.108	512	1.79	57	367.554	409	1.43
28	71.120	1660	5.81	58	367.573	205	0.72
29	72.080	13232	46.29	59	526.213	98	0.34
30	72.117	199	0.70				

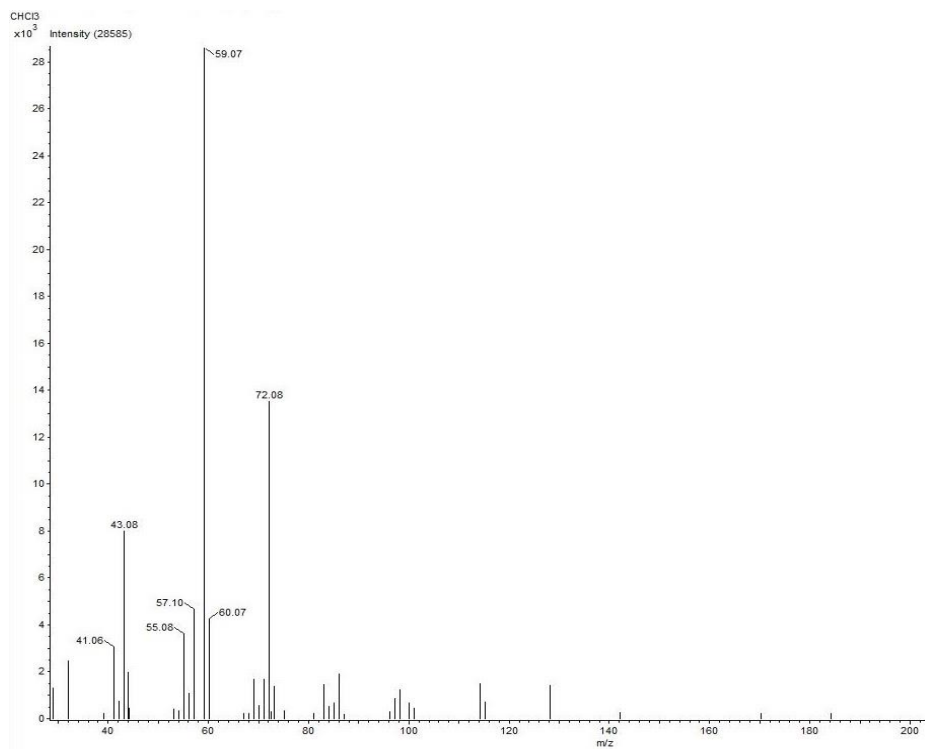


Figure 40. Mass-spectra of dodecanamide (Rt = 25.55) in F3 fraction from ethyl acetate extract of *C. militaris* detected by GC-MS.

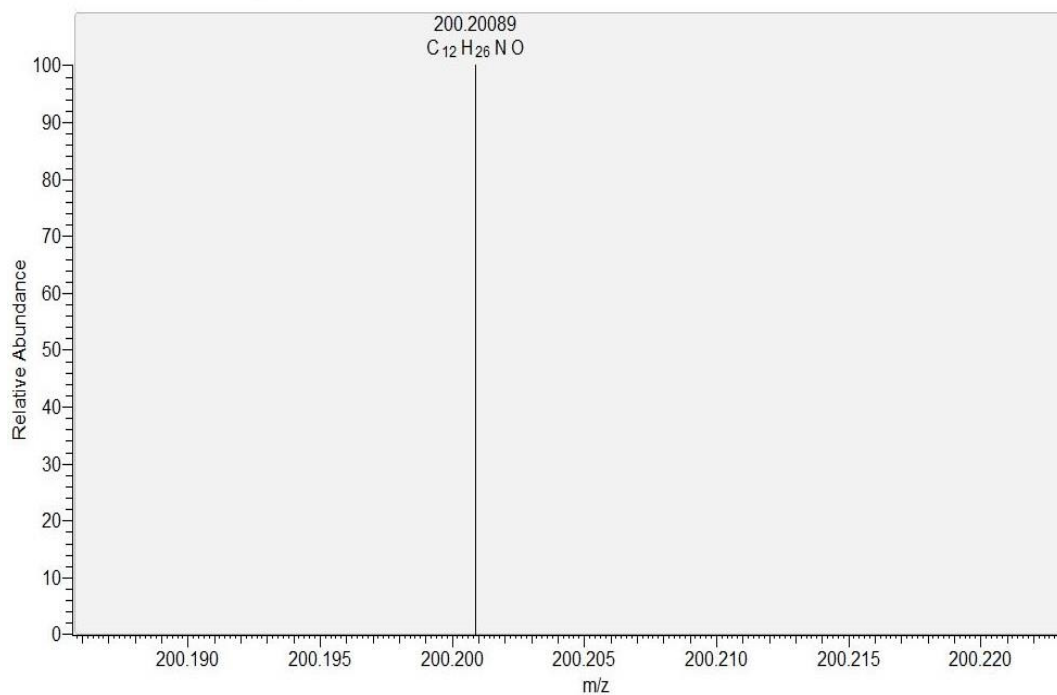


Figure 41. ESI-MS spectra of dodecanamide in F3 fraction from ethyl acetate extract of *C. militaris*.

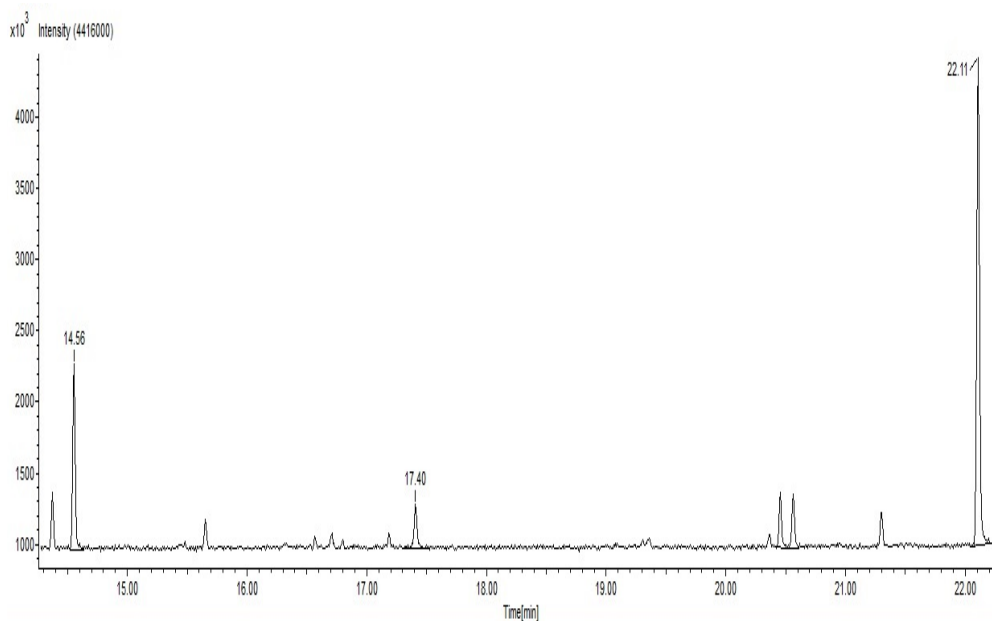


Figure 42. GC-MS chromatogram of F4 fraction from ethyl acetate extract of *C. militaris*.

Table 27. Fragmentation pattern of pentadecanal (retention time = 14.56) in F4 fraction from ethyl acetate extract of *C. militaris* detected by GC-MS

Peak#	m/z	Intensity	Relative Intensity (%)	Peak#	m/z	Intensity	Relative Intensity (%)
1	29.017	1041	4.70	26	71.120	5332	24.09
2	29.053	9474	42.81	27	72.092	1448	6.54
3	39.043	2549	11.52	28	79.093	861	3.89
4	40.051	632	2.86	29	81.110	6863	31.01
5	41.060	18760	84.76	30	82.118	13588	61.40
6	42.067	3967	17.93	31	83.126	7702	34.80
7	43.040	1024	4.63	32	84.134	2710	12.25
8	43.076	22131	100.00	33	85.107	801	3.62
9	44.048	7380	33.35	34	85.143	2978	13.45
10	44.080	873	3.95	35	95.132	5933	26.81
11	45.056	2945	13.31	36	96.140	7799	35.24
12	53.065	1197	5.41	37	97.148	4604	20.80
13	54.073	3227	14.58	38	98.155	1439	6.50
14	55.082	14988	67.72	39	99.128	607	2.74
15	56.090	6441	29.10	40	109.154	2782	12.57
16	57.062	8041	36.33	41	110.161	2331	10.53
17	57.098	13727	62.02	42	111.170	1654	7.47
18	58.069	1007	4.55	43	112.180	901	4.07
19	58.102	799	3.61	44	123.176	1113	5.03
20	66.079	1682	7.60	45	124.184	1096	4.95
21	67.087	8159	36.87	46	137.200	715	3.23
22	68.096	9535	43.09	47	138.206	791	3.58
23	69.104	8506	38.44	48	180.275	947	4.28
24	70.112	4731	21.37	49	182.289	956	4.32
25	71.084	2531	11.44				

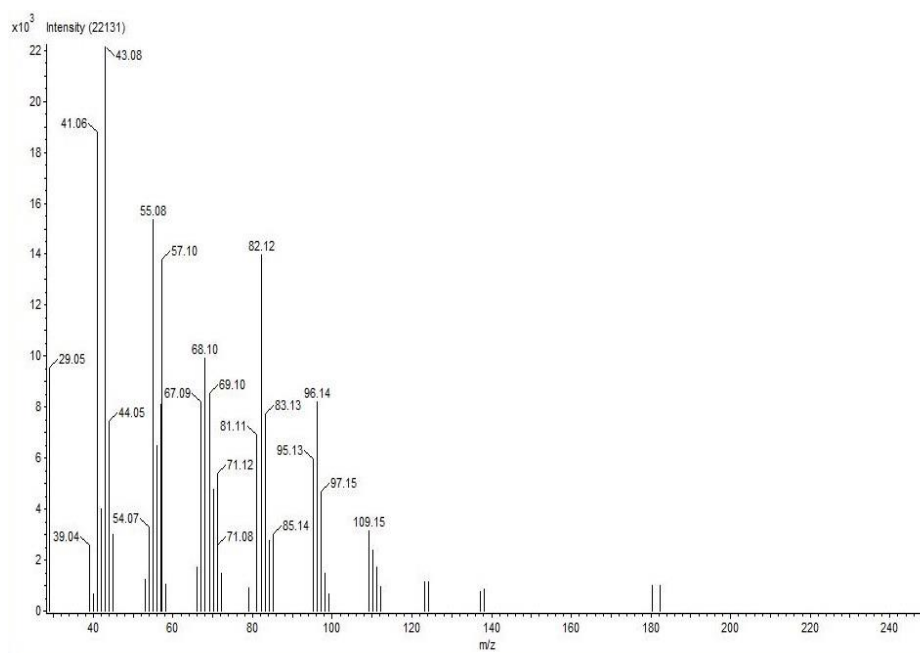


Figure 43. Mass-spectra of pentadecanal (Rt = 14.56) in F4 fraction from ethyl acetate extract of *C. militaris* detected by GC-MS.

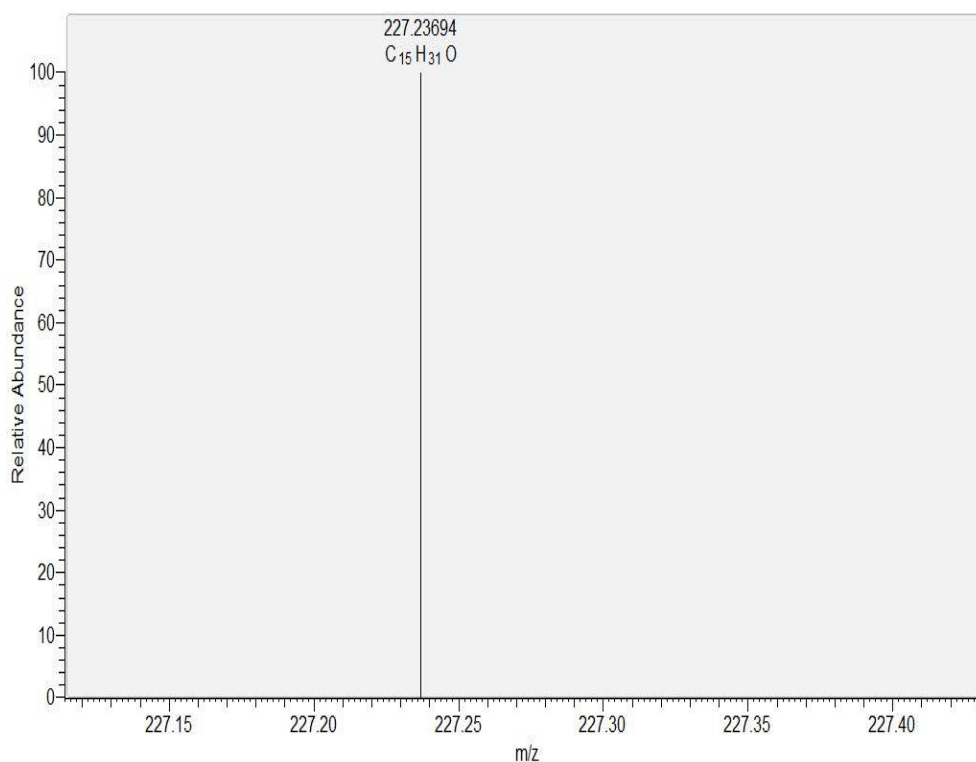


Figure 44. ESI-MS spectra of pentadecanal in F4 fraction from ethyl acetate extract of *C. militaris*.

Table 28. Fragmentation pattern of 2-oxopalmitic acid methyl ester (retention time = 17.40) in F4 fraction from ethyl acetate extract of *C. militaris* detected by GC-MS

Peak#	m/z	Intensity	Relative Intensity (%)	Peak#	m/z	Intensity	Relative Intensity (%)
1	29.053	2656	26.38	14	67.088	1162	11.54
2	31.034	1394	13.84	15	69.104	2661	26.42
3	32.002	342	3.40	16	71.121	5562	55.23
4	39.043	812	8.06	17	74.074	474	4.71
5	41.060	6092	60.49	18	81.111	1192	11.83
6	42.068	1343	13.34	19	83.127	1755	17.43
7	43.039	685	6.80	20	85.142	3199	31.77
8	43.076	9780	97.11	21	95.132	1690	16.78
9	55.082	4411	43.81	22	97.148	708	7.03
10	56.089	981	9.74	23	109.153	536	5.32
11	57.098	10071	100.00	24	109.161	356	3.54
12	58.070	563	5.59	25	225.329	6738	66.90
13	58.102	630	6.25	26	226.335	1217	12.09

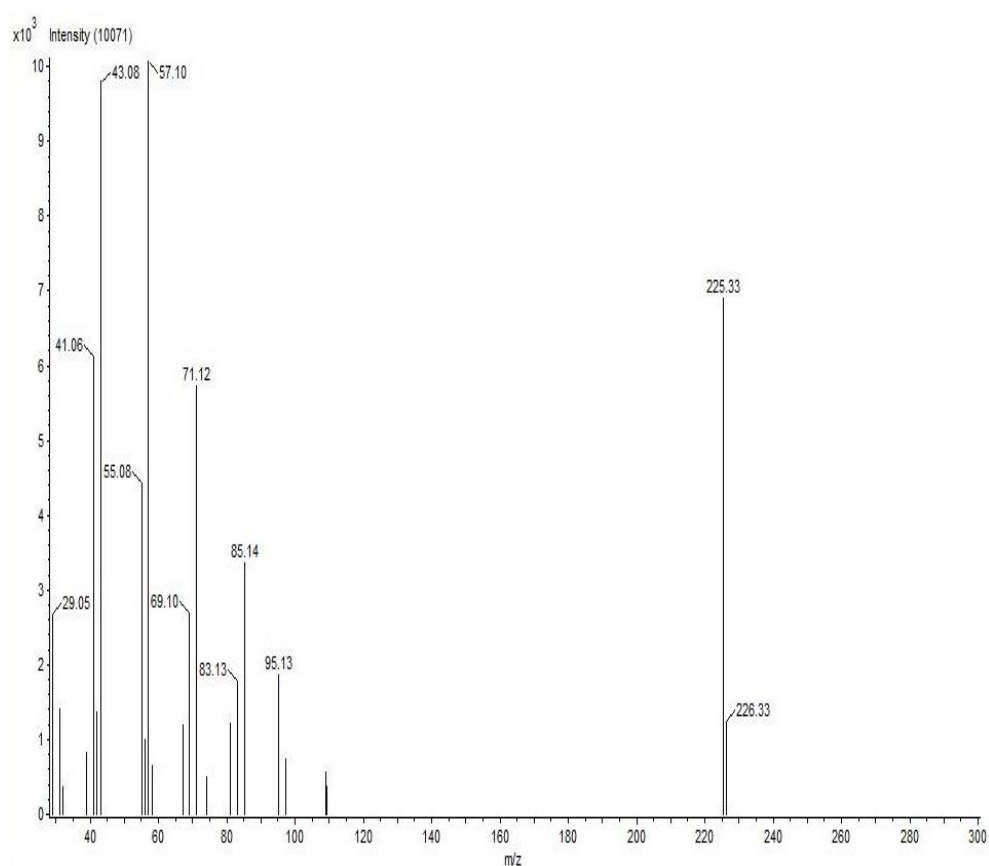


Figure 45. Mass-spectra of 2-oxopalmitic acid methyl ester (Rt = 17.40) in F4 fraction from ethyl acetate extract of *C. militaris* detected by GC-MS.

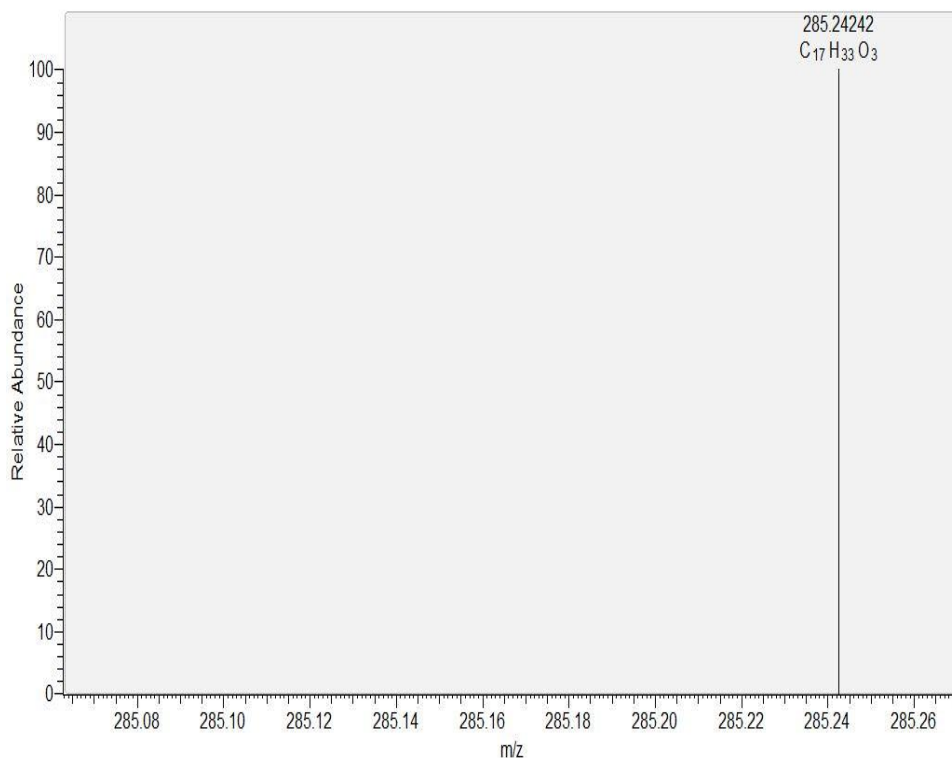


Figure 46. ESI-MS spectra of 2-oxopalmitic acid methyl ester in F4 fraction from ethyl acetate extract of *C. militaris*.

Table 29. Fragmentation pattern of octadecanal (retention time = 22.11) in F4 fraction from ethyl acetate extract of *C. militaris* detected by GC-MS

Peak#	m/z	Intensity	Relative Intensity (%)	Peak#	m/z	Intensity	Relative Intensity (%)
1	29.017	750	1.56	51	83.091	439	0.91
2	29.053	10112	20.97	52	83.126	21753	45.12
3	32.001	226	0.47	53	83.161	301	0.62
4	39.043	1784	3.70	54	83.196	480	0.99
5	40.050	567	1.18	55	84.097	338	0.70
6	41.059	24459	50.73	56	84.133	4281	8.88
7	41.115	703	1.46	57	85.107	1630	3.38
8	42.067	5368	11.13	58	85.143	8394	17.41
9	43.040	1046	2.17	59	86.114	803	1.66
10	43.076	48217	100.00	60	86.147	723	1.50
11	43.110	312	0.65	61	93.116	876	1.82
12	43.130	1086	2.25	62	94.124	1307	2.71
13	44.048	11721	24.31	63	95.132	13515	28.03
14	44.080	1633	3.39	64	96.140	20855	43.25
15	45.056	4309	8.94	65	97.148	14630	30.34
16	53.066	1413	2.93	66	98.155	2624	5.44
17	54.073	4982	10.33	67	99.128	825	1.71
18	55.046	434	0.90	68	99.164	1339	2.78
19	55.082	30253	62.74	69	100.137	430	0.89
20	55.109	291	0.60	70	108.145	746	1.55
21	55.140	433	0.90	71	109.154	6562	13.61
22	55.150	229	0.47	72	110.162	5896	12.23

23	56.090	10262	21.28	73	111.170	5421	11.24
24	57.062	11480	23.81	74	112.177	1334	2.77
25	57.098	37304	77.37	75	113.187	758	1.57
26	57.144	172	0.36	76	122.167	428	0.89
27	57.161	857	1.78	77	123.176	3688	7.65
28	58.069	1324	2.75	78	124.183	3135	6.50
29	58.102	1686	3.50	79	125.192	2082	4.32
30	59.077	367	0.76	80	126.199	707	1.47
31	66.079	3790	7.86	81	127.210	502	1.04
32	67.087	15469	32.08	82	137.198	2093	4.34
33	68.096	20459	42.43	83	138.206	2110	4.38
34	69.104	20655	42.84	84	139.212	1034	2.14
35	70.075	993	2.06	85	140.223	445	0.92
36	70.112	7677	15.92	86	151.220	771	1.60
37	71.084	3899	8.09	87	152.228	1081	2.24
38	71.121	16055	33.30	88	166.251	621	1.29
39	71.154	229	0.47	89	180.273	648	1.34
40	72.092	1856	3.85	90	208.321	507	1.05
41	72.124	974	2.02	91	222.334	600	1.24
42	73.101	579	1.20	92	236.363	668	1.38
43	79.094	1517	3.15	93	250.383	556	1.15
44	80.101	1469	3.05	94	264.393	160	0.33
45	81.110	14744	30.58	95	264.405	192	0.40
46	82.118	35493	73.61	96	264.415	120	0.25
47	82.160	232	0.48	97	264.425	379	0.79
48	82.187	335	0.69	98	292.453	1686	3.50
49	82.194	113	0.24	99	320.496	2915	6.05
50	82.201	219	0.45	100	321.501	732	1.52

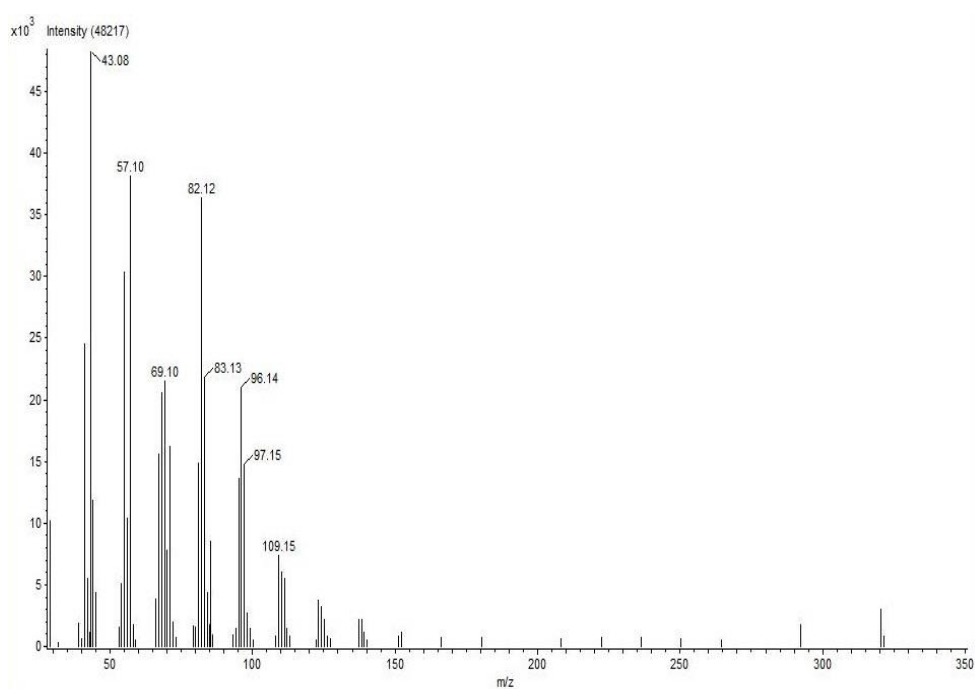


Figure 47. Mass-spectra of octadecanal (Rt = 22.11) in F4 fraction from ethyl acetate extract of *C. militaris* detected by GC-MS.

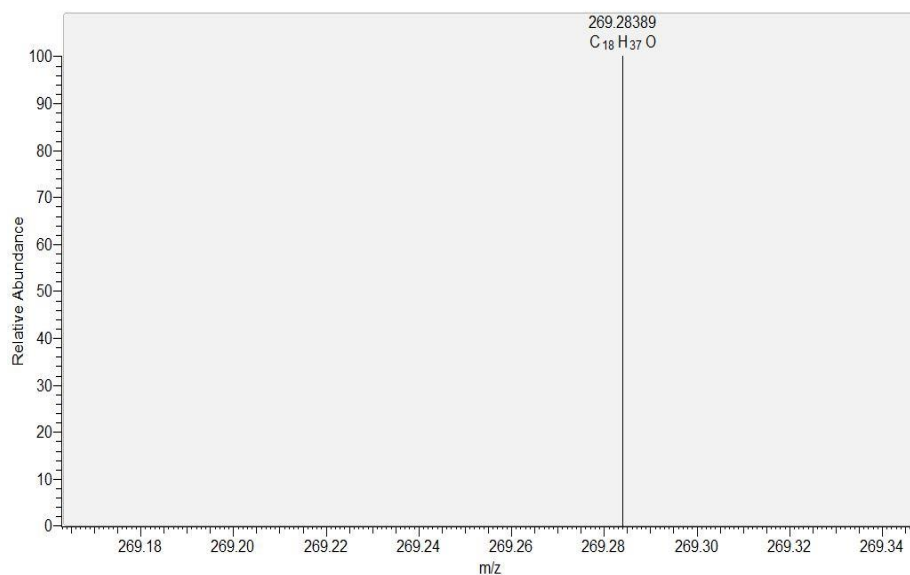


Figure 48. ESI-MS spectra of octadecanal in F4 fraction from ethyl acetate extract of *C. militaris*.

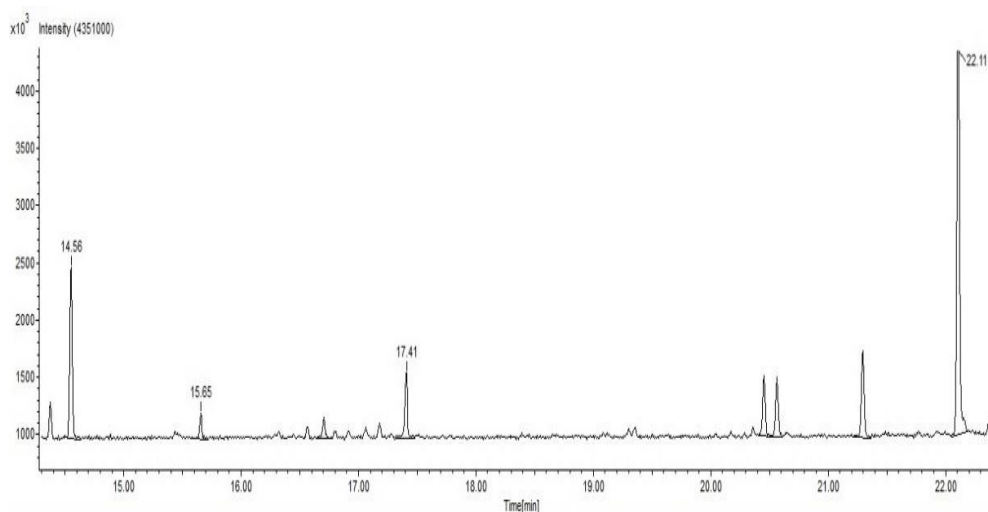


Figure 49. GC-MS chromatogram of F5 fraction from ethyl acetate extract of *C. militaris*.

Table 30. Fragmentation pattern of pentadecanal (retention time = 14.56) in F5 fraction from ethyl acetate extract of *C. militaris* detected by GC-MS

Peak#	m/z	Intensity	Relative Intensity (%)	Peak#	m/z	Intensity	Relative Intensity (%)
1	29.017	1052	4.74	34	80.102	629	2.84
2	29.053	9290	41.90	35	81.110	6787	30.61
3	31.034	314	1.42	36	82.118	13654	61.58
4	39.043	2390	10.78	37	83.126	7520	33.91
5	40.050	532	2.40	38	84.134	2583	11.65
6	41.060	18824	84.89	39	85.106	775	3.50
7	42.067	4084	18.42	40	85.143	2817	12.70

8	43.040	1021	4.61	41	86.114	374	1.69
9	43.076	22173	100.00	42	93.113	405	1.82
10	43.100	223	1.00	43	94.123	468	2.11
11	43.130	418	1.89	44	95.132	5847	26.37
12	44.048	7250	32.70	45	96.140	7695	34.71
13	44.080	834	3.76	46	97.148	4671	21.07
14	45.056	2856	12.88	47	98.155	1476	6.66
15	53.065	1371	6.18	48	99.128	529	2.39
16	54.073	3192	14.40	49	99.164	419	1.89
17	55.046	421	1.90	50	109.154	2879	12.98
18	55.082	15025	67.76	51	110.161	2188	9.87
19	56.090	6331	28.55	52	111.170	1794	8.09
20	57.062	8066	36.38	53	112.179	807	3.64
21	57.098	13741	61.97	54	123.176	1377	6.21
22	58.069	851	3.84	55	124.184	1099	4.96
23	58.102	573	2.58	56	125.192	581	2.62
24	66.079	1602	7.22	57	126.200	500	2.25
25	67.087	8097	36.52	58	137.200	817	3.69
26	68.096	9357	42.20	59	138.208	906	4.08
27	69.104	8871	40.01	60	140.224	699	3.15
28	70.078	499	2.25	61	152.227	971	4.38
29	70.112	4936	22.26	62	180.275	837	3.78
30	71.084	2627	11.85	63	182.290	1156	5.21
31	71.120	5419	24.44	64	208.311	177	0.80
32	72.092	1314	5.93	65	208.323	305	1.38
33	79.093	967	4.36				

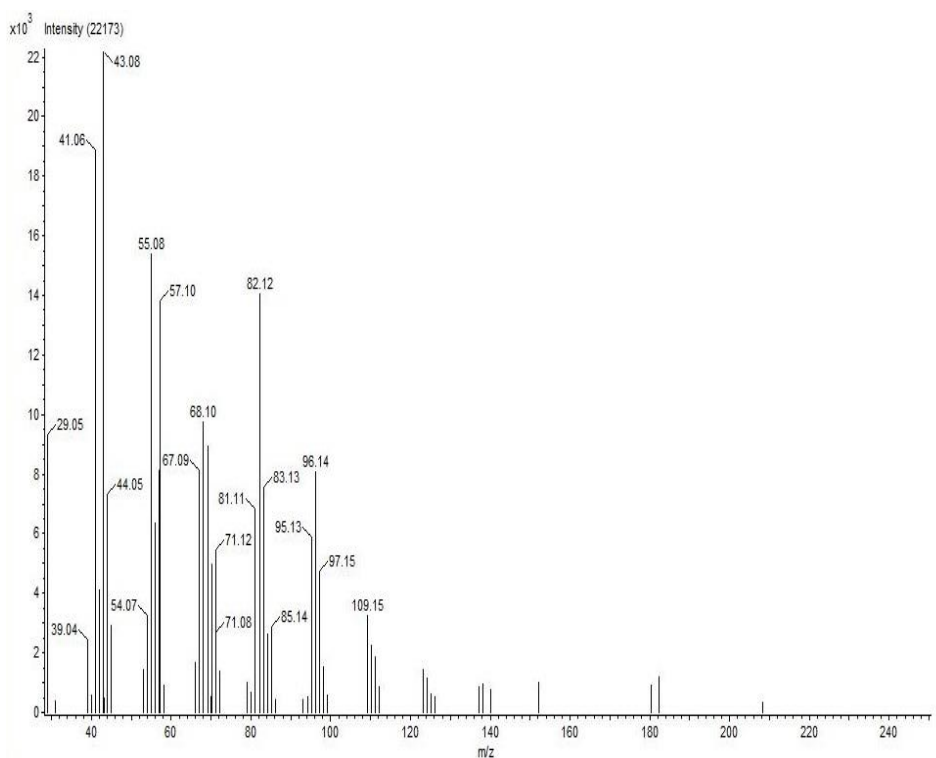


Figure 50. Mass-spectra of pentadecanal (Rt = 14.56) in F5 fraction from ethyl acetate extract of *C. militaris* detected by GC-MS.

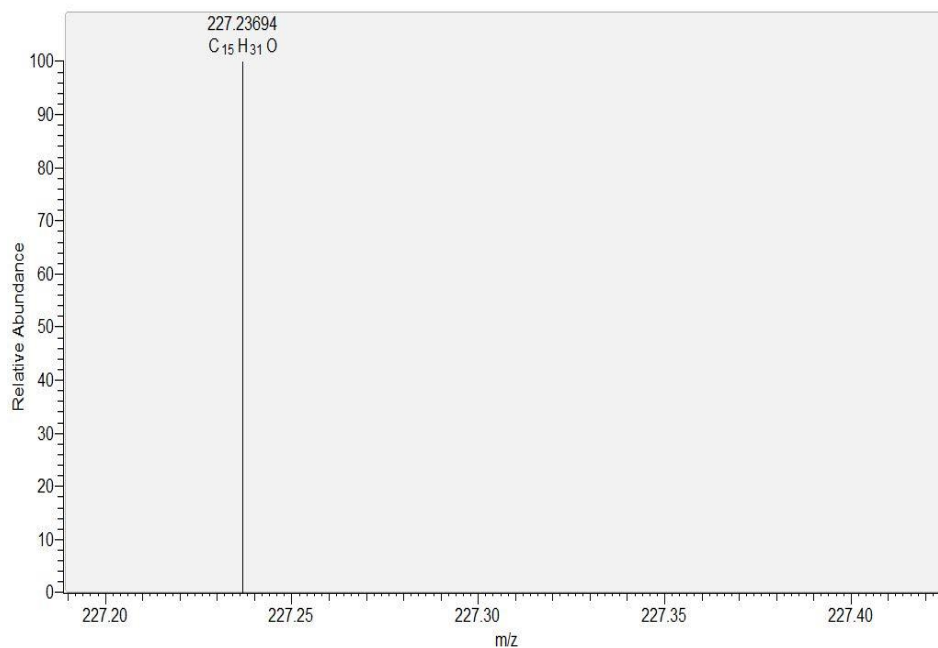


Figure 51. ESI-MS spectra of pentadecanal in F5 fraction from ethyl acetate extract of *C. militaris*.

Table 31. Fragmentation pattern of hexadecanal (retention time = 15.65) in F5 fraction from ethyl acetate extract of *C. militaris* detected by GC-MS

Peak#	m/z	Intensity	Relative Intensity (%)	Peak#	m/z	Intensity	Relative Intensity (%)
1	29.048	15677	13.78	37	82.102	909	0.80
2	31.028	717	0.63	38	83.074	1658	1.46
3	39.035	3693	3.25	39	83.111	6396	5.62
4	40.044	874	0.77	40	84.083	2596	2.28
5	41.052	33958	29.86	41	84.118	938	0.82
6	42.024	832	0.73	42	85.127	2099	1.85
7	42.059	6744	5.93	43	87.071	70771	62.23
8	43.032	8216	7.22	44	87.145	1541	1.35
9	43.068	40454	35.57	45	88.077	5909	5.20
10	43.091	267	0.23	46	93.098	771	0.68
11	44.072	1435	1.26	47	95.114	1398	1.23
12	45.047	1410	1.24	48	97.094	2477	2.18
13	53.055	1880	1.65	49	97.131	2908	2.56
14	54.063	2563	2.25	50	98.103	2246	1.97
15	55.035	4134	3.63	51	101.091	4578	4.03
16	55.072	27714	24.37	52	109.133	668	0.59
17	56.079	5552	4.88	53	111.113	1225	1.08
18	57.052	1373	1.21	54	111.151	993	0.87
19	57.088	17100	15.04	55	115.110	1539	1.35
20	58.093	929	0.82	56	129.129	4524	3.98
21	59.031	8862	7.79	57	143.149	9728	8.55
22	59.068	4016	3.53	58	144.154	1002	0.88
23	67.075	3431	3.02	59	147.109	3045	2.68
24	68.083	1496	1.32	60	171.188	2106	1.85

25	69.092	15520	13.65	61	185.207	2596	2.28
26	70.098	2388	2.10	62	199.227	1907	1.68
27	71.071	982	0.86	63	213.246	1301	1.14
28	71.108	4888	4.30	64	221.151	1270	1.12
29	73.070	11383	10.01	65	227.267	7560	6.65
30	74.059	113733	100.00	66	228.270	1346	1.18
31	74.159	709	0.62	67	239.306	4774	4.20
32	74.187	788	0.69	68	241.286	2530	2.22
33	75.067	20171	17.74	69	270.333	10127	8.90
34	76.067	1582	1.39	70	271.336	1797	1.58
35	79.079	897	0.79	71	281.132	1727	1.52
36	81.095	2235	1.97				

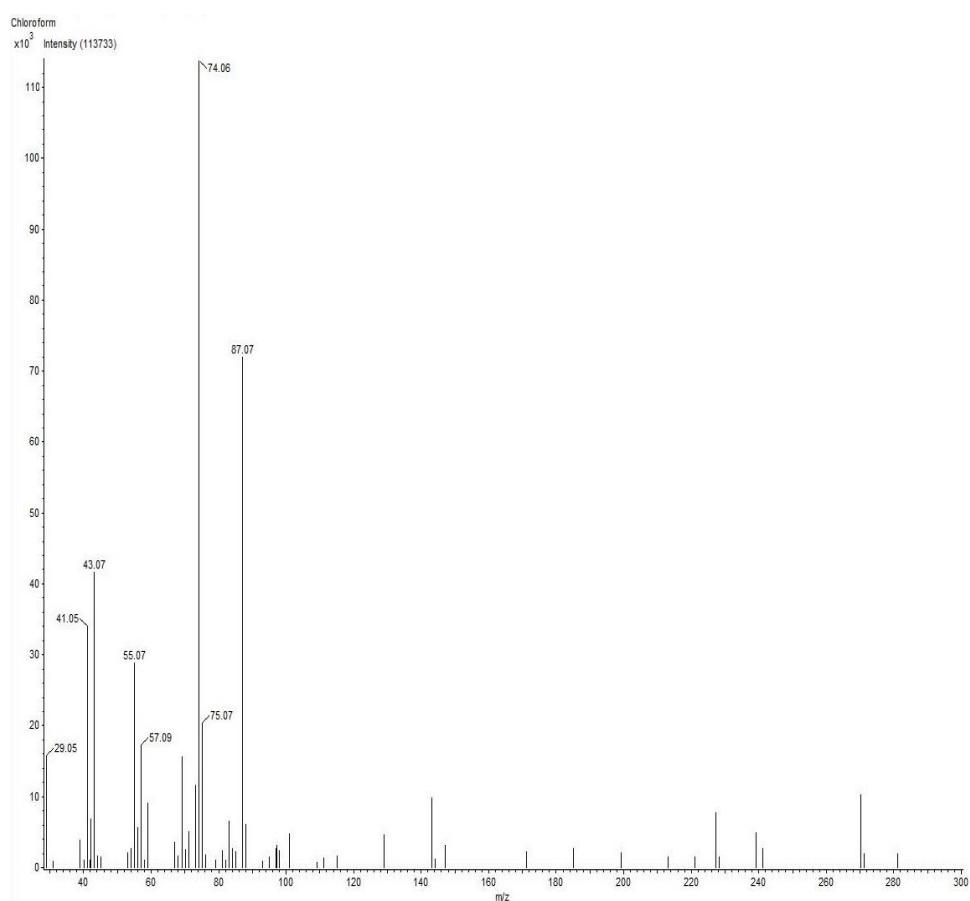


Figure 52. Mass-spectra of hexadecanal (Rt = 15.65) in F5 fraction from ethyl acetate extract of *C. militaris* detected by GC-MS.

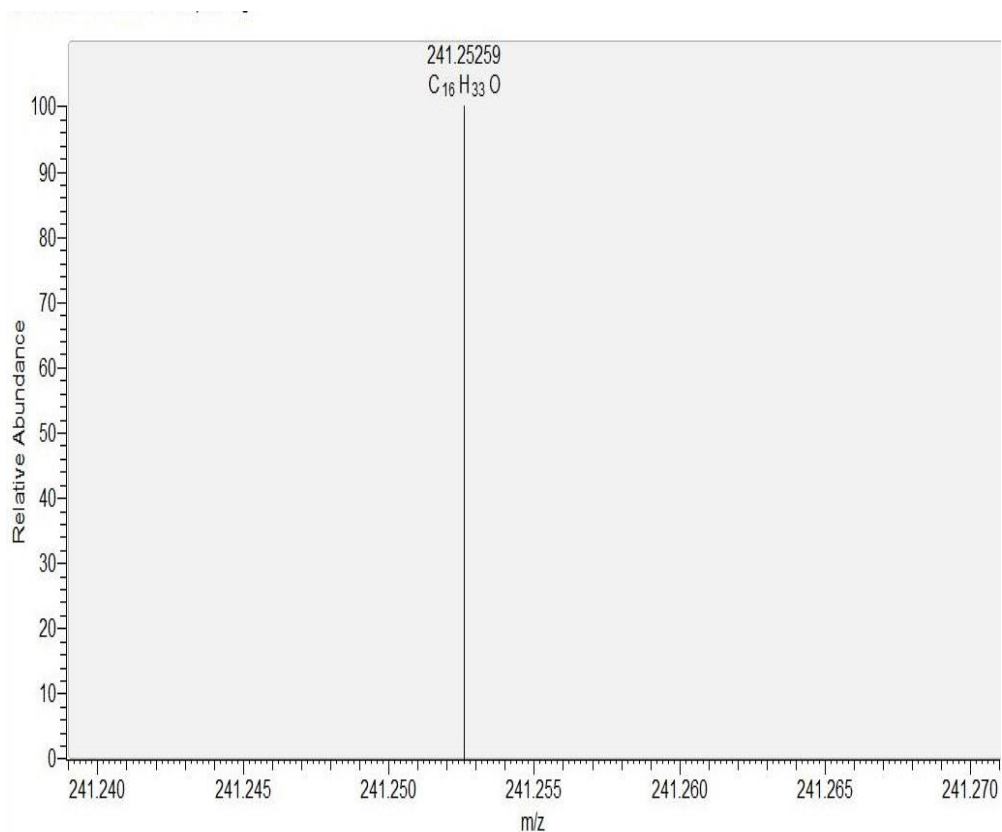


Figure 53. ESI-MS spectra of hexadecanal in F5 fraction from ethyl acetate extract of *C. militaris*.

Table 32. Fragmentation pattern of 2-oxopalmitic acid methyl ester (retention time = 17.41) in F4 fraction from ethyl acetate extract of *C. militaris* detected by GC-MS

Peak#	m/z	Intensity	Relative Intensity (%)	Peak#	m/z	Intensity	Relative Intensity (%)
1	29.048	1756	28.64	11	67.078	566	9.24
2	31.028	1233	20.12	12	69.093	1269	20.70
3	31.996	718	11.71	13	71.108	2537	41.39
4	39.036	538	8.78	14	73.070	1513	24.68
5	41.052	3692	60.24	15	81.095	629	10.27
6	42.060	1205	19.66	16	83.111	720	11.74
7	43.068	6129	100.00	17	85.128	1315	21.46
8	55.073	2698	44.02	18	95.117	605	9.86
9	56.079	683	11.14	19	225.290	4627	75.49
10	57.089	5167	84.29	20	226.291	800	13.06

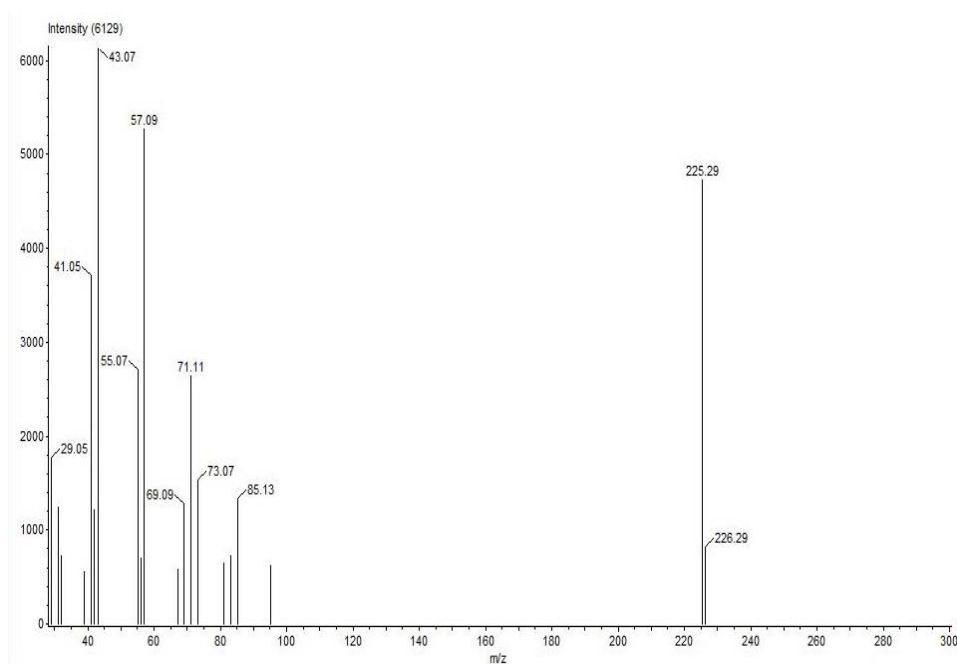


Figure 54. Mass-spectra of 2-oxopalmitic acid methyl ester ($R_t = 17.41$) in F4 fraction from ethyl acetate extract of *C. militaris* detected by GC-MS.

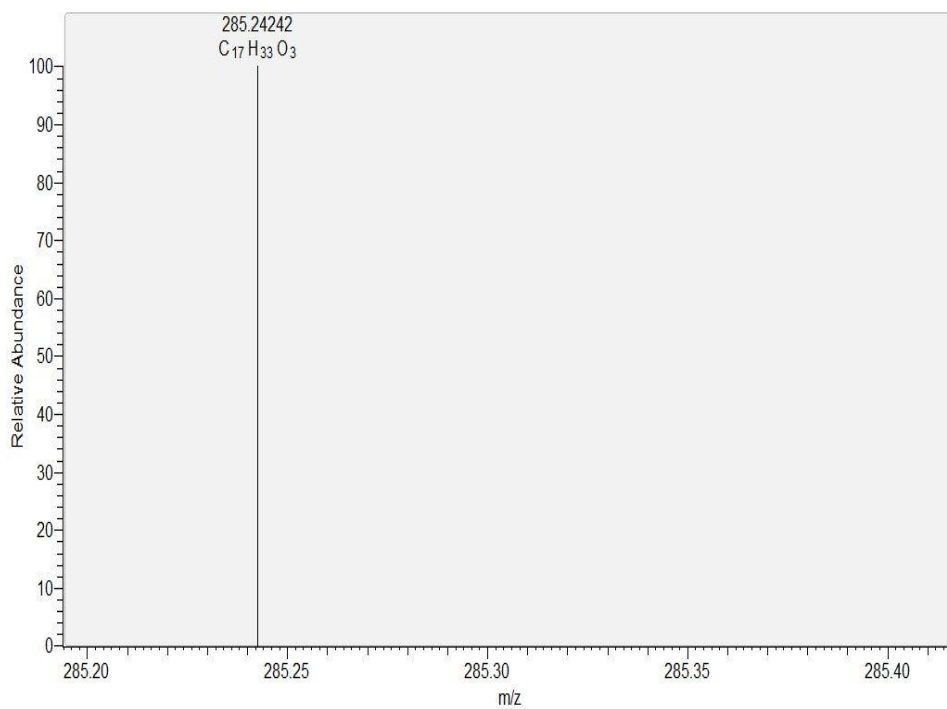


Figure 55. ESI-MS spectra of 2-oxopalmitic acid methyl ester in F5 fraction from ethyl acetate extract of *C. militaris*.

Table 33. Fragmentation pattern of octadecanal (retention time = 22.11) in F5 fraction from ethyl acetate extract of *C. militaris* detected by GC-MS

Peak#	m/z	Intensity	Relative Intensity (%)	Peak#	m/z	Intensity	Relative Intensity (%)
1	29.017	694	1.62	49	82.202	202	0.47
2	29.053	8864	20.73	50	83.126	19379	45.33
3	32.001	277	0.65	51	83.162	195	0.46
4	39.043	1575	3.68	52	83.196	181	0.42
5	40.051	536	1.25	53	84.097	353	0.83
6	41.059	21377	50.00	54	84.133	3895	9.11
7	41.114	149	0.35	55	85.107	1592	3.72
8	42.067	4892	11.44	56	85.143	7672	17.94
9	43.040	964	2.26	57	86.114	699	1.64
10	43.076	42754	100.00	58	86.146	617	1.44
11	43.109	278	0.65	59	93.116	682	1.59
12	43.119	161	0.38	60	94.124	1161	2.71
13	43.129	823	1.92	61	95.132	12270	28.70
14	44.048	10493	24.54	62	96.140	18592	43.49
15	44.080	1516	3.55	63	97.148	13136	30.73
16	45.056	3759	8.79	64	98.155	2589	6.06
17	53.065	1318	3.08	65	99.128	778	1.82
18	54.073	4458	10.43	66	99.164	1260	2.95
19	55.046	423	0.99	67	108.144	641	1.50
20	55.082	26879	62.87	68	109.154	5877	13.75
21	55.108	278	0.65	69	110.162	5390	12.61
22	55.140	248	0.58	70	111.170	4805	11.24
23	55.150	206	0.48	71	112.177	1211	2.83
24	56.090	9115	21.32	72	113.188	760	1.78
25	57.062	10194	23.84	73	122.165	511	1.19
26	57.098	32820	76.76	74	123.176	3541	8.28
27	57.135	205	0.48	75	124.183	2943	6.88
28	57.143	209	0.49	76	125.192	1969	4.61
29	57.162	751	1.76	77	126.198	572	1.34
30	58.069	1150	2.69	78	137.198	1897	4.44
31	58.102	1482	3.47	79	138.206	1801	4.21
32	66.079	3544	8.29	80	139.212	819	1.92
33	67.087	13848	32.39	81	140.224	470	1.10
34	68.096	18447	43.15	82	151.221	620	1.45
35	69.104	18414	43.07	83	152.228	1115	2.61
36	70.072	862	2.02	84	166.251	586	1.37
37	70.112	6593	15.42	85	180.274	708	1.66
38	71.084	3417	7.99	86	208.321	714	1.67
39	71.121	14317	33.49	87	250.382	211	0.49
40	71.154	220	0.51	88	250.401	254	0.59
41	72.092	1601	3.75	89	264.405	317	0.74
42	72.124	841	1.97	90	264.416	112	0.26
43	73.101	681	1.59	91	264.425	120	0.28
44	79.094	1245	2.91	92	292.453	1113	2.60
45	80.101	1371	3.21	93	320.496	2737	6.40
46	81.110	13334	31.19	94	321.494	256	0.60
47	82.118	31588	73.88	95	321.504	434	1.02
48	82.187	413	0.97				

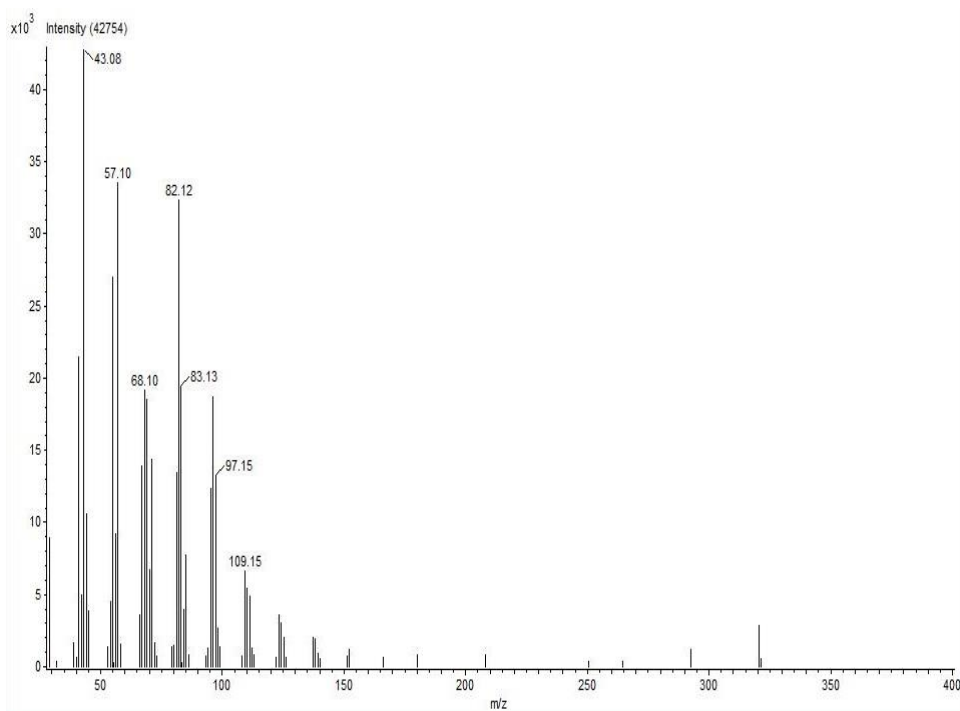


Figure 56. Mass-spectra of octadecanal (Rt = 22.11) in F5 fraction from ethyl acetate extract of *C. militaris* detected by GC-MS.

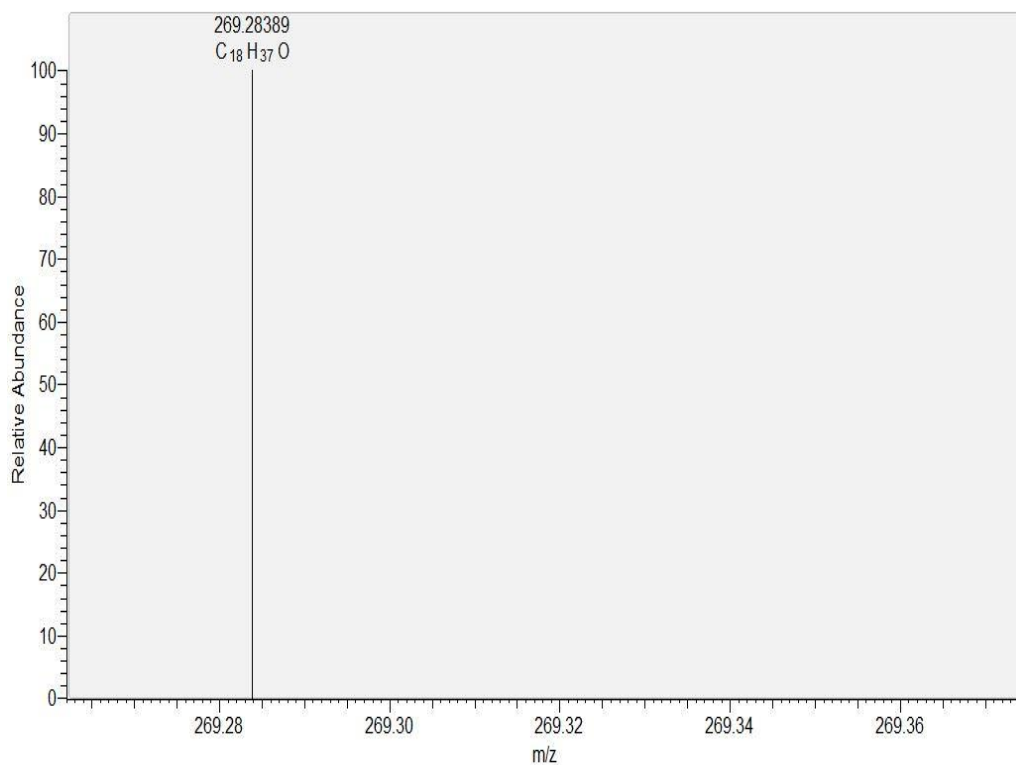


Figure 57. ESI-MS spectra of octadecanal in F5 fraction from ethyl acetate extract of *C. militaris*.

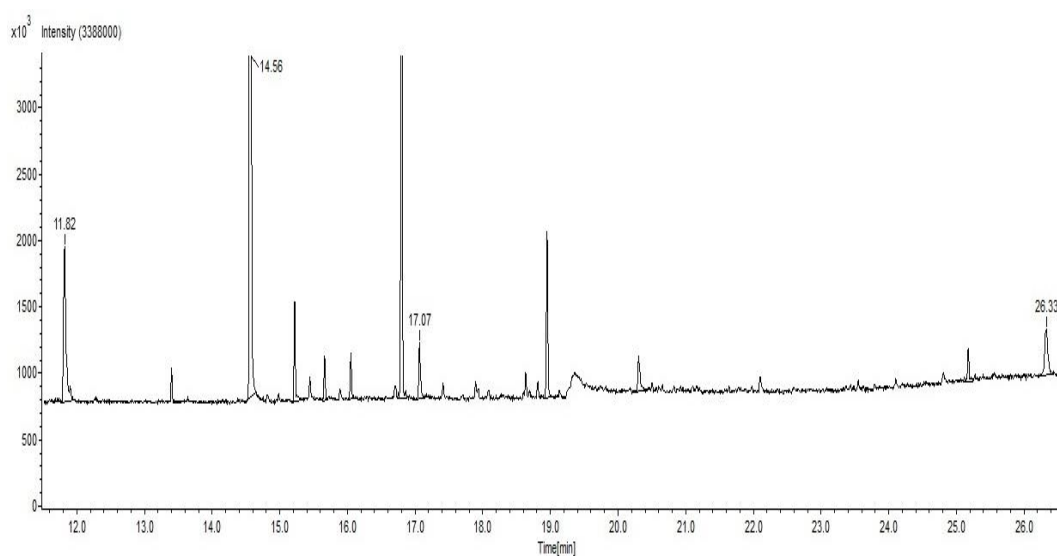


Figure 58. GC-MS chromatogram of F6 fraction from ethyl acetate extract of *C. militaris*.

Table 34. Fragmentation pattern of 1,6-anhydro- β -D-glucopyranose (retention time = 11.82) in F6 fraction from ethyl acetate extract of *C. militaris* detected by GC-MS

Peak#	m/z	Intensity	Relative Intensity (%)	Peak#	m/z	Intensity	Relative Intensity (%)
1	29.015	11571	19.31	28	59.038	784	1.31
2	29.051	3925	6.55	29	60.046	59918	100.00
3	30.023	1455	2.43	30	60.130	223	0.37
4	31.031	9648	16.10	31	60.147	380	0.63
5	31.043	125	0.21	32	60.157	454	0.76
6	39.040	2449	4.09	33	61.053	4212	7.03
7	39.975	365	0.61	34	62.052	337	0.56
8	40.047	472	0.79	35	69.026	514	0.86
9	41.056	3549	5.92	36	69.063	4894	8.17
10	42.028	8051	13.44	37	70.071	7991	13.34
11	42.064	1720	2.87	38	71.043	4944	8.25
12	43.037	9739	16.25	39	71.078	943	1.57
13	43.072	721	1.20	40	72.051	4235	7.07
14	44.008	294	0.49	41	73.059	19945	33.29
15	44.044	6410	10.70	42	74.067	4039	6.74
16	45.016	466	0.78	43	75.067	427	0.71
17	45.053	5236	8.74	44	81.066	694	1.16
18	47.033	5105	8.52	45	85.063	942	1.57
19	53.062	774	1.29	46	87.082	742	1.24
20	54.033	544	0.91	47	89.061	1839	3.07
21	55.042	7144	11.92	48	97.069	2682	4.48
22	56.049	9851	16.44	49	98.077	4174	6.97
23	57.058	26237	43.79	50	99.083	1056	1.76
24	57.083	197	0.33	51	101.066	1235	2.06
25	57.119	778	1.30	52	102.073	1846	3.08
26	58.032	548	0.91	53	115.087	827	1.38
27	58.062	1119	1.87	54	144.101	771	1.29

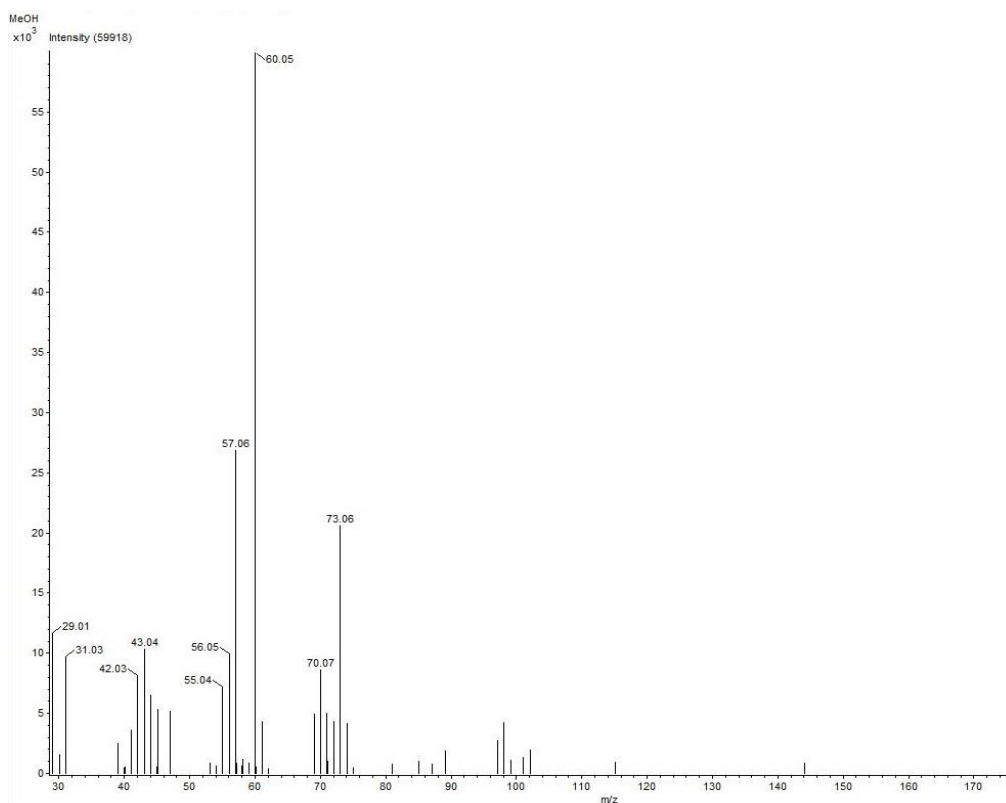


Figure 59. Mass-spectra of 1,6-anhydro- β -D-glucopyranose (Rt = 11.82) in F6 fraction from ethyl acetate extract of *C. militaris* detected by GC-MS.

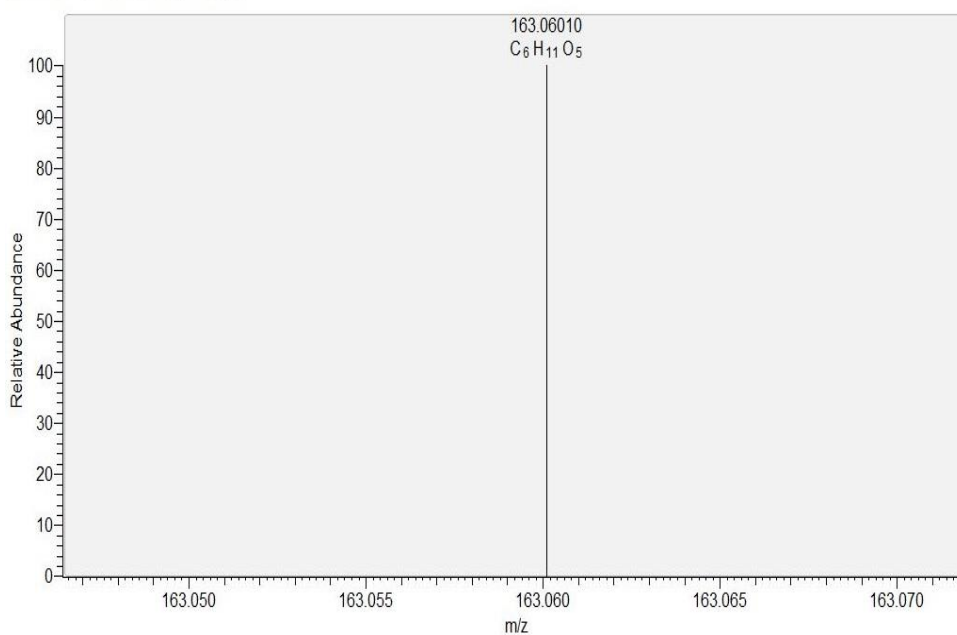


Figure 60. ESI-MS spectra of 1,6-anhydro- β -D-glucopyranose in F6 fraction from ethyl acetate extract of *C. militaris*.

Table 35. Fragmentation pattern of pentadecanal (retention time = 14.56) in F6 fraction from ethyl acetate extract of *C. militaris* detected by GC-MS

Peak#	m/z	Intensity	Relative Intensity (%)	Peak#	m/z	Intensity	Relative Intensity (%)
1	29.015	11564	4.14	55	81.104	95319	34.16
2	29.051	109896	39.38	56	81.175	2284	0.82
3	29.071	1169	0.42	57	82.112	215871	77.36
4	29.094	2452	0.88	58	82.221	1123	0.40
5	30.055	2649	0.95	59	82.241	2064	0.74
6	31.031	3132	1.12	60	83.085	3041	1.09
7	32.005	1695	0.61	61	83.120	116391	41.71
8	39.040	27975	10.03	62	83.193	2822	1.01
9	40.048	6208	2.22	63	84.093	1859	0.67
10	41.057	229086	82.10	64	84.128	37308	13.37
11	41.136	988	0.35	65	85.101	10895	3.90
12	41.145	922	0.33	66	85.137	39732	14.24
13	41.153	1001	0.36	67	86.108	4756	1.70
14	42.029	1979	0.71	68	86.140	2779	1.00
15	42.064	50354	18.05	69	93.109	3469	1.24
16	43.037	10547	3.78	70	94.117	5563	1.99
17	43.073	279037	100.00	71	95.126	84328	30.22
18	43.163	3818	1.37	72	96.133	114348	40.98
19	44.009	1165	0.42	73	96.212	2336	0.84
20	44.045	95977	34.40	74	97.106	1309	0.47
21	44.077	13547	4.86	75	97.141	70289	25.19
22	45.053	36362	13.03	76	98.113	1263	0.45
23	53.062	13966	5.01	77	98.149	21533	7.72
24	54.070	42896	15.37	78	99.122	6483	2.32
25	55.042	4853	1.74	79	99.157	6220	2.23
26	55.078	201872	72.35	80	108.139	1830	0.66
27	56.086	85867	30.77	81	109.147	37277	13.36
28	57.058	108134	38.75	82	110.155	34132	12.23
29	57.094	197896	70.92	83	111.163	26130	9.36
30	57.199	2794	1.00	84	112.171	10830	3.88
31	58.065	10731	3.85	85	113.143	1830	0.66
32	58.098	8001	2.87	86	113.178	3230	1.16
33	59.074	2188	0.78	87	122.159	1939	0.70
34	65.067	2838	1.02	88	123.168	18534	6.64
35	66.075	22694	8.13	89	124.176	18818	6.74
36	67.083	111277	39.88	90	125.183	9065	3.25
37	67.149	2654	0.95	91	126.192	7272	2.61
38	68.091	141163	50.59	92	127.199	2522	0.90
39	68.156	3267	1.17	93	137.189	10478	3.76
40	69.063	1361	0.49	94	138.197	11171	4.00
41	69.099	126379	45.29	95	139.204	4115	1.47
42	69.146	799	0.29	96	140.215	5672	2.03
43	69.166	2375	0.85	97	151.211	5911	2.12
44	70.071	4618	1.65	98	152.218	9975	3.57
45	70.107	69103	24.76	99	153.225	2453	0.88
46	71.079	35622	12.77	100	154.236	4897	1.75
47	71.116	78494	28.13	101	165.232	2598	0.93
48	71.182	2086	0.75	102	166.240	3794	1.36
49	72.087	18330	6.57	103	180.262	12233	4.38
50	72.120	5513	1.98	104	181.266	1853	0.66
51	73.095	2726	0.98	105	182.279	15718	5.63
52	77.072	1911	0.68	106	183.282	2597	0.93

53	79.088	9712	3.48	107	198.280	2671	0.96
54	80.096	7754	2.78	108	208.306	7673	2.75

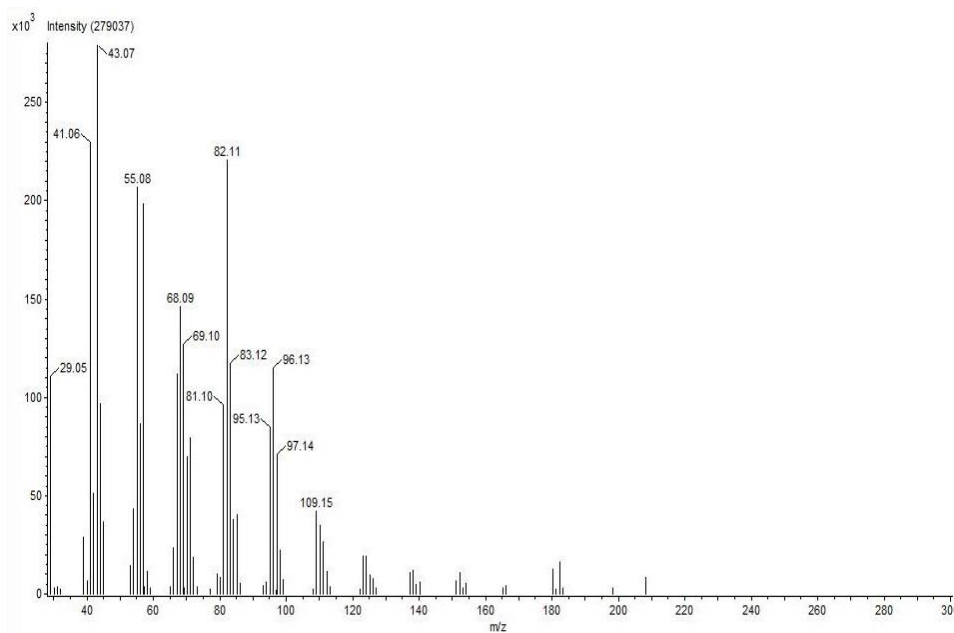


Figure 61. Mass-spectra of pentadecanal (Rt = 14.56) in F6 fraction from ethyl acetate extract of *C. militaris* detected by GC-MS.

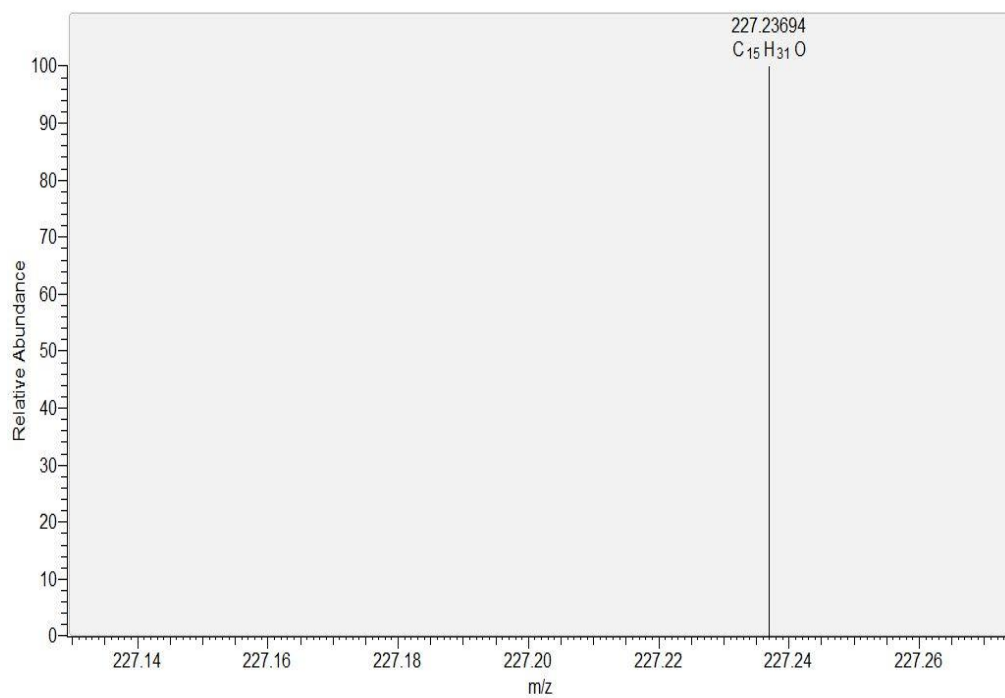
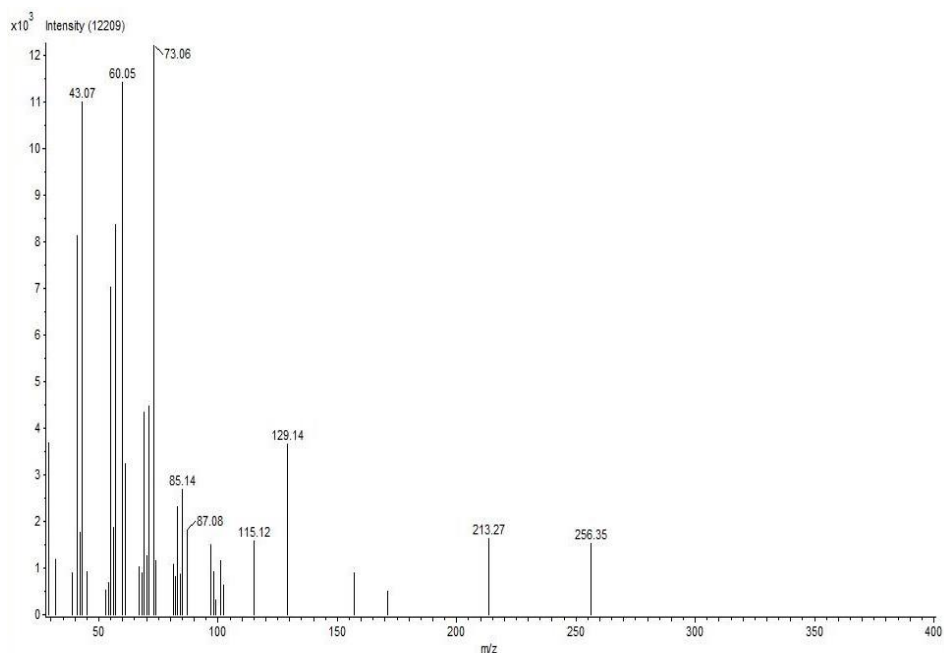


Figure 62. ESI-MS spectra of pentadecanal in F6 fraction from ethyl acetate extract of *C. militaris*.

Table 36. Fragmentation pattern of palmitic acid (retention time = 17.07) in F6 fraction from ethyl acetate extract of *C. militaris* detected by GC-MS

Peak#	m/z	Intensity	Relative Intensity (%)	Peak#	m/z	Intensity	Relative Intensity (%)
1	29.051	3662	30.00	25	81.104	1062	8.70
2	32.007	1166	9.55	26	82.111	778	6.37
3	39.040	865	7.09	27	83.082	344	2.82
4	41.057	8113	66.45	28	83.089	265	2.17
5	42.064	1726	14.14	29	83.120	2302	18.86
6	43.037	1263	10.35	30	84.091	848	6.94
7	43.073	10778	88.28	31	84.126	742	6.07
8	45.053	883	7.23	32	85.137	2478	20.29
9	53.062	499	4.09	33	87.080	1800	14.74
10	54.070	669	5.48	34	97.105	652	5.34
11	55.042	621	5.09	35	97.142	1479	12.12
12	55.078	6991	57.26	36	98.111	894	7.32
13	56.086	1839	15.07	37	99.154	273	2.23
14	57.094	8328	68.21	38	99.162	281	2.30
15	60.046	11215	91.86	39	101.102	1128	9.24
16	61.054	3210	26.29	40	102.109	593	4.86
17	67.083	995	8.15	41	115.123	1381	11.31
18	68.092	865	7.08	42	129.144	3455	28.30
19	69.099	4312	35.32	43	157.182	871	7.14
20	70.107	1237	10.13	44	171.204	335	2.75
21	71.115	4437	36.34	45	171.211	463	3.79
22	73.059	12209	100.00	46	213.272	1426	11.68
23	73.091	636	5.21	47	256.347	1307	10.71
24	74.065	1142	9.35				

**Figure 63.** Mass-spectra of palmitic acid (Rt = 17.07) in F6 fraction from ethyl acetate extract of *C. militaris* detected by GC-MS.

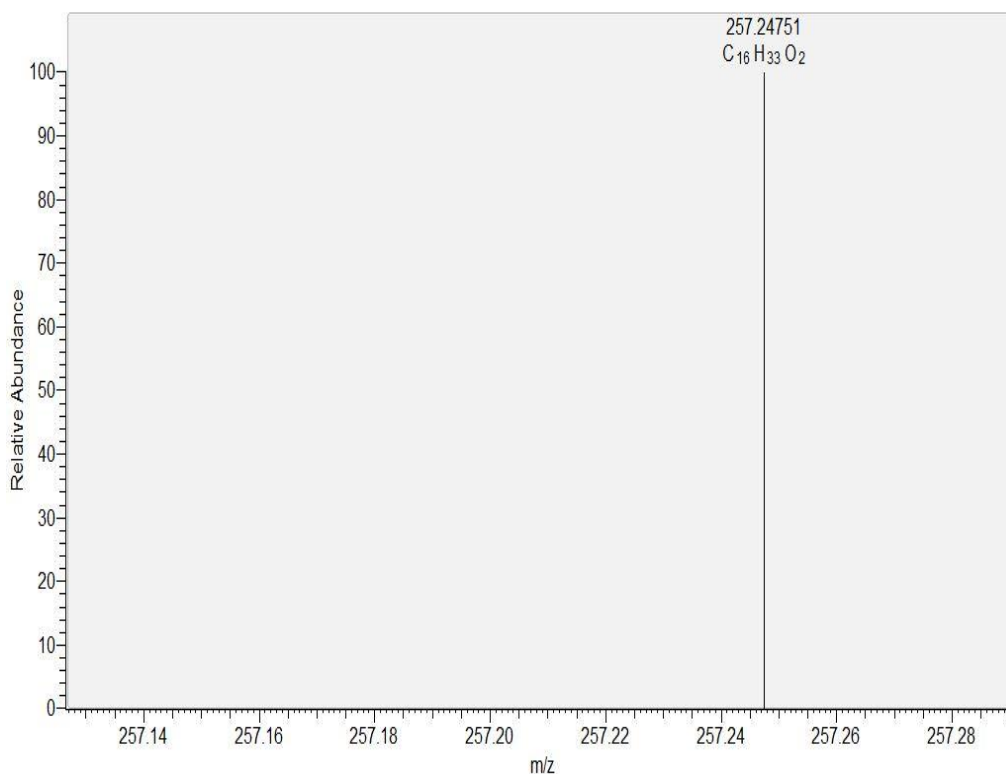


Figure 64. ESI-MS spectra of palmitic acid in F6 fraction from ethyl acetate extract of *C. militaris*.

Table 37. Fragmentation pattern of 1-heneicosanol (retention time = 26.33) in F6 fraction from ethyl acetate extract of *C. militaris* detected by GC-MS

Peak#	m/z	Intensity	Relative Intensity (%)	Peak#	m/z	Intensity	Relative Intensity (%)
1	29.052	1023	11.58	19	82.113	2952	33.42
2	31.031	663	7.50	20	83.122	6180	69.96
3	32.008	1015	11.49	21	84.129	1769	20.02
4	41.057	3227	36.53	22	85.138	2761	31.25
5	42.065	1248	14.13	23	95.125	625	7.07
6	43.074	7578	85.79	24	96.135	1484	16.81
7	54.071	745	8.43	25	97.143	5570	63.06
8	55.079	6555	74.20	26	98.150	1097	12.42
9	56.087	3165	35.83	27	99.158	565	6.39
10	57.095	8834	100.00	28	110.157	411	4.65
11	58.100	519	5.87	29	111.164	2461	27.86
12	67.083	1065	12.06	30	112.172	688	7.79
13	68.092	2330	26.38	31	125.185	1295	14.66
14	69.100	5968	67.56	32	139.204	552	6.25
15	70.108	2801	31.70	33	147.129	1349	15.27
16	71.117	4427	50.11	34	221.176	887	10.05
17	73.081	1606	18.18	35	281.164	701	7.93
18	81.107	1042	11.79				

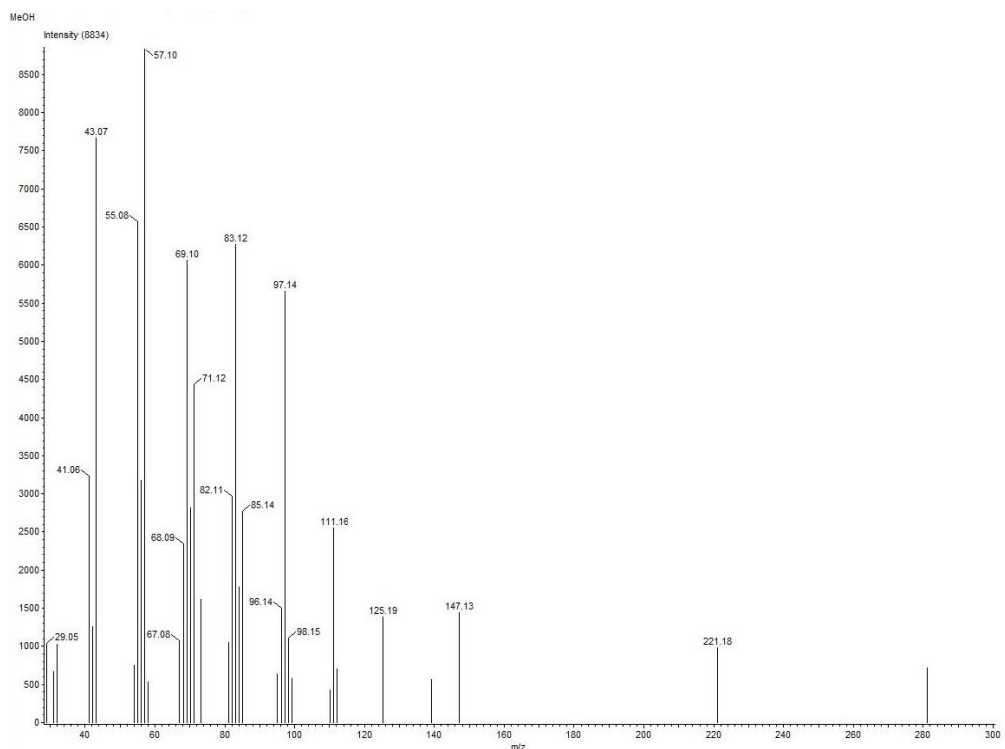


Figure 65. Mass-spectra of 1-heneicosanol (Rt = 26.33) in F6 fraction from ethyl acetate extract of *C. militaris* detected by GC-MS.

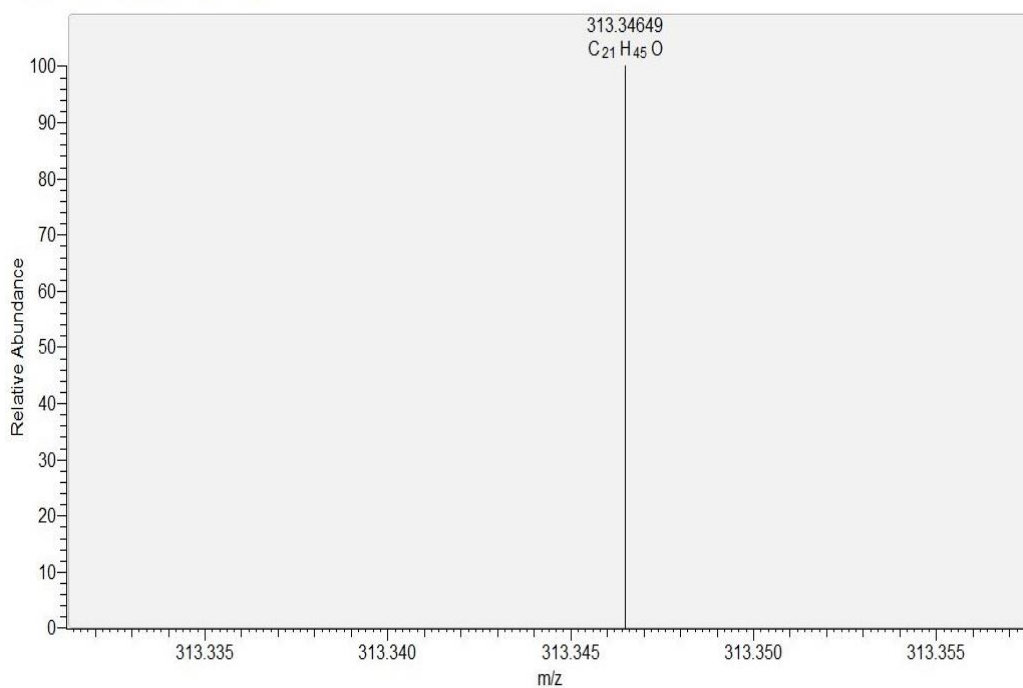


Figure 66. ESI-MS spectra of 1-heneicosanol in F6 fraction from ethyl acetate extract of *C. militaris*.

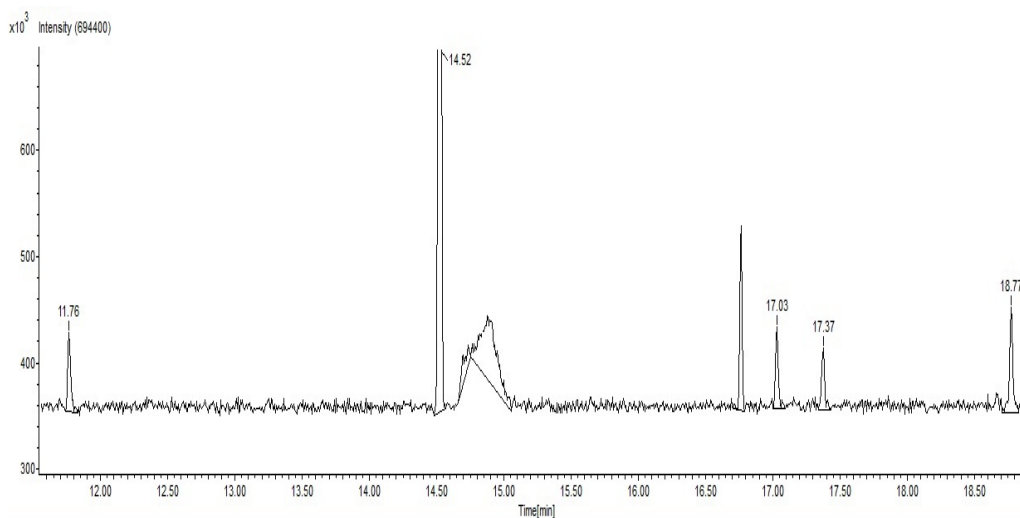


Figure 67. GC-MS chromatogram of F7 fraction from ethyl acetate extract of *C. militaris*.

Table 38. Fragmentation pattern of 1,6-anhydro- β -D-glucopyranose (retention time = 11.76) in F7 fraction from ethyl acetate extract of *C. militaris* detected by GC-MS

Peak#	m/z	Intensity	Relative Intensity (%)	Peak#	m/z	Intensity	Relative Intensity (%)
1	29.015	11992	19.85	28	59.037	768	1.27
2	29.051	3951	6.54	29	60.046	60411	100.00
3	30.023	1452	2.40	30	60.129	182	0.30
4	31.031	9578	15.86	31	60.148	425	0.70
5	32.038	383	0.63	32	60.156	233	0.39
6	39.040	2581	4.27	33	60.165	338	0.56
7	39.979	418	0.69	34	61.053	4130	6.84
8	40.048	391	0.65	35	62.052	355	0.59
9	41.056	3494	5.78	36	69.026	556	0.92
10	42.028	8197	13.57	37	69.063	4801	7.95
11	42.064	1559	2.58	38	70.071	8211	13.59
12	43.036	9748	16.14	39	71.043	4908	8.12
13	43.072	721	1.19	40	71.077	1120	1.85
14	44.044	6513	10.78	41	72.050	4315	7.14
15	45.018	406	0.67	42	73.059	20327	33.65
16	45.053	5150	8.52	43	74.067	3978	6.59
17	47.033	5327	8.82	44	81.067	666	1.10
18	53.062	811	1.34	45	85.064	893	1.48
19	54.033	587	0.97	46	87.081	780	1.29
20	55.042	7390	12.23	47	89.060	1964	3.25
21	56.049	10230	16.93	48	97.069	2959	4.90
22	57.058	26212	43.39	49	98.077	4022	6.66
23	57.083	214	0.35	50	99.084	1168	1.93
24	57.107	277	0.46	51	101.066	1272	2.11
25	57.118	493	0.82	52	102.073	1563	2.59
26	58.032	528	0.87	53	115.087	825	1.37
27	58.062	1082	1.79	54	144.100	708	1.17

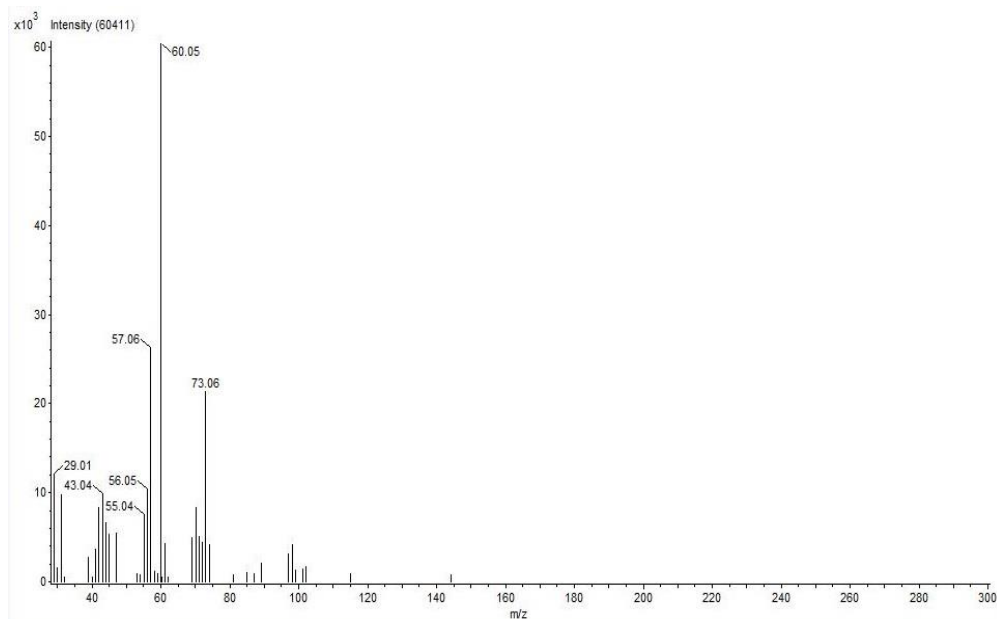


Figure 68. Mass-spectra of 1,6-anhydro- β -D-glucopyranose ($R_t = 11.76$) in F7 fraction from ethyl acetate extract of *C. militaris* detected by GC-MS.

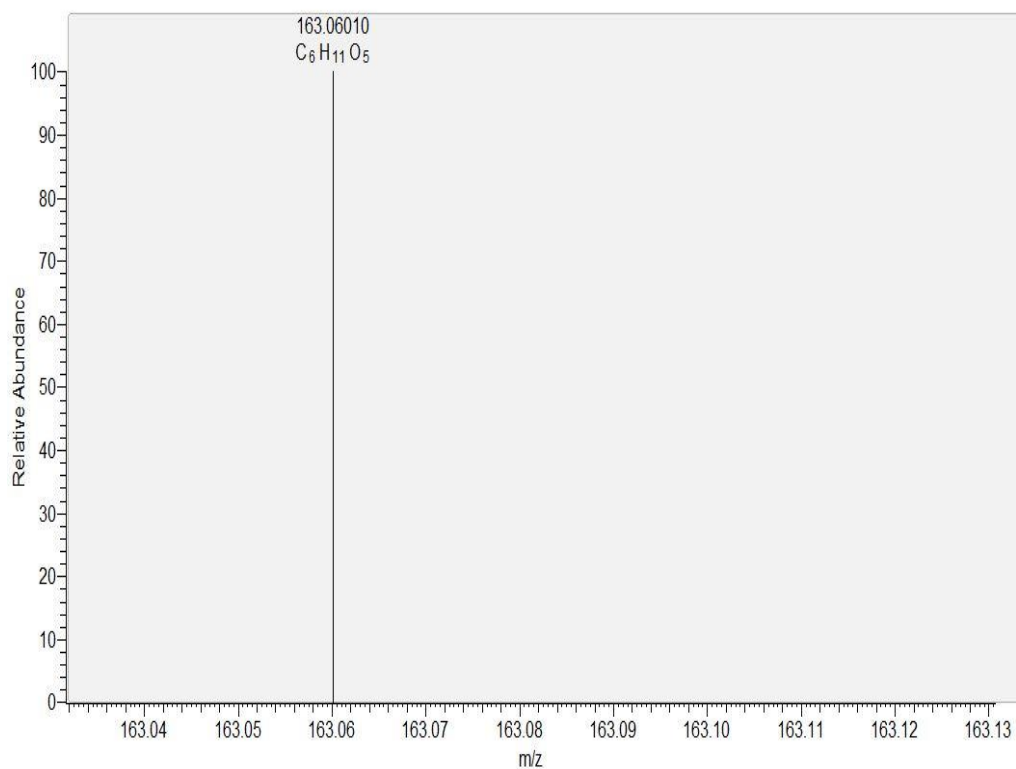


Figure 69. ESI-MS spectra of 1,6-anhydro- β -D-glucopyranose in F7 fraction from ethyl acetate extract of *C. militaris*.

Table 39. Fragmentation pattern of pentadecanal (retention time = 14.52) in F7 fraction from ethyl acetate extract of *C. militaris* detected by GC-MS

Peak#	m/z	Intensity	Relative Intensity (%)	Peak#	m/z	Intensity	Relative Intensity (%)
1	29.012	6408	4.61	49	77.064	976	0.70
2	29.049	60336	43.41	50	79.080	4670	3.36
3	29.068	559	0.40	51	80.088	3208	2.31
4	29.091	1241	0.89	52	81.096	39643	28.52
5	30.053	1628	1.17	53	82.104	80344	57.81
6	31.028	1785	1.28	54	82.146	204	0.15
7	39.036	15507	11.16	55	82.154	394	0.28
8	40.044	3510	2.53	56	82.177	1852	1.33
9	41.053	120357	86.60	57	83.076	1219	0.88
10	42.025	829	0.60	58	83.112	44659	32.13
11	42.060	25037	18.01	59	84.083	820	0.59
12	43.032	5103	3.67	60	84.120	14840	10.68
13	43.069	138979	100.00	61	85.092	4467	3.21
14	43.160	1668	1.20	62	85.129	15856	11.41
15	44.041	45499	32.74	63	86.099	1760	1.27
16	44.073	5067	3.65	64	86.132	937	0.67
17	44.093	560	0.40	65	93.100	2000	1.44
18	44.100	364	0.26	66	94.108	2188	1.57
19	45.049	16913	12.17	67	95.116	33492	24.10
20	53.057	7385	5.31	68	96.124	43506	31.30
21	54.065	19282	13.87	69	97.132	26822	19.30
22	55.037	2156	1.55	70	98.106	639	0.46
23	55.073	93852	67.53	71	98.139	7996	5.75
24	55.114	550	0.40	72	99.112	2634	1.90
25	55.132	1861	1.34	73	99.147	2541	1.83
26	56.080	37300	26.84	74	109.136	14099	10.14
27	57.053	48389	34.82	75	110.144	12642	9.10
28	57.089	84680	60.93	76	111.151	9640	6.94
29	58.059	4972	3.58	77	112.160	4431	3.19
30	58.093	3762	2.71	78	113.167	1195	0.86
31	59.068	940	0.68	79	123.155	6834	4.92
32	65.060	1704	1.23	80	124.164	7105	5.11
33	66.068	9064	6.52	81	125.171	3552	2.56
34	67.076	48468	34.87	82	126.180	2486	1.79
35	68.084	56863	40.91	83	137.175	3848	2.77
36	68.114	770	0.55	84	138.183	4460	3.21
37	68.150	1330	0.96	85	139.191	1639	1.18
38	69.057	771	0.56	86	140.199	2291	1.65
39	69.092	53759	38.68	87	151.195	2074	1.49
40	69.122	404	0.29	88	152.203	4521	3.25
41	69.156	1505	1.08	89	153.210	1200	0.86
42	70.065	2081	1.50	90	154.220	1617	1.16
43	70.100	28547	20.54	91	165.215	1003	0.72
44	71.072	14527	10.45	92	166.223	1578	1.14
45	71.109	31218	22.46	93	180.243	4641	3.34
46	72.080	6690	4.81	94	182.259	5911	4.25
47	72.112	1678	1.21	95	183.263	1064	0.77
48	73.088	1085	0.78	96	208.282	2871	2.07

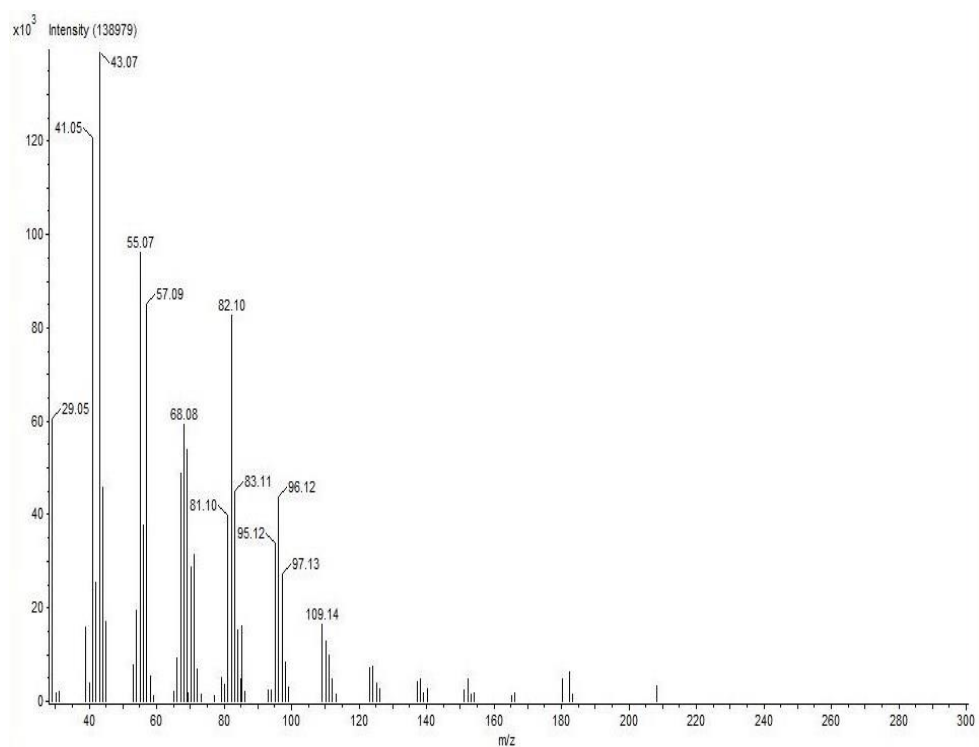


Figure 70. Mass-spectra of pentadecanal (Rt = 14.52) in F7 fraction from ethyl acetate extract of *C. militaris* detected by GC-MS.

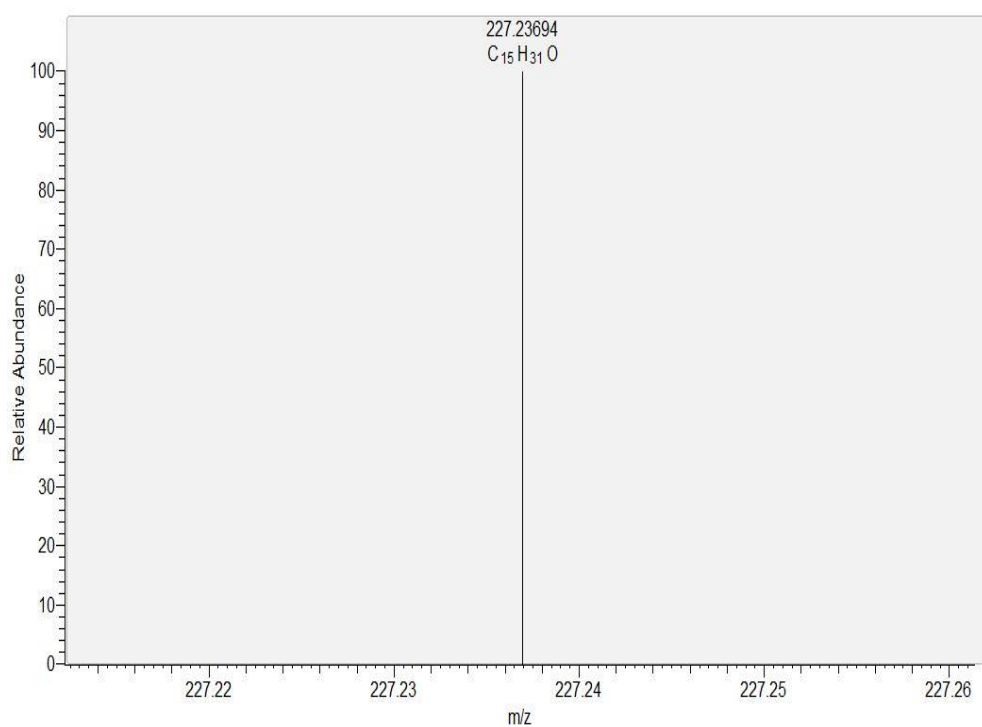
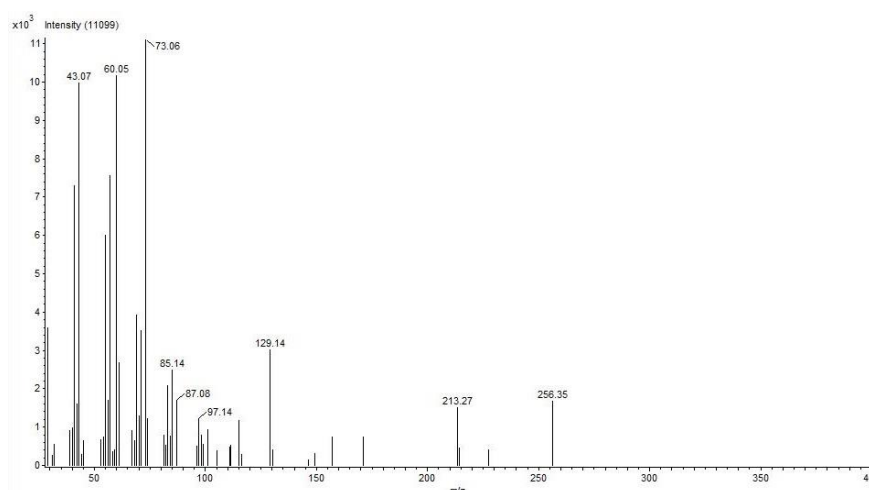


Figure 71. ESI-MS spectra of pentadecanal in F6 fraction from ethyl acetate extract of *C. militaris*.

Table 40. Fragmentation pattern of palmitic acid (retention time = 17.03) in F7 fraction from ethyl acetate extract of *C. militaris* detected by GC-MS

Peak#	m/z	Intensity	Relative Intensity (%)	Peak#	m/z	Intensity	Relative Intensity (%)
1	29.015	578	5.21	32	81.104	776	6.99
2	29.051	3564	32.11	33	82.112	514	4.63
3	31.034	239	2.15	34	83.085	587	5.29
4	32.008	516	4.65	35	83.120	2047	18.44
5	39.040	874	7.88	36	84.091	734	6.62
6	39.978	951	8.57	37	84.127	574	5.17
7	41.057	7282	65.61	38	85.136	2290	20.63
8	42.064	1575	14.19	39	87.081	1664	14.99
9	43.036	1153	10.39	40	96.133	485	4.37
10	43.073	9785	88.16	41	97.103	805	7.25
11	44.077	262	2.36	42	97.142	1198	10.79
12	45.017	319	2.87	43	98.112	758	6.83
13	45.053	629	5.66	44	98.152	417	3.75
14	53.063	638	5.75	45	99.158	522	4.70
15	54.070	728	6.56	46	101.102	908	8.18
16	55.042	620	5.59	47	105.114	360	3.25
17	55.078	5981	53.88	48	111.126	457	4.12
18	56.086	1675	15.09	49	111.166	503	4.53
19	57.094	7546	67.99	50	115.122	1138	10.25
20	58.099	338	3.04	51	115.138	179	1.62
21	59.076	391	3.52	52	116.128	253	2.28
22	60.046	9965	89.78	53	129.144	2826	25.46
23	61.055	2648	23.86	54	130.149	394	3.55
24	67.083	892	8.04	55	146.294	123	1.11
25	68.091	633	5.71	56	149.091	286	2.58
26	69.099	3902	35.16	57	157.187	727	6.55
27	70.107	1257	11.32	58	171.209	721	6.49
28	71.115	3497	31.50	59	213.274	1308	11.79
29	73.059	11099	100.00	60	214.289	438	3.95
30	73.094	658	5.93	61	227.286	377	3.39
31	74.066	1186	10.68	62	256.349	1483	13.36

**Figure 72.** Mass-spectra of palmitic acid (Rt = 17.03) in F7 fraction from ethyl acetate extract of *C. militaris* detected by GC-MS.

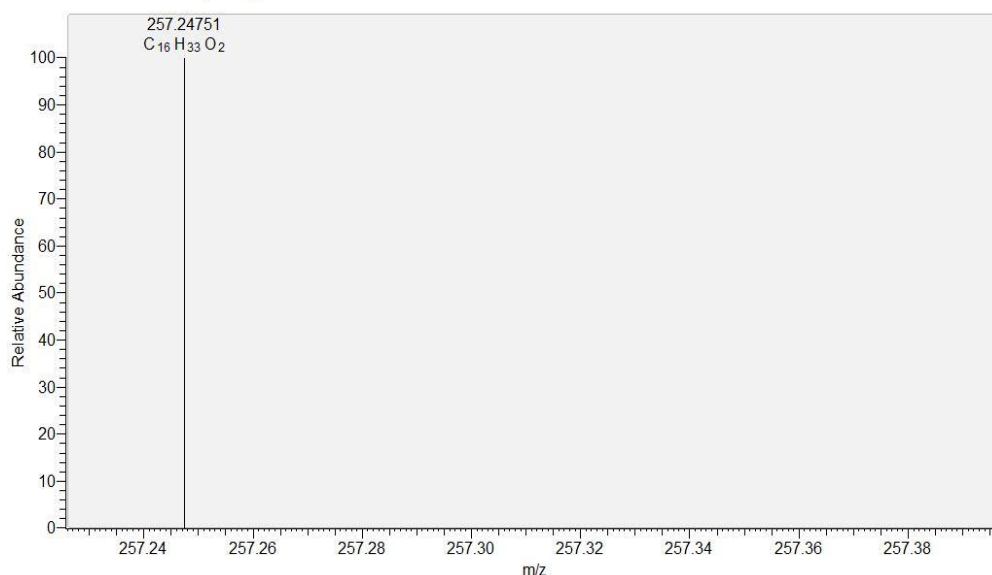


Figure 73. ESI-MS spectra of palmitic acid in F7 fraction from ethyl acetate extract of *C. militaris*.

Table 41. Fragmentation pattern of 2-oxopalmitic acid methyl ester (retention time = 17.40) in F9 fraction from ethyl acetate extract of *C. militaris* detected by GC-MS

Peak#	m/z	Intensity	Relative Intensity (%)	Peak#	m/z	Intensity	Relative Intensity (%)
1	29.049	6091	27.17	29	71.109	11288	50.36
2	31.029	3761	16.78	30	72.112	754	3.36
3	39.037	1472	6.57	31	74.060	1297	5.78
4	41.053	13198	58.88	32	75.067	743	3.31
5	42.024	366	1.63	33	79.076	216	0.96
6	42.060	3140	14.01	34	79.082	251	1.12
7	43.032	1310	5.85	35	81.096	2709	12.09
8	43.069	22415	100.00	36	82.103	906	4.04
9	44.008	385	1.72	37	83.075	620	2.77
10	44.071	950	4.24	38	83.113	2770	12.36
11	45.049	659	2.94	39	84.084	469	2.09
12	53.058	926	4.13	40	84.120	330	1.47
13	54.065	756	3.37	41	85.129	6251	27.89
14	55.037	1318	5.88	42	86.133	494	2.20
15	55.073	10236	45.67	43	87.073	746	3.33
16	56.042	424	1.89	44	93.095	189	0.85
17	56.050	218	0.97	45	93.102	320	1.43
18	56.080	2435	10.86	46	95.116	3314	14.79
19	57.089	21641	96.55	47	97.098	671	2.99
20	58.060	1138	5.08	48	97.132	1374	6.13
21	58.093	1134	5.06	49	98.104	672	3.00
22	59.069	623	2.78	50	99.148	632	2.82
23	67.076	2282	10.18	51	109.135	1511	6.74
24	68.084	998	4.45	52	111.151	441	1.97
25	69.092	5315	23.71	53	123.156	854	3.81
26	70.064	404	1.80	54	225.291	14642	65.32
27	70.099	929	4.14	55	226.294	2470	11.02
28	71.071	955	4.26				

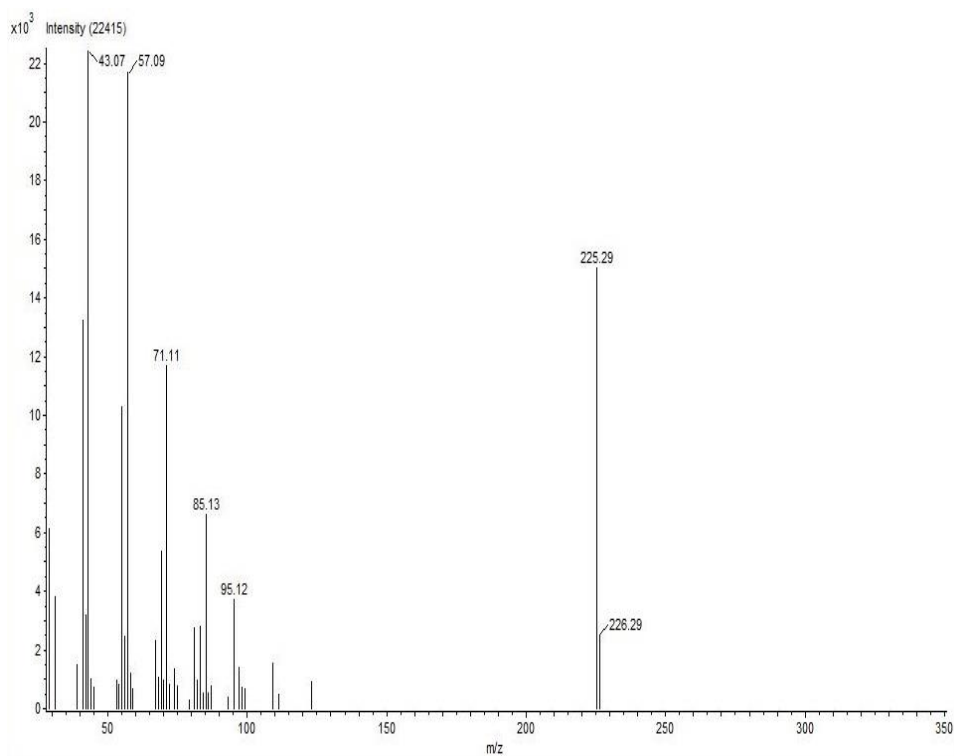


Figure 74. Mass-spectra of 2-oxopalmitic acid methyl ester (Rt = 17.40) in F9 fraction from ethyl acetate extract of *C. militaris* detected by GC-MS.

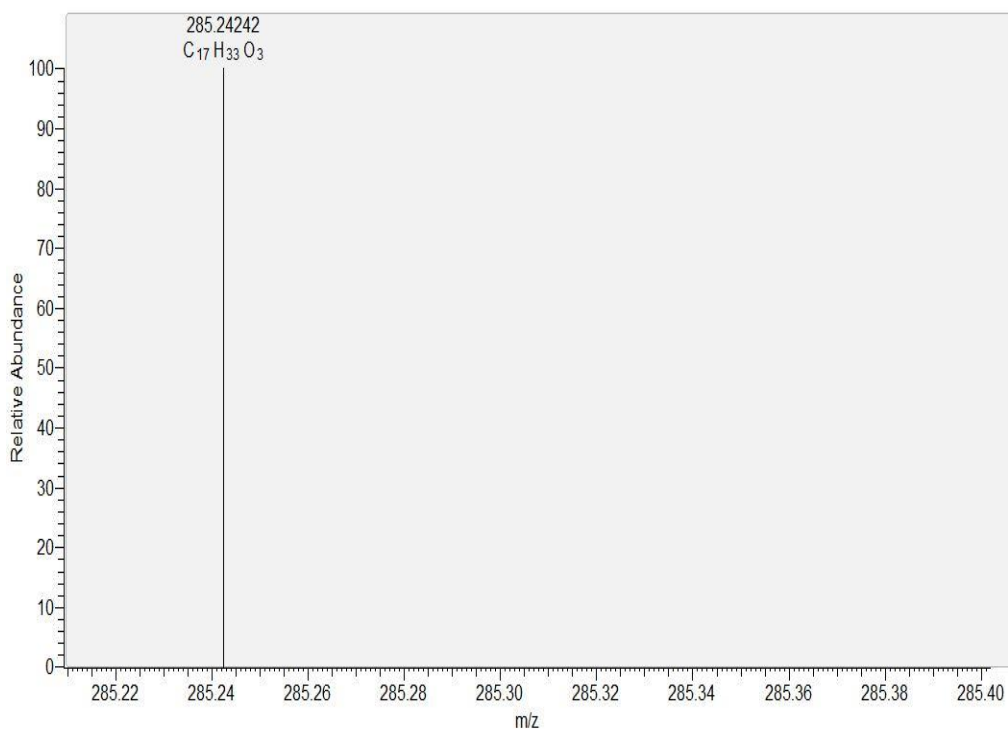


Figure 75. ESI-MS spectra of 2-oxopalmitic acid methyl ester in F9 fraction from ethyl acetate extract of *C. militaris*.

Table 42. Fragmentation pattern of Octanamide, N-(2-hydroxyethyl) (retention time = 18.77) in F7 fraction from ethyl acetate extract of *C. militaris* detected by GC-MS

Peak#	m/z	Intensity	Relative Intensity (%)	Peak#	m/z	Intensity	Relative Intensity (%)
1	29.049	1779	5.52	27	85.079	32226	100.00
2	31.994	423	1.31	28	85.125	422	1.31
3	39.036	472	1.46	29	85.132	246	0.76
4	39.970	392	1.22	30	85.158	490	1.52
5	41.052	4884	15.15	31	85.169	221	0.68
6	42.053	1299	4.03	32	86.084	2336	7.25
7	43.069	4724	14.66	33	90.780	114	0.35
8	44.002	318	0.99	34	96.113	290	0.90
9	44.064	2010	6.24	35	98.091	12817	39.77
10	45.049	223	0.69	36	98.131	82	0.25
11	53.056	313	0.97	37	99.098	2339	7.26
12	54.053	478	1.48	38	112.110	1987	6.17
13	54.066	178	0.55	39	126.129	689	2.14
14	55.036	452	1.40	40	140.151	2185	6.78
15	55.073	3549	11.01	41	141.152	366	1.13
16	56.073	990	3.07	42	154.170	1112	3.45
17	57.089	1873	5.81	43	168.189	639	1.98
18	67.073	652	2.02	44	182.214	513	1.59
19	68.066	104	0.32	45	196.228	254	0.79
20	68.074	543	1.69	46	196.240	291	0.90
21	69.092	1320	4.10	47	210.257	489	1.52
22	70.094	142	0.44	48	213.022	98	0.31
23	70.098	188	0.58	49	238.292	744	2.31
24	71.104	229	0.71	50	252.307	224	0.70
25	82.092	440	1.37	51	252.320	235	0.73
26	83.111	591	1.83				

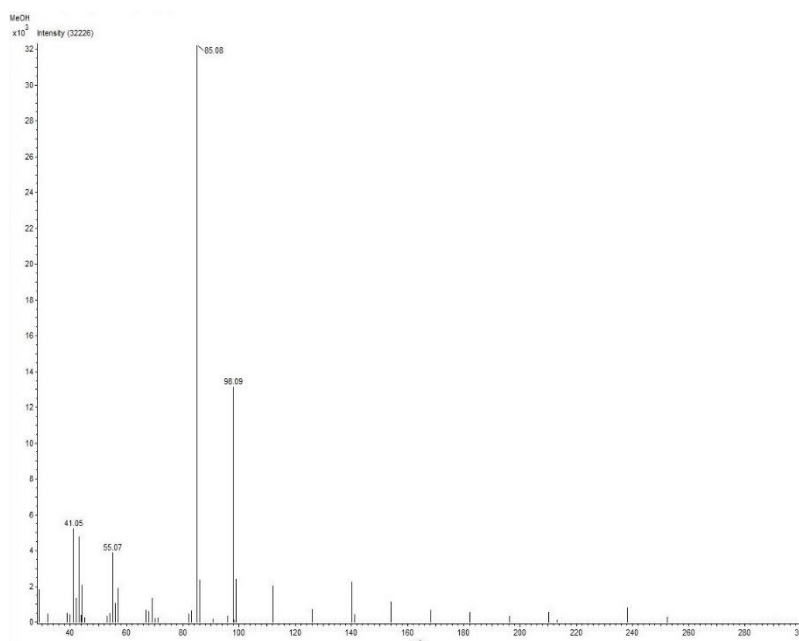


Figure 76. Mass-spectra of Octanamide, N-(2-hydroxyethyl) (Rt = 18.77) in F7 fraction from ethyl acetate extract of *C. militaris* detected by GC-MS.

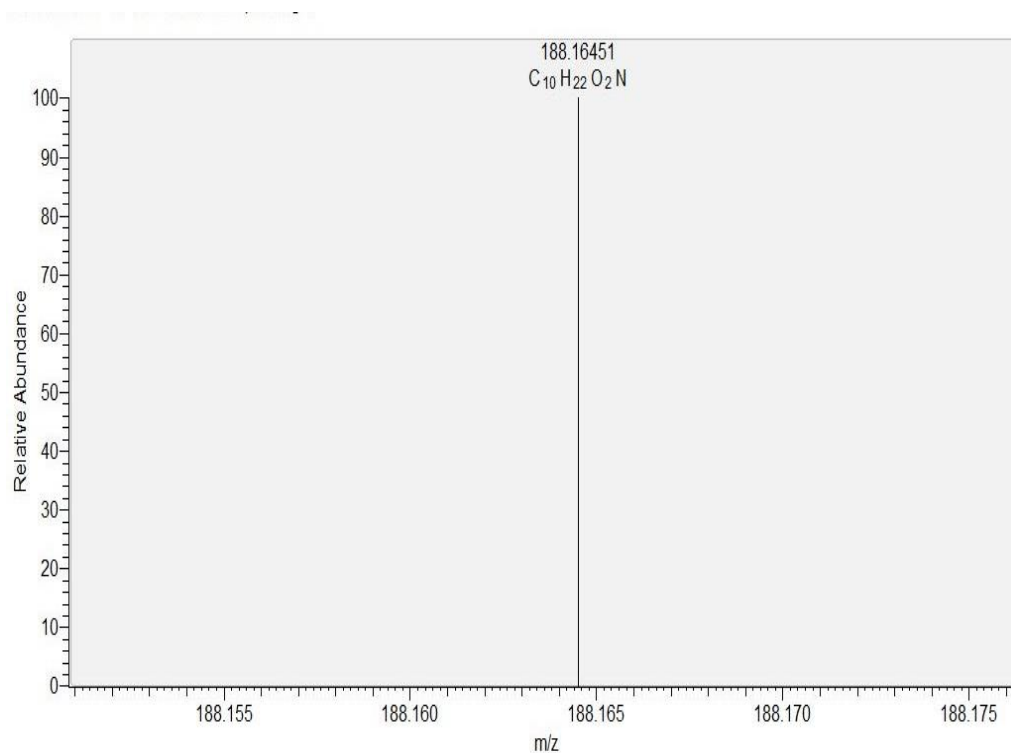


Figure 77. ESI-MS spectra of Octanamide, N-(2-hydroxyethyl) in F7 fraction from ethyl acetate extract of *C. militaris*.

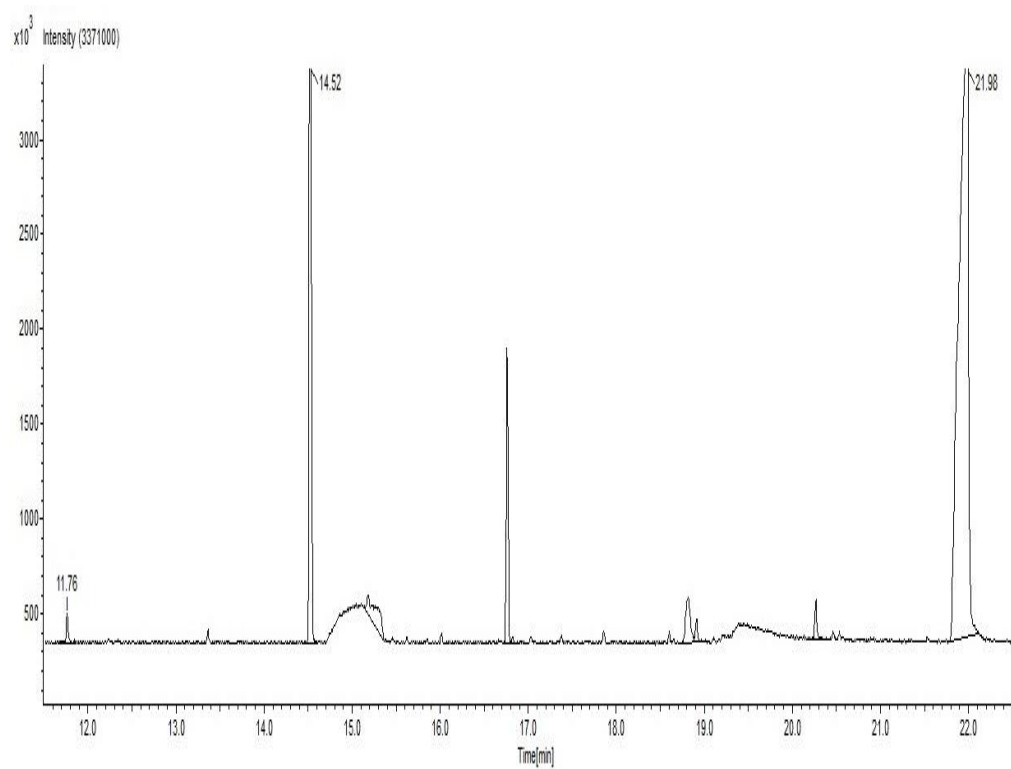


Figure 78. GC-MS chromatogram of F8 fraction from ethyl acetate extract of *C. militaris*.

Table 43. Fragmentation pattern of 1,6-anhydro- β -D-glucopyranose (retention time = 11.76) in F8 fraction from ethyl acetate extract of *C. militaris* detected by GC-MS

Peak#	m/z	Intensity	Relative Intensity (%)	Peak#	m/z	Intensity	Relative Intensity (%)
1	29.012	2748	22.10	13	56.045	2160	17.37
2	29.049	1101	8.85	14	57.053	5111	41.10
3	31.029	2569	20.65	15	60.041	12436	100.00
4	31.997	1212	9.74	16	61.047	883	7.10
5	39.037	1142	9.18	17	69.057	1275	10.25
6	41.052	917	7.38	18	70.065	1568	12.61
7	42.025	1958	15.75	19	71.036	1310	10.53
8	43.033	2622	21.08	20	72.045	646	5.19
9	44.041	1630	13.11	21	73.053	3819	30.71
10	45.049	1480	11.90	22	74.061	882	7.09
11	47.029	1312	10.55	23	98.067	688	5.54
12	55.037	1605	12.91				

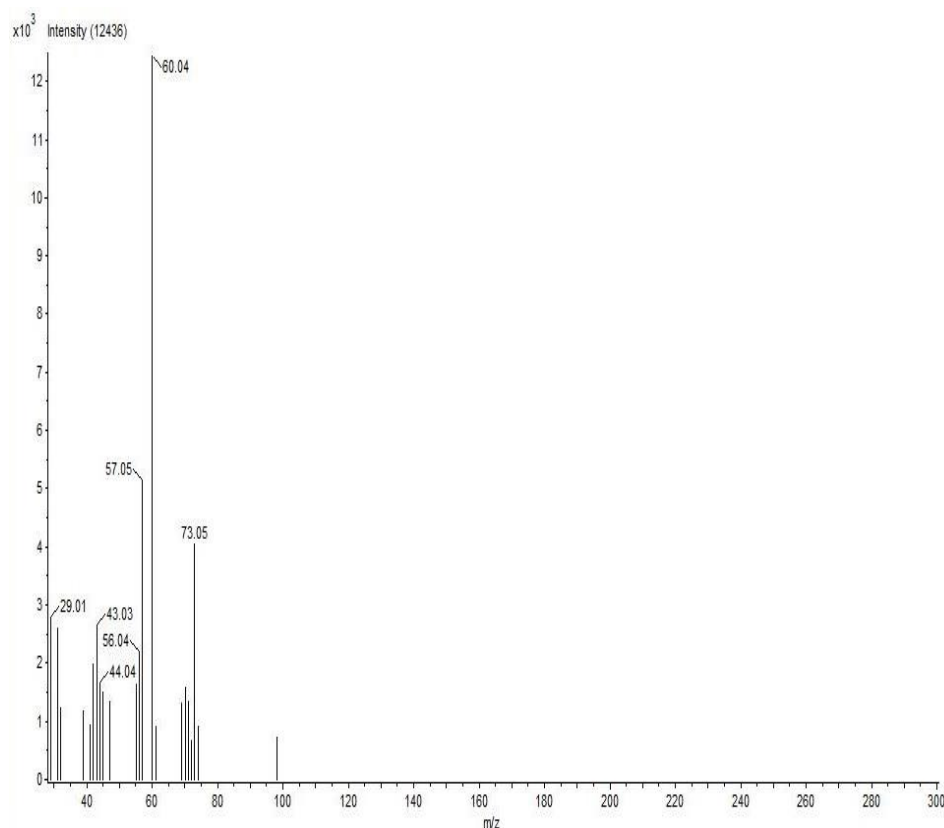


Figure 79. Mass-spectra of 1,6-anhydro- β -D-glucopyranose (Rt = 11.76) in F8 fraction from ethyl acetate extract of *C. militaris* detected by GC-MS.

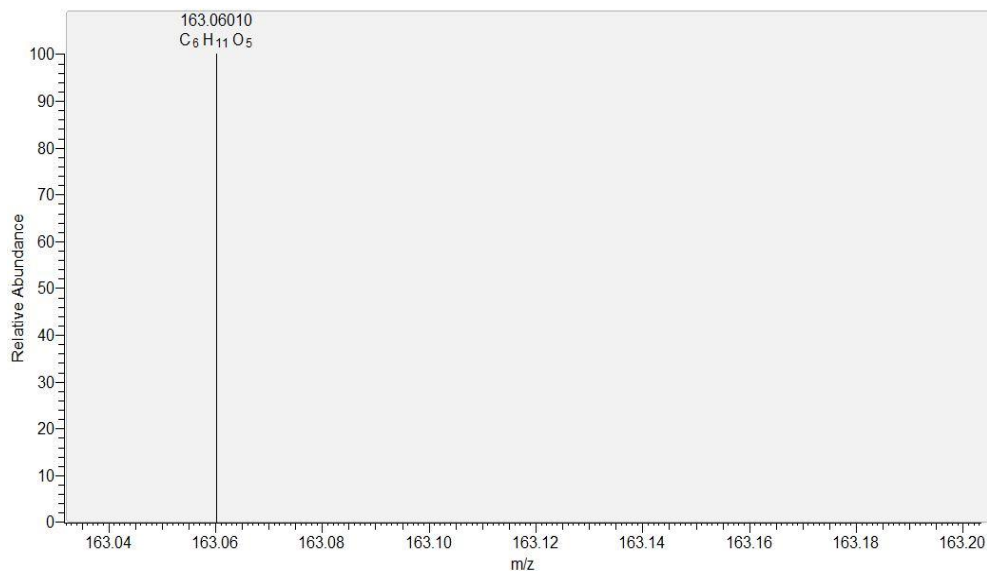


Figure 80. ESI-MS spectra of 1,6-anhydro- β -D-glucopyranose in F8 fraction from ethyl acetate extract of *C. militaris*.

Table 44. Fragmentation pattern of pentadecanal (retention time = 14.52) in F8 fraction from ethyl acetate extract of *C. militaris* detected by GC-MS

Peak#	m/z	Intensity	Relative Intensity (%)	Peak#	m/z	Intensity	Relative Intensity (%)
1	29.012	10019	4.13	63	81.097	67287	27.73
2	29.049	102051	42.06	64	81.137	214	0.09
3	29.092	2541	1.05	65	81.169	1349	0.56
4	30.053	2608	1.07	66	82.105	142015	58.53
5	31.029	2746	1.13	67	82.228	1951	0.80
6	31.998	1946	0.80	68	83.077	2111	0.87
7	39.037	25856	10.66	69	83.113	75585	31.15
8	40.044	5446	2.24	70	83.163	592	0.24
9	41.053	204843	84.43	71	83.186	1494	0.62
10	41.328	78	0.03	72	84.085	1391	0.57
11	41.368	257	0.11	73	84.120	25115	10.35
12	42.025	1381	0.57	74	85.093	7514	3.10
13	42.061	41790	17.22	75	85.129	26846	11.06
14	42.116	853	0.35	76	86.100	3257	1.34
15	43.033	8711	3.59	77	86.133	1727	0.71
16	43.069	242628	100.00	78	91.083	781	0.32
17	43.363	514	0.21	79	93.100	2429	1.00
18	43.370	725	0.30	80	94.108	3817	1.57
19	43.393	774	0.32	81	95.117	56223	23.17
20	44.041	76259	31.43	82	95.197	1165	0.48
21	44.073	8560	3.53	83	96.124	72554	29.90
22	44.133	83	0.03	84	96.172	293	0.12
23	45.049	28575	11.78	85	96.203	1446	0.60
24	46.052	817	0.34	86	97.096	867	0.36
25	51.041	895	0.37	87	97.132	45410	18.72
26	53.057	12138	5.00	88	98.104	1142	0.47
27	54.065	33174	13.67	89	98.140	13548	5.58
28	55.037	3924	1.62	90	99.113	4459	1.84
29	55.073	158228	65.21	91	99.148	3864	1.59

30	55.173	1223	0.50	92	100.119	923	0.38
31	55.187	593	0.24	93	108.128	1241	0.51
32	56.043	647	0.27	94	109.137	23587	9.72
33	56.081	63350	26.11	95	110.144	21427	8.83
34	56.108	313	0.13	96	111.152	16144	6.65
35	56.141	640	0.26	97	112.160	7498	3.09
36	57.053	81099	33.43	98	113.133	1143	0.47
37	57.089	142478	58.72	99	113.168	2031	0.84
38	58.060	8503	3.50	100	122.148	1098	0.45
39	58.093	6444	2.66	101	123.157	11725	4.83
40	59.068	1758	0.72	102	124.164	11819	4.87
41	65.061	2266	0.93	103	125.172	5863	2.42
42	66.069	15360	6.33	104	126.180	4490	1.85
43	67.077	82548	34.02	105	127.187	1421	0.59
44	67.121	516	0.21	106	137.176	7016	2.89
45	67.142	1655	0.68	107	138.184	7459	3.07
46	68.085	97800	40.31	108	139.192	2406	0.99
47	69.057	798	0.33	109	140.200	3841	1.58
48	69.093	90228	37.19	110	141.208	725	0.30
49	69.159	1064	0.44	111	151.196	3324	1.37
50	70.065	3587	1.48	112	152.204	6395	2.64
51	70.101	48046	19.80	113	153.211	1938	0.80
52	70.169	840	0.35	114	154.221	2952	1.22
53	71.073	24919	10.27	115	165.216	1702	0.70
54	71.109	54236	22.35	116	166.224	2553	1.05
55	71.157	356	0.15	117	179.235	1168	0.48
56	71.178	1263	0.52	118	180.244	7714	3.18
57	72.081	11831	4.88	119	181.250	1148	0.47
58	72.113	2898	1.19	120	182.260	10218	4.21
59	73.088	1857	0.77	121	183.263	1983	0.82
60	77.065	1633	0.67	122	198.260	1623	0.67
61	79.081	7358	3.03	123	208.283	4552	1.88
62	80.088	5884	2.43				

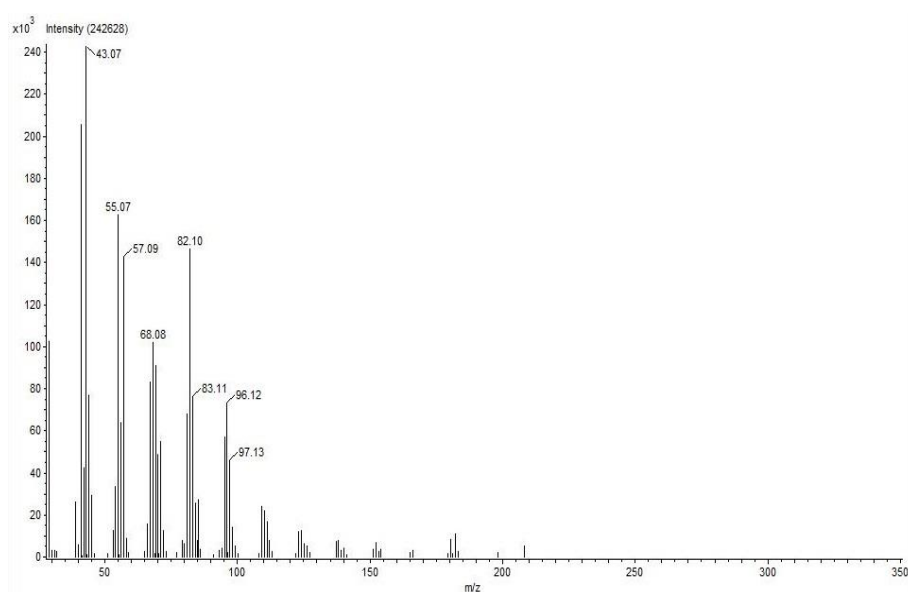


Figure 81. Mass-spectra of pentadecanal ($R_t = 14.52$) in F8 fraction from ethyl acetate extract of *C. militaris* detected by GC-MS.

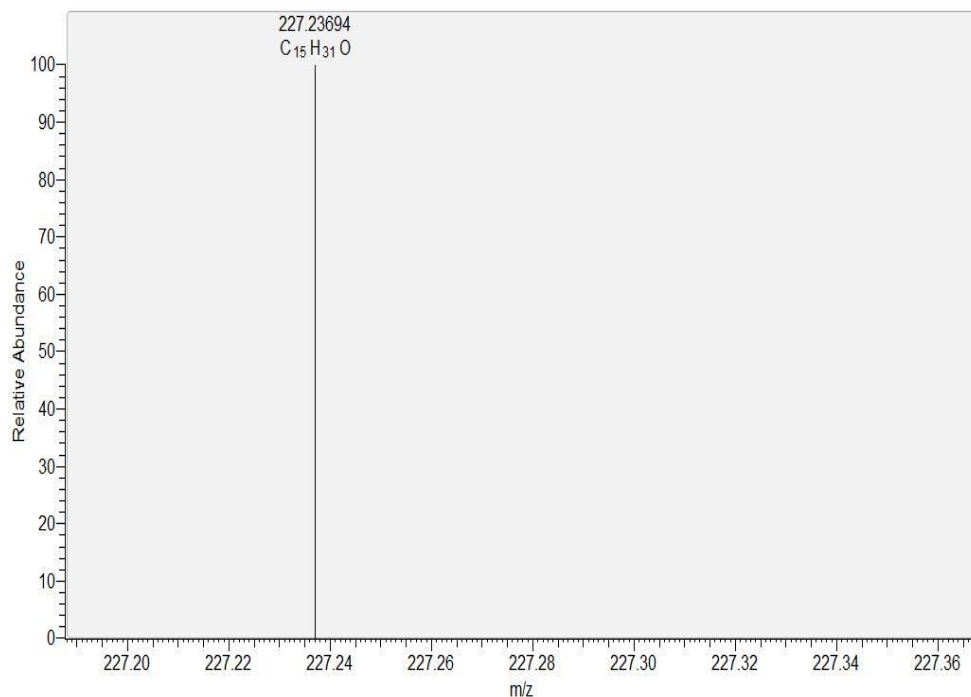


Figure 82. ESI-MS spectra of pentadecanal in F8 fraction from ethyl acetate extract of *C. militaris*.

Table 45. Fragmentation pattern of cordycepin (retention time = 21.98) in F8 fraction from ethyl acetate extract of *C. militaris* detected by GC-MS

Peak#	m/z	Intensity	Relative Intensity (%)	Peak#	m/z	Intensity	Relative Intensity (%)
1	29.012	20499	7.15	49	93.064	4897	1.71
2	29.036	5285	1.84	50	94.071	7414	2.59
3	29.049	9391	3.28	51	95.079	3396	1.18
4	30.020	1521	0.53	52	99.076	7526	2.62
5	30.044	5603	1.95	53	107.071	2870	1.00
6	31.029	37061	12.92	54	108.078	94206	32.85
7	38.016	1889	0.66	55	108.162	2065	0.72
8	39.037	15378	5.36	56	109.084	11798	4.11
9	40.032	12042	4.20	57	116.084	1639	0.57
10	41.053	39661	13.83	58	117.093	1248	0.44
11	42.025	2802	0.98	59	119.074	22947	8.00
12	42.061	16203	5.65	60	120.081	3718	1.30
13	43.034	25759	8.98	61	121.090	4478	1.56
14	43.069	15459	5.39	62	122.097	1260	0.44
15	44.041	8214	2.86	63	133.095	1227	0.43
16	45.050	6819	2.38	64	134.092	5250	1.83
17	47.029	3803	1.33	65	135.097	286745	100.00
18	51.033	1773	0.62	66	136.105	130251	45.42
19	52.036	3740	1.30	67	137.107	9171	3.20
20	53.032	9243	3.22	68	145.098	1459	0.51
21	53.057	14171	4.94	69	147.113	1932	0.67
22	54.040	22577	7.87	70	148.110	26161	9.12
23	55.046	17008	5.93	71	149.116	7042	2.46

24	55.073	623	0.22	72	161.120	1521	0.53
25	56.055	4650	1.62	73	162.129	4818	1.68
26	57.053	41327	14.41	74	163.102	2368	0.83
27	58.059	2701	0.94	75	164.109	152326	53.12
28	59.069	1118	0.39	76	164.294	1071	0.37
29	60.041	2179	0.76	77	165.112	12593	4.39
30	61.049	997	0.35	78	173.125	3196	1.11
31	65.036	6922	2.41	79	174.133	5882	2.05
32	66.044	25084	8.75	80	175.140	9068	3.16
33	67.052	21058	7.34	81	176.147	3555	1.24
34	68.058	8147	2.84	82	177.121	1884	0.66
35	69.057	35222	12.28	83	178.129	35404	12.35
36	69.092	1101	0.38	84	179.131	3675	1.28
37	70.063	9807	3.42	85	192.149	5705	1.99
38	71.037	1897	0.66	86	193.154	2290	0.80
39	71.073	14239	4.97	87	202.136	9167	3.20
40	73.053	6530	2.28	88	203.143	5183	1.81
41	77.039	1654	0.58	89	204.151	2599	0.91
42	79.055	2584	0.90	90	215.148	4163	1.45
43	80.052	6090	2.12	91	216.154	2010	0.70
44	81.060	21147	7.37	92	220.152	6124	2.14
45	82.067	5780	2.02	93	221.160	16543	5.77
46	85.057	1805	0.63	94	222.163	2043	0.71
47	91.048	1258	0.44	95	234.172	1803	0.63
48	92.055	8573	2.99	96	251.180	3630	1.27

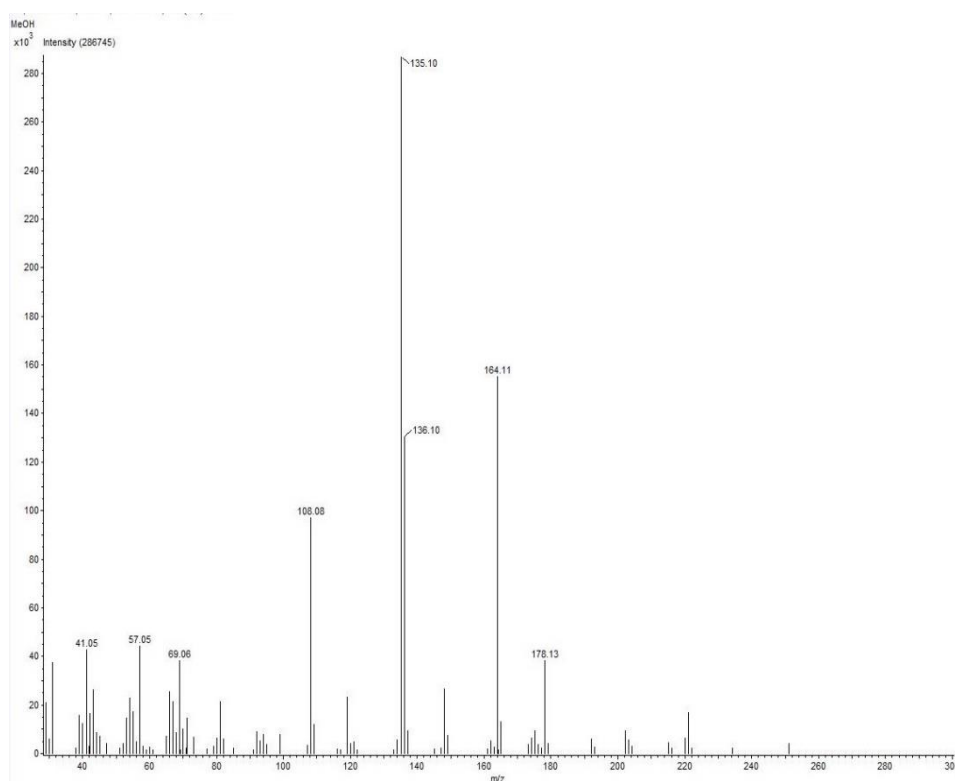


Figure 83. Mass-spectra of cordycepin ($R_t = 21.98$) in F8 fraction from ethyl acetate extract of *C. militaris* detected by GC-MS.

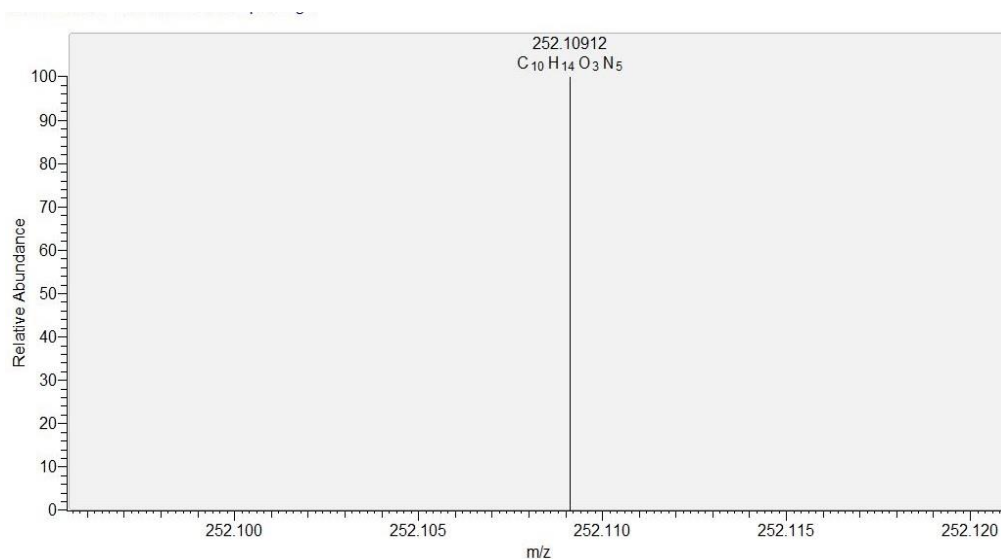


Figure 84. ESI-MS spectra of cordycepin in F8 fraction from ethyl acetate extract of *C. militaris*.

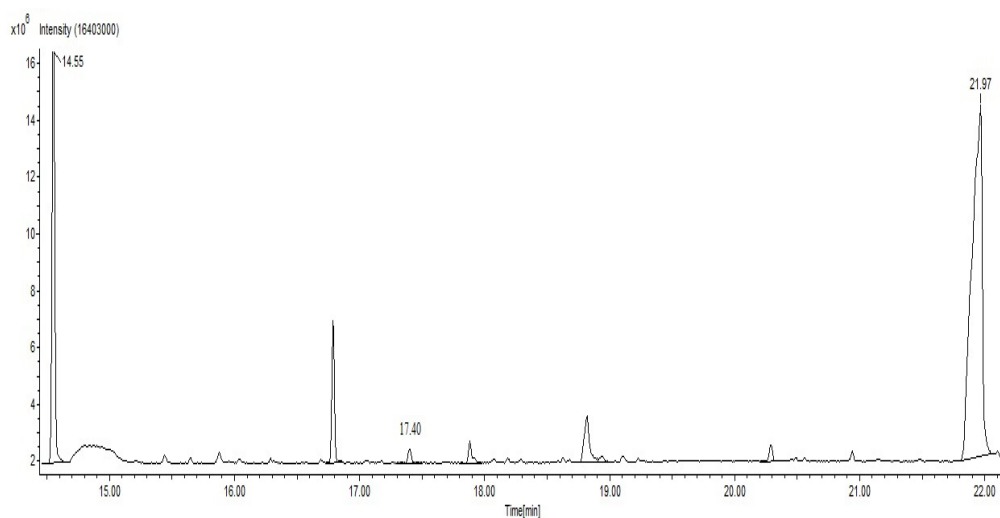


Figure 85. GC-MS chromatogram of F9 fraction from ethyl acetate extract of *C. militaris*.

Table 46. Fragmentation pattern of pentadecanal (retention time = 14.55) in F9 fraction from ethyl acetate extract of *C. militaris* detected by GC-MS

Peak#	m/z	Intensity	Relative Intensity (%)	Peak#	m/z	Intensity	Relative Intensity (%)
1	29.013	11824	4.33	65	77.064	1947	0.71
2	29.049	115544	42.27	66	79.081	8513	3.11
3	29.118	35	0.01	67	80.089	6470	2.37
4	29.125	43	0.02	68	81.097	75699	27.70
5	30.053	2902	1.06	69	81.169	1615	0.59
6	31.029	3324	1.22	70	82.105	155514	56.90
7	39.037	28612	10.47	71	83.077	2681	0.98
8	40.044	6219	2.28	72	83.113	86190	31.53
9	41.053	239366	87.58	73	83.211	352	0.13

10	41.336	1525	0.56	74	83.228	666	0.24
11	41.346	195	0.07	75	83.243	907	0.33
12	41.352	511	0.19	76	84.084	1377	0.50
13	41.370	742	0.27	77	84.121	28025	10.25
14	42.025	1472	0.54	78	85.093	8378	3.07
15	42.061	47468	17.37	79	85.129	29924	10.95
16	42.084	357	0.13	80	86.101	3568	1.31
17	42.114	799	0.29	81	86.133	1963	0.72
18	43.033	9991	3.66	82	91.085	1053	0.39
19	43.069	273317	100.00	83	93.101	3120	1.14
20	43.304	496	0.18	84	94.109	4276	1.56
21	43.370	242	0.09	85	95.117	61705	22.58
22	43.378	110	0.04	86	95.150	418	0.15
23	43.393	304	0.11	87	95.197	1413	0.52
24	44.041	86731	31.73	88	96.125	81458	29.80
25	44.073	9495	3.47	89	96.175	473	0.17
26	44.129	1165	0.43	90	96.203	1648	0.60
27	45.049	32863	12.02	91	97.098	954	0.35
28	46.052	998	0.37	92	97.133	50805	18.59
29	51.041	891	0.33	93	98.105	1346	0.49
30	52.050	953	0.35	94	98.140	14962	5.47
31	53.057	13801	5.05	95	99.113	4740	1.73
32	54.065	36992	13.53	96	99.148	4506	1.65
33	55.037	4492	1.64	97	100.120	1031	0.38
34	55.073	180342	65.98	98	108.128	1459	0.53
35	55.176	2144	0.78	99	109.137	27540	10.08
36	56.044	707	0.26	100	110.144	23762	8.69
37	56.081	71631	26.21	101	111.153	18806	6.88
38	56.109	401	0.15	102	112.161	8209	3.00
39	56.141	1076	0.39	103	113.133	1214	0.44
40	57.053	91415	33.45	104	113.169	2296	0.84
41	57.089	168237	61.55	105	122.148	1310	0.48
42	58.060	8759	3.20	106	123.157	13397	4.90
43	58.093	6555	2.40	107	124.164	13334	4.88
44	59.069	1967	0.72	108	125.172	6802	2.49
45	65.061	2883	1.05	109	126.181	5181	1.90
46	66.069	17069	6.25	110	127.188	1529	0.56
47	67.077	92324	33.78	111	137.177	7244	2.65
48	67.143	1932	0.71	112	138.184	8183	2.99
49	68.085	110087	40.28	113	139.192	2514	0.92
50	68.194	1628	0.60	114	140.201	4245	1.55
51	69.057	1214	0.44	115	141.205	1224	0.45
52	69.093	102825	37.62	116	151.197	3919	1.43
53	69.160	2036	0.74	117	152.205	7375	2.70
54	70.065	4149	1.52	118	153.212	1825	0.67
55	70.101	54388	19.90	119	154.221	3304	1.21
56	70.132	664	0.24	120	165.217	1854	0.68
57	70.162	666	0.24	121	166.225	2574	0.94
58	70.172	791	0.29	122	179.237	1128	0.41
59	71.073	27915	10.21	123	180.245	8784	3.21
60	71.109	61506	22.50	124	181.249	1544	0.56
61	71.178	1561	0.57	125	182.261	11705	4.28
62	72.081	13558	4.96	126	183.264	1786	0.65
63	72.113	3364	1.23	127	198.262	1866	0.68
64	73.088	2331	0.85	128	208.284	5605	2.05

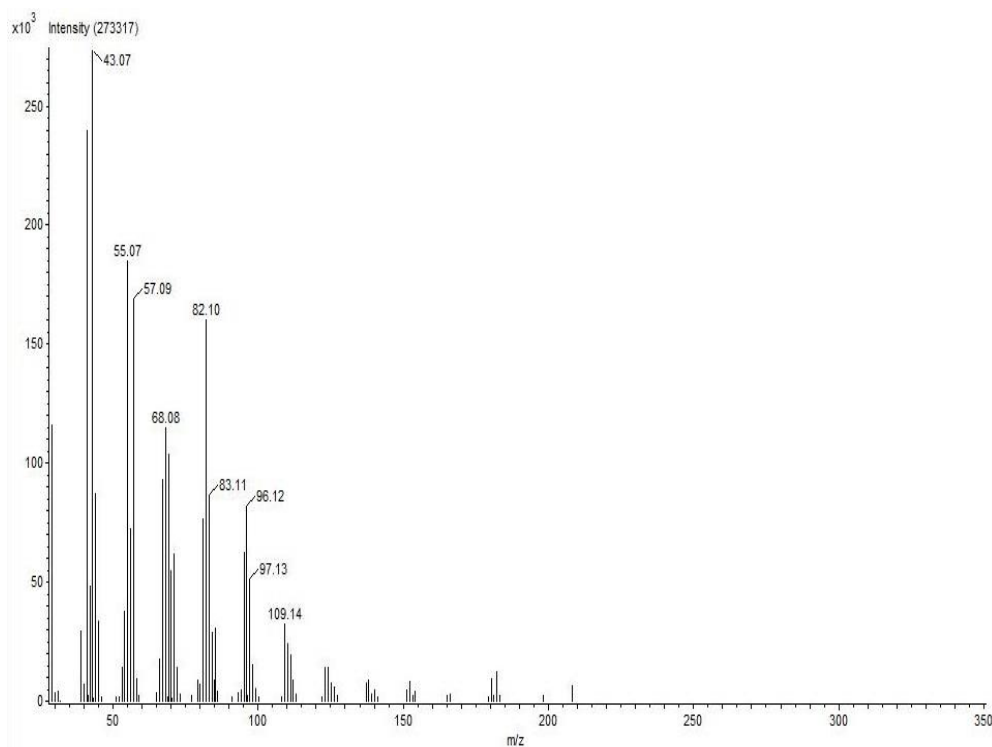


Figure 86. Mass-spectra of pentadecanal (Rt = 14.55) in F9 fraction from ethyl acetate extract of *C. militaris* detected by GC-MS.

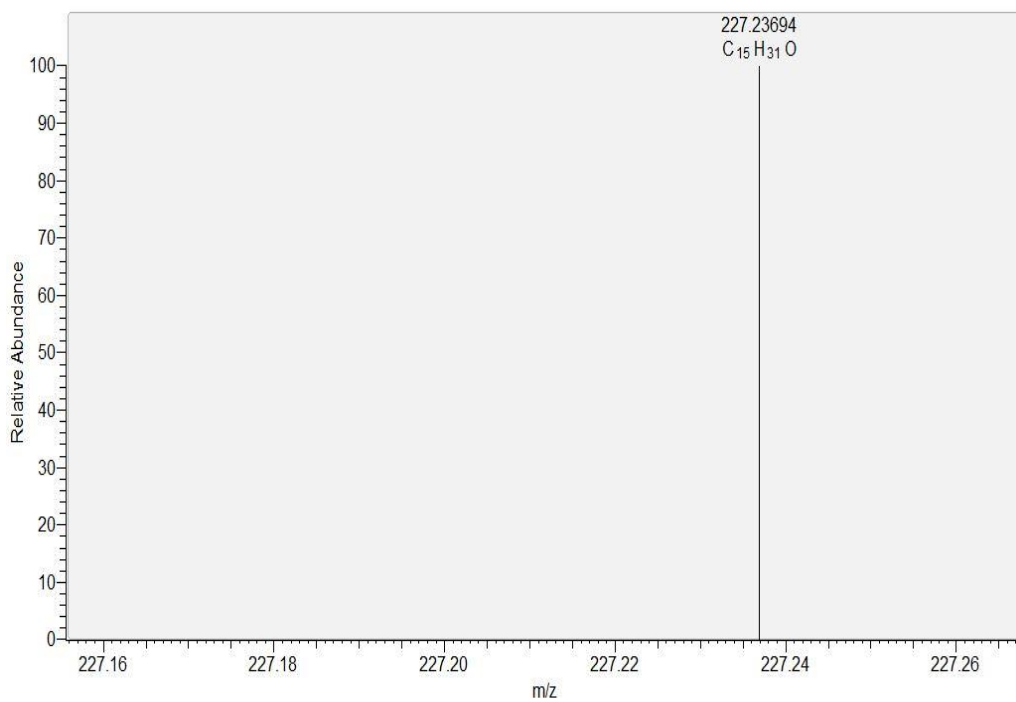


Figure 87. ESI-MS spectra of pentadecanal in F9 fraction from ethyl acetate extract of *C. militaris*.

Table 47. Fragmentation pattern of 2-oxopalmitic acid methyl ester (retention time = 17.40) in F9 fraction from ethyl acetate extract of *C. militaris* detected by GC-MS

Peak#	m/z	Intensity	Relative Intensity (%)	Peak#	m/z	Intensity	Relative Intensity (%)
1	29.049	4142	27.61	23	70.100	519	3.46
2	31.029	2417	16.11	24	70.106	189	1.26
3	31.994	353	2.35	25	71.072	470	3.13
4	39.037	853	5.69	26	71.109	7830	52.19
5	41.053	9152	61.00	27	72.109	313	2.09
6	42.061	2325	15.50	28	72.114	334	2.22
7	43.032	1005	6.70	29	74.061	706	4.71
8	43.069	14336	95.56	30	75.070	548	3.65
9	44.073	639	4.26	31	81.097	1869	12.46
10	53.060	394	2.63	32	82.104	546	3.64
11	54.065	999	6.66	33	83.076	541	3.60
12	55.038	879	5.86	34	83.113	1798	11.98
13	55.073	7159	47.72	35	85.130	4293	28.61
14	56.081	1845	12.30	36	87.072	500	3.33
15	57.054	769	5.13	37	95.117	2383	15.89
16	57.089	15003	100.00	38	97.135	824	5.49
17	58.063	849	5.66	39	98.104	620	4.14
18	58.092	705	4.70	40	99.149	459	3.06
19	67.077	1635	10.90	41	109.136	1200	8.00
20	68.085	866	5.78	42	123.159	831	5.54
21	69.093	3827	25.51	43	225.294	10025	66.82
22	70.064	440	2.93	44	226.297	1385	9.23

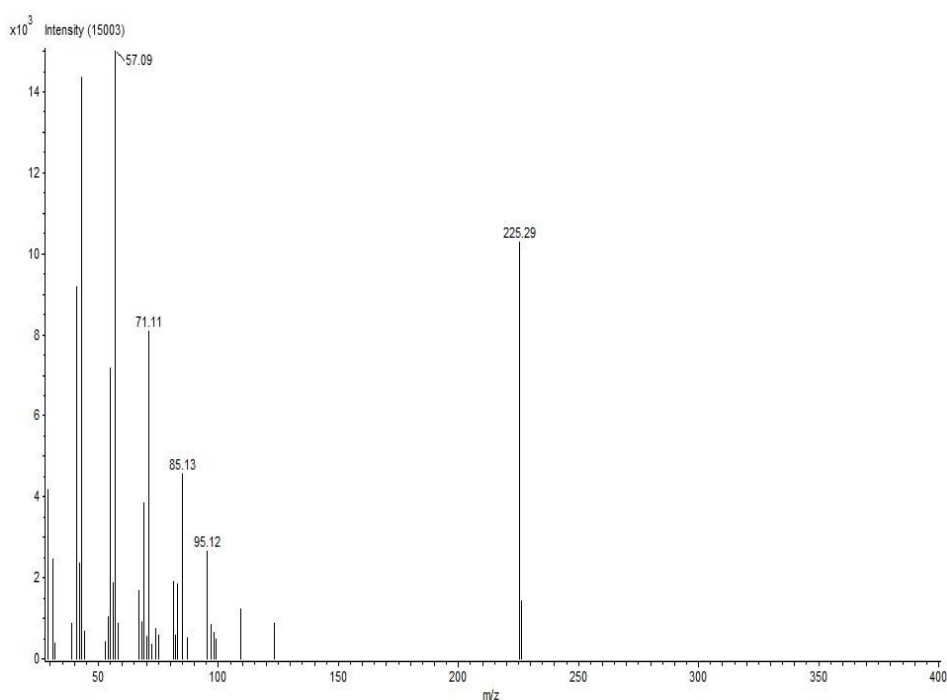


Figure 88. Mass-spectra of 2-oxopalmitic acid methyl ester (Rt = 17.40) in F9 fraction from ethyl acetate extract of *C. militaris* detected by GC-MS.

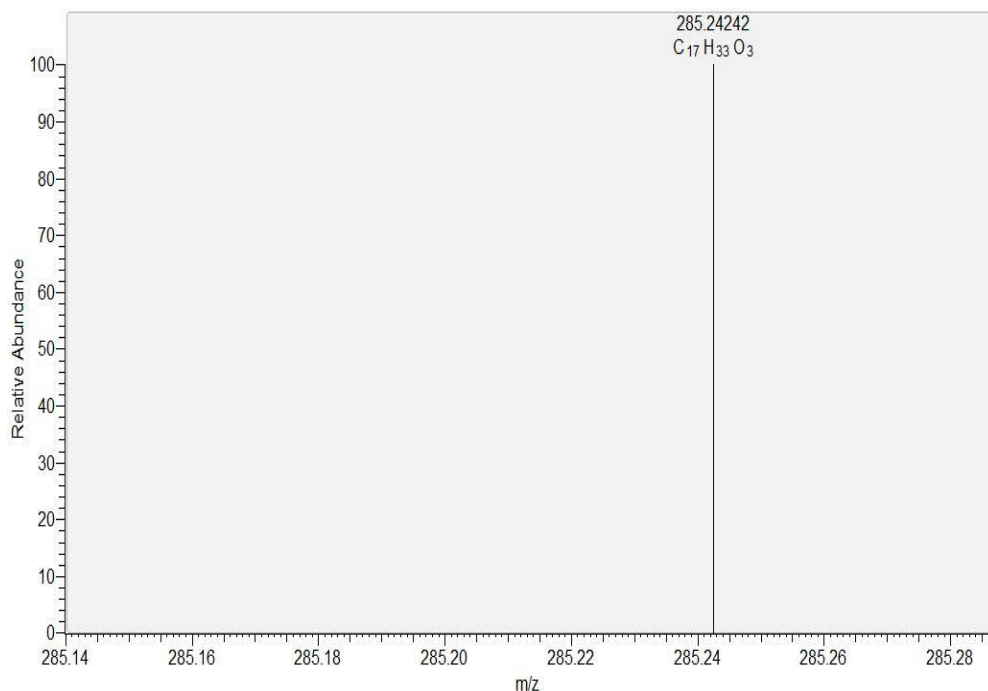


Figure 89. ESI-MS spectra of 2-oxopalmitic acid methyl ester in F9 fraction from ethyl acetate extract of *C. militaris*.

Table 48. Fragmentation pattern of cordycepin (retention time = 21.97) in F9 fraction from ethyl acetate extract of *C. militaris* detected by GC-MS

Peak#	m/z	Intensity	Relative Intensity (%)	Peak#	m/z	Intensity	Relative Intensity (%)
1	29.013	30067	7.47	80	100.081	874	0.22
2	29.036	8251	2.05	81	104.061	982	0.24
3	29.049	14021	3.48	82	105.070	989	0.25
4	29.078	370	0.09	83	106.075	1272	0.32
5	30.020	2117	0.53	84	107.072	3963	0.98
6	30.045	7846	1.95	85	108.079	135148	33.56
7	31.029	53388	13.26	86	109.085	18069	4.49
8	31.059	337	0.08	87	110.091	1887	0.47
9	31.074	1082	0.27	88	116.085	2353	0.58
10	32.005	789	0.20	89	117.094	1448	0.36
11	32.034	907	0.23	90	118.072	1715	0.43
12	38.016	2598	0.65	91	119.075	32420	8.05
13	39.037	21564	5.35	92	120.082	5523	1.37
14	40.033	17081	4.24	93	121.091	6545	1.63
15	41.053	56220	13.96	94	122.098	1636	0.41
16	41.077	464	0.12	95	131.079	1117	0.28
17	41.088	348	0.09	96	132.095	1124	0.28
18	41.104	1091	0.27	97	133.095	1696	0.42
19	42.025	4141	1.03	98	134.093	7232	1.80
20	42.061	23005	5.71	99	135.098	402708	100.00
21	43.034	37322	9.27	100	135.514	711	0.18
22	43.069	23161	5.75	101	135.676	6760	1.68
23	43.115	196	0.05	102	135.749	719	0.18
24	43.125	875	0.22	103	135.988	998	0.25

25	44.005	472	0.12	104	136.105	196829	48.88
26	44.041	11252	2.79	105	136.486	1034	0.26
27	44.068	1462	0.36	106	136.523	3955	0.98
28	45.050	9755	2.42	107	136.682	1101	0.27
29	47.029	5429	1.35	108	137.108	13463	3.34
30	51.032	2404	0.60	109	145.099	1938	0.48
31	52.037	5219	1.30	110	146.104	1524	0.38
32	53.032	13003	3.23	111	147.114	2724	0.68
33	53.057	20487	5.09	112	148.111	37378	9.28
34	54.040	32613	8.10	113	148.209	755	0.19
35	55.046	25784	6.40	114	149.117	9719	2.41
36	56.056	6040	1.50	115	150.122	2020	0.50
37	57.053	58922	14.63	116	152.107	900	0.22
38	58.026	654	0.16	117	160.114	1162	0.29
39	58.059	3793	0.94	118	161.121	2214	0.55
40	59.034	925	0.23	119	162.130	6741	1.67
41	59.069	1561	0.39	120	163.104	3255	0.81
42	60.041	2850	0.71	121	164.110	232350	57.70
43	61.049	1440	0.36	122	164.360	727	0.18
44	64.029	1388	0.34	123	164.622	712	0.18
45	65.036	9752	2.42	124	164.643	294	0.07
46	66.044	34946	8.68	125	164.684	1205	0.30
47	66.074	516	0.13	126	164.711	196	0.05
48	66.108	711	0.18	127	164.746	1489	0.37
49	67.052	29641	7.36	128	165.112	20824	5.17
50	68.059	11504	2.86	129	165.264	1422	0.35
51	69.057	52243	12.97	130	166.115	1787	0.44
52	69.123	1310	0.33	131	173.126	4749	1.18
53	70.064	14077	3.50	132	174.134	8585	2.13
54	71.037	2782	0.69	133	175.141	13824	3.43
55	71.073	20494	5.09	134	176.147	5244	1.30
56	71.109	693	0.17	135	177.122	2530	0.63
57	72.075	1300	0.32	136	178.130	52154	12.95
58	73.053	9018	2.24	137	178.235	1202	0.30
59	74.060	685	0.17	138	179.133	5254	1.30
60	77.040	2286	0.57	139	186.138	675	0.17
61	78.050	1714	0.43	140	190.135	693	0.17
62	79.056	3725	0.93	141	192.150	8297	2.06
63	80.052	8877	2.20	142	193.156	3281	0.81
64	81.060	29873	7.42	143	194.131	1136	0.28
65	82.067	8671	2.15	144	202.138	13378	3.32
66	83.074	1367	0.34	145	203.144	7678	1.91
67	84.050	850	0.21	146	204.152	3813	0.95
68	85.057	2626	0.65	147	205.159	770	0.19
69	86.065	879	0.22	148	214.141	1050	0.26
70	87.072	745	0.19	149	215.149	5932	1.47
71	91.049	1537	0.38	150	216.156	2862	0.71
72	92.056	12244	3.04	151	220.154	8944	2.22
73	93.064	6926	1.72	152	221.161	24401	6.06
74	94.072	10955	2.72	153	222.164	2897	0.72
75	95.079	4854	1.21	154	233.164	1329	0.33
76	96.084	622	0.15	155	234.174	2704	0.67
77	97.061	814	0.20	156	251.181	5292	1.31
78	98.069	847	0.21	157	252.186	752	0.19
79	99.077	11270	2.80				

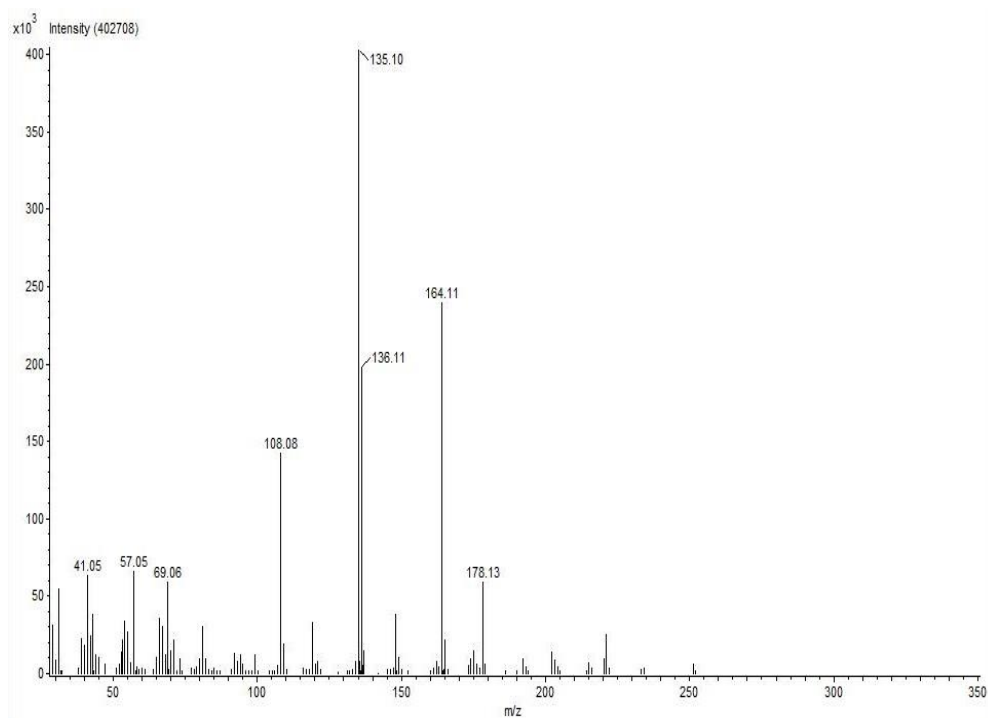


Figure 90. Mass-spectra of cordycepin (Rt = 21.97) in F9 fraction from ethyl acetate extract of *C. militaris* detected by GC-MS.

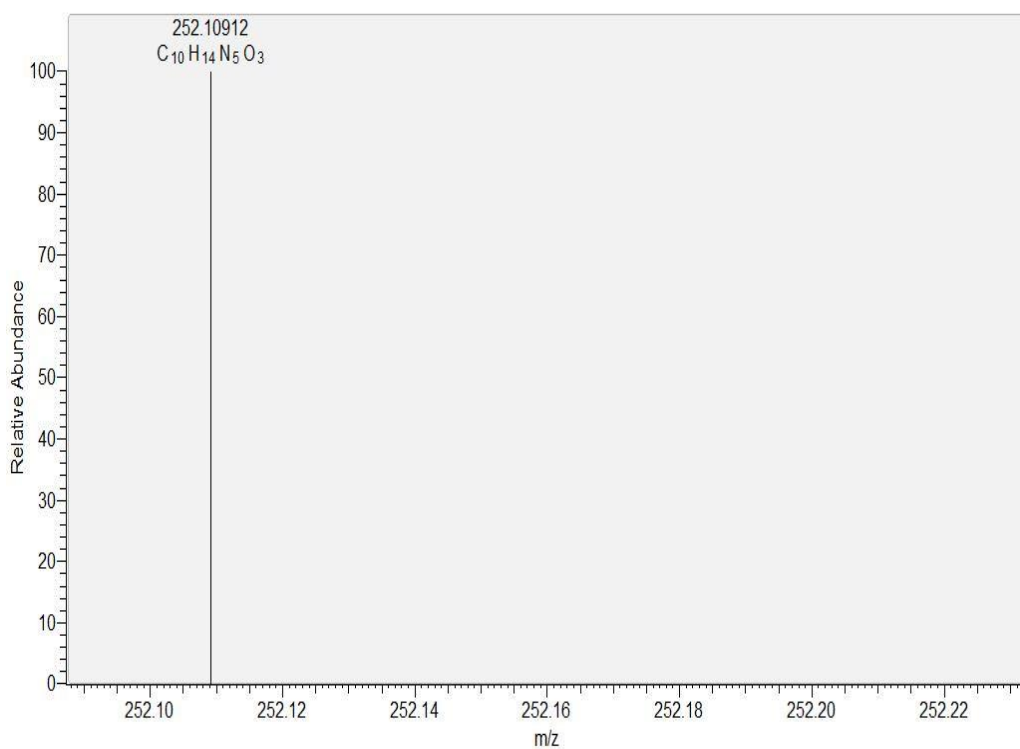


Figure 91. ESI-MS spectra of cordycepin in F9 fraction from ethyl acetate extract of *C. militaris*.

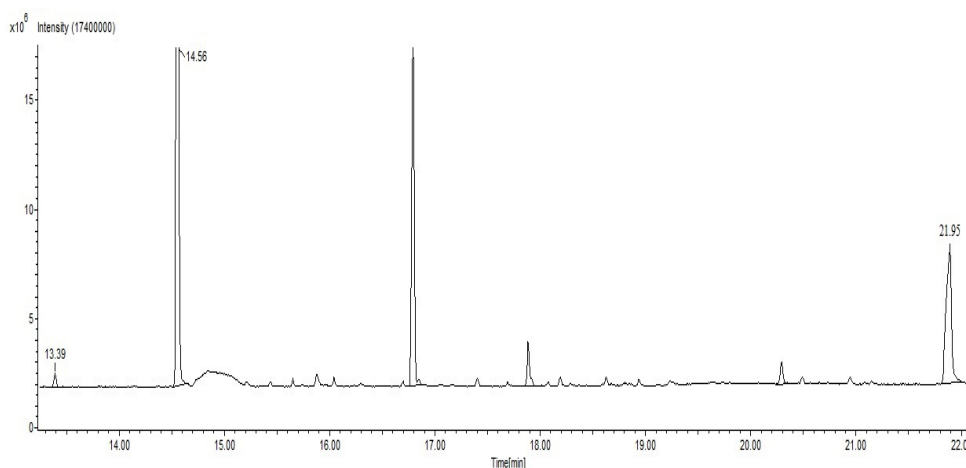


Figure 92. GC-MS chromatogram of F10 fraction from ethyl acetate extract of *C. militaris*.

Table 49. Fragmentation pattern of tetradecanal (retention time = 13.39) in F10 fraction from ethyl acetate extract of *C. militaris* detected by GC-MS

Peak#	m/z	Intensity	Relative Intensity (%)	Peak#	m/z	Intensity	Relative Intensity (%)
1	29.013	799	5.67	32	72.082	816	5.80
2	29.049	6804	48.31	33	79.083	907	6.44
3	32.002	778	5.52	34	80.087	242	1.72
4	39.037	1967	13.96	35	80.092	199	1.41
5	39.973	1058	7.51	36	81.098	3953	28.07
6	40.045	372	2.64	37	82.106	8083	57.39
7	41.053	13564	96.31	38	83.081	459	3.26
8	42.061	3258	23.14	39	83.114	4459	31.66
9	43.033	643	4.56	40	84.122	1955	13.88
10	43.070	14084	100.00	41	85.093	595	4.23
11	44.041	4871	34.58	42	85.130	1663	11.81
12	44.074	772	5.48	43	95.117	3525	25.03
13	45.049	1960	13.92	44	96.126	4083	28.99
14	53.058	1275	9.06	45	97.133	2527	17.94
15	54.066	2246	15.95	46	98.141	999	7.09
16	55.074	9367	66.51	47	109.138	1447	10.27
17	56.082	4560	32.38	48	110.146	1372	9.74
18	57.054	5396	38.31	49	111.154	892	6.33
19	57.090	8472	60.15	50	112.159	458	3.25
20	58.060	321	2.28	51	112.170	203	1.44
21	58.065	137	0.97	52	123.160	755	5.36
22	58.094	422	3.00	53	124.166	854	6.06
23	65.062	161	1.15	54	137.179	775	5.51
24	66.069	1241	8.81	55	138.188	933	6.63
25	67.078	5177	36.76	56	140.200	89	0.63
26	67.151	181	1.28	57	149.117	686	4.87
27	68.086	5857	41.59	58	166.220	449	3.19
28	69.093	5769	40.96	59	166.235	209	1.48
29	70.101	3242	23.02	60	168.241	1087	7.72
30	71.074	1943	13.80	61	194.269	188	1.33
31	71.110	3226	22.91				

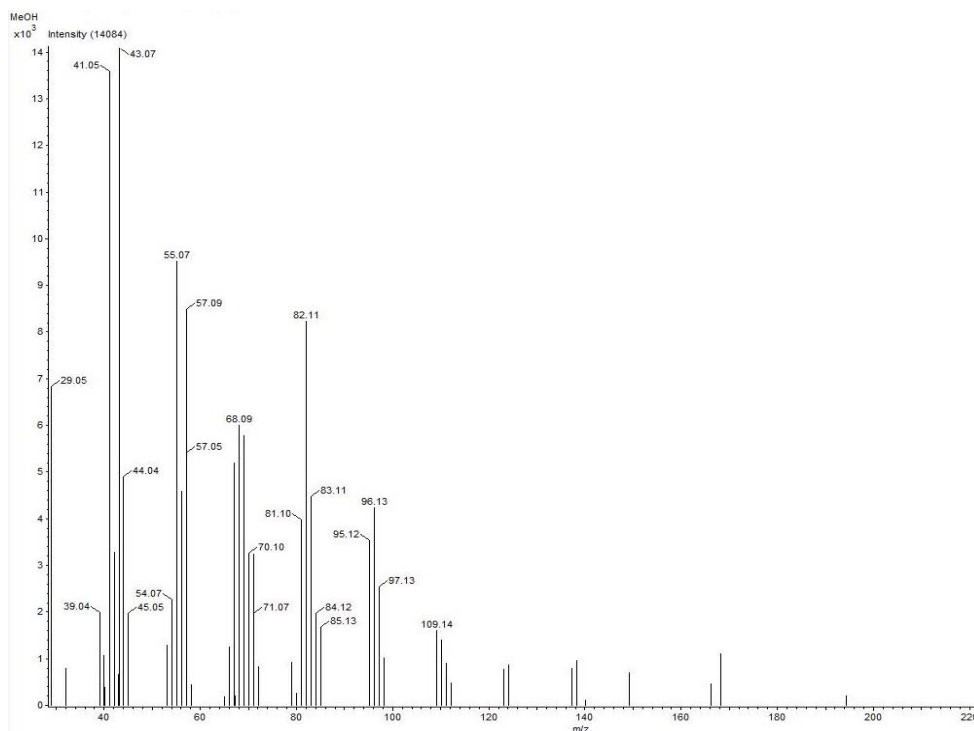


Figure 93. Mass-spectra of tetradecanal ($R_t = 13.39$) in F10 fraction from ethyl acetate extract of *C. militaris* detected by GC-MS

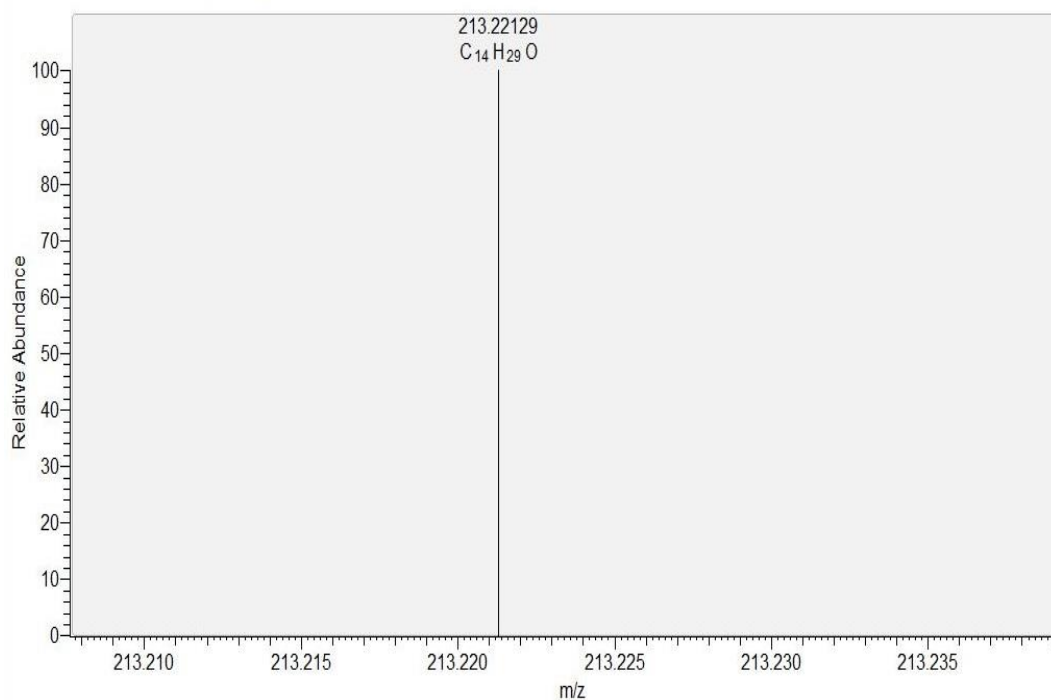


Figure 94. ESI-MS spectra of tetradecanal in F10 fraction from ethyl acetate extract of *C. militaris*.

Table 50. Fragmentation pattern of pentadecanal (retention time = 14.56) in F10 fraction from ethyl acetate extract of *C. militaris* detected by GC-MS

Peak#	m/z	Intensity	Relative Intensity (%)	Peak#	m/z	Intensity	Relative Intensity (%)
1	29.013	18601	4.33	134	68.495	706	0.16
2	29.049	197637	45.99	135	69.058	2569	0.60
3	29.153	1166	0.27	136	69.094	178336	41.50
4	29.242	250	0.06	137	69.392	304	0.07
5	29.274	206	0.05	138	69.416	229	0.05
6	29.286	99	0.02	139	69.423	170	0.04
7	29.292	92	0.02	140	69.429	104	0.02
8	29.297	66	0.02	141	69.436	172	0.04
9	29.303	55	0.01	142	69.448	187	0.04
10	29.316	197	0.05	143	69.469	731	0.17
11	30.018	422	0.10	144	69.486	115	0.03
12	30.053	4681	1.09	145	69.505	728	0.17
13	31.029	5249	1.22	146	70.066	6064	1.41
14	38.029	514	0.12	147	70.102	89784	20.89
15	39.037	46732	10.87	148	70.209	438	0.10
16	39.060	358	0.08	149	70.222	286	0.07
17	39.081	242	0.06	150	71.074	45813	10.66
18	39.089	565	0.13	151	71.110	100474	23.38
19	40.045	10098	2.35	152	71.411	694	0.16
20	41.053	393186	91.49	153	71.443	468	0.11
21	41.179	1226	0.29	154	71.494	638	0.15
22	41.283	719	0.17	155	72.081	22261	5.18
23	41.339	2492	0.58	156	72.114	5840	1.36
24	41.369	939	0.22	157	72.149	795	0.19
25	41.405	6	0.00	158	73.089	3359	0.78
26	41.410	8	0.00	159	77.065	2896	0.67
27	41.550	37	0.01	160	78.073	819	0.19
28	41.561	49	0.01	161	79.082	13552	3.15
29	41.566	14	0.00	162	80.089	10001	2.33
30	41.599	696	0.16	163	81.063	498	0.12
31	41.637	7	0.00	164	81.098	125139	29.12
32	41.819	48	0.01	165	81.543	368	0.09
33	41.828	39	0.01	166	82.106	257906	60.01
34	41.838	67	0.02	167	82.430	532	0.12
35	41.845	49	0.01	168	82.456	453	0.11
36	41.852	52	0.01	169	82.466	303	0.07
37	41.860	32	0.01	170	82.479	320	0.07
38	41.866	15	0.00	171	82.515	2089	0.49
39	42.025	2322	0.54	172	82.553	1591	0.37
40	42.061	78508	18.27	173	82.586	518	0.12
41	42.161	207	0.05	174	82.607	950	0.22
42	42.337	74	0.02	175	82.835	18	0.00
43	42.351	84	0.02	176	82.845	35	0.01
44	42.355	85	0.02	177	82.855	50	0.01
45	42.359	266	0.06	178	82.867	50	0.01
46	42.382	331	0.08	179	82.882	138	0.03
47	43.033	16353	3.80	180	82.901	24	0.01
48	43.070	429776	100.00	181	82.911	60	0.01
49	43.305	906	0.21	182	82.922	25	0.01
50	43.365	4839	1.13	183	82.929	13	0.00
51	43.394	1821	0.42	184	83.078	3937	0.92
52	43.442	366	0.09	185	83.113	142192	33.09

53	43.559	80	0.02	186	83.287	77	0.02
54	43.567	9	0.00	187	83.472	52	0.01
55	43.575	18	0.00	188	83.481	4	0.00
56	43.623	1684	0.39	189	83.486	13	0.00
57	43.675	10	0.00	190	83.566	992	0.23
58	43.683	28	0.01	191	83.613	2	0.00
59	43.828	369	0.09	192	83.629	47	0.01
60	43.834	218	0.05	193	84.085	2412	0.56
61	43.842	247	0.06	194	84.121	46835	10.90
62	43.850	251	0.06	195	84.195	1050	0.24
63	43.882	2051	0.48	196	84.224	220	0.05
64	43.918	608	0.14	197	84.243	363	0.08
65	44.004	310	0.07	198	84.259	450	0.10
66	44.041	143912	33.49	199	85.094	13269	3.09
67	44.073	15565	3.62	200	85.130	48673	11.33
68	44.281	310	0.07	201	86.101	5750	1.34
69	44.343	1795	0.42	202	86.134	2930	0.68
70	44.368	1104	0.26	203	87.108	907	0.21
71	44.390	397	0.09	204	91.085	1741	0.41
72	44.399	190	0.04	205	93.102	4941	1.15
73	44.404	118	0.03	206	94.109	7000	1.63
74	44.410	576	0.13	207	95.118	104833	24.39
75	44.601	282	0.07	208	96.125	143548	33.40
76	44.608	284	0.07	209	96.314	372	0.09
77	45.049	52342	12.18	210	97.133	84526	19.67
78	45.126	161	0.04	211	97.270	274	0.06
79	45.138	344	0.08	212	98.106	1939	0.45
80	45.151	297	0.07	213	98.141	25009	5.82
81	46.052	1566	0.36	214	99.114	7815	1.82
82	51.042	1481	0.34	215	99.149	7439	1.73
83	52.049	1007	0.23	216	100.120	1581	0.37
84	53.058	22453	5.22	217	100.155	693	0.16
85	54.065	61590	14.33	218	107.122	744	0.17
86	54.125	1198	0.28	219	108.129	2256	0.52
87	55.037	6945	1.62	220	109.138	46035	10.71
88	55.074	305608	71.11	221	109.192	401	0.09
89	55.218	394	0.09	222	109.219	845	0.20
90	55.340	410	0.10	223	109.236	237	0.06
91	55.374	160	0.04	224	110.145	40129	9.34
92	55.408	525	0.12	225	110.225	1148	0.27
93	55.439	718	0.17	226	111.153	30728	7.15
94	55.473	59	0.01	227	111.237	707	0.16
95	55.679	136	0.03	228	112.124	573	0.13
96	55.684	202	0.05	229	112.161	13733	3.20
97	55.693	374	0.09	230	113.134	1859	0.43
98	55.704	352	0.08	231	113.169	3658	0.85
99	55.713	216	0.05	232	114.139	599	0.14
100	55.721	292	0.07	233	121.140	814	0.19
101	55.729	272	0.06	234	122.149	1742	0.41
102	56.045	1439	0.33	235	123.158	22181	5.16
103	56.081	119143	27.72	236	124.165	22217	5.17
104	56.165	219	0.05	237	125.173	10796	2.51
105	56.185	1182	0.27	238	126.182	8466	1.97
106	57.054	151237	35.19	239	127.153	860	0.20
107	57.090	275836	64.18	240	127.189	2361	0.55
108	57.242	1130	0.26	241	136.170	1100	0.26
109	57.324	382	0.09	242	137.178	12128	2.82
110	57.361	754	0.18	243	138.185	13575	3.16
111	57.430	4393	1.02	244	139.193	4604	1.07

112	57.463	1991	0.46	245	140.202	6169	1.44
113	57.498	474	0.11	246	141.173	441	0.10
114	57.702	3556	0.83	247	141.207	1715	0.40
115	57.767	679	0.16	248	151.198	6562	1.53
116	57.995	67	0.02	249	152.206	12489	2.91
117	58.006	124	0.03	250	153.212	3378	0.79
118	58.022	63	0.01	251	154.222	5292	1.23
119	58.060	14652	3.41	252	155.227	1067	0.25
120	58.094	10737	2.50	253	165.218	3086	0.72
121	59.069	3199	0.74	254	166.226	4192	0.98
122	65.062	4411	1.03	255	167.230	755	0.18
123	66.069	27619	6.43	256	170.222	796	0.19
124	67.077	158217	36.81	257	179.238	1544	0.36
125	67.449	447	0.10	258	180.246	14292	3.33
126	67.457	365	0.09	259	181.250	2021	0.47
127	68.049	464	0.11	260	182.262	18202	4.24
128	68.085	187046	43.52	261	183.266	2916	0.68
129	68.381	526	0.12	262	193.256	753	0.18
130	68.416	807	0.19	263	198.262	2790	0.65
131	68.429	284	0.07	264	208.286	9044	2.10
132	68.447	483	0.11	265	209.290	1474	0.34
133	68.464	836	0.19	266	226.303	927	0.22

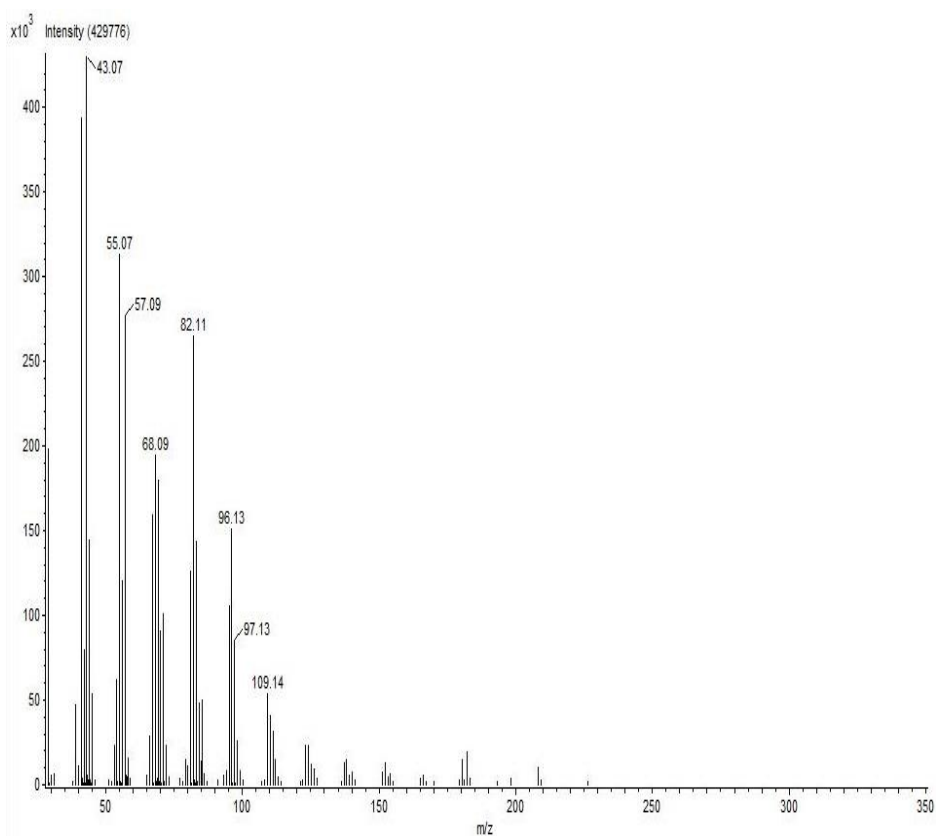


Figure 95. Mass-spectra of pentadecanal (Rt = 14.56) in F10 fraction from ethyl acetate extract of *C. militaris* detected by GC-MS.

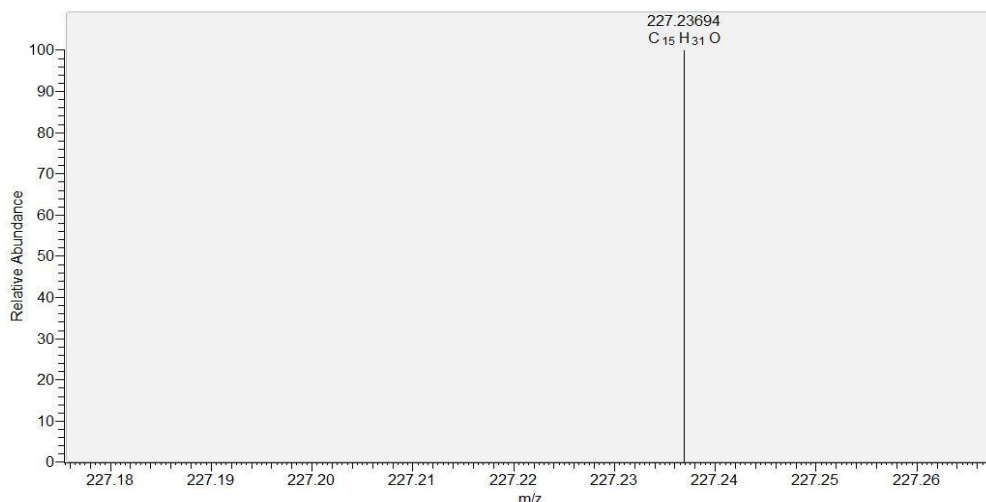


Figure 96. ESI-MS spectra of pentadecanal in F10 fraction from ethyl acetate extract of *C. militaris*.

Table 51. Fragmentation pattern of cordycepin (retention time = 21.95) in F10 fraction from ethyl acetate extract of *C. militaris* detected by GC-MS

Peak#	m/z	Intensity	Relative Intensity (%)	Peak#	m/z	Intensity	Relative Intensity (%)
1	29.013	17485	7.51	69	104.057	264	0.11
2	29.036	4900	2.11	70	104.064	316	0.14
3	29.049	8209	3.53	71	105.069	639	0.27
4	30.021	1293	0.56	72	106.076	927	0.40
5	30.045	4571	1.96	73	107.073	2388	1.03
6	31.029	30971	13.31	74	108.080	77113	33.14
7	31.050	292	0.13	75	108.197	502	0.22
8	32.005	817	0.35	76	109.085	10210	4.39
9	32.034	575	0.25	77	110.081	386	0.17
10	38.016	1265	0.54	78	110.091	491	0.21
11	39.037	12588	5.41	79	116.086	1353	0.58
12	40.033	9788	4.21	80	117.095	793	0.34
13	41.053	32776	14.09	81	118.073	1074	0.46
14	41.104	695	0.30	82	119.075	18798	8.08
15	42.025	2231	0.96	83	120.083	3067	1.32
16	42.061	13645	5.86	84	121.092	3785	1.63
17	43.034	21909	9.42	85	122.098	1029	0.44
18	43.070	12758	5.48	86	131.081	699	0.30
19	44.006	478	0.21	87	133.095	1084	0.47
20	44.041	6939	2.98	88	134.093	4263	1.83
21	44.070	872	0.37	89	135.099	232683	100.00
22	45.050	5661	2.43	90	135.319	293	0.13
23	47.030	3179	1.37	91	135.331	491	0.21
24	51.030	1437	0.62	92	135.583	1200	0.52
25	52.037	3181	1.37	93	135.607	405	0.17
26	53.032	7772	3.34	94	135.632	898	0.39
27	53.057	11764	5.06	95	135.676	1975	0.85
28	54.040	18794	8.08	96	136.050	434	0.19
29	55.047	14900	6.40	97	136.106	109405	47.02
30	56.056	3661	1.57	98	136.272	398	0.17
31	57.054	35149	15.11	99	136.285	389	0.17

32	57.114	655	0.28	100	136.523	707	0.30
33	58.025	435	0.19	101	137.108	7419	3.19
34	58.059	2228	0.96	102	145.100	1206	0.52
35	59.033	575	0.25	103	146.104	1184	0.51
36	59.070	939	0.40	104	147.115	1605	0.69
37	60.042	1819	0.78	105	148.111	21643	9.30
38	61.050	823	0.35	106	149.118	5624	2.42
39	64.029	811	0.35	107	150.122	1093	0.47
40	65.037	5766	2.48	108	152.107	599	0.26
41	66.045	20255	8.70	109	157.102	700	0.30
42	67.053	17392	7.47	110	160.115	758	0.33
43	68.059	6477	2.78	111	161.122	1331	0.57
44	69.057	30127	12.95	112	162.131	3848	1.65
45	70.064	8266	3.55	113	163.104	1829	0.79
46	71.038	1622	0.70	114	164.111	123110	52.91
47	71.074	11747	5.05	115	165.113	10574	4.54
48	72.077	692	0.30	116	166.115	1294	0.56
49	73.054	5349	2.30	117	173.127	2737	1.18
50	77.040	1522	0.65	118	174.135	4769	2.05
51	78.049	1067	0.46	119	175.142	7535	3.24
52	79.056	2258	0.97	120	176.148	3125	1.34
53	80.053	5084	2.18	121	177.124	1626	0.70
54	81.060	17229	7.40	122	178.131	28998	12.46
55	82.068	4719	2.03	123	179.134	2794	1.20
56	83.069	366	0.16	124	192.151	4714	2.03
57	83.076	427	0.18	125	193.157	1743	0.75
58	85.058	1458	0.63	126	202.139	7199	3.09
59	86.065	472	0.20	127	203.146	4233	1.82
60	91.048	1009	0.43	128	204.154	2020	0.87
61	92.056	6786	2.92	129	215.151	3503	1.51
62	93.065	4039	1.74	130	216.158	1661	0.71
63	94.072	6449	2.77	131	220.155	5058	2.17
64	95.080	3142	1.35	132	221.163	13364	5.74
65	97.058	279	0.12	133	222.164	1607	0.69
66	97.064	247	0.11	134	233.166	746	0.32
67	99.077	6292	2.70	135	234.174	1577	0.68
68	100.082	457	0.20	136	251.182	3015	1.30

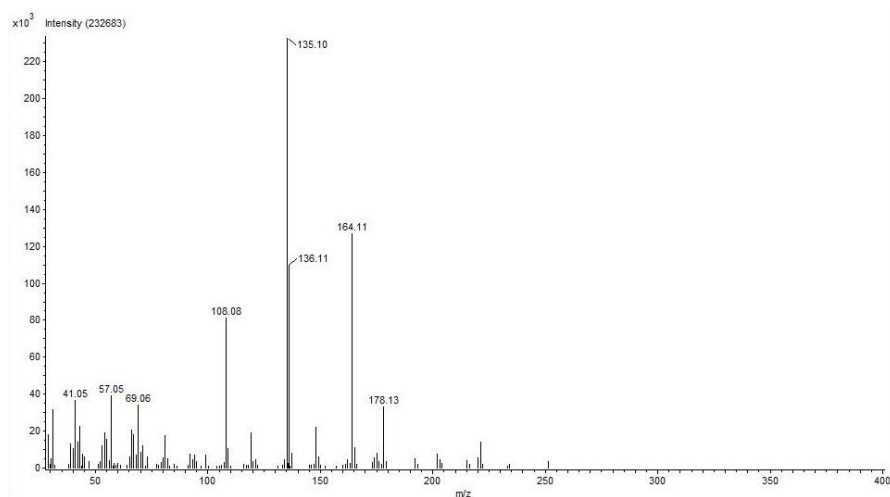


Figure 97. Mass-spectra of cordycepin (Rt = 21.95) in F10 fraction from ethyl acetate extract of *C. militaris* detected by GC-MS.

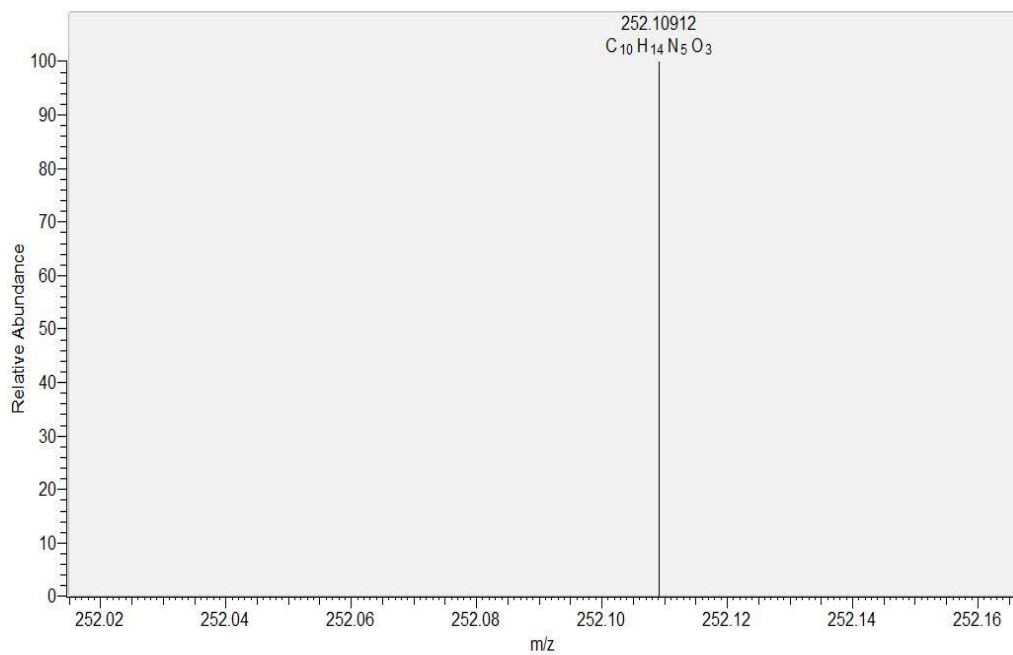


Figure 98. ESI-MS spectra of cordycepin in F10 fraction from ethyl acetate extract of *C. militaris*.

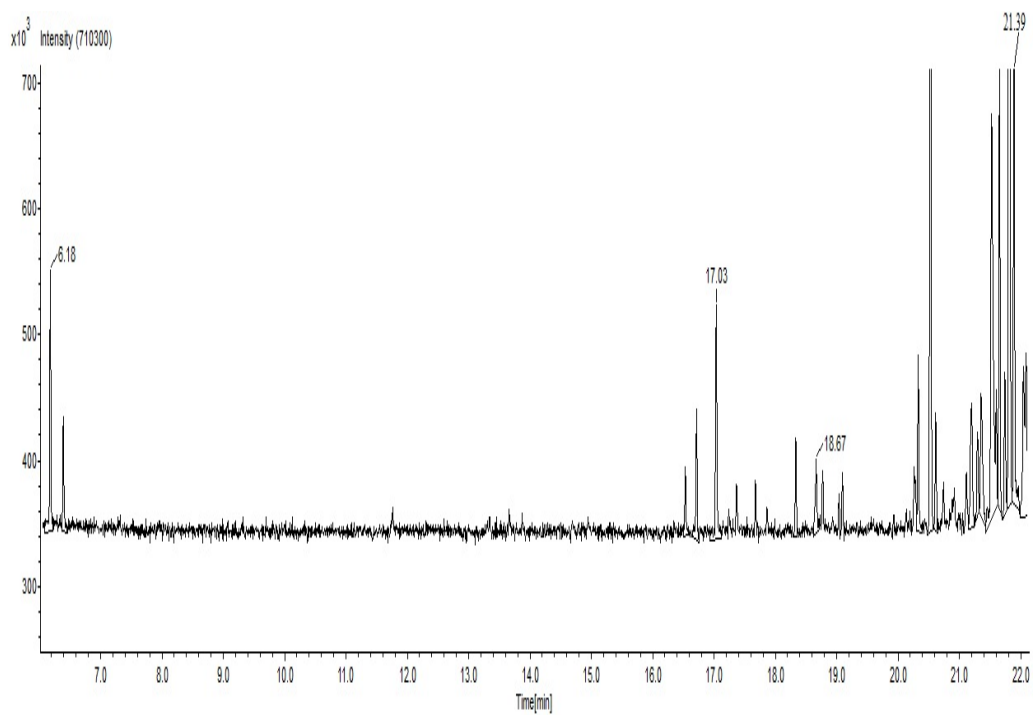


Figure 99. GC-MS chromatogram of F11 fraction from ethyl acetate extract of *C. militaris*

Table 52. Fragmentation pattern of malic acid (retention time = 6.18) in F11 fraction from ethyl acetate extract of *C. militaris* detected by GC-MS

Peak#	m/z	Intensity	Relative Intensity (%)	Peak#	m/z	Intensity	Relative Intensity (%)
1	29.012	1238	8.16	11	53.059	365	2.40
2	29.049	691	4.55	12	55.036	531	3.50
3	31.999	513	3.38	13	55.073	456	3.00
4	39.036	410	2.70	14	57.053	1813	11.94
5	41.052	1364	8.98	15	71.073	5957	39.23
6	42.023	359	2.37	16	71.101	149	0.98
7	43.032	15184	100.00	17	72.080	3113	20.50
8	43.069	2768	18.23	18	75.070	648	4.27
9	44.039	667	4.39	19	89.089	6295	41.46
10	45.049	4723	31.11	20	90.094	515	3.39

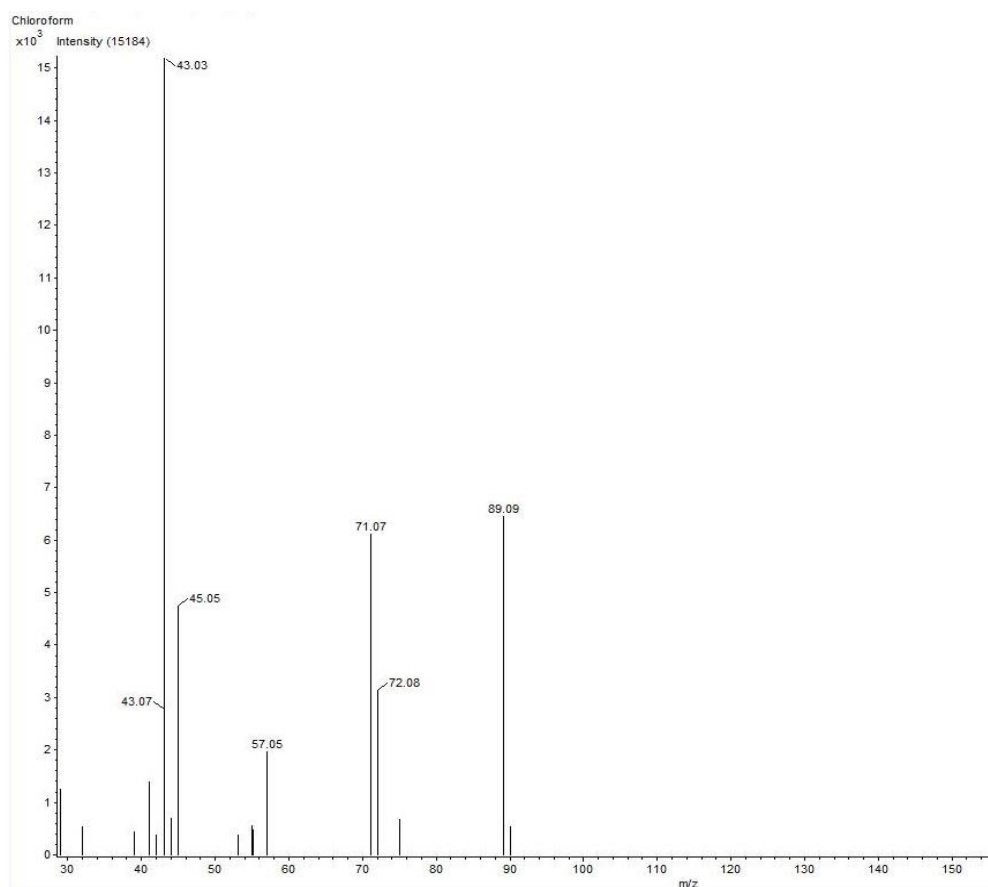


Figure 100. Mass-spectra of malic acid (Rt = 6.18) in F11 fraction from ethyl acetate extract of *C. militaris* detected by GC-MS.

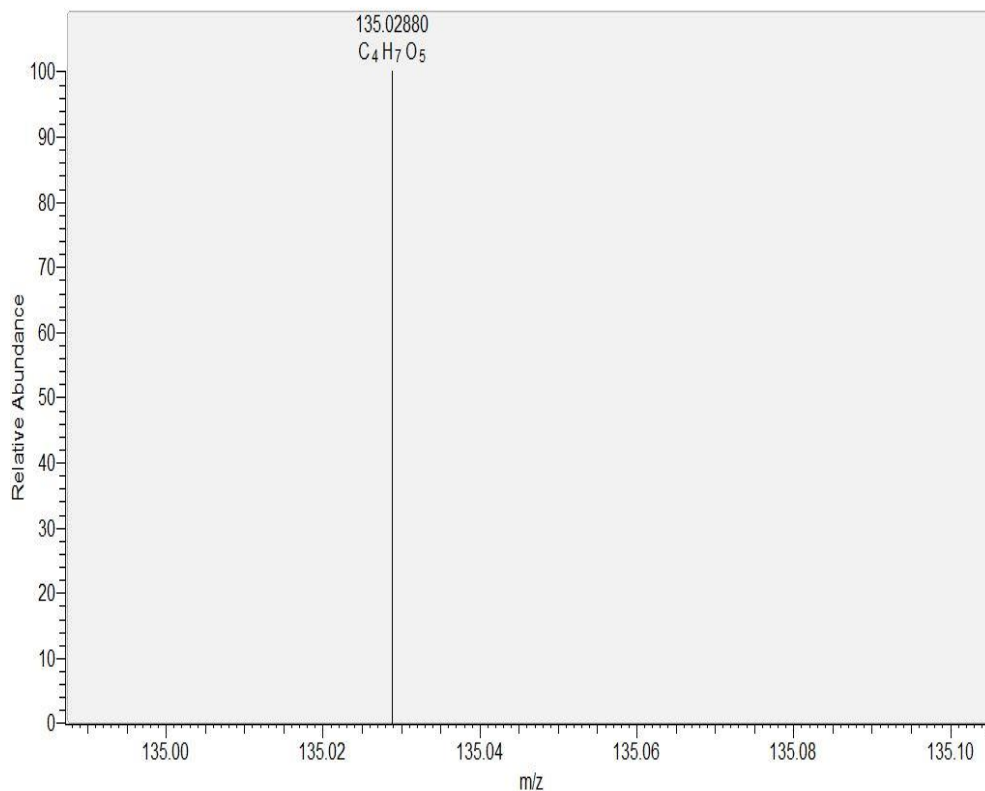


Figure 101. ESI-MS spectra of malic acid in F11 fraction from ethyl acetate extract of *C. militaris*.

Table 53. Fragmentation pattern of palmitic acid (retention time = 17.03) in F11 fraction from ethyl acetate extract of *C. militaris* detected by GC-MS

Peak#	m/z	Intensity	Relative Intensity (%)	Peak#	m/z	Intensity	Relative Intensity (%)
1	29.048	2650	47.58	14	69.093	1813	32.55
2	39.036	707	12.69	15	70.097	274	4.92
3	41.052	4763	85.49	16	70.103	196	3.52
4	42.060	1066	19.13	17	71.109	1443	25.90
5	43.032	507	9.10	18	73.052	4512	80.99
6	43.069	5571	100.00	19	83.112	679	12.19
7	45.049	347	6.23	20	85.128	831	14.93
8	55.072	3744	67.20	21	87.072	665	11.94
9	56.080	897	16.11	22	97.133	617	11.07
10	57.089	3137	56.30	23	129.133	1029	18.46
11	60.040	4972	89.25	24	213.250	501	9.00
12	61.049	1328	23.83	25	256.315	910	16.34
13	67.077	458	8.22				

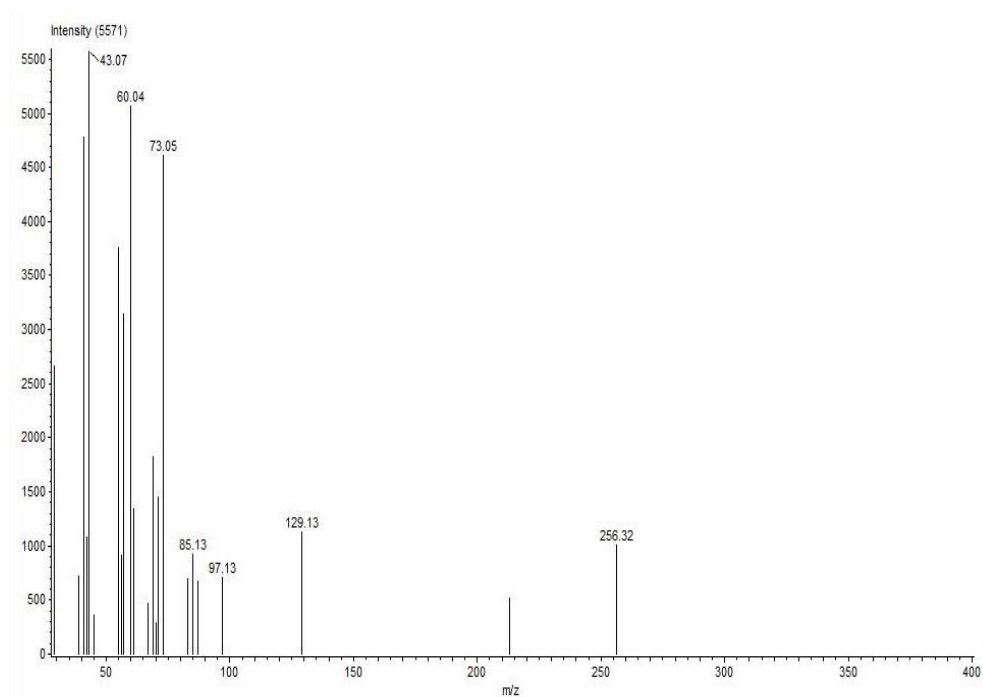


Figure 102. Mass-spectra of palmitic acid ($R_t = 17.03$) in F11 fraction from ethyl acetate extract of *C. militaris* detected by GC-MS.

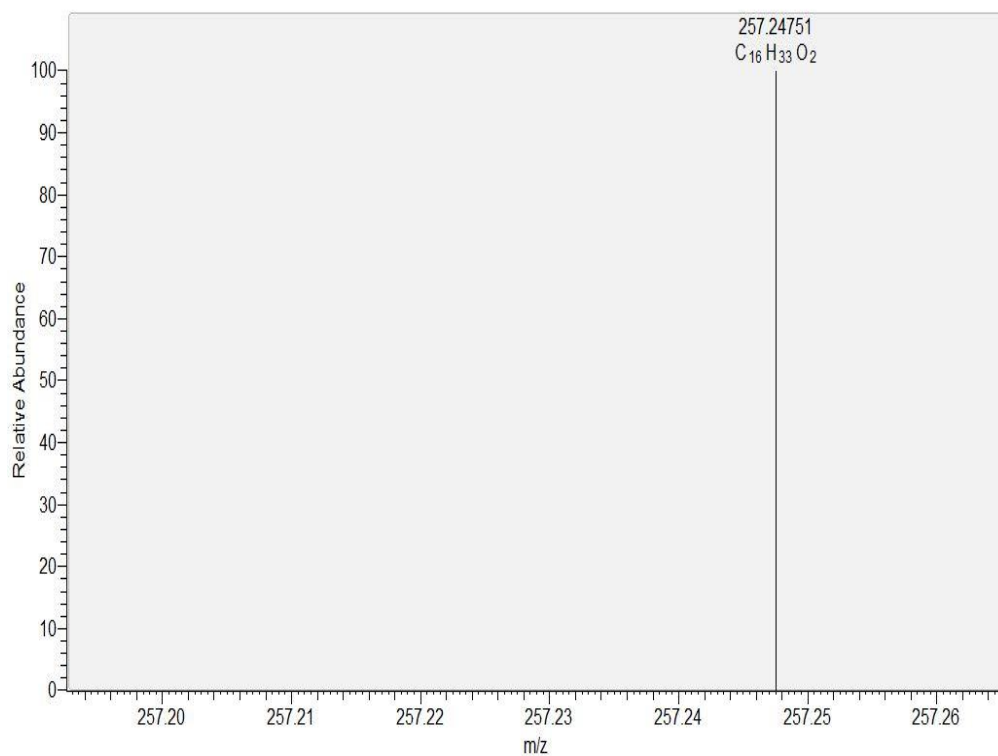
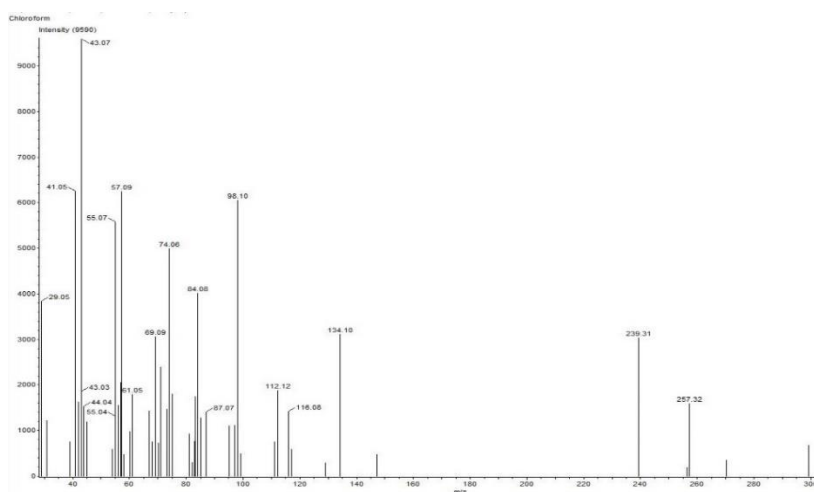


Figure 103. ESI-MS spectra of palmitic acid in F11 fraction from ethyl acetate extract of *C. militaris*.

Table 54. Fragmentation pattern of 2-palmitoylglycerol (retention time = 21.89) in F11 fraction from ethyl acetate extract of *C. militaris* detected by GC-MS

Peak#	m/z	Intensity	Relative Intensity (%)	Peak#	m/z	Intensity	Relative Intensity (%)
1	29.012	432	4.50	30	75.068	1791	18.67
2	29.048	3821	39.84	31	81.096	915	9.54
3	31.028	1197	12.48	32	82.102	283	2.95
4	39.036	734	7.66	33	82.108	207	2.16
5	41.052	6245	65.12	34	83.077	751	7.83
6	42.024	499	5.20	35	83.112	1724	17.98
7	42.060	1619	16.89	36	84.084	3913	40.81
8	43.032	1838	19.16	37	85.090	350	3.65
9	43.069	9590	100.00	38	85.128	1260	13.14
10	44.041	1521	15.86	39	87.072	1394	14.54
11	45.049	1180	12.31	40	95.116	1094	11.40
12	54.064	573	5.97	41	97.096	764	7.96
13	55.036	1305	13.61	42	97.132	1102	11.49
14	55.073	5570	58.08	43	98.104	5953	62.07
15	56.044	1443	15.05	44	99.115	479	4.99
16	56.080	1544	16.10	45	111.115	739	7.71
17	57.052	2044	21.31	46	112.124	1777	18.53
18	57.089	6140	64.02	47	116.084	1401	14.60
19	58.062	461	4.80	48	117.075	575	6.00
20	60.041	962	10.04	49	129.092	280	2.92
21	61.048	1696	17.68	50	129.101	271	2.82
22	67.077	1416	14.77	51	134.100	3006	31.34
23	68.085	745	7.77	52	147.111	458	4.78
24	69.092	2960	30.86	53	239.310	2928	30.53
25	70.100	711	7.42	54	256.315	150	1.56
26	71.069	499	5.20	55	256.325	181	1.88
27	71.109	2378	24.79	56	257.322	1497	15.61
28	73.052	1458	15.20	57	270.336	344	3.59
29	74.060	4890	50.99	58	299.346	667	6.96

**Figure 104.** Mass-spectra of 2-palmitoylglycerol (Rt = 21.89) in F11 fraction from ethyl acetate extract of *C. militaris* detected by GC-MS.

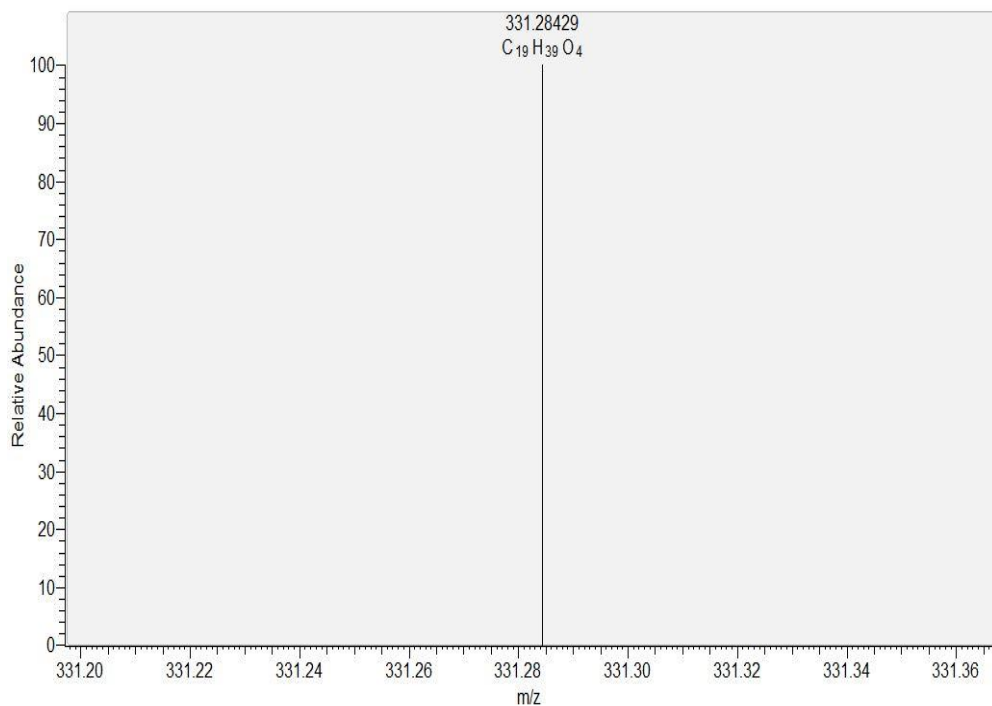


Figure 105. ESI-MS spectra of 2-palmitoylglycerol in F11 fraction from ethyl acetate extract of *C. militaris*.

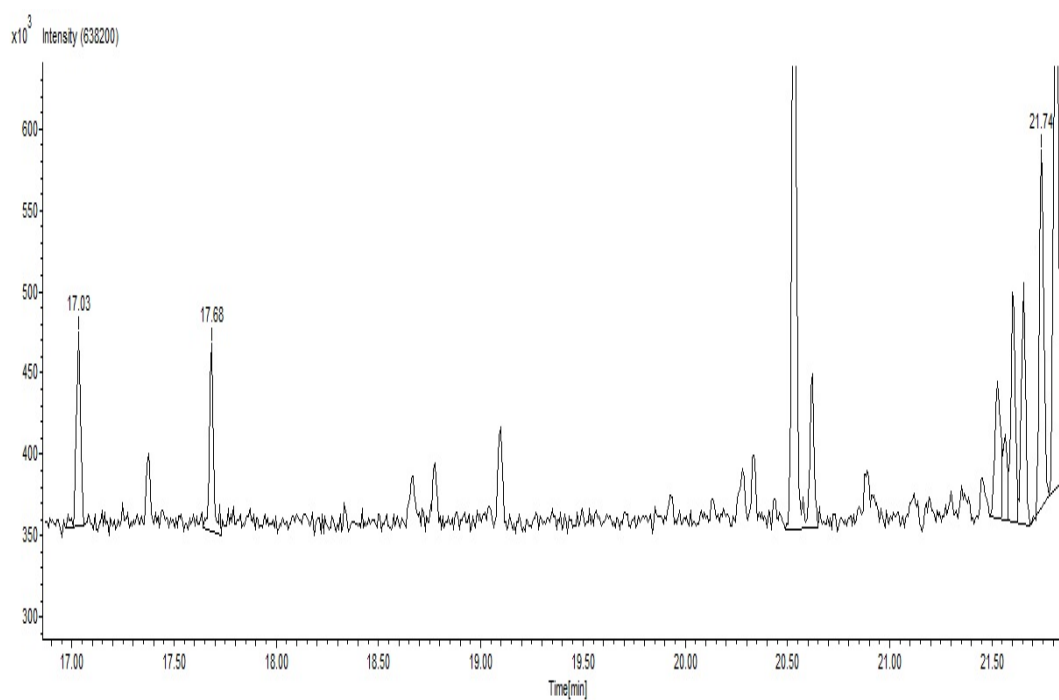


Figure 106. GC-MS chromatogram of F12 fraction from ethyl acetate extract of *C. militaris*.

Table 55. Fragmentation pattern of palmitic acid (retention time = 17.03) in F12 fraction from ethyl acetate extract of *C. militaris* detected by GC-MS

Peak#	m/z	Intensity	Relative Intensity (%)	Peak#	m/z	Intensity	Relative Intensity (%)
1	29.048	1655	47.43	12	60.039	3134	89.79
2	31.996	484	13.88	13	61.048	750	21.48
3	39.033	452	12.96	14	69.092	1525	43.68
4	41.052	3045	87.24	15	70.102	423	12.13
5	42.060	704	20.17	16	71.108	1115	31.94
6	43.031	312	8.93	17	73.051	2702	77.41
7	43.068	3490	100.00	18	83.110	534	15.29
8	55.038	206	5.90	19	85.129	656	18.79
9	55.072	1852	53.06	20	87.070	662	18.98
10	56.078	645	18.49	21	129.130	487	13.94
11	57.088	1989	56.99	22	256.308	563	16.13

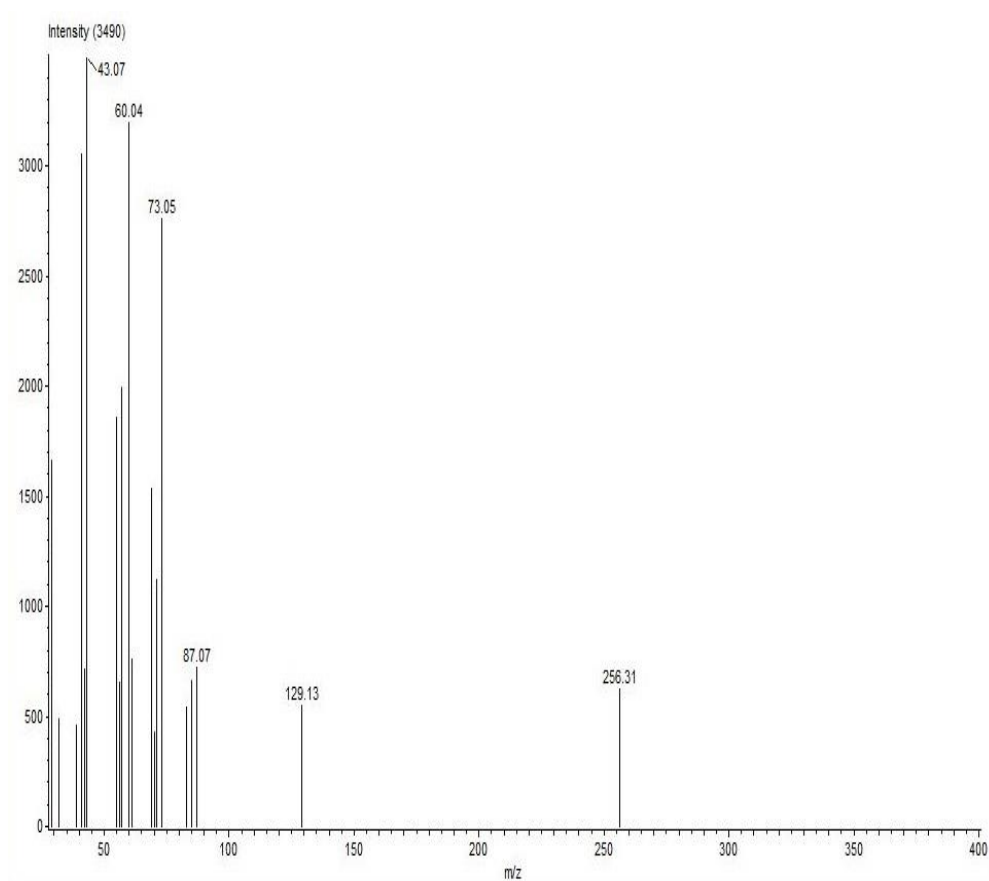


Figure 107. Mass-spectra of palmitic acid (Rt = 17.03) in F12 fraction from ethyl acetate extract of *C. militaris* detected by GC-MS.

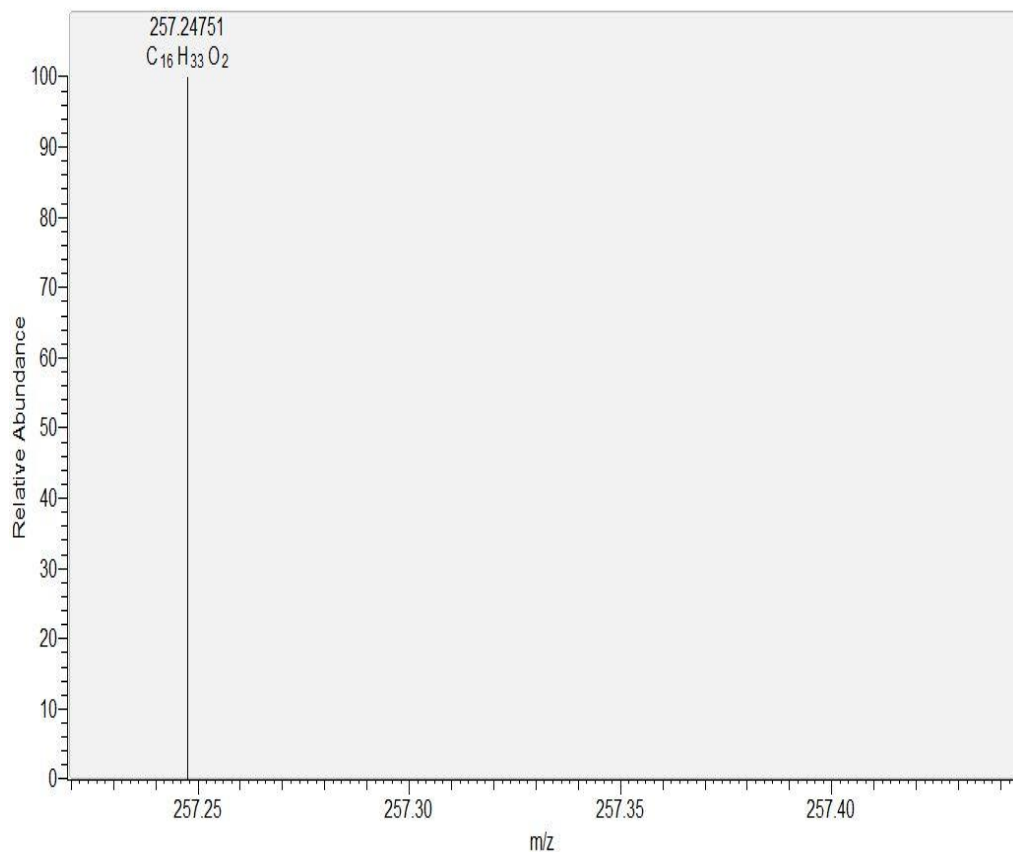


Figure 108. ESI-MS spectra of palmitic acid in F12 fraction from ethyl acetate extract of *C. militaris*.

Table 56. Fragmentation pattern of 1, E-11, Z-13-octadecatriene (retention time = 17.68) in F12 fraction from ethyl acetate extract of *C. militaris* detected by GC-MS

Peak#	m/z	Intensity	Relative Intensity (%)	Peak#	m/z	Intensity	Relative Intensity (%)
1	29.048	2479	32.55	36	78.071	290	3.81
2	32.002	699	9.17	37	79.079	2874	37.73
3	35.394	117	1.53	38	80.086	1572	20.64
4	39.035	1144	15.03	39	81.095	5060	66.44
5	40.040	80	1.05	40	82.102	2515	33.02
6	40.044	148	1.94	41	83.083	254	3.34
7	41.052	6137	80.58	42	83.111	945	12.41
8	41.075	147	1.93	43	85.089	170	2.24
9	42.023	195	2.56	44	91.083	829	10.88
10	42.058	714	9.37	45	93.098	735	9.65
11	43.032	549	7.21	46	94.105	448	5.88
12	43.068	1736	22.79	47	95.115	2770	36.37
13	45.011	540	7.09	48	96.122	1636	21.48
14	45.047	583	7.66	49	97.095	97	1.28
15	53.056	1150	15.10	50	97.119	97	1.27
16	54.063	3833	50.32	51	97.130	400	5.25

17	55.035	505	6.63	52	107.119	346	4.54
18	55.072	5260	69.06	53	108.125	281	3.68
19	56.078	533	7.00	54	109.134	1153	15.13
20	57.014	85	1.11	55	110.142	955	12.54
21	57.051	102	1.34	56	121.138	436	5.73
22	57.088	495	6.50	57	122.143	253	3.32
23	59.066	191	2.51	58	123.155	611	8.02
24	60.039	1379	18.11	59	124.164	530	6.95
25	65.059	658	8.64	60	137.173	227	2.98
26	66.067	610	8.01	61	197.437	60	0.78
27	67.075	7616	100.00	62	280.319	603	7.92
28	67.103	191	2.50	63	280.350	128	1.67
29	67.151	99	1.30	64	313.987	165	2.17
30	68.083	3276	43.02	65	420.319	129	1.70
31	69.091	2265	29.74	66	441.046	181	2.38
32	70.098	293	3.85	67	476.420	64	0.84
33	71.068	168	2.21	68	501.843	49	0.65
34	73.051	567	7.45	69	654.088	233	3.06
35	77.063	1072	14.07	70	654.665	144	1.89

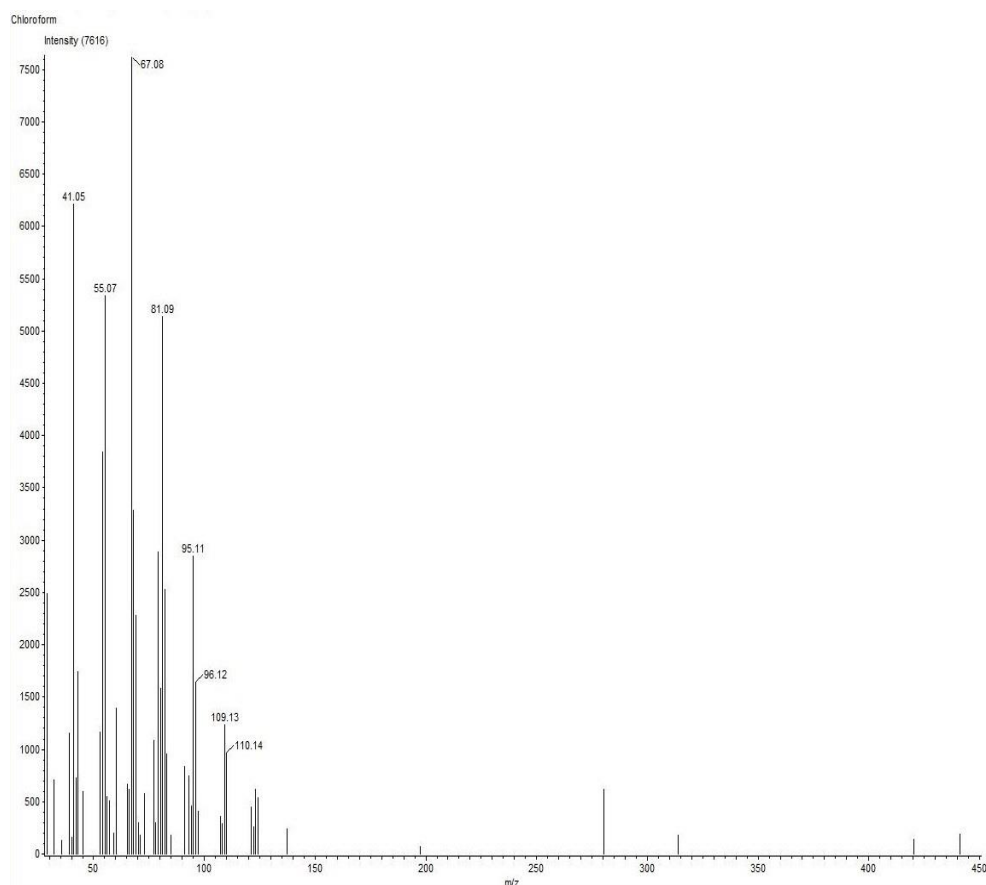


Figure 109. Mass-spectra of 1, E-11, Z-13-octadecatriene (Rt = 17.68) in F12 fraction from ethyl acetate extract of *C. militaris* detected by GC-MS.

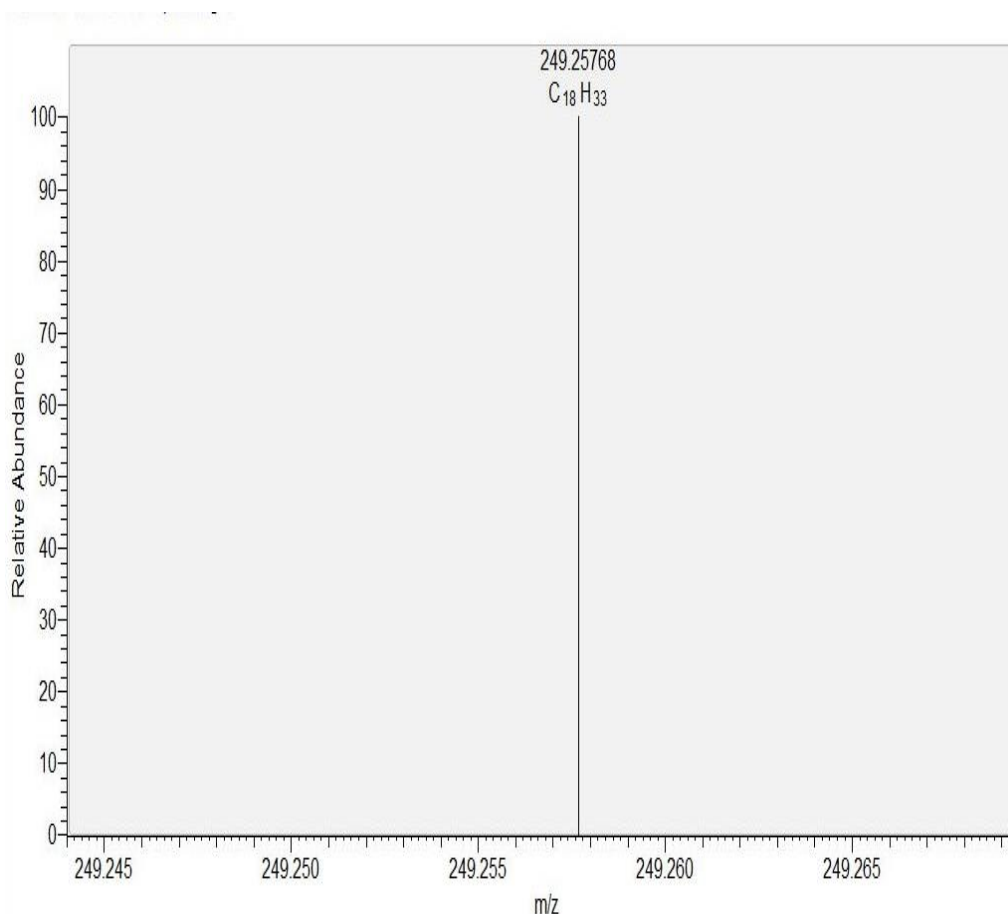


Figure 110. ESI-MS spectra of 1, E-11, Z-13-octadecatriene in F12 fraction from ethyl acetate extract of *C. militaris*.

Table 57. Fragmentation pattern of 1-n-hexadecylindan (retention time = 21.74) in F12 fraction from ethyl acetate extract of *C. militaris* detected by GC-MS

Peak#	m/z	Intensity	Relative Intensity (%)	Peak#	m/z	Intensity	Relative Intensity (%)
1	29.047	806	10.43	67	98.101	561	7.27
2	31.995	462	5.99	68	101.072	905	11.72
3	41.052	1367	17.70	69	116.065	493	6.38
4	43.068	2423	31.37	70	117.072	7724	100.00
5	55.071	1119	14.49	71	118.060	109	1.42
6	56.079	429	5.55	72	118.073	741	9.60
7	57.089	1227	15.89	73	119.067	766	9.92
8	59.049	628	8.13	74	129.076	882	11.42
9	69.093	627	8.12	75	130.084	1728	22.37
10	71.107	464	6.01	76	131.090	1307	16.92
11	75.049	814	10.55	77	190.115	518	6.71
12	84.083	688	8.90	78	313.343	493	6.38
13	89.069	804	10.40	132	313.367	185	2.40

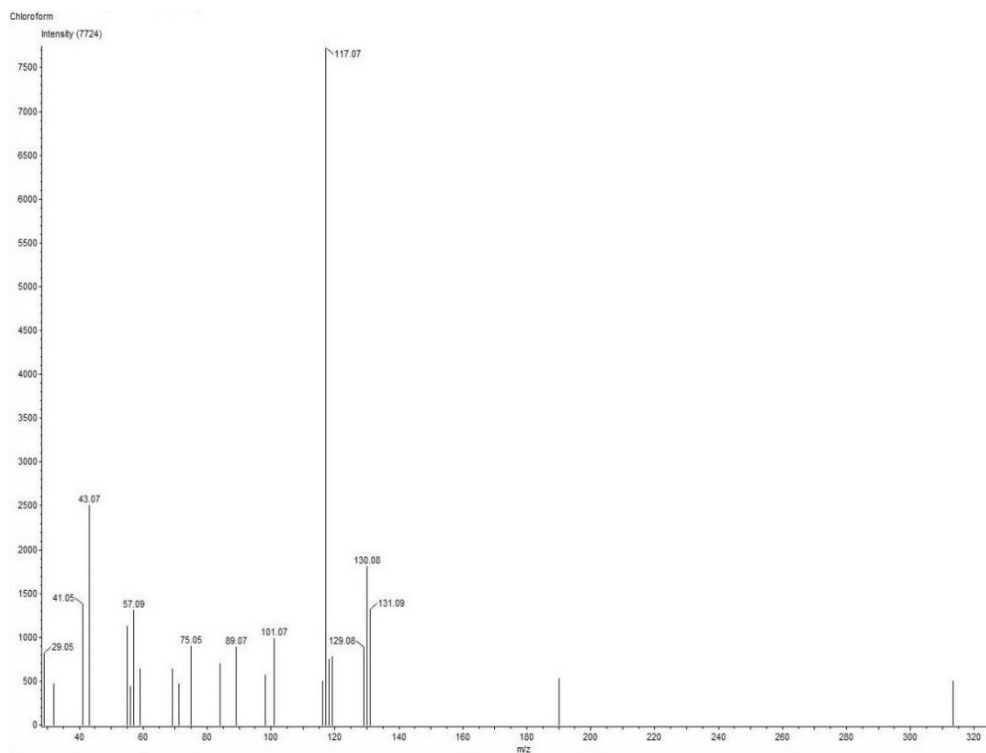


Figure 111. Mass-spectra of 1-n-hexadecylindan (Rt = 21.74) in F12 fraction from ethyl acetate extract of *C. militaris* detected by GC-MS.

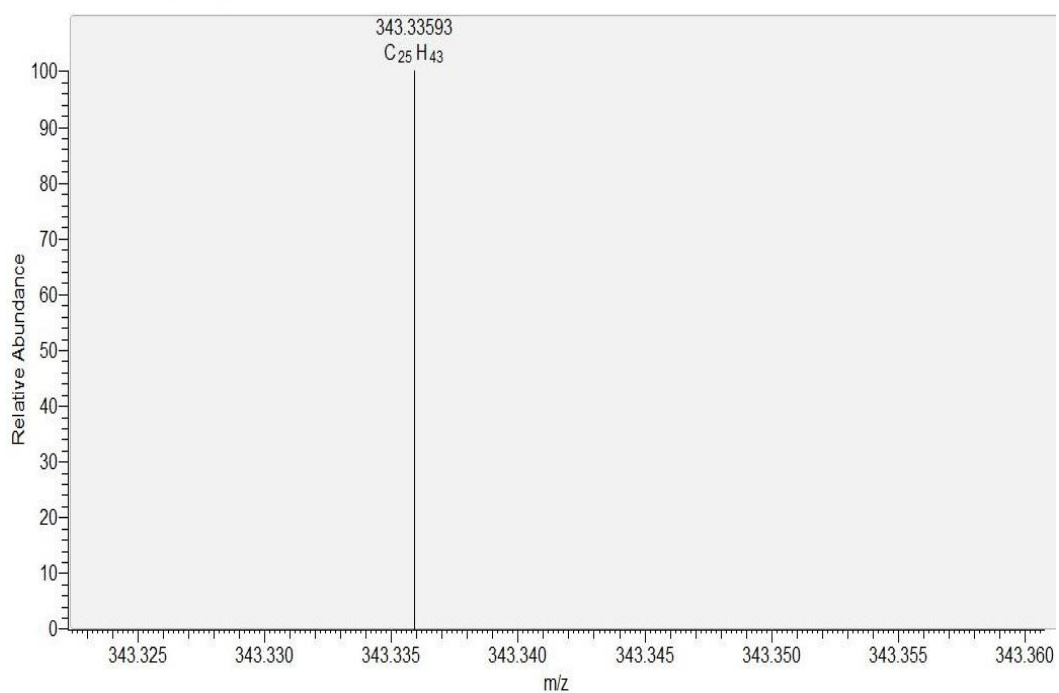


Figure 112. ESI-MS spectra of 1-n-hexadecylindan in F12 fraction from ethyl acetate extract of *C. militaris*.

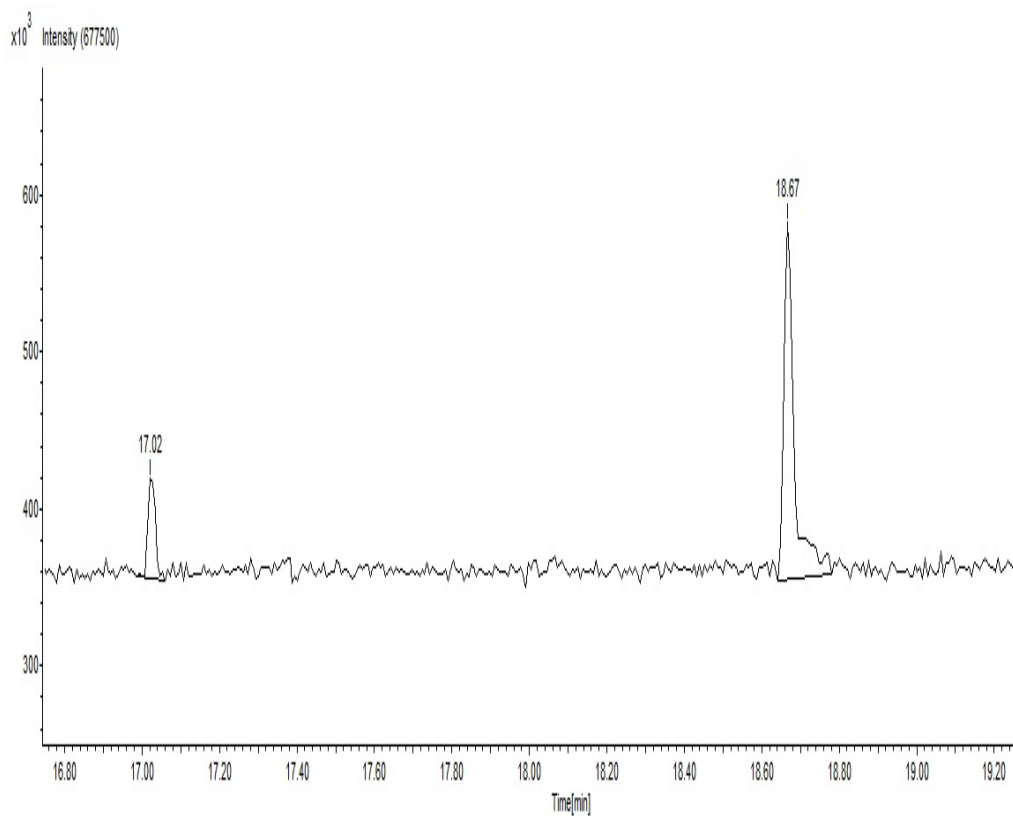


Figure 113. GC-MS chromatogram of F13 fraction from ethyl acetate extract of *C. militaris*.

Table 58. Fragmentation pattern of palmitic acid (retention time = 17.02) in F13 fraction from ethyl acetate extract of *C. militaris* detected by GC-MS

Peak#	m/z	Intensity	Relative Intensity (%)	Peak#	m/z	Intensity	Relative Intensity (%)
1	29.048	2964	44.70	15	67.078	697	10.52
2	31.997	415	6.26	16	69.092	2347	35.40
3	39.036	787	11.87	17	70.100	564	8.51
4	41.052	5854	88.31	18	71.109	1971	29.73
5	42.060	1408	21.23	19	73.052	5924	89.36
6	43.033	627	9.46	20	74.059	579	8.74
7	43.069	6629	100.00	21	83.112	883	13.32
8	45.049	526	7.94	22	85.128	1131	17.06
9	55.036	491	7.40	23	87.073	807	12.17
10	55.072	4471	67.45	24	97.133	633	9.54
11	56.080	1055	15.92	25	98.107	448	6.76
12	57.089	4032	60.82	26	129.133	1335	20.14
13	60.041	6183	93.28	27	213.251	529	7.98
14	61.049	1474	22.24	28	256.317	1174	17.71

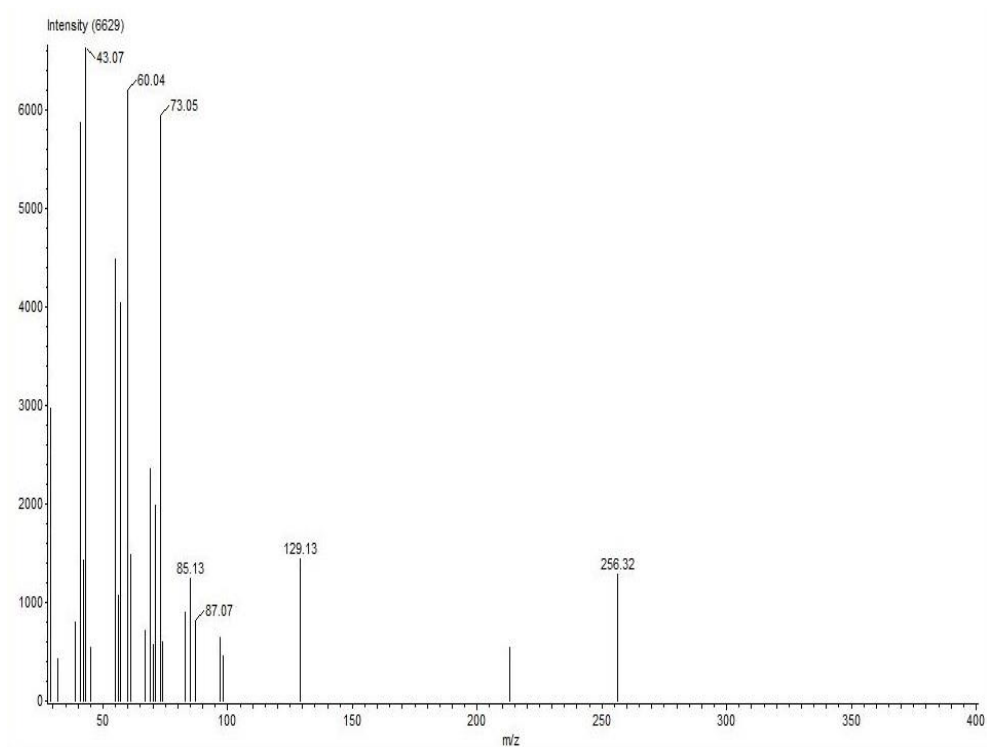


Figure 114. Mass-spectra of palmitic acid ($R_t = 17.02$) in F13 fraction from ethyl acetate extract of *C. militaris* detected by GC-MS.

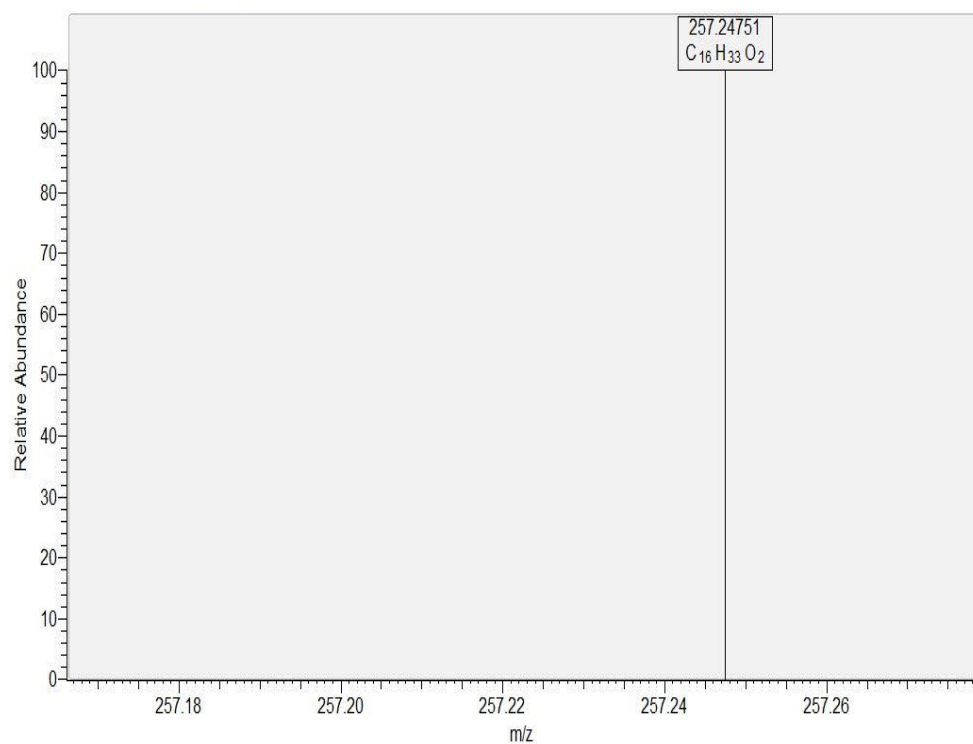


Figure 115. ESI-MS spectra of palmitic acid in F13 fraction from ethyl acetate extract of *C. militaris*.

Table 59. Fragmentation pattern of 1, E-11, Z-13-octadecatriene (retention time = 18.67) in F13 fraction from ethyl acetate extract of *C. militaris* detected by GC-MS

Peak#	m/z	Intensity	Relative Intensity (%)	Peak#	m/z	Intensity	Relative Intensity (%)
1	29.048	3953	32.52	23	70.097	508	4.18
2	32.002	496	4.08	24	73.052	654	5.38
3	39.035	1751	14.40	25	77.063	1663	13.68
4	41.052	9503	78.18	26	79.079	4464	36.73
5	42.023	312	2.56	27	80.087	2181	17.94
6	42.058	947	7.79	28	81.095	7857	64.64
7	43.032	832	6.84	29	82.102	3948	32.48
8	43.068	2672	21.98	30	83.111	1367	11.25
9	45.011	737	6.07	31	91.083	1225	10.08
10	45.047	683	5.62	32	93.098	1015	8.35
11	53.055	1656	13.62	33	94.106	681	5.61
12	54.063	5929	48.77	34	95.115	4510	37.10
13	55.035	560	4.61	35	96.122	2391	19.67
14	55.072	7999	65.80	36	97.129	642	5.28
15	56.077	682	5.61	37	107.120	496	4.08
16	57.088	774	6.37	38	108.126	570	4.69
17	60.039	1989	16.36	39	109.134	1917	15.77
18	65.058	1092	8.99	40	110.142	1316	10.83
19	66.067	890	7.32	41	123.157	647	5.32
20	67.075	12156	100.00	42	124.163	586	4.82
21	68.083	5083	41.81	43	280.320	982	8.08
22	69.091	3513	28.90				

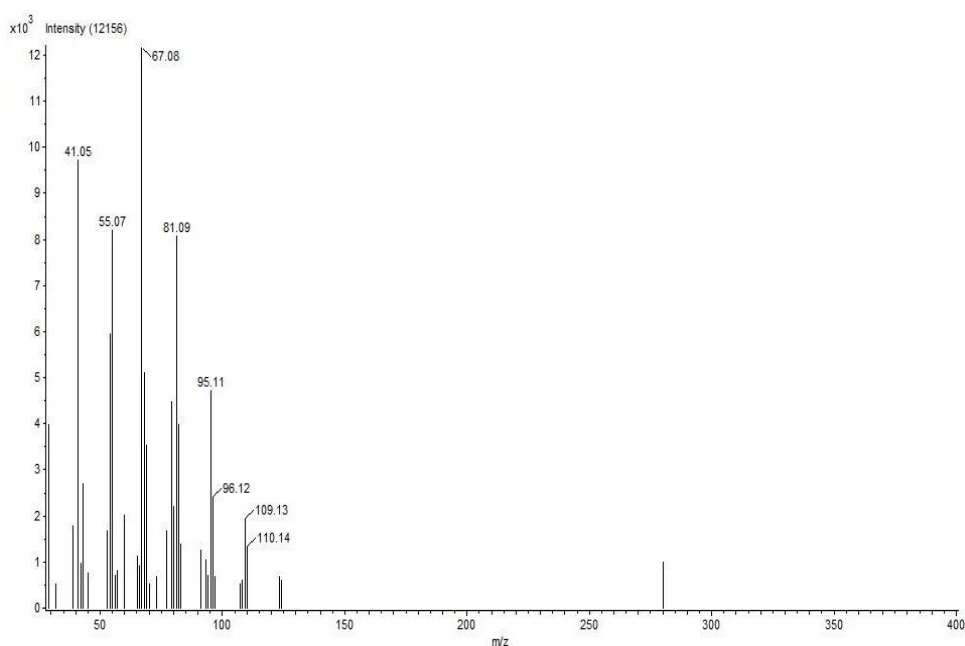


Figure 116. Mass-spectra of 1, E-11, Z-13-octadecatriene (Rt = 18.67) in F13 fraction from ethyl acetate extract of *C. militaris* detected by GC-MS.

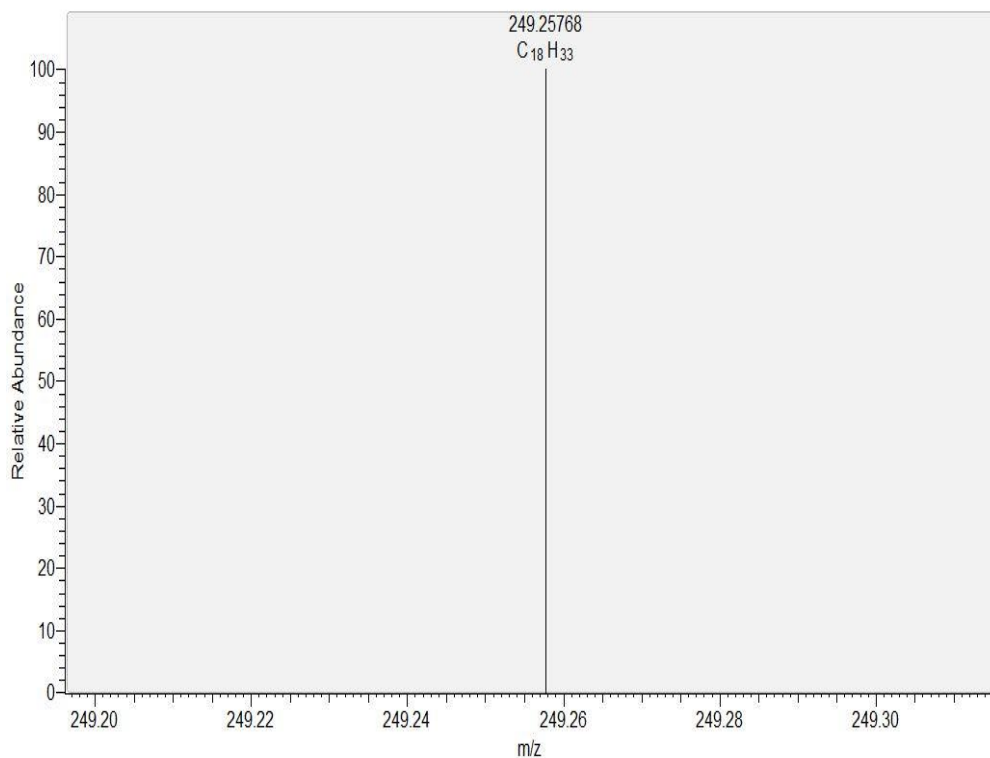


Figure 117. ESI-MS spectra of 1, E-11, Z-13-octadecatriene in F13 fraction from ethyl acetate extract of *C. militaris*.

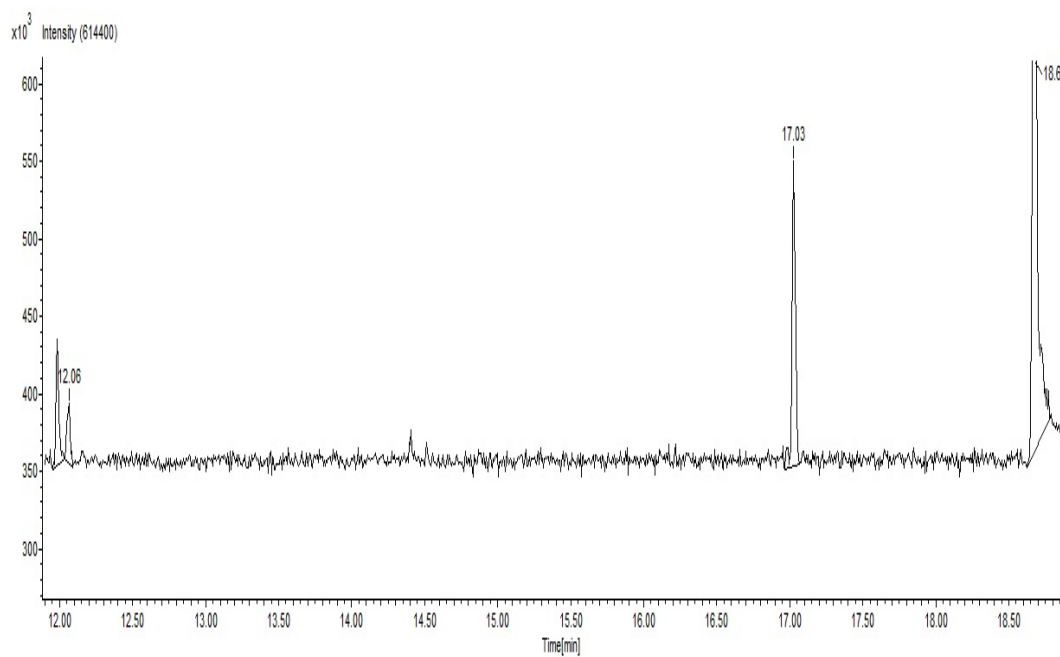


Figure 118. GC-MS chromatogram of F14 fraction from ethyl acetate extract of *C. militaris*.

Table 60. Fragmentation pattern of carbamic acid (3-methylphenyl) methyl ester (retention time = 7.00) in F14 fraction from ethyl acetate extract of *C. militaris* detected by GC-MS

Peak#	m/z	Intensity	Relative Intensity (%)	Peak#	m/z	Intensity	Relative Intensity (%)
1	29.011	1719	22.19	15	79.019	5761	74.35
2	30.019	481	6.20	16	80.999	1329	17.15
3	31.028	1421	18.34	17	81.012	125	1.61
4	42.022	502	6.48	18	82.007	993	12.82
5	43.032	876	11.30	19	84.103	298	3.84
6	44.039	938	12.10	20	84.110	292	3.76
7	45.047	709	9.16	21	93.004	401	5.17
8	46.983	2412	31.13	22	95.018	390	5.03
9	47.992	496	6.40	23	99.016	1482	19.13
10	56.068	446	5.75	24	107.024	668	8.62
11	57.050	735	9.49	25	108.030	7749	100.00
12	65.002	585	7.55	26	109.036	687	8.87
13	77.002	713	9.21	27	537.370	272	3.51
14	78.012	1254	16.19				

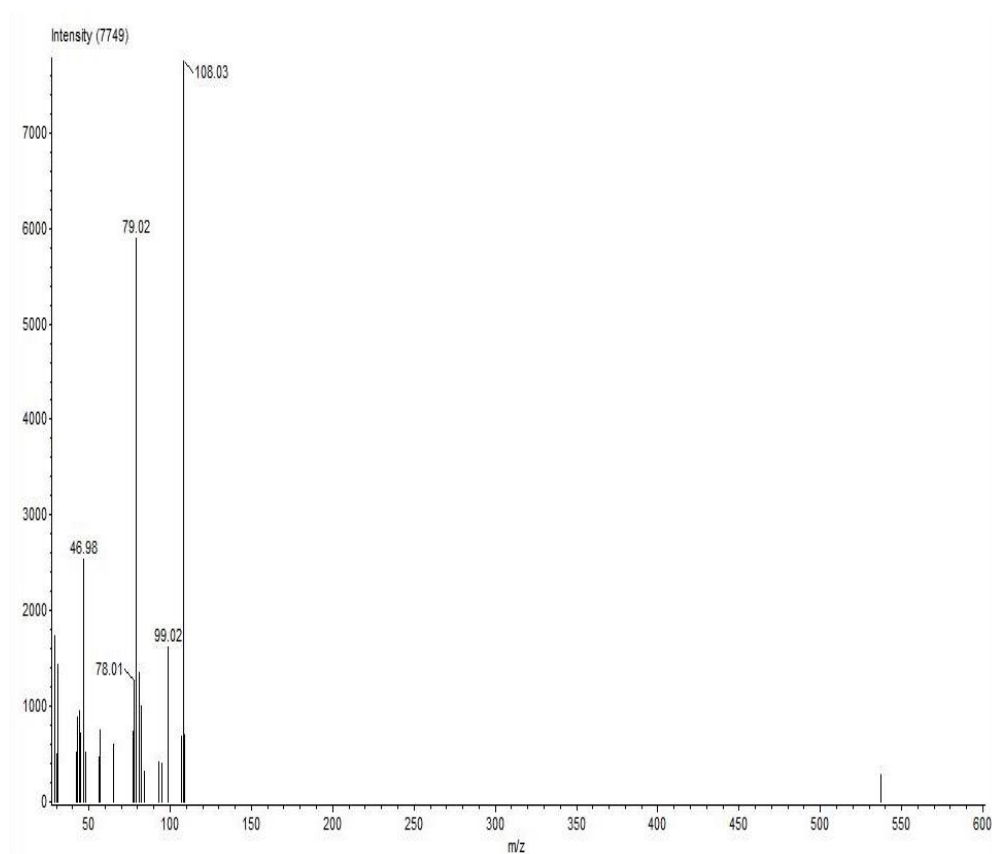


Figure 119. Mass-spectra of carbamic acid (3-methylphenyl) methyl ester (Rt = 7.00) in F14 fraction from ethyl acetate extract of *C. militaris* detected by GC-MS.

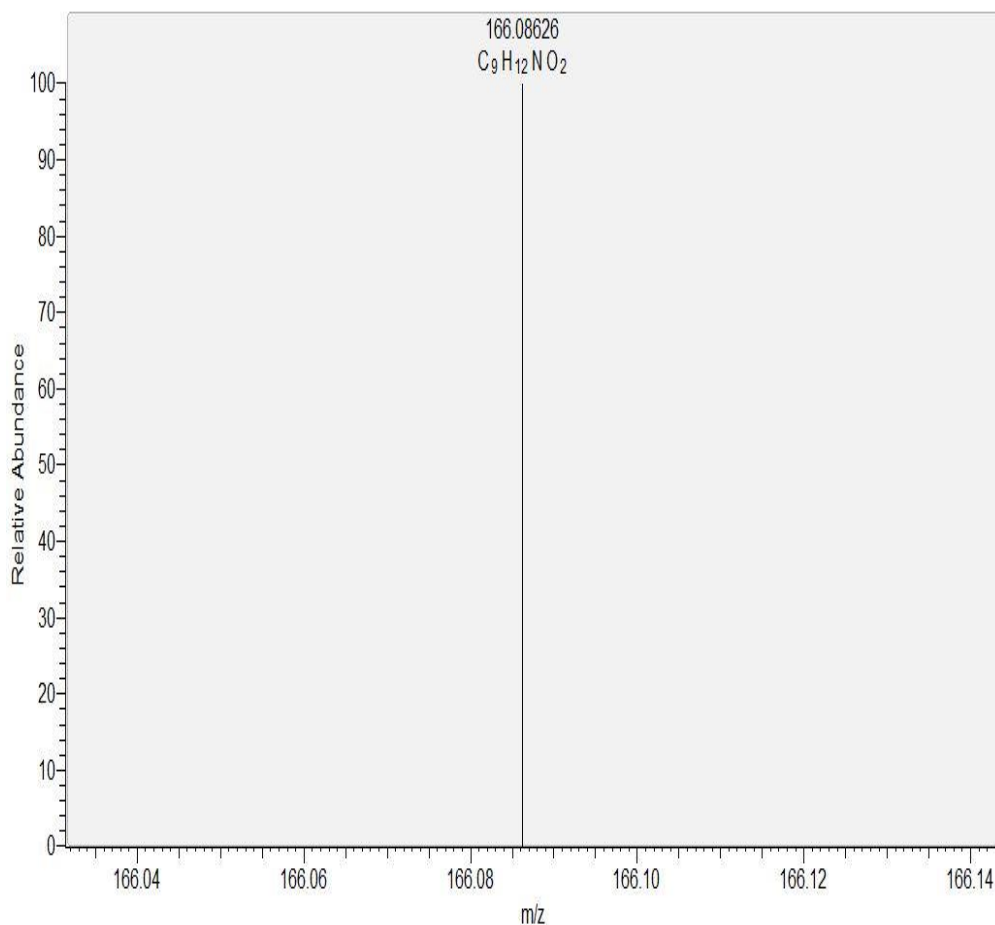


Figure 120. ESI-MS spectra of carbamic acid (3-methylphenyl) methyl ester in F14 fraction from ethyl acetate extract of *C. militaris*.

Table 61. Fragmentation pattern of palmitic acid (retention time = 17.03) in F14 fraction from ethyl acetate extract of *C. militaris* detected by GC-MS

Peak#	m/z	Intensity	Relative Intensity (%)	Peak#	m/z	Intensity	Relative Intensity (%)
1	29.048	2159	38.76	12	61.047	1386	24.88
2	39.035	698	12.52	13	69.092	2118	38.03
3	41.052	4720	84.73	14	71.108	1217	21.85
4	42.059	955	17.14	15	73.051	4266	76.58
5	43.032	719	12.91	16	83.111	905	16.24
6	43.068	5571	100.00	17	85.126	802	14.40
7	45.048	511	9.17	18	87.071	663	11.90
8	55.072	3233	58.03	19	97.132	592	10.63
9	56.080	1156	20.75	20	129.130	1239	22.23
10	57.088	3235	58.07	21	256.317	958	17.20
11	60.040	4531	81.33				

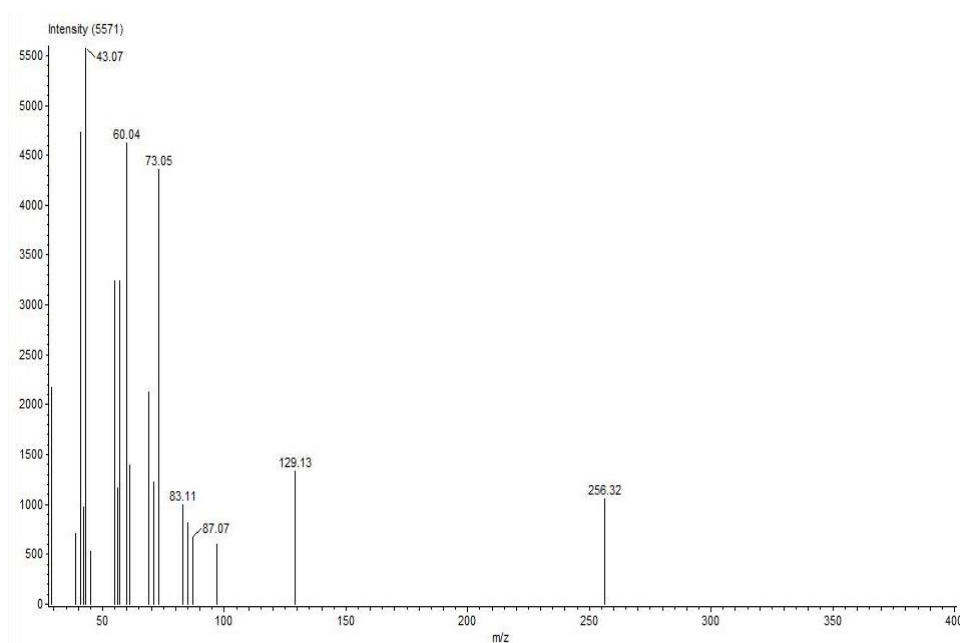


Figure 121. Mass-spectra of palmitic acid ($R_t = 17.03$) in F14 fraction from ethyl acetate extract of *C. militaris* detected by GC-MS.

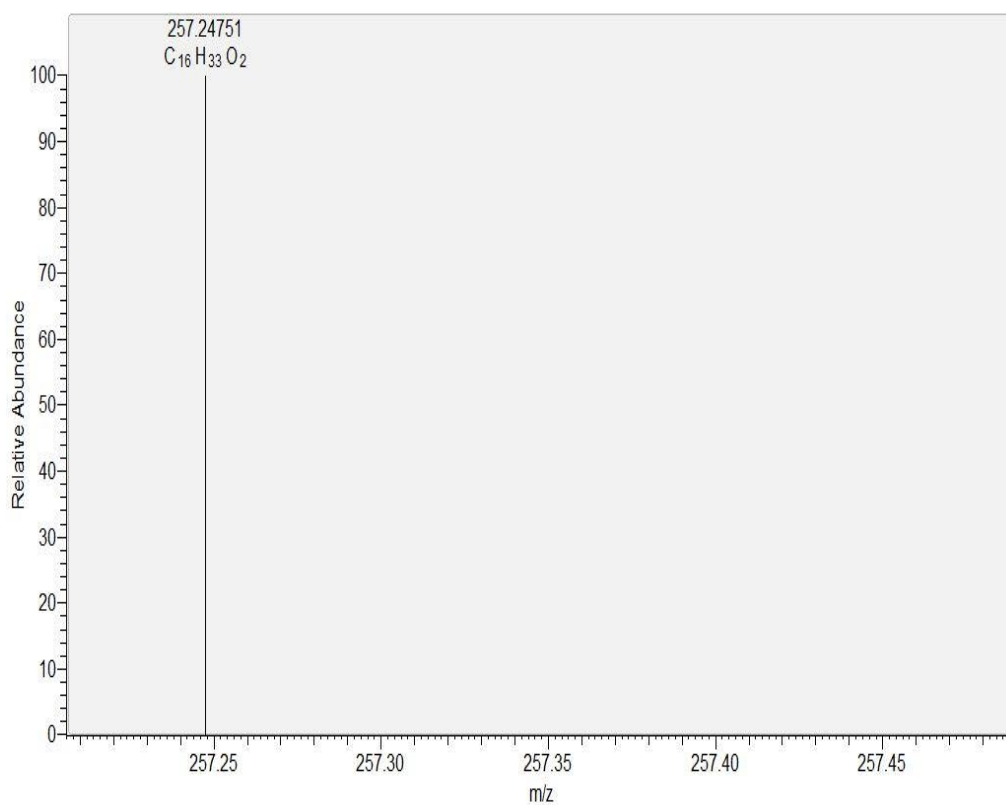


Figure 122. ESI-MS spectra of palmitic acid in F14 fraction from ethyl acetate extract of *C. militaris*.

Table 62. Fragmentation pattern of 1, E-11, Z-13-octadecatriene (retention time = 18.67) in F14 fraction from ethyl acetate extract of *C. militaris* detected by GC-MS

Peak#	m/z	Intensity	Relative Intensity (%)	Peak#	m/z	Intensity	Relative Intensity (%)
1	29.048	2733	30.58	20	69.091	2504	28.02
2	39.036	1202	13.45	21	73.052	528	5.91
3	41.052	7048	78.86	22	77.063	1319	14.76
4	42.058	754	8.44	23	79.079	3285	36.76
5	43.032	547	6.12	24	80.086	1532	17.14
6	43.068	2056	23.01	25	81.095	5598	62.64
7	45.011	527	5.90	26	82.102	2844	31.82
8	45.048	538	6.02	27	83.111	950	10.63
9	53.056	1253	14.02	28	91.083	888	9.94
10	54.063	4330	48.45	29	93.098	749	8.39
11	55.035	555	6.21	30	94.106	596	6.67
12	55.072	5945	66.52	31	95.115	3392	37.96
13	56.077	525	5.87	32	96.122	1836	20.54
14	57.088	602	6.74	33	97.130	482	5.39
15	60.039	1448	16.20	34	107.119	446	5.00
16	65.058	786	8.80	35	109.134	1314	14.71
17	66.067	691	7.73	36	110.142	1094	12.24
18	67.075	8937	100.00	37	123.157	427	4.78
19	68.083	3840	42.96	38	280.321	760	8.51

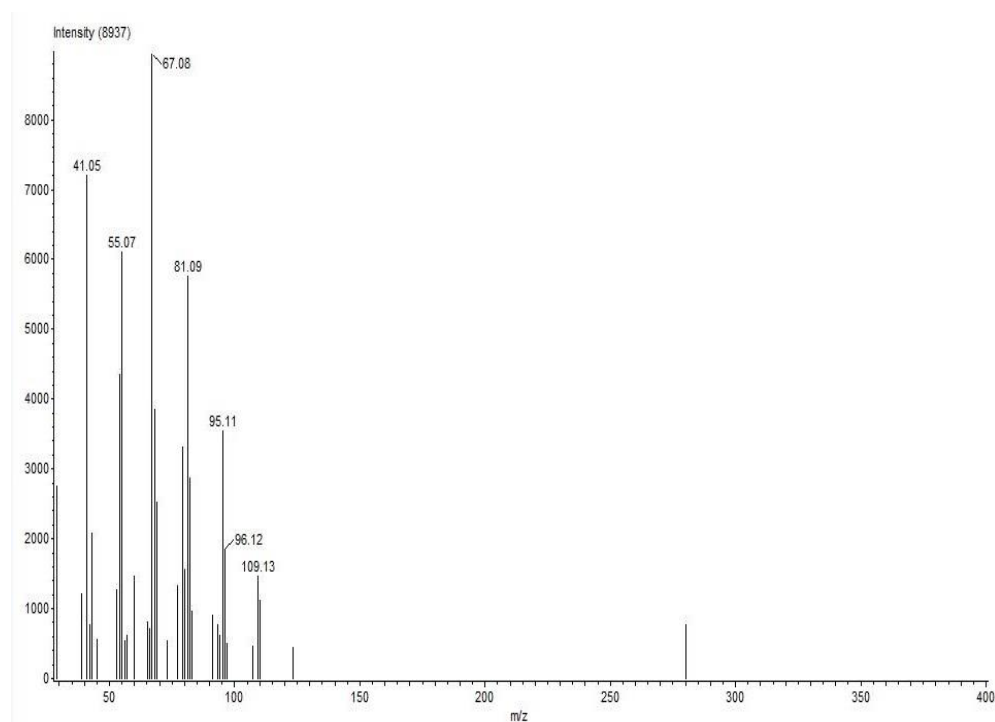


Figure 123. Mass-spectra of 1, E-11, Z-13-octadecatriene (Rt = 18.67) in F14 fraction from ethyl acetate extract of *C. militaris* detected by GC-MS

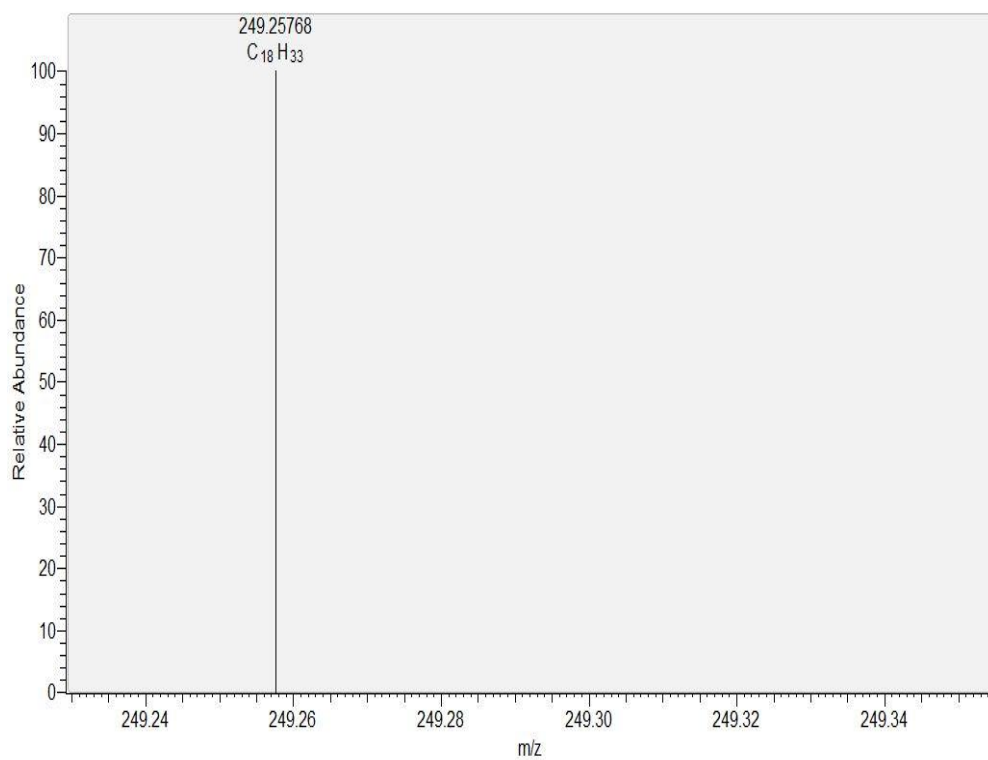


Figure 124. ESI-MS spectra of 1, E-11, Z-13-octadecatriene in F14 fraction from ethyl acetate extract of *C. militaris*.

Appendix B: Identification of the most active fraction and cordycepin of *C. militaris* on allelopathic activity

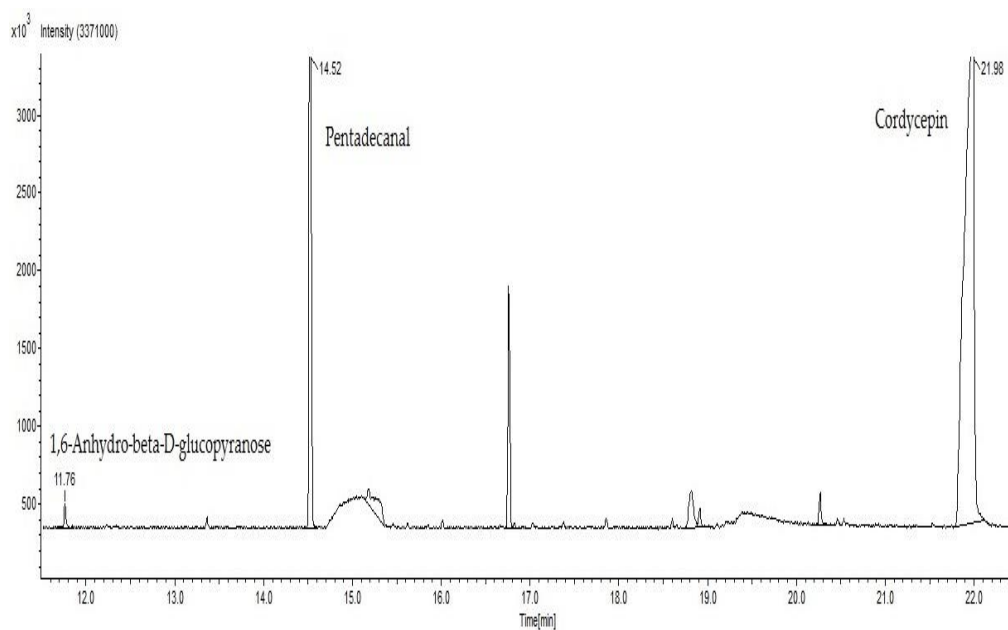


Figure 125. GC-MS chromatogram of CM4 fraction from ethyl acetate extract of *C. militaris*.

Table 63. Fragmentation pattern of cordycepin (retention time = 21.98) in CM4 fraction from ethyl acetate extract of *C. militaris* detected by GC-MS

Peak#	m/z	Intensity	Relative Intensity (%)	Peak#	m/z	Intensity	Relative Intensity (%)
1	29.012	20499	7.15	49	93.064	4897	1.71
2	29.036	5285	1.84	50	94.071	7414	2.59
3	29.049	9391	3.28	51	95.079	3396	1.18
4	30.020	1521	0.53	52	99.076	7526	2.62
5	30.044	5603	1.95	53	107.071	2870	1.00
6	31.029	37061	12.92	54	108.078	94206	32.85
7	38.016	1889	0.66	55	108.162	2065	0.72
8	39.037	15378	5.36	56	109.084	11798	4.11
9	40.032	12042	4.20	57	116.084	1639	0.57
10	41.053	39661	13.83	58	117.093	1248	0.44
11	42.025	2802	0.98	59	119.074	22947	8.00
12	42.061	16203	5.65	60	120.081	3718	1.30
13	43.034	25759	8.98	61	121.090	4478	1.56
14	43.069	15459	5.39	62	122.097	1260	0.44
15	44.041	8214	2.86	63	133.095	1227	0.43
16	45.050	6819	2.38	64	134.092	5250	1.83
17	47.029	3803	1.33	65	135.097	286745	100.00
18	51.033	1773	0.62	66	136.105	130251	45.42
19	52.036	3740	1.30	67	137.107	9171	3.20
20	53.032	9243	3.22	68	145.098	1459	0.51
21	53.057	14171	4.94	69	147.113	1932	0.67
22	54.040	22577	7.87	70	148.110	26161	9.12
23	55.046	17008	5.93	71	149.116	7042	2.46
24	55.073	623	0.22	72	161.120	1521	0.53
25	56.055	4650	1.62	73	162.129	4818	1.68
26	57.053	41327	14.41	74	163.102	2368	0.83

27	58.059	2701	0.94	75	164.109	152326	53.12
28	59.069	1118	0.39	76	164.294	1071	0.37
29	60.041	2179	0.76	77	165.112	12593	4.39
30	61.049	997	0.35	78	173.125	3196	1.11
31	65.036	6922	2.41	79	174.133	5882	2.05
32	66.044	25084	8.75	80	175.140	9068	3.16
33	67.052	21058	7.34	81	176.147	3555	1.24
34	68.058	8147	2.84	82	177.121	1884	0.66
35	69.057	35222	12.28	83	178.129	35404	12.35
36	69.092	1101	0.38	84	179.131	3675	1.28
37	70.063	9807	3.42	85	192.149	5705	1.99
38	71.037	1897	0.66	86	193.154	2290	0.80
39	71.073	14239	4.97	87	202.136	9167	3.20
40	73.053	6530	2.28	88	203.143	5183	1.81
41	77.039	1654	0.58	89	204.151	2599	0.91
42	79.055	2584	0.90	90	215.148	4163	1.45
43	80.052	6090	2.12	91	216.154	2010	0.70
44	81.060	21147	7.37	92	220.152	6124	2.14
45	82.067	5780	2.02	93	221.160	16543	5.77
46	85.057	1805	0.63	94	222.163	2043	0.71
47	91.048	1258	0.44	95	234.172	1803	0.63
48	92.055	8573	2.99	96	251.180	3630	1.27

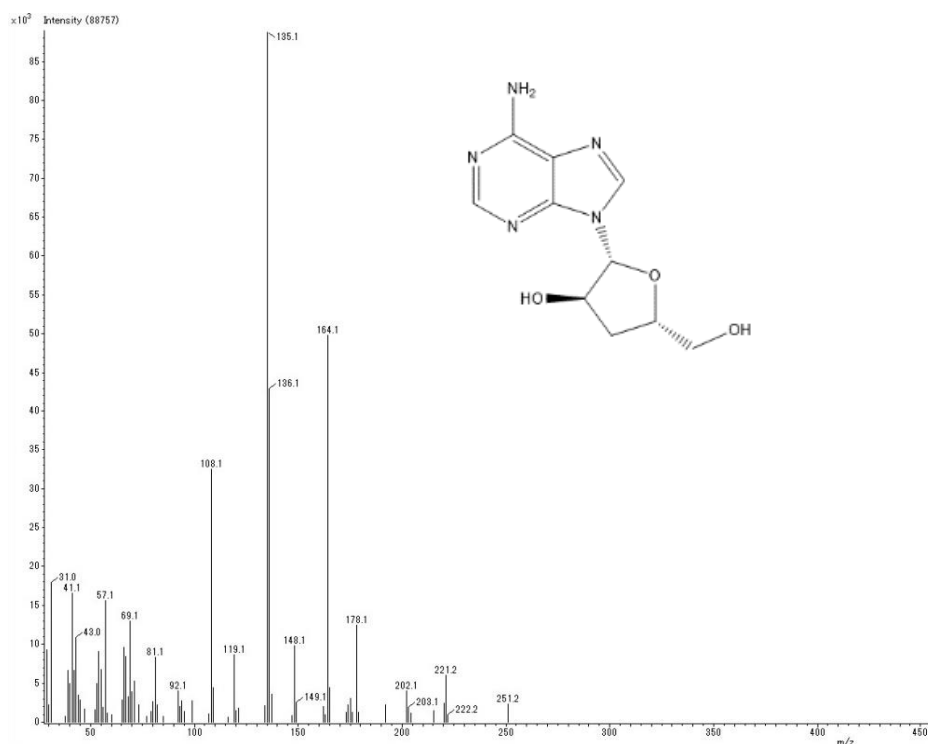


Figure 126. Mass-spectra of cordycepin (Rt = 21.98) in CM4 fraction from ethyl acetate extract of *C. militaris* detected by GC-MS.

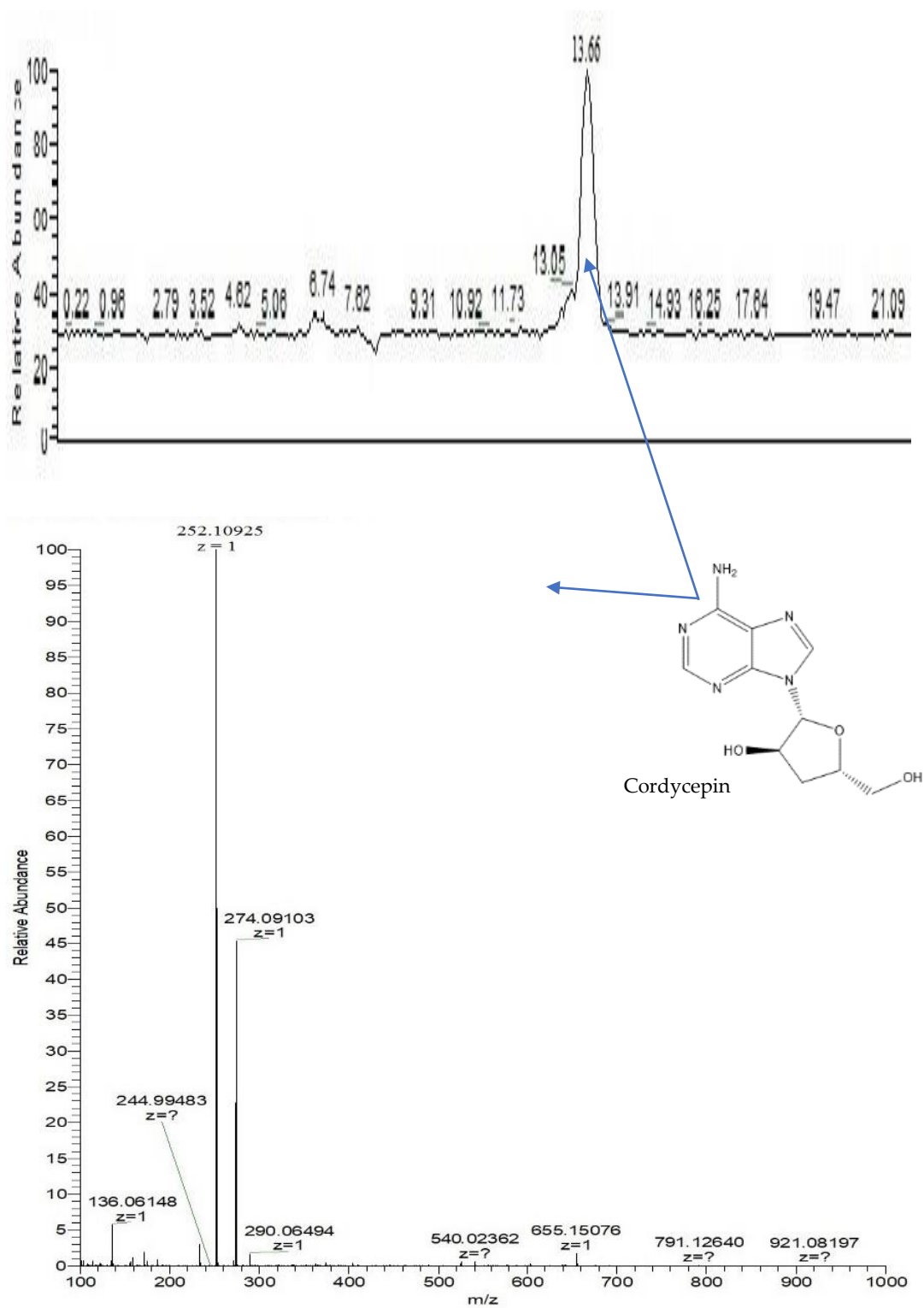


Figure 127. Total ion chromatogram and mass spectra of standard cordycepin by LC-ESI-MS ($[M + Na]^+$ m/z: 274.1; $[M+H]^+$ m/z: 252.1).

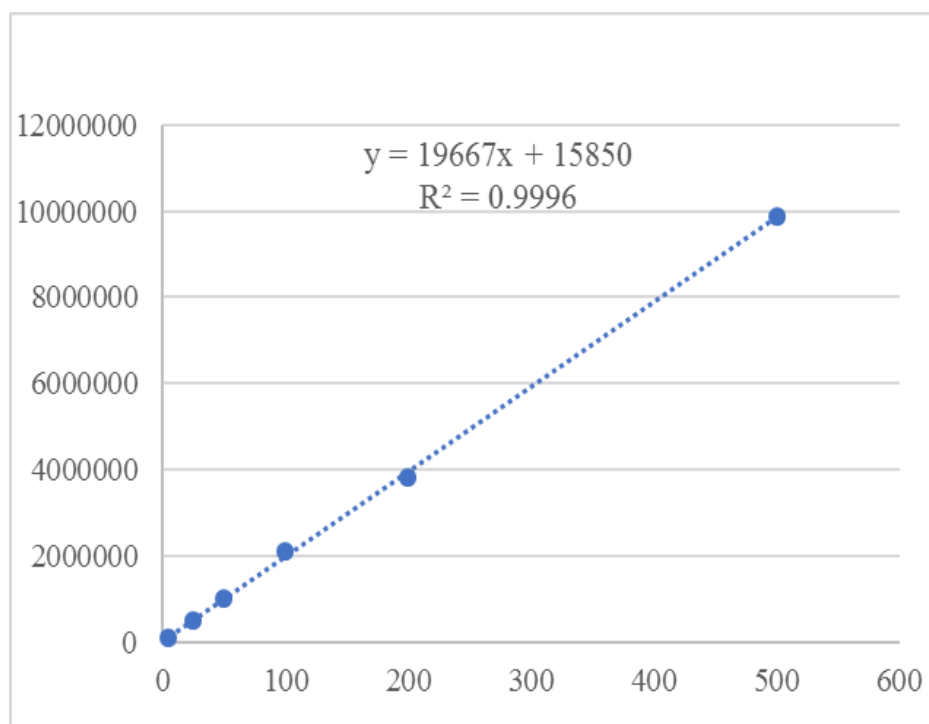


Figure 128. HPLC standard curve of cordycepin.

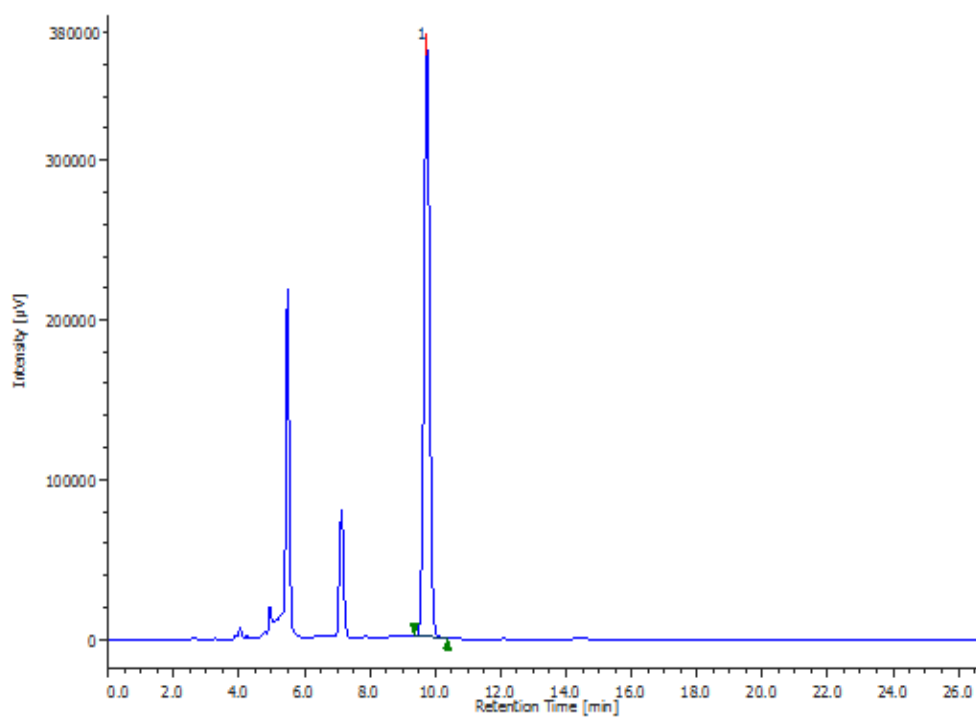


Figure 129. HPLC chromatogram of cordycepin in CM4 fraction from ethyl acetate extract of *C. militaris*.